2020

INVESTIGATING THE ROLE OF TAM (TYRO3, AXL AND MERTK) FAMILY RECEPTORS IN MERLIN-DEFICIENT TUMOURS

Dave, Foram

http://hdl.handle.net/10026.1/15791

UNIVERSITY OF PLYMOUTH

INVESTIGATING THE ROLE OF TAM (TYRO3, AXL AND MERTK) FAMILY RECEPTORS IN MERLIN-DEFICIENT TUMOURS

by

FORAM SANJAYKUMAR DAVE

A thesis submitted to the University of Plymouth

in partial fulfilment for the degree of

DOCTOR OF PHILOSOPHY

Peninsula Medical School

March 2019

<u>Acknowledgements</u>

AUTHOR'S DECLARATION

At no time during the registration for the degree of Doctor of Philosophy has the author been registered for any other University award without prior agreement of the Doctoral College Quality Sub-Committee.

Work submitted for this research degree at the University of Plymouth has not formed part of any other degree either at the University of Plymouth or at another establishment.

Publications (or public presentation of creative research outputs):

Provenzano L, Ryan Y, Hilton D *et al.* (2017). Cellular prion protein (PrPC) in the development of Merlin-deficient tumours. Oncogene. 2017 Nov 2;36(44):6132-6142. doi: 10.1038/onc.2017.200.

Presentation at conferences:

BNOS conference 2016, Leeds, UK. June 29-July 1, 2016. Poster presentation.

BNOS conference 2017, Edinburgh, UK. June 21-13, 2017. Oral presentation.

Next generation immune-oncology conference, London, UK. March 13-14, 2017. Poster presentation

Word count of main body of thesis: 58786

Signed

Date

Foram Sanjaykumar Dave

INVESTIGATING THE ROLE OF TAM (TYRO3, AXL AND MERTK)

FAMILY RECEPTORS IN MERLIN DEFICIENT TUMOURS

Abstract

Mutations in the *NF2* gene, which codes for the tumour suppressor Merlin, is responsible for the development of all Neurofibromatosis Type 2 (NF2)-related tumours including schwannomas, meningiomas and ependymomas. These tumours can also occur spontaneously in non-NF2 patients. The only available treatments for this group of tumours are surgery and radiosurgery/radiotherapy. Hence, there is an urgent need for new effective drug-based treatments.

TAM (TYRO3, AXL and MERTK) family receptors are involved in tumour development, progression, metastasis and resistance to targeted therapies in several cancers. Our group previously showed overexpression and hyper-activation of all three TAM family receptors and their ligand Gas6 in schwannomas. The key role of AXL in promoting tumour development by altering proliferation, adhesion and survival of human schwannoma primary cells *in vitro* was also established. The aim of this project is to explore the role of TYRO3 and MERTK in schwannomas' and all three TAM members in meningiomas' pathogenesis.

Western blotting demonstrated that AXL, MERTK, TYRO3 and their ligand Gas6 are highly expressed and activated in Merlin-deficient meningioma tissues and cells. The expression of AXL, MERTK and TYRO3, but not Gas6, appear to be Merlin-dependent in meningiomas. MERTK forms a complex with TYRO3 but not with AXL in both

meningioma and schwannoma tissues, and its expression is mandatory to maintain AXL and TYRO3 levels in both cell-types.

MERTK and AXL contribute to increased proliferation and survival of schwannoma and meningioma cells *in vitro*. MERTK acts via JNK, FAK and cyclin-D1 in meningiomas, and via JNK, AKT, FAK and cyclin-D1 in schwannomas. Pathological proliferation and survival of both cell-types was successfully reversed by AXL inhibitor BGB324 and MERTK inhibitor UNC2025 *in vitro*, with UNC2025 being more effective. TYRO3 had no effect on cell proliferation of either schwannoma or meningioma cells.

In conclusion, AXL and MERTK are important in schwannoma and meningioma pathogenesis and are potentially good therapeutic targets. MERTK inhibitor UNC2025 has the potential to be used as a common candidate for the treatment of NF2-related tumours.

Contents

List of Figures

List of Tables

Abbreviations

AAF	Alanyl-alanyl-phenylalanyl-aminoluciferin
AML	Acute myeloid leukemia
AP1	Activator protein1
AP-2α	Activating enhancer binding Protein-2 alpha
ARID1A	AT-rich interactive domain-containing protein 1A
ARID1B	AT-rich interactive domain-containing protein 1B
BM-I	Ben-Men-I
BSA	Bovine serum albumin
BVS	Bilateral vestibular schwannoma
CAL	Café-au-lait
CCR	Coil-coil region
CD44	Cluster of differentiation 44
CHK2	Checkpoint kinase 2
CLH-22/CTCL1	Catherin heavy chain polypeptide gene
CML	Chronic myelogenous leukemia
CN	Cranial Nerve
CNS	Central Nervous System
CRC	Colorectal cancer
CREB	cAMP response element-binding protein
CSF	Cerebrospinal fluid
DDR1	Discoidin domain receptor family, member 1
DMEM	Dulbecco's modified eagle medium
DMSO	Dimethyl sulphoxide
ECL	Enhanced chemical luminescence
ECM	Extra-cellular matrix
EGF	Epidermal growth factor
EGFR	Epidermal growth factor receptor
ELISA	Enzyme-linked immunosorbent assay
ERK	Extracellular signal-regulated kinase
EtOH	Etanol
FAK	Focal adhesion kinase
FBS	Fetal bovine serum
FISH	Fluorescence in-Situ hybridization
FOXM1	Forkhead box protein M1
GAP	GTPase activating protein
Gas6	Growth arrest-specific 6
GBM	Glioblastoma multiforme
GFAP	Glial fibrillary acid protein
Gla	Glutamic acid
HCC	Hepatocellular carcinoma
HDAC	Histone deacetylase
HGG	High grade glioma
HNCC	Head and neck cancer
IBMX	3-isobutyl-1-methylxamthine
IFNγ	Interferon gamma
IGFR1	Insulin-like growth factor receptor-1
IHC	Immunohistochemistry
IRS-1	Insulin receptor substrate 1

JNK	c-Jun N-terinal kinase
Kb	Kilobase pair
KLF4	Kruppel like factor 4
LA	Laminin
LG	Laminin G
LOH	Loss of heterozygosity
LZTRI	Leucine-zipper-like transcriptional regulator 1
MAPK	Mitogen activated protein kinase
MD-MSC	Merlin deficient-mouse Schwann cells
Merlin	Moesin ezrin Rrdixin Llke protein
MLPA	Multiple ligation-dependent probe amplification
MOI	Multiplicity of infection
MPNST	Malignant Peripheral Nerve Sheath Tumour
mTORC	Mammalian target of rapamycin complex
MZF1	Myeloid zinc finger1
NCAM	Neural cell adhesion molecule
NF	Neurofibromatosis
NGS	Next generation sequencing
NIH	National institute of health
NK cells	Natural killer cells
NSCLC	Non-small cell lung cancer
PBS	Phosphate buffered saline
PDGFR	Platelet derived growth factor receptor
Pen/strep	Penicillin/streptomycin
PFA	Paraformaldehyde
PLL	Poly-l-lysine
PNS	Peripheral nervous system
PS	Phosphatidylserine
PVDF	Polyvinylidene fluoride
RIPA	Radioimmunoprecipitation assay buffer
RPE	Retinal pigment epithelium
RT	Radiation therapy
RTK	Receptor tyrosine kinase
SDS	Sodium dodecyl sulphate
SHBG	Sex hormone binding domain
SMARCB1	SWI/SNF-related matrix-associated actin-dependent regulator of chromatin subfamily B member 1
SMO	Signaling member smoothened
TAM	TYRO3, AXL, MERTK
TBST	Tris-buffered saline with 0.1% tween
TERT	Telomerase reverse transcriptase
TKI	Tyrosine kinase inhibitor
TRAF7	TNF receptor-associated factor 7
UVS	Unilateral sestibular schwannoma
VEGF	Vascular endothelial growth factor
VEGFR	Vascular endothelial growth factor receptor
VS	Vestibular schwannoma
WHO	World health organization

Chapter 1.0 - Introduction

1.1 Neurofibromatosis

Neurofibromatosis (NF) is an autosomal dominant genetic condition, primarily described by multiple cutaneous lesions and the tumours of central and peripheral nervous system. The term neurofibromatosis was first described by the German pathologist Friedrich Daniel von Recklinghausen in 1822 (Madigan and Shaw, 1988). In 1982, Riccardi classified the heterogenous disorder into eight categories with designations, clinical features and the pattern of an inheritance (Riccardi, 1982). Later, in 1987 National Institute of Health (NIH) published the basis for a current guideline of NF diagnosis. NIH consensus panel classified NF into two distinguish genetic conditions according to the characteristic features of each and numbered them as Neurofibromatosis type 1 (NF1), previously known as Recklinghausen's disease or peripheral neuroma and Neurofibromatosis type 2 (NF2), referred as central neurofibroma (NIH Consensus Development Conference, 1988)

1.1.1   Neurofibromatosis type 1 (NF1)

NF1 is the most common genetic condition, affecting 1 in 3500 individuals. The gene for NF1 is located on chromosome 17q11.2 and encodes the protein neurofibromin (Boyd et al., 2009). Neurofibromin is GTPase-activating protein (GAP) and is expressed by many cell-types including neurons, glial cells, Schwann cells and melanocytes (Boyd et al., 2009). Neurofibromin maintains cell proliferation and differentiation by negatively regulating mitogenic RAS signaling. Hence, the loss of tumour suppressor neurofibromin leads to pathogenesis of NF1 by RAS stimulated RAF/MEK/ERK and PI3K/AKT/mTOR pathway (Bollag et al., 1996). The most common clinical features associated with the disease includes café-au-lait spots (CAL), neurofibromas, skin freckling, lisch nodules and optic gliomas. Neurofibromas originally arise from Schwann cells and café-au-lait spots from melanocytes. Both cell-types harbor mutation in both *NF1* alleles, including a

germline and an acquired somatic mutation. In addition, patients can also exhibit other symptoms like learning disabilities, malignant peripheral nerve sheath tumours (MPNST) and bone deformities such as curvature of the spine (scoliosis) and congenital pseudarthrosis of the tibia (CPT) (Friedman, 2002). MPNST are highly aggressive malignancies with lifetime incidences in NF1 patients is 8-13% and the five years survival of only ~50% (Watson et al., 2017, Kahn et al., 2014).

1.1.2 Neurofibromatosis type 2 (NF2)

NF2 is characterized by the development of multiple benign (non-cancerous) tumours of nervous system. Bilateral vestibular schwannomas (BVS) of the eigth cranial nerve is a hallmark of the disease (Figure 1.1). Moreover, 50-60% of NF2 patients also develop intracranial meningiomas and 75% of patients develop spinal schwannomas, meningiomas and/or ependymomas. Since the initial guidelines of NF2 diagnosis criteria proposed in 1987, continuous revisions have been made over years as more knowledge about the condition and its genetics become available (NIH Consensus Statement, 1987) (Gutmann et al., 1997) (Baser et al., 2011). The most up-to-date, revised diagnostic criteria were presented in 2018 which involves mandatory molecular testing of individuals with unilateral vestibular schwannomas (UVS) for *NF2* or *Leucine-zipper-like transcriptional regulator 1 (LZTR1)* to rule out schwannomatosis associated schwannomas (more information in chapter-1.1.3) (Table-1.1).

Current and revised Manchester Criteria for diagnosis of NF2	
1	Bilateral vestibular schwannomas (BVS) less than 70 years of age
2	First degree relative (FDR) family history of NF2 AND unilateral vestibular schwannoma (UVS) before age 70 years OR
3	FDR family history of NF2 OR UVS AND any two of meningiomas, cataract, glioma, neurofibroma, schwannoma, cerebral classification OR UVS and negative LZTR1 testing
4	Multiple meningiomas (two or more) AND two of: UVS, cataract, glioma, neurofibroma, schwannoma, cerebral classification, OR
5	Constitutional pathogenetic NF2 gene variant in blood or identical in two tumours

Table 1. 1 - The Manchester Diagnostic criteria for NF2 (Evans et al., 2018).

The estimated prevalence rate of NF2 is 1 in 25,000 individuals. Interestingly, despite not occurring as frequently as NF1, the tumour types associated with NF2 are the most common in neuro-oncology and can cause significant morbidity and mortality in majority of the patients depending on the size and location of the tumour (Gerber et al., 2009). Hearing impairment is a primary symptom of almost all NF2 patients and that attributes to vestibular schwannomas (VS). At the time of onset, hearing loss is mostly unilateral which may be accompanied or preceded by tinnitus. Many NF2 patients also experience dizziness and balance issues as primary symptoms of the disease. Other symptoms present in NF2 patients are due to intracranial meningiomas, spinal tumours and cutaneous schwannomas. Seizures, headaches, impaired vision and cognitive and behavioral problems are common indications associated with meningiomas. Spinal tumours usually cause muscle pain, weakness and paresthesia and many NF2 patients become wheelchair bound by adulthood. Vertigo, blindness, numbness, tingling, nausea and vomiting are less common symptoms in the beginning and usually evident of later stages of the disease (Evans et al., 1992, O'Shaughnessy and Bussieres, 2006).

1.1.3 Schwannomatosis

Schwannomatosis shares significant clinical overlap with NF2 and is characterized by the development of multiple schwannomas but rarely meningiomas ((Merker et al., 2012). The estimated prevalence rate of schwannomatosis is 1/40,000-1/70,000 (Koontz et al., 2013). Once considered as an attenuated form of NF2, schwannomatosis was recognized as genetically and clinically distinct form of NF in late 90's (MacCollin et al., 1996, Jacoby et al., 1997).

Most patients with schwannomatosis develop initial symptoms of the disease in second or third decade of their life, the majority of the cases being sporadic without any family history unlike NF2. Chronic pain is a hallmark of the disease and most often associated with depression and anxiety in many patients (Merker et al., 2012). Moreover, there is an increased concern of malignancy in patients with schwannomatosis compared to NF2, specifically for malignant peripheral nerve sheath tumour (MPNST) (Gonzalvo et al., 2011).

Schwannomas linked to schwannomatosis usually affect spine and peripheral nerves but are not associated with BVS, which is characteristic feature of NF2. Schwannomatosis patients may develop UVS and care should be taken not to misdiagnose it as NF2 (Smith et al., 2012). Moreover, intradermal schwannomas, ependymomas, cataract and retinal abnormalities that are commonly observed in NF2 patients, are absent in schwannomatosis (Smith et al., 2015).

Recent molecular studies identified two novel genes *SWI/SNF-related matrix-associated actin-dependent regulator of chromatin subfamily B member 1 (SMARCB1)* and *LZTR1* on chromosome 22 as responsible for the pathogenesis of schwannomatosis ((Piotrowski et al., 2014)). Moreover, *NF2* somatic mutations affecting both alleles are often present, schwannomas linked to schwannomatosis lack classical *NF2* genetic mutation seen in

NF2 patients. Tumourogenesis is believed to occur via four-hit, where patient carry germline mutation in *SMARCB1* (1 hit), followed by loss of portion of chromosome 22 which harbors second *SMARCB1* allele and one *NF2* allele (hit 2 and 3), subsequently mutation in the raminaing *NF2* allele (hit 4) (Plotkin et al., 2013). The genetic differences in molecular etiology of two conditions provide the basis of molecular testing that distinguish NF2 and schwannomatosis from each other. Patient's blood and tumour samples are now routinely checked for mutations in *SMARCB1, LZRT1* and *NF2* genes to improve diagnosis (Piotrowski et al., 2014, Sestini et al., 2008).

1.2   NF2 related tumours

1.2.1   Schwannomas

Schwannomas are benign and encapsulated tumours of peripheral nerves, composed purely of Schwann cells. They can arise as a part of the hereditary condition NF2, schwannomatosis or sporadically and account for about 20% of adult nervous system tumours. Schwannomas associated with NF2 affect less than 5% of population and more than 90% of patients develop unilateral sporadic schwannomas. The chances of schwannomas undergoing malignant transformation is very rare but may occur following therapeutic irradiation (Mahboubi et al., 2015, Hilton and Hanemann, 2014).

VS of the eigth cranial nerve (CN) are the most common CN schwannoma, with overall lifetime risk of approximately 1 in 1000 (Figure 1.1) (Hanemann, 2008, Laws and Thapar, 1993, Evans et al., 2005). Other CN rarely found affected by schwannoma involves; trigeminal nerve (CN V), the facial nerve (CN VII), glossopharyngeal (CN IX) the vagal (CN X), accessory (CN XI) or hypoglossal nerve (CN XII) (Laws and Thapar, 1993). Schwannomas arising from nerves within spinal canal are also very common and account for 3% of all spinal tumours with the annual incidences of 0.3-0.5/100,00 (Rustagi et al., 2012, Conti et al., 2004). While the most cases of sporadic schwannomas are diagnosed between 50-60 years of age, NF2-related schwannomas affect individuals in their 20s or 30s with no gender bias and often develop at multiple locations within the nervous system (Evans et al., 2005, Mahboubi et al., 2015).
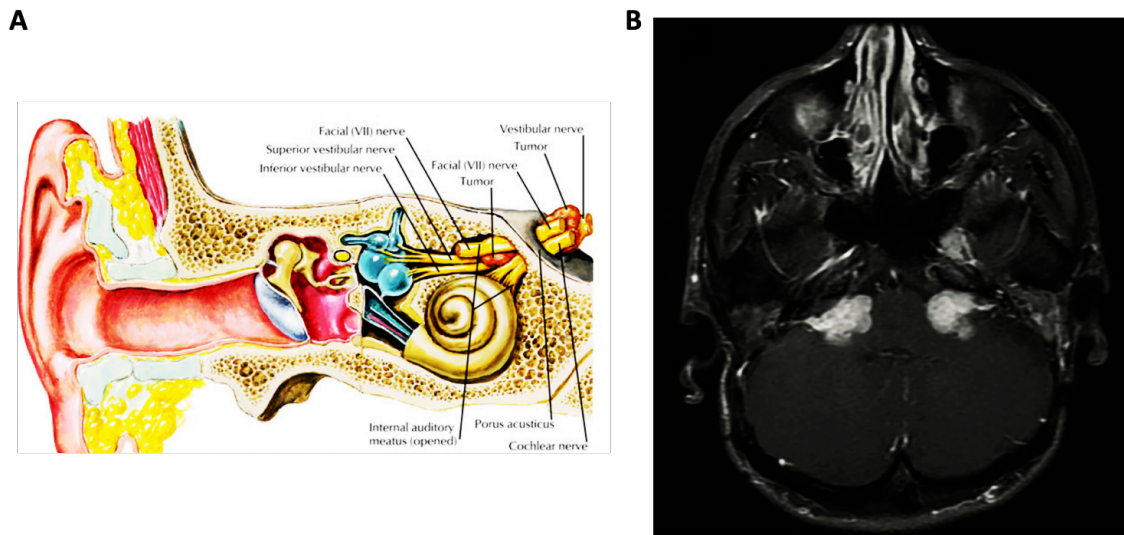
Figure 1. 1: Images of vestibular schwannoma. Illustration showing small vestibular schwannoma arising from superior vestibular nerve in internal auditory meatus and protruding into posterior fossa (Image is taken from (Lam, 2016)) **A)**; MRI image of a 28-year old male with bilateral vestibular schwannomas (BVS) (Image is taken from (L, 2019)) **B)**.

Histologically, schwannomas consist of two distinct cellular growth patterns: Antoni A regions described by highly dense cellular areas and Antoni B regions composed of loosely arranged tumour cells. Sometimes schwannomas show parallel arrays of two rows of palisading nuclei, forming the unique structure called Verocay bodies (Hilton and Hanemann, 2014). Compared to normal healthy Schwann cells which are slim elongated and bipolar in nature; schwannoma cells in culture show increased spreading, multiple membrane extensions and enhanced cell-matrix adhesion (Figure 1.2) (Hanemann, 2008) . The tumour cells demonstrate strong and diffuse staining of S-100, a calcium binding protein and routinely used as a diagnostic marker for schwannomas (Boulagnon-Rombi et al., 2017). Small subsets of schwannomas are positive for glial fibrillary acid protein (GFAP) (Kawahara et al., 1988). Moreover, Sox-10, calretinin and podoplannin are also increasingly use as a positive marker for schwannomas (Choi et al., 2017, Jokinen et al., 2008, Fine et al., 2004). Although mostly homogenous with limited range of cellular components, schwannomas still show few interesting histological diversities. Histological variants other than classical schwannomas reported so far involve; cellular

schwannomas, plexiform schwannomas and melanotic schwannomas (Hilton and Hanemann, 2014).
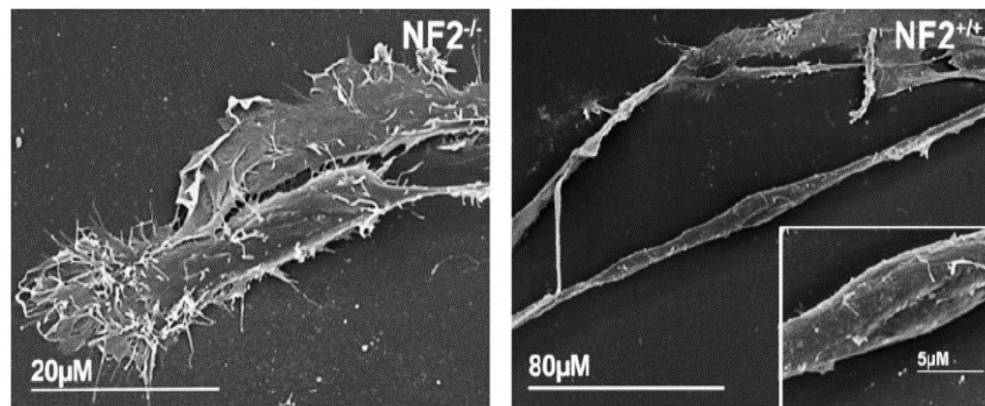
Figure 1. 2: Electron microscopic pictures showing differences in cell shape of Schwann cells and schwannoma cells. Schwannoma cells (NF2-/-) show increased spreading and membrane ruffling (left panel) whereas schwann cells (NF2+/+) show thin, elongated bipolar structure (right panel) (Image is taken from (Hanemann, 2008)).

Early cytogenetic analysis revealed partial or complete loss of chromosome 22 as the main characteristic feature of schwannomas and proposed *NF2* as a candidate gene responsible for the formation of schwannomas (Stenman et al., 1991, Bijlsma et al., 1992). Other rare chromosomal changes observed to date by different investigators; involves loss of chromosome 9p, 1p, 11q, 13q and copy gains on chromosome 9q, 10q, 17q, 19p, 19q (Koutsimpelas et al., 2011, Leone et al., 1998, Warren et al., 2003). However, chromosome 22 is the only consistently reported genetic alteration associated with schwannomas; further clinical relevance of all other chromosomal changes is needed.

The bi-allelic inactivating mutation of *NF2* gene by Knudson's two-hit model, which leads to complete loss of Merlin, is responsible for all NF2 related schwannomas as well as 30-60% of sporadic schwannomas (Lee et al., 2012, Ikeda et al., 2005). The recent genomic sequencing data reveals that at least ~40% of sporadic VS cases are due to a single mutation in *NF2* gene and are associated with a less aggressive phenotype compared to their bi-allelic counterpart. Moreover, bi-allelic mutation or 'two-hit' is more common in younger individuals and may be responsible for the clinical progression of

the tumours (Chen et al., 2017). This newly published data provides biological background to the previously published reports which have shown the correlation between tumour growth speed and younger age (Mohyuddin et al., 2015). In addition to *NF2*, loss of chromatin-modifying genes *AT-rich interactive domain-containing protein 1A* (*ARID1A)* and *AT-rich interactive domain-containing protein 1B (ARID1B)* as well as mutation in *discoidin domain receptor family, member 1 (DDR1)* genes were found to be responsible for around 29% and 11% of sporadic schwannoma cases respectively. The subset of schwannomas harbors the balanced chromosomal translocation on chromosome 10q which results in a fusion of *SH3PXD2A-HTR1A,* with higher predominance in males and leads to increased proliferation and invasion of the tumour (Agnihotri et al., 2016). In addition to genetic factors, hay fever, exposure to high level of sounds, ionizing and non-ionizing radiation are some of the environmental risk factors proposed to be responsible for schwannoma's etiology (Corona et al., 2009).

1.2.2   Meningiomas

Meningiomas are the most common primary brain tumour and arise from the meningeal covering of the brain and spinal cord. The meniges are composed of three protective layers; the dura mater (the outermost layer), the arachnoid mater (the middle layer) and the pia mater (the innermost layer) **(Haines D, 2018)**. Meningiomas are thought to originate from arachnoid cells of the meninges and may occur anywhere arachnoid cells are present (Figure 1.3).
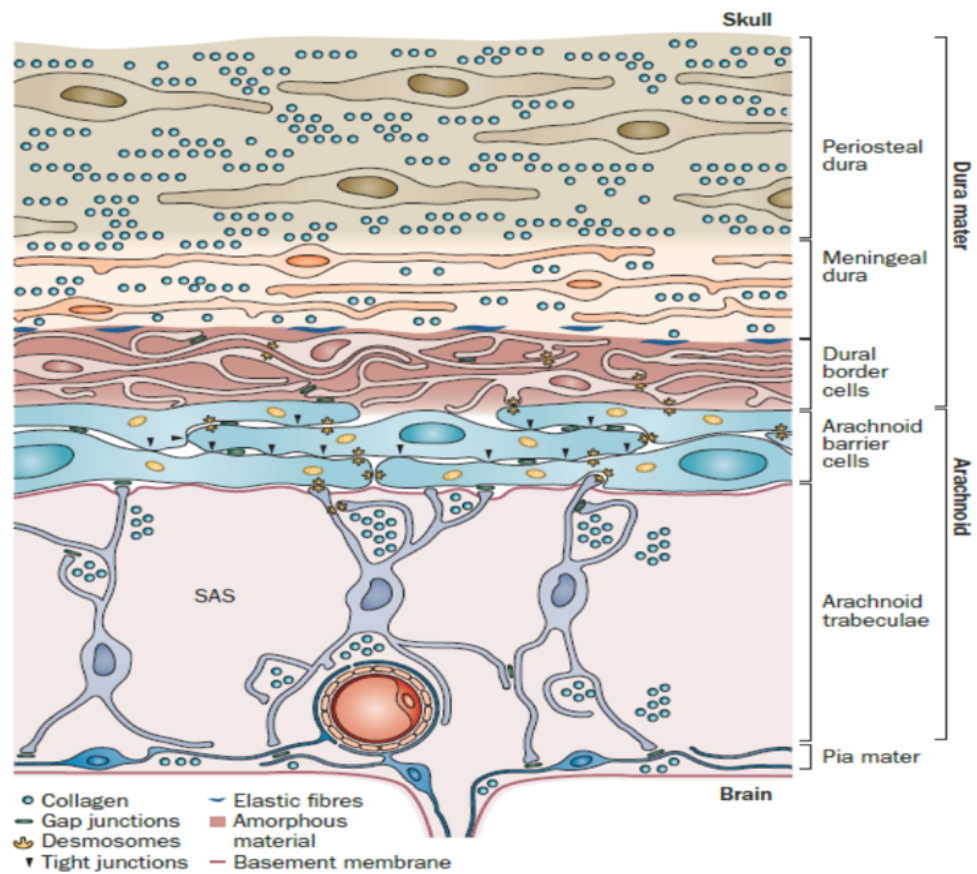
Figure 1. 3: The structure of Meninges. Schematic representation of the meninges showing three layers; the dura mater, arachnoid mater and pia mater. Meningiomas are thought to originate from arachnoid cells (Image is taken from (Kolias et al., 2014)).

Meningiomas account for 20-30% of primary intracranial tumours and high proportion of the meningiomas are found to be located in the region of convexity, parasagittal and sphenoid (Figure 1.4). Spinal location is rare but found to be a primary site in 12% of meningioma patients (Bondy and Ligon, 1996, Buetow et al., 1991) . Meningiomas are mostly sporadic in nature but approximately 50% of meningiomas are associated with the genetic condition- NF2 (Smith et al., 2011). Females have a two-fold higher incidence of meningioma compared to males, except for atypical and anaplastic meningiomas which show higher predominance in males (Liang et al., 2014). The incidence of meningiomas increases with age in both males and females, with peak incidences reported after age 65. The correlation between age and grade of meningiomas is still a controversial topic with some reports suggesting that younger patients are more prone to higher grade

meningiomas. Liang *et al*. however, found no correlation between meningioma tumour grade and age (Wang et al., 2013, Liang et al., 2014)
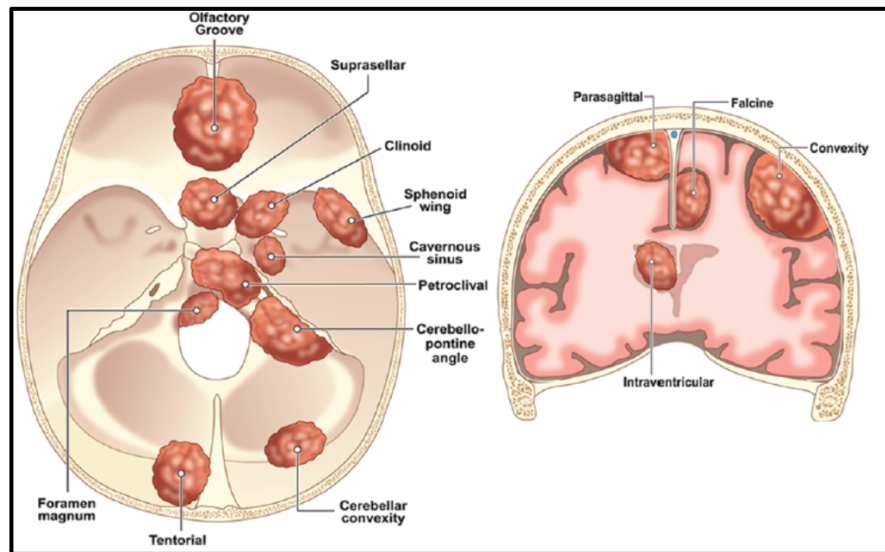
Figure 1. 4: **Illustration of intracranial meningiomas.** Schematic diagram shows the locations of skull base tumours (left) and the locations of parasagittal, falcine, covexity and intraventricular tumours (right) (Image is taken from (Nanda et al., 2017)).

WHO (World Health Organization) classification categorizes meningiomas into 15 different subtypes depending on the histological and biological diversity of the tumours (Table-1.2). The WHO grade I (G-I) comprises nine variants that represents 80% of all meningiomas with meningothelial, fibroblastic and transitional subtypes are being the most common. G-I meningiomas are histologically benign in nature with less than 4 mitoses/10 microscopic high-power field (HPF) (Louis et al., 2007, Louis et al., 2016). The WHO grade-II (G-II) and grade-III (G-III) meningiomas have higher recurrence rates with aggressive tumour biology. WHO G-II or atypical meningiomas account for 15-20% of all cases and are characterized by increased mitotic activity; 4-19 mitoses/10 microscopic HPF or the presence of 3 out 5 of the following features: sheet-like growth, spontaneous necrosis, high nuclear to cytoplasmic ratio, prominent nucleoli and tumour necrosis (Maier et al., 1992). Chordoid and clear-cell meningiomas are the variants of G-II meningiomas (Zorludemir et al., 1995, Couce et al., 2000). Meningiomas with 20 or

more mitoses/10 HPF and resemblance to sarcoma or carcinoma, are considered as G-III or anaplastic meningiomas. G-III meningiomas involve rhabdoid and papillary subtypes with the incidence rate of only 1-2% but are associated with high recurrence rate (~50-80% of cases) and usually cause death within two years of diagnosis (Perry et al., 1999, Pasquier et al., 1986, Kepes et al., 1998).

In accordance with schwannomas, loss of chromosome 22 is the most consistent cytogenetic abnormality in meningiomas with ~50% of the tumours showing chromosome 22 monosomy (Zang, 2001). In addition, loss of chromosome 1p, 14q, 9p21 and abnormality in chromosome 10 and 17q is frequently associated with tumorigenesis and progression to higher grade meningiomas (Alahmadi and Croul, 2011, Cai et al., 2001). Especially, the loss of chromosome 1p is associated with high recurrence rate and is mostly found in meningiomas located at the convexity but not in skull base or spinal meningiomas (Ketter et al., 2008)

	Grade-I	**Grade-II**	**Grade-III**
WHO Histological subtypes	Meningiothelial	Atypical	Anaplastic
	Fibrous	Chordoid	Rhabdoid
	Transitional	Clear-cell	Papillary
	Psammomatous		
	Angiomatous		
	Microcystic		
	Secretory		
	Lymphoplamacyte-rich		
	Metaplastic		
WHO diagnostic criteria	Mitosis <4/10 hpf	Mitosis 4-19/10 hpf	Mitosis ≥20/10 hpf or
		3/5 of following:	
		Necrosis	
		High nuclear/cytoplasmic ratio	
		Prominent nucleoli	
		Architectural sheeting	
		Hypercellularity or	
		Brain invasion	
Gene mutations	TRAF7	SMARCE1	BAP1
	KLF4	NF2	NF2
	AKT1	PPM1D	PPM1D
	POLR2A	AKT1	ARID1A
	PIK3CA		FOXM1
	NF2		
	SMO		
Chromosome alterations	Monosomy 22	Monosomy 22	Monosomy 22
	Gain on chromosome 5	Gain on chromosome	Gain on chromosome
		1q, 9q, 12q, 15q, 17q and 20q	1q, 9q, 12q, 15q, 17q and 20q
		Loss on chromosome	Loss on chromosome
		1p, 6q, chromosome 10, 14q and 18q	1p, 6q, 9p, chromosome 10, 14q and 18q

Table 1. 2 - Table showing histological subtypes, WHO diagnostic criteria, mutations and chromosomal alterations across meningiomas (Adapted from (Bi et al., 2016)).

Mutations in the *NF2* gene is responsible for 40-60% of sporadic meningiomas, in addition to familial meningiomas. The role of the *NF2* gene in meningioma's pathogenesis is still conflicting, with many reports suggesting *NF2* mutation as an early

event in tumorigenesis (Perry et al., 2000, Menon et al., 1997). However, Peyre *et al* argued this, showing in *NF2* knock-out mouse that *NF2* cooperates with *cdkn2ab* and is responsible for progression of G-I meningioma to G- II/III (Peyre et al., 2013). Moreover, *NF2* mutated meningiomas are prone to higher chromosomal instability during malignant progression and are larger in tumour size compared to their *NF2*-wild type counterparts (Goutagny et al., 2010, Yuzawa et al., 2016). In addition to *NF2*, chromosome 22 harbors genes like *SMARCB1*, *checkpoint kinase 2* (*CHEK2*) and *clathrin heavy chain polypeptide gene* (*CLH-22/CTCL1*) which have been shown to be responsible for meningioma pathogenesis (Yang et al., 2012, van den Munckhof et al., 2012). Isolated cases of familial meningiomas have also been observed due to genetic mutation in *SMARCE1* and *SUFU* gene, which causes multiple non-NF2 spinal and cranial meningiomas (Smith et al., 2014, Aavikko et al., 2012).

The recent data from the next generation DNA sequencing has identified new somatic recurrent mutation responsible for benign meningiomas. These non-*NF2* mutations are specific to G-I meningiomas and involve pro-apoptotic E3 ubiquitin ligase *TNF receptor-associated factor 7 (TRAF7),* the proto-oncogene *v-Akt murine thymoma viral oncogene homolog 1 (AKT1),* the pluripotency transcription factor *kruppel like factor 4 (KLF4),* the Hedgehog pathway *signaling member smoothened (SMO).* In conclusion, non-*NF2* recurrent somatic mutations represent ~40% of sporadic meningioma cases and are enriched in the skull base tumours in contrast to *NF2* tumours which are most commonly found in calvarium (Brastianos et al., 2013, Clark et al., 2013, Abedalthagafi et al., 2016, Yuzawa et al., 2016). A recurrent mutation in *KLF4^{K409Q}* on chromosome 9q31 which results in a lysine to glutamine substitution at codon 409 has shown to be responsible for ~15% of G-I meningiomas. *KLF4^{K409Q}* is the second highest mutation after *TRAF7* located on 16p13*,* which causes ~25% of benign meningiomas. The remaining *AKT1* and *SMO*

mutations occur almost at similar frequencies and harbor ~5-8% of benign meningiomas (Clark et al., 2013, Abedalthagafi et al., 2016). *TRAF7* mutations in most cases co-occur with mutations in *KLF4* and *AKT1* but independent of *NF2* and *SMO*. Moreover, *KLF4* and *AKT1* mutation occurs mutually exclusive of each other and mutations in all three genes (*KLF4, AKT1 and TRAF7*) are exclusive of *SMO, NF2* or chromosome 22 loss (Figure-1.5) (Clark et al., 2013).
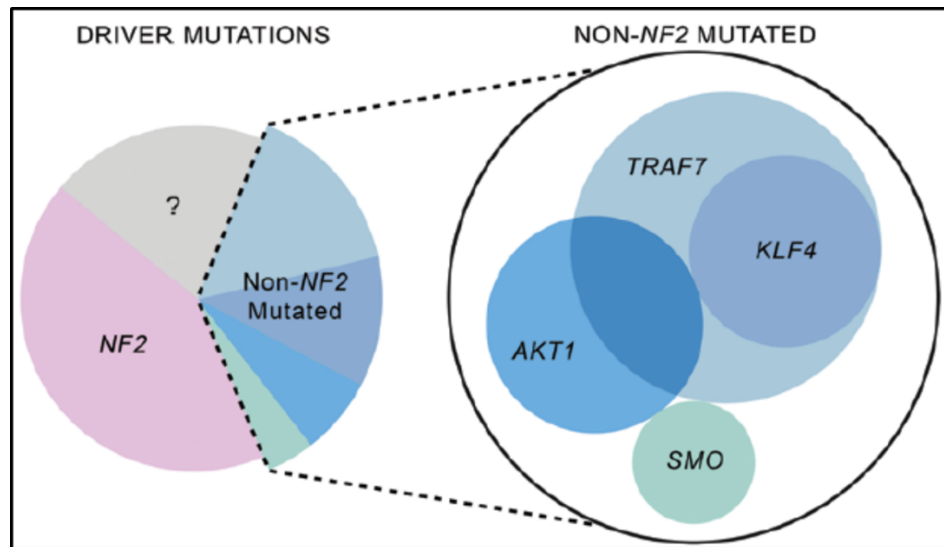
Figure 1. 5- Graph showing distribution of NF2 and non-NF2 mutations in G-I meningiomas. Mutation in TRAF7, KLF4, AKT1 and SMO occurs in mutually exclusive pattern of NF2. The proportion of overlap of AKT1 and KLF4 with TRAF7 has represented in Venn diagram (Image is taken from (Bi et al., 2016)).

Mutations in certain genes have associated with higher grades of meningiomas. The mutation in *telomerase reverse transcriptase* (*TERT)* promoter that leads to higher expression of TERT protein is indicative of progression to higher grade meningiomas (Goutagny et al., 2014, Stogbauer et al., 2019, Collord et al., 2018). Transformation of atypical (G-II) meningiomas to the rhabdoid subtype, the most aggressive form of G-III meningiomas, is associated with lack of ARID1A protein due to frameshift deletion of *ARID1A* (Bujko et al., 2017)*.* Higher expression of *PPM1D* in G-II and G-III meningiomas is the predictive marker for progression (Fukami et al., 2016). Recently, Vasudevan *et al*. linked the higher expression of *forkhead box protein M1* (*FOXM1)*,

which is negatively regulated by *NF2*, with poor clinical outcomes and aggressive forms of meningiomas (Vasudevan et al., 2018).

The genetic alteration profile of meningiomas correlates to specific grade and histologic subtypes. *NF2* mutation is a common occurrence in fibroblastic and transitional subtypes of G-I meningiomas while *AKT1*E17K is associated with meningothelial subtypes but rarely seen in G-II and G-III meningiomas (Wellenreuther et al., 1997, Sahm et al., 2013). Almost all cases of secretory meningiomas appeared to have mutation in *TRAF7* and *KLF4* [K409Q]. *SMARCE1* is the signature mutation associated with cranial and spinal clear cell meningiomas (Smith et al., 2013, Smith et al., 2014). Multiple chromosomal polysomies on chromosome 5 are linked to angiomatous subtype of G-I meningiomas and unbalanced translocation between chromosome 1 and 3 is the marker for G-II chordoid meningiomas (Abedalthagafi et al., 2014, Steilen-Gimbel et al., 1999).

Despite recent advances in the understanding of molecular markers for meningiomas, the current diagnosis of meningiomas grade is based solely on tumour histology. Although of high prognostic value, the current histology based WHO classification system for meningiomas many times results in interobserver and sampling bias in accurately determining the meningioma grade and to predict the associated risk of tumour recurrence for individual patients (Rogers et al., 2016). To solve this key problem, Sahm *et al*. recently classified meningiomas into six sub-groups based on DNA- methylation profiling by combine knowledge of histology and molecular markers. The methylation classes MC ben-1, MC ben-2, MC ben-3 and MC int-A are mostly composed of G-I tumours. MC ben G-I tumours have ~50-60% higher chances of progression free survival compared to MC int G-I tumours at 72 months. The grade-II tumours fall into MC int-A and MC int-B categories with a small subset belongs to MC ben. The progression free survival rate of G-II MC int-A and MC int-B at 72 months is ~28% and ~23%

respectively, whereas MC ben G-II tumours have 70% higher chances of being progression free at 72 months compared to MC int G-IIs. The probability of progression free survival for G-III tumours is only 15-18% at 24 months, these tumours belong to MC mal class of methylation (Sahm et al., 2017). This new innovative and precise DNA-based classification system may be a key turning point for the diagnosis and treatment decision-making of meningiomas.

In addition to genetic factors, ionizing radiation is the most consistently reported environmental factor known to increase the risk of meningiomas. Occupational exposure to certain metals like lead and iron increase the chances of meningiomas, especially in women (Sadetzki et al., 2016, Wesseling et al., 2002). Certain health conditionals like epilepsy, diabetes and hypertension have been linked to meningioma risk (Schwartzbaum et al., 2005, Schneider et al., 2005). Other common risk factors involve endogenous and exogenous hormone use, cell-phone use, cigarette smoking and allergies (Custer et al., 2006, Schneider et al., 2005, Phillips et al., 2005).

1.2.3   Ependymomas

Ependymoma is a type of glioma, arising from the ependymal cells at different locations throughout the brain and spinal cord. It is the least frequent out of three tumours linked to NF2 condition and accounts for ~5% of all intracranial tumours. Approximately 29-38% of ependymomas show mutation in *NF2* or loss of heterozygosity (LOH) on chromosome arm 22q. *NF2* mutation and Merlin loss is more common in spinal ependymomas than cranial (Hanemann, 2008). Ependymomas has not been studied in this project and will not be dicussed further, however, due to a common aetiology of subset of ependymomas with schwannomas and meningiomas, the findings presented in this study may also be relevant for *NF2*-mutated ependymomas.

1.3 Challenges in the management of NF2-related tumours

The classical mainstay management options for schwannomas and meningiomas are surgery, radiosurgery/radiotherapy as well as 'wait and scan' strategy. Although drastic improvements in the diagnostic and surgical techniques have been made in last few decades, post-operative neurological complications based on tumour location are not rare. The preservation of hearing and facial nerve functions is the most common challenge while performing complete resection of tumours as well as with radiation treatment. The patients who undergo sub-total resection of tumour to preserve the nerve function or other complications face high recurrence rates compared to patients with total resected tumours. Furthermore, total resected tumours are not guaranteed to be recurrence free and up to 60% of tumours come back after ~15 years. Post-operative cerebrospinal fluid (CSF) leaks may further complicate the patient's condition and increases the chances of meningitis. In most cases, patients require re-operation and repair (Apra et al., 2018, Halliday et al., 2018)

Surgery and radiosurgery/radiotherapy (RT) is an unattractive option for VS and meningiomas especially in NF2. NF2-related VS are multifocal and tend to grow faster compared to sporadic VS. The preservation of cochlear nerve is very difficult in NF2-related VS and almost all NF2 patients become completely deaf (Evans, 2009). NF2-related meningiomas located at the skull-base, cavernous sinuses and orbits are challenging to operate on and the success rate of RT is also limited (Blakeley and Plotkin, 2016). Moreover, there are reports showing concern of increased chances of malignancy following RT in NF2 patients compared to patients with sporadic tumours (Evans et al., 2006). Many patients with NF2 die or become wheel-chair bound by their early 20s or 30s, adversely affecting the quality of life (Evans, 2009). This demands for new non-invasive and effective drug-based treatments for NF2-related tumours.

As mutations in the *NF2* gene is a common event of all NF2-related tumours, a better understanding of how *NF2* mutation primes the upregulation of oncogenic signaling pathways and tumour development, will help us to define the best therapeutic target and treatment.

1.4   NF2 gene and Merlin

NF2 was discovered in 1993, by two different groups individually, as an inactivated tumour suppressor gene, in the familial inherited disorder, Neurofibromatosis Type 2 (NF2) (Rouleau et al., 1993, Trofatter et al., 1993). The ~95 kilobase pair (kb) *NF2* gene consists of 17 exons and undergoes alternate splicing to generate multiple isoforms. Isoform I, which lacks exon 16 and isoform II that contains all 17 exons, are the most predominant isoforms of the gene. The diversity in NF2 isoforms are thought to be due to the presence of multiple polyadenylation sites (Chang et al., 2002)

The wide variety of mutations in *NF2* gene has been discovered which defines the severity of the disease. Protein truncating mutations such as frameshift insertion/deletion and nonsense mutations, which cause a severe phenotype with decreased survival rates amongst, NF2 patients, are the most common. Patients with constitutional missense mutations, large deletions and somatic mosaicism experience a comparatively milder phenotype. The germline *NF2* splice-site mutation causes greater variability in the disease severity depending on the exons affected. Mutations in exons 13-15 cause a milder phenotype compared to mutations in exons 1-5 (Evans, 2009). In addition to mutational inactivation, loss of heterozygosity (LOH) and transcriptional inactivation are also major cause of NF2-related tumours. 60% of VS and 26% of sporadic meningiomas found to have methylation in *NF2* promoter which correlate to decreased promoter activity and mRNA expression (Kino et al., 2001, Lomas et al., 2005).

NF2 gene encodes the tumour suppressor protein Merlin (<u>m</u>oesin <u>e</u>zrin <u>r</u>adixin <u>li</u>ke <u>p</u>rotein). Merlin belongs to the protein 4.1 superfamily of cytoskeleton-associated proteins and has a high structural similarity to the other members of the family; Ezrin, Radixin, Moesin (ERM) proteins. Merlin is composed of three functional domains; an amino terminal (N-terminal) FERM domain which corresponds to exons 1-9, α helical

coil-coil domain corresponds to exons 10-13 and a carboxy terminal (C-terminal) domain corresponding to exons 14-17 of *NF2* gene, mirroring the structure of ERM proteins (Figure-1.6). Unique from other ERM proteins however, Merlin interacts with the actin cytoskeleton through an actin-binding motif at the N-terminus instead of the C-terminus portion of the protein (Zhou and Hanemann, 2012).
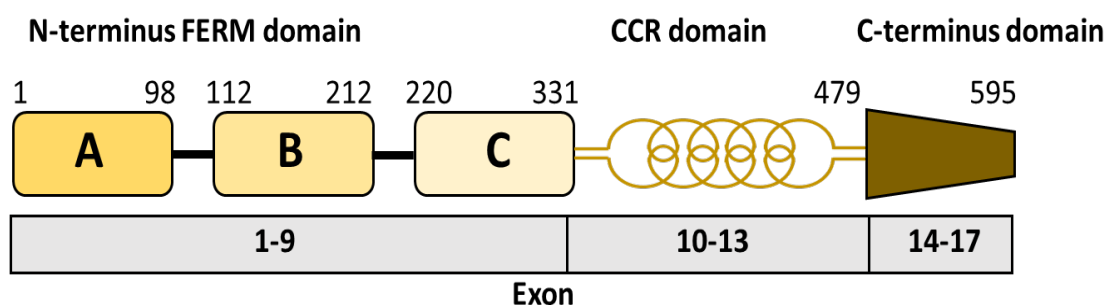
Figure 1. 6- The structure of protein Merlin. A schematic representation of the structure of protein Merlin shows the FERM domain in N-terminus followed by α-helical coil-coil region (CCR) and C-terminus domain (adapted from (Sun et al., 2002)).

Merlin is ubiquitously expressed in all tissues during embryonic development. Homozygous deletion of *NF2* in mice lead to embryonic failure (McClatchey et al., 1997), underlining the importance of Merlin in normal embryonic development. Expression of Merlin is restricted to certain tissues in adulthood including testis, ovaries, adrenal glands, lens, retina and neuronal tissues. In neuronal tissues, Merlin is expressed by both glial cells and neurons of CNS and PNS (Hanemann, 2008).

In Schwann cells, the role of Merlin is not just restricted to a tumour suppressive function but is critical for organization of Schwann cell contacts. Here Merlin promotes the alignment of Schwann cells to axons thus, influencing myelin segment length. At a sub-cellular level, Merlin is enriched in actin-rich cellular compartments like membrane ruffles and lamellipodia as well as cell-cell and cell-matrix contact sites in association with focal adhesion proteins (Hanemann, 2008, Schulz et al., 2014).

1.4.1 Merlin as a tumour suppressor

Merlin works at multiple levels to regulate cellular proliferation. It acts as a tumour suppressor protein at the cell membrane by regulating the expression and activation of integrins and receptor tyrosine kinases (RTKs) and in the nucleus by suppressing the E3 ubiquitin ligase CRL4^{DCAF1} (Figure-1.7) (Hanemann, 2008).

1.4.1.1 Merlin's role in contact dependent inhibition

Merlin plays an important role in contact-dependent inhibition, the process by which normal cells undergo senescence and stop proliferating upon contact with neighbouring cells. Healthy cells recruit Merlin at cell-cell contacts where Merlin facilitates cadherin mediated cell-cell adhesion and inhibits the cell-growth (Lallemand et al., 2003). When Merlin is depleted, cadherin junctions are destabilized, Rac1 is recruited to the plasma membrane and there is an enhanced activity of RTK and Rac/PAK signaling, leading to tumour proliferation (Curto et al., 2007, Okada et al., 2005). In addition, Merlin can also associate with cluster of differentiation 44 (CD44) - hyaluronic acid receptor and paxillin to mediate contact-dependent cell inhibition of growth (Morrison et al., 2001, Fernandez-Valle et al., 2002).

1.4.1.2 Merlin's role in regulation of RTKs and integrins

RTKs are cell-surface receptors that mediate signaling pathways leading to cell-proliferation, survival, differentiation and cell-migration. Over-expression and activation of RTKs is the most common event in the development of malignant as well as benign tumours, including Merlin-deficient tumours (Paul and Mukhopadhyay, 2004, Hanemann, 2008)

A study in *Drosophila* shows that Merlin controls the availability of RTKs at the plasma membrane by regulating endocytosis. Defective endocytosis and degradation of RTKs due to loss of Merlin and the related tumour suppressor Expanded in Drosophila, leads to

upregulation of several RTKs including epidermal growth factor receptor (EGFR) (Maitra et al., 2006). Further direct evidence comes from a study in mouse primary Schwann cells, where Merlin restricts the delivery of several RTKs to plasma membrane. Loss of Merlin leads to accumulation of ErbB2, ErbB3, insulin-like growth factor receptor-1 (IGFR1) and platelet derived growth factor receptor 1 (PDGFR-1) at the plasma membrane in both NF-2 mutant mice and human NF2-deficient schwannomas (Lallemand et al., 2009)(Ammoun et al., 2008). Both of these studies point to a complex level of regulation of RTKs by Merlin at the plasma membrane but helps to explain the link between loss of Merlin and overexpression/hyper activation of mitogenic signaling pathways such as Ras/Raf/MEK/ERK, PI3K/AKT, FAK/Src and Rac/PAK/JNK pathways downstream of RTKs in Merlin deficient tumours (Zhou and Hanemann, 2012, Ammoun and Hanemann, 2011).

Integrins are heterodimeric cell surface adhesion receptors. Integrin mediate adhesion to the extra-cellular matrix (ECM) is a crucial regulator of cell-proliferation, migration and survival (Schwartz and Assoian, 2001) Merlin is known to regulate the expression of integrins α6, β1 and β4 (Hanemann et al., 2006). High expression and activation of integrins in the absence of Merlin leads to a cascade of Rac/PAK/JNK, FAK/Src as well as mTORC1/Cyclin-D1 signaling. All of these pathways are known to enhance integrin-mediated pathological adhesion, proliferation and survival (Xiao et al., 2002, Ammoun et al., 2012, Lopez-Lago et al., 2009).

Co-operation between integrins and growth factor receptors is often essential to regulate cell proliferation and survival. In Merlin-deficient tumours, RTK mediated signaling and integrin mediated signaling every so often synergize. For example, in schwannoma cells activation of AXL receptor kinase and integrins, independently by their respective ligands, leads to phosphorylation of FAK molecule and increase in cell-proliferation,

adhesion and survival of schwannomas (Ammoun et al., 2012, Ammoun et al., 2014). In addition, to regulate the mitogenic signaling directly at plasma membrane, active Merlin can also enter the nucleus and indirectly regulate the activity of RTKs at the membrane by inhibiting promitogenic E3 ubiquitin ligase CRL4/DCAF1 in nucleus (Figure-1.3) (Li et al., 2010).

As is clear from the above reports, RTKs are directly or indirectly involved in promoting key signaling pathways which leads to cell-proliferation, differentiation, migration and survival of Merlin-deficient tumours. Hence, targeting RTKs appears to be a good therapeutic strategy for these tumours.
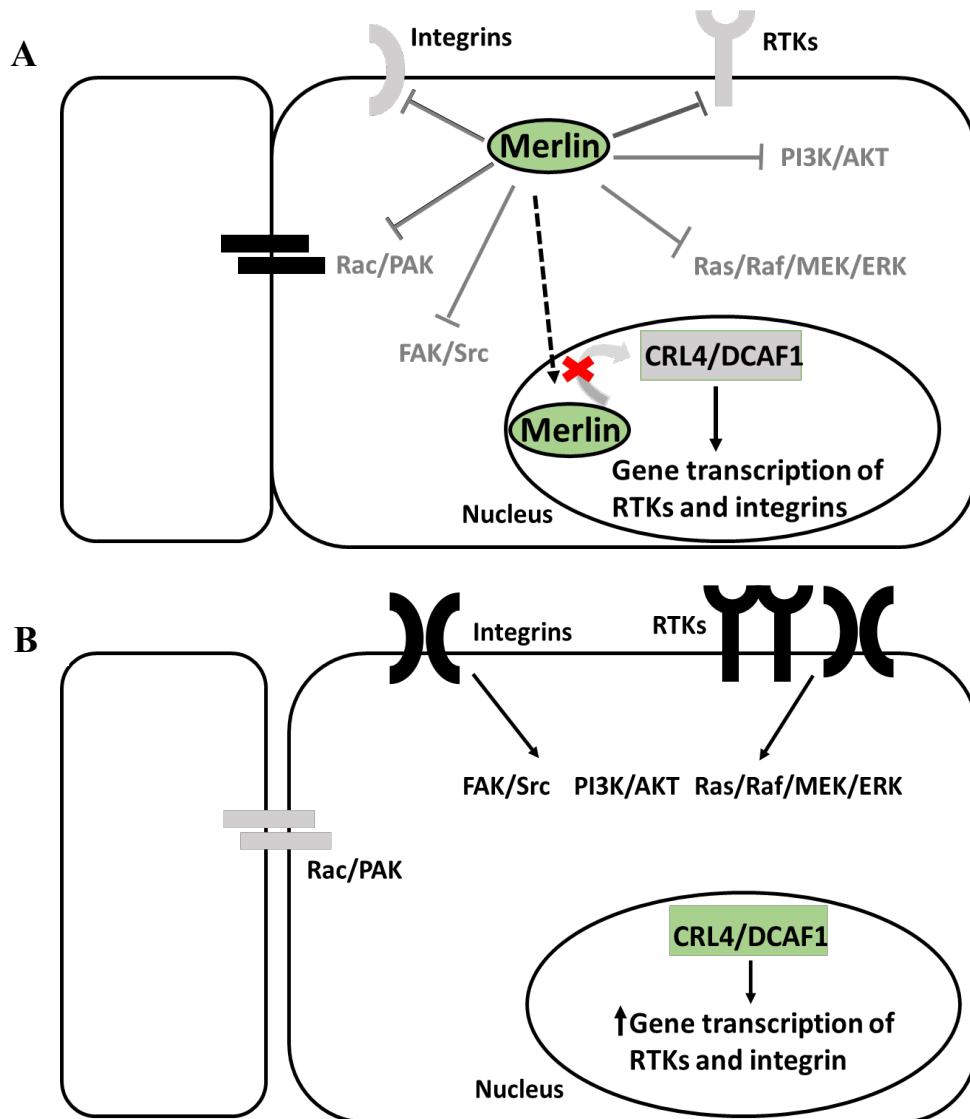
Figure 1. 7- A schematic diagram of Merlin's role as tumor suppressor at the membrane and in nucleus; functional Merlin A) and loss of Merlin B). At the membrane Merlin inhibits RTK and integrin mediated Ras/Raf/MER/ERK, PI3K/AKT, FAK/Src and Rac/PAK/JNK signaling. In nucleus, it inhibits the E3 ubiquitin ligase CRL4/DCAF1 complex. CRL4/DCAF1 can also regulate the expression of RTK and integrins and therefore is link to membrane signaling **A)**; Loss of Merlin leads to upregulation of CRL4/DCAF1 in nucleus and membrane signaling of RTKs and integrins and enhances cell-proliferation, adhesion, survival and migration of cells **B)** (adapted from (Hanemann, 2008, Zhou and Hanemann, 2012)).

1.5   Molecular targeted therapy for NF2 tumours

Due to advances in the understanding of the molecular pathways responsible for the development of NF2-related tumours, many new potential therapeutic targets have recently emerged. It is now possible to reprofile many drug candidates which are already approved in the clinical setting for other conditions including but not exclusively, cancer, as well as to develop new therapeutic agents to benefit NF2 patients. Below I have summarised the candidates which are approved for or are currently in clinical trial for NF2-related tumours.

Bevacizumab is a monoclonal antibody against vascular endothelial growth factor (VEGF). VEGF and its receptor vascular endothelial growth factor receptor-1 (VEGFR-1) are highly expressed in schwannomas and their expression corelate with increased tumour growth. The efficacy of bevacizumab was tested in small group of NF2 patients with progressive VS. Results showed that more than 50% of patients achieved radiographic response, defined as >20% decrease in tumour volume and audiological response, defined as significant increase in word-recognition score. 54% of patients had stable or decreased tumour size and 61% had stable or improved hearing after three years of treatment (Plotkin et al., 2012). Bevacizumab response in meningioma is poor but conversely, ependymomas responded impressively to the drug (Goutagny et al., 2011, Farschtschi et al., 2016). Long-term use of bevacizumab was associated with manageable toxicity including hypertension and proteinuria. However, one team reported the death of a patient due to cerebral hemorrhage, possibly linked to bevacizumab treatment. Despite good therapeutic response, close follow-up of NF2 patients treated with the drug is required to avoid long term drug related toxicity or further complications (Slusarz et al., 2014, Alanin et al., 2015). VEGFR inhibitor- axitinib which demonstrated inhibition of tumour growth in a breast cancer xenograft model (Wilmes et al., 2007) and showed

partial responses in renal cell carcinoma patients (Karam et al., 2014) is now underway in a phase-II clinical trial for NF2 patients to determine the effect of the drug on NF2 related tumours (NCT02129647).

Since EGFR pathways are involved in the pathogenesis of all NF2-related tumours-schwannomas, meningiomas and ependymomas, various EGFR kinase inhibitors have been investigated in pre-clinical and clinical studies. Erlotinib, an oral EGFR kinase inhibitor was administrated to 11 NF2 patients with progressive VS, who were poor candidates for standard therapy. Neither significant decrease in tumour volume nor improvement in hearing were observed. In fact, two patients developed progressive hearing loss whilst taking part in the trial (Plotkin et al., 2010). Results of erlotinib (NABTC 01-03) as well as another EGFR kinase inhibitor- gefitinib (NABTC 00-01) were discouraging also for meningiomas. Erlotinib is no longer in use for the treatment of NF2 patients. Icotinib another EGFR kinase inhibitor which has been shown to have modest therapeutic effect in non-small-cell lung cancer patients (Yang et al., 2017), is now in phase-II clinical trial for NF2 patients (NCT02934256). There are no published reports of EGFR inhibitors that have been or are being tested for ependymomas.

Following promising results of pre-clinical study using human schwannoma primary cell model (Ammoun et al., 2010), lapatinib- a dual EGFR/ErbB2 kinase inhibitor was tested in phase-II clinical trial for NF2 patients with progressive VS (NCT00973739) and meningiomas (NCT00973739). 17 out of 21 VS patients experienced ≥15% decrease in tumour volume and nearly one third of evaluated patients had hearing improvement. However, ≥20% reduction in tumour volume is required to be considered as a significant response and hence, the trial results were categorized as a minor response (Karajannis et al., 2012). Karajannis *et al* suggested that combination therapy of lapatinib together with bevacizumab which has shown a good response in phase-II metastatic breast cancer trial

(Rugo et al., 2012), would be more efficient in NF2 patients. Progressive meningioma patients treated with lapatinib showed significant tumour shrinkage with best volumetric response of 26.1%. The drug was well tolerated among patients with minimum toxicity (Osorio et al., 2018).

Mammalian target of rapamycin complex- 1 (mTORC1) is negatively regulated by Merlin. Activation of mTORC1 in the absence of Merlin is responsible for the growth of schwannomas and meningiomas *in vitro* and *in vivo* which can be reversed by mTORC1inhibitors- rapamycin and everolimus (James et al., 2009, Pachow et al., 2013, Giovannini et al., 2014). Based on pre-clinical data and safety profile of everolimus in other diseases, three phase-II clinical trials were conducted. In the first study, everolimus was administrated orally to 9 NF2 patients with progressive VS for 12 months. None of the 9 patients experienced volumetric or hearing response and the study concluded that everolimus did not have clinical anti-tumour activity against progressive VS in NF2 patients (Karajannis et al., 2014). The second study showed that although unable to induce tumour shrinkage, everolimus maintained stable disease condition in 5 out of 9 patients with manageable mild toxicity. However, tumour resumed in this group of patients within 3-6 months of treatment discontinuation (Goutagny et al., 2015). Third, phase-II study for everolimus (NCT01345136) is ongoing.

AZD2014 is an mTORC1/mTORC2 dual kinase inhibitor. In the laboratory, AZD2014 has proved its anti-tumour effect by blocking cellular pathways responsible for the growth and survival of meningiomas (Beauchamp et al., 2015). Although not approved by food and drug administration (FDA) yet, the first in human-pharmacokinetic and pharmacodynamic study of AZD2014 for multiple cancers have allowed investigators to determine the dose to achieve anti-tumour effect with minimum side effects (Basu et al., 2015). Two phase-II clinical studies of AZD2014 are underway for NF2 patients with

progressive or symptomatic meningiomas (NCT02831257) and for patients with recurrent G-II and III meningiomas (NCT03071874). The main objective of both studies being to learn if AZD2014 can shrink or slow the tumour growth.

Sorafenib (PDGFR/cRaf kinase inhibitor) and nilotinib (PDGFR kinase inhibitor) have been tested in human schwannomas *in vitro* by Ammoun *et al* in two separate studies. Both kinase inhibitors were able to decrease PDGFR-mediated ERK1/2 activity and proliferation of human schwannoma primary cells. Sorafenib was slightly more effective than the nilotinib *in vitro* which could be due to its inhibitory effect not only on PDGFR but also on the downstream Raf/MEK1/2/ERK1/2 pathway, which is activated in schwannomas not only by PDGF-DD but also by other growth factors released by schwannoma cells (Ammoun et al., 2008, Ammoun et al., 2011). Based on *in vitro* data, sorafenib has being assessed in phase 0 clinical trial (ISRCTN49989464) but was subsequently found to be insignificant (Ammoun et al., 2019). Due to the crucial role of Raf/MEK1/2/ERK1/2 pathway in schwannoma development, a combination of nilotinib and the MEK kinase inhibitor-selumitinib has also been tested in human schwannoma primary cells. Indeed, combination therapy of these two drugs resulted in a significant increase in the effectiveness of nilotinib towards decreasing schwannoma growth, suggesting nilotinib and selumitinib combination therapy could be beneficial for NF2 patients (Ammoun et al., 2011). In 2017, a phase-II trial for selumitinib (NCT03095248) started recruiting patients with NF2-related tumours to determine if selumitinib is capable of inhibiting tumour growth, improve hearing and physical and emotional health in this group of patients. The trial is still ongoing with the results are scheduled to be released in 2021.

AR-42, a novel histone deacetylase (HDAC) inhibitor has gained attention for a treatment of schwannomas and meningiomas recently. Bush and colleagues showed that AR-42

inhibited cell-growth, induced apoptosis, decreased phosphorylation of AKT in Merlin-deficient mouse and human schwannoma and meningioma primary cells as well as meningioma cell-line Ben-Men-I *in vitro* and schwannoma xenograft model *in vivo* (Bush et al., 2011). Subsequently AR-42 (NCT02282917) phase-0 clinical trial began for treatment of vestibular schwannomas and meningiomas in September 2015, the results of which are yet to be published.

Recently, the effect of cabozantinib (XL184, Cabometyx™, Exelixis) and saracatinib (AZD0530, AstraZenca) was tested in Merlin-deficient primary mouse Schwann cells *in vitro* and *in vivo*. Cabozantinib is a c-Met inhibitor, FDA approved for the treatment of medullary thyroid cancer (Bentzien et al., 2013) and renal cell carcinoma (Singh et al., 2017). It has previously shown great potential in inhibiting the growth of NF1-associated MPNST *in vitro* and *in vivo* (Torres et al., 2011, Lock et al., 2016). Saracatinib is a dual kinase inhibitor of c-Src and Abl which has shown excellent pre-clinical activity in bladder cancer (Green et al., 2009). Moreover, it enhanced the sensitivity to the c-Met inhibitor (PHA-665752) in gastric cancer (Bertotti et al., 2010). When Merlin-deficient mouse Schwann cells (MD-MSC) are treated with cabozantinib and saracatinib as single agents, the cells demonstrated cell-cycle arrest at G1 phase. However, when treated in combination, cabozantinib and saracatinib induced caspase-dependent apoptosis and more than ~80% inhibition in the cell growth compared to vehicle in MD-MSC orthotopic allograft mouse model. c-Met and Src dual inhibition could be a good potential therapy for the treatment of NF2-related schwannomas (Fuse et al., 2017).

Although there have been advances in clinical therapeutics in recent years, there are not yet any FDA approved drug treatments for NF2 patients. Most of the drugs tested in clinical trials, have shown limited efficacy only in a small group of patients. Moreover, drug resistance due to activation of alternate signaling pathways is a major limitation in

cancer therapeutics (McCubrey et al., 2015). Therefore, comprehensive dissection of all signaling pathways involved in the pathogenesis of all NF2-related tumours is required for designing the most effective therapy that is simultaneously effective against all NF2-related tumours- schwannomas, meningiomas and ependymomas.
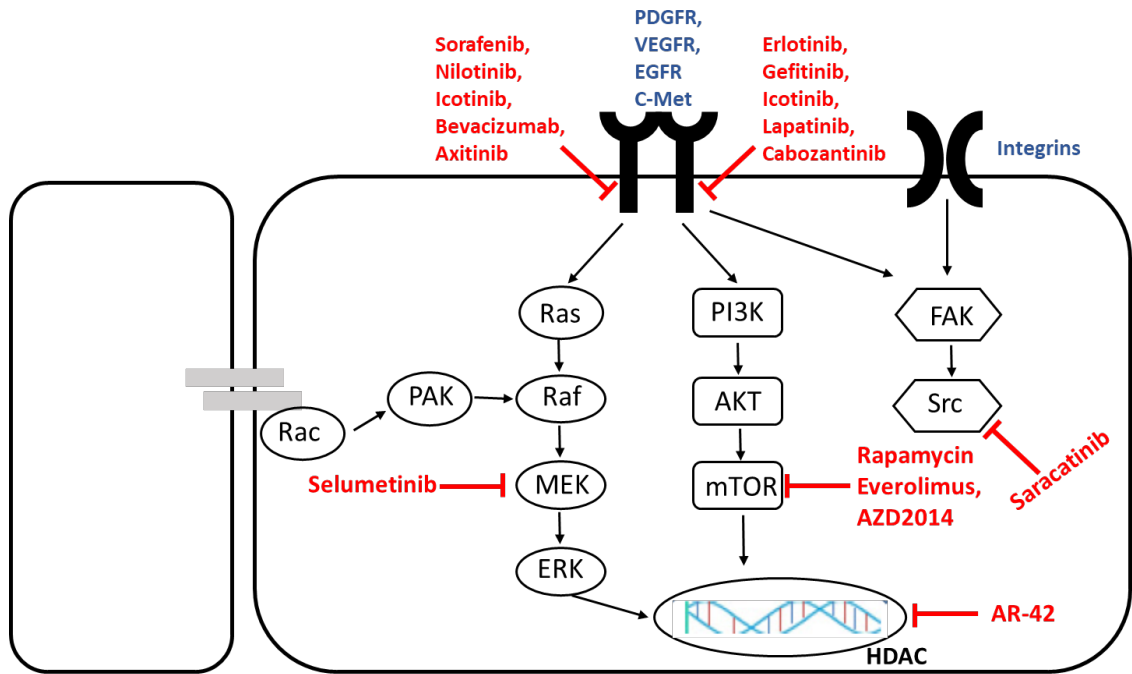
Figure 1. 8- A known drug targets in Merlin-deficient tumours. Figure shows the aberrant activation of multiple growth factor receptors and downstream signaling pathways in Merlin-deficient tumour and kinase inhibitors with known effect in Merlin-deficient tumours (adapted from (Agarwal et al., 2014)).

1.6   TAM family receptor tyrosine kinases

The TAM family of receptors are a recently identified family of receptor tyrosine kinases (RTK) that consist of three members; AXL, TYRO3 and MERTK. Interestingly, all members of TAM family were discovered in early 1990s in span of only three years. AXL was discovered in 1991 by three individual research groups. One group discovered the gene from chronic myelogenous leukemia (CML) and named *AXL-anexelekto*, meaning 'uncontrolled' in Greek (O'Bryan et al., 1991). The second group identified the same gene from patients with myeloproliferative disorder and termed it UFO for its unknown function whilest the third group called it *ark*-adhesion related kinase (Janssen et al., 1991, Rescigno et al., 1991). In the same year, second member of the family-*TYRO3* was discovered from rat cells in an effort search for novel genes that regulate neural development (Lai and Lemke, 1991). Later in 1993, another group cloned human *TYRO3* gene from human tetocarcinoma cells, bone marrow and melanocyte cDNA libraries (Polvi et al., 1993). In 1994, Graham *et al* cloned human ortholog of avian MERTK and named for its presence in monocytes, epithelial and reproductive tissues (Graham et al., 1994).

1.6.1   Structure and expression pattern of TAM receptors

Like other RTKs, TAM family receptors are composed of an extracellular domain, a transmembrane and an intracellular tyrosine kinase domain (Figure-1.9). An extracellular domain structure of the TAM family members consists of two immunoglobulin (Ig)-like domains through which it binds to ligand and two fibronectin type-III (FN-III) domains that regulate ligand binding. The transmembrane domain consists of an α-helix chain, responsible for promoting the stabilization of the dimeric receptor chain. Finally, the intrinsic tyrosine kinase domain activates down-stream signaling pathways responsible for proliferation, survival, migration and invasion. The neural cell adhesion molecule

(NCAM)-like structure in the extra-cellular region and unique KW(I/L)A(I/L)ES conserved amino acid sequence in the tyrosine kinase domain, distinguishes TAM family receptors from other RTKs (Linger et al., 2008, Niu et al., 2019).

Within the TAM family, AXL and TYRO3 have highly similar genomic structure sharing same number (20) and size of exons, whereas AXL and MERTK have the most similar amino acid sequence within tyrosine kinase domain. Overall, TAM family receptors share ~30% amino acid sequence identity within the extracellular region and over 50% sequence identity within the tyrosine kinase domain. The full length TYRO3, AXL, and MERTK proteins consist of 890, 894, and 999 amino acids and have predicted protein sizes of 97, 98, and 110 kDa, respectively. However, actual molecular weight of the proteins varies due to post-translational modifications such as glycosylation, phosphorylation, and ubiquitination. The post-translation modification of the protein is accountable for variations in TAM family's tissue and cell-specific function (Linger et al., 2008)
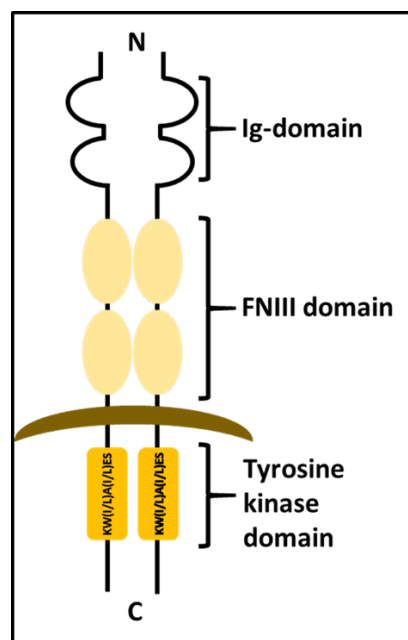
Figure 1. 9- The structure of AXL/TYRO3/MERTK (TAM) receptor. The figure represents two Immunoglobulin (Ig)-like domains and two Fibronectin type-III (FNIII) domains in extracellular region, followed by transmembrane domain and intracellular tyrosine kinase domain. N= N terminal; C= C terminal (adapted from (Linger et al., 2008)).

TAM receptors have an overlapping but unique expression profile in adult tissues. All three receptors are expressed diversely by brain, heart, ovary, testis, lung, kidney and retina (Linger et al., 2008). Expression of AXL receptor is universal with prominent expression found in hippocampus and cerebellum. TYRO3 is highly expressed in nervous system and MERTK is rich in hematopoietic cells such as monocytes/macrophages, dendritic cells, natural-killer (NK) cells and platelets (Brandao et al., 2011).

TAMs are widely distributed in the nervous system but TYRO3 is most highly expressed compared to AXL and MERTK. In brain, TYRO3 is abundantly expressed in the olfactory bulbs, cerebral cortex, and piriform cortex, all cortical layers of the cerebellum, the amygdala, and hippocampus. In addition, expression of TYRO3 increases during CNS development. All three receptors are expressed at variable level by non-neuronal cells of the CNS such as endothelial cells, oligodendrocytes, glia, Schwann cells and astrocytes (Pierce and Keating, 2014, Goudarzi et al., 2016).

1.6.2 Function of TAM receptors in normal physiological processes

At the cellular level, TAM family receptors play an important role in promoting phagocytosis of apoptotic cells, a process which is essential for maintaining normal tissue homeostasis. Even though they are expressed throughout embryonic development, TAM family receptors, appear not to play an important role in embryogenesis (Lu et al., 1999). This is evident from single, double and even triple knock-out mice that were born without any obvious signs of developmental birth defects. However, around four week of post-birth, the mice start developing enlarged spleens and lymph nodes at an abnormal rate and by the age of one year, their spleen weights were on average 10 times higher compared to wild type. The triple mutant mice eventually developed autoimmunity, likely due to delayed clearance of apoptotic cells (Lu and Lemke, 2001).

TAM receptors involvement in the clearance of apoptotic cells is cell and tissue-type specific. Macrophage-mediated phagocytosis appears to involve all thee TAM receptors, but dendritic cells (DCs)-mediated phagocytosis, mainly involves only AXL or TYRO3. Moreover, MERTK but not AXL and TYRO3 appears essential for the maintenance of the retinal tissues (Seitz et al., 2007). This was in accordance with previous study reporting that MERTK knock-out mice developed retinitis pigmentosa due to defective phagocytosis of photoreceptors on the outer segment of the membrane of retinal pigment epithelium (RPE) (D'Cruz et al., 2000).

Moreover, TAM family receptors also play an important role in the regulation of inflammatory responses. TAM triple knock-out mice produce elevated inflammatory response and hyperactivation of macrophages (Lu and Lemke, 2001). This was further supported by another group who showed that MERTK works by negatively regulating the activation of nuclear factor kappa B (NFκB) signaling in dendritic cells and dampens NFκB-mediated proinflammatory response by decreasing tumour necrosis factor alpha (TNFα) production (Sen et al., 2007).

In the CNS, TAM family receptors play an important role in maintaining adult brain neurogenesis. TAM receptors are expressed by astrocytes and microglial-like immune cells in CNS where they regulate brain immunity. Microglial cells of TAM triple knock-out mice produce high level of proinflammatory cytokines such as IL-1β, IL-6 and TNF-α, which adversely affect the neurogenesis process. Furthermore, TAMs play a direct role in maintaining the neurogenesis process by supporting neural stem cells (NSCs) survival, proliferation and neuronal differentiation (Ji et al., 2013, Ji et al., 2014). Moreover, TYRO3 has been shown to be expressed in axons and dendritic compartments of cortical and hippocampal neurons where it thought to be important for neuronal plasticity via activation of MAPK and PI3K pathways (Prieto et al., 2007).

TAMs promote gonadotropin-releasing hormone (GnRH) neuronal survival and migration. GnRH neurons are brain cells that control reproduction and thus affect normal reproductive function (Pierce et al., 2008). AXL-mediated activation of ERK and PI3K pathways rescues GnRH neurons from cell death and promotes their migration in GnRH neuronal development (Allen et al., 2002). Loss of GnRH neurons in AXL/TYRO3 null mice resulted in an abnormal estrous cycle and reproductive malfunction due to impaired sex hormone-induced gonadotropin surge (Pierce et al., 2011).

Another important role of TAM family receptors in nervous system involve the regulation of myelination process. Oligodendrocytes are myelin-producing cells of CNS whereas Schwann cells produce myelin for peripheral nervous system (PNS). Expression and activation of all three TAM receptors promotes survival and proliferation of oligodendrocytes and Schwann cells (Binder et al., 2008, Ammoun et al., 2014, Goudarzi et al., 2016). TAM family receptors are highly expressed and activated in white matter both before and during the myelination process (Binder and Kilpatrick, 2009). TYRO3 has the largest pro-myelin effect of all the TAM family receptors. The loss of TYRO3 on oligodendrocytes and Schwann cells, impairs the pro-myelination process and results in delayed myelination and production of thinner myelin (Miyamoto et al., 2015, Goudarzi et al., 2016, Akkermann et al., 2017). AXL is not directly involved in either myelin or demyelination but is important for remyelination process. The loss of AXL causes delayed phagocytosis, delayed removal of myelin debris and enhanced inflammation which ultimately leads to the inhibition of remyelination and prolonged axonal damage (Hoehn et al., 2008). The role of MERTK in the myelination process has not well studied yet.

1.6.3 Regulation of TAM activity

TAM family receptors were originally cloned from the cancer cells which manifests their oncogenic potential. All three members of the TAM receptor kinases are overexpressed in a broad spectrum of human cancers and non-cancerous tumours, including schwannomas, and their aberrant activation is related to cancer progression, metastasis and resistance to targeted therapies (Linger et al., 2008, Ammoun et al., 2014). Despite the high oncogenic potential of TAM receptors in many cancers, there is limited reseach in understanding the mechanisms that cause aberrant expression of TAM receptors. Some of the explored mechanism are described below.

1.6.3.1 Genetic variation

DNA copy number variation has emerged as a potential mechanism underlying the overexpression of TAM receptors in many cancers. Evidence supporting this notion comes from two separate studies around the similar time; one in GBM patients and another in lapatinib resistant breast cancer cell-line. Both studies showed that AXL gene amplification was the potential cause for overexpression of the protein (Margareto et al., 2009, Liu et al., 2009). Additionally, fluorescence in situ hybridization (FISH) on AXL-expressing colorectal cancer (CRC) samples identified that AXL overexpression in 5.4% of cases were due to the gene amplification (Martinelli et al., 2015). Mutations in TAM family receptors have reported recently but the functional significance of these mutations in promoting malignancy are still not fully understood. Mutation within TYRO3 kinase domain has reported in primary tumour samples of colon cancer (M592I), lung cancer (N615K), melanoma (W708fs*5), brain cancer (A709T) and AML (C690R). Mutations in the extra-cellular region of TYRO3 have been found in melanoma (Q67 and H60Q) and lung cancer (E340) which result in a premature stop codon (Smart et al., 2018). Most

reported *MERTK* human mutations have been linked to retinal dystrophy and retinitis pigmentosa (Jinda et al., 2016). *MERTK* missense mutations have been found in 5.8% of head and neck cancer (HNSCC) cases but the significance of this mutation in cancer development is not clear (von Massenhausen et al., 2016). However, a mutation in *MERTK* kinase domain in melanoma cell-lines (P802S) was found to be responsible for impaired phosphorylation of the MERTK receptor and affected melanoma cell motility (Tworkoski et al., 2013).

1.6.3.2 Transcription regulation

Several vital up-stream transcriptional regulators have been described for AXL, TYRO3 and MERTK. Many studies showed that sp1/sp3, activating enhancer binding Protein 2 alpha (AP-2α), myeloid zinc finger-1 (MZF1) and activator protein-1 (AP1) can directly interact with the AXL promoter and regulate the transcriptional activity of the gene (Mudduluru and Allgayer, 2008, Mudduluru et al., 2010a, Mudduluru et al., 2010b, Orso et al., 2009). In addition, the proximal region of AXL contains hypoxia-response element (HRE) binding sites for hypoxia-inducible factor 1 (HIF1) and hypoxia-inducible factor 2 (HIF2). Rankin *et al* showed that HIF1 and HIF2 can activate the transcription of AXL in hypoxic renal cancer cells by direct binding to HRE sites in the promoter region (Rankin et al., 2014). AXL is believed to be a transcriptional target of Yes-associated protein (YAP). In hepatocellular carcinoma (HCC) and non-small cell lung cancer (NSCLC), AXL mediates YAP-dependent oncogenic function and knock-down or pharmacological inhibition of AXL decrease the proliferation and invasion of YAP-expressing HCC and lung cancer cell-line (Xu et al., 2011, Ghiso et al., 2017). P53 has also been shown to regulate AXL gene expression directly or indirectly (Vaughan et al., 2012). Circadian regulator nuclear receptor subfamily 1 group D membra 2 (NR1D2) has

recently been shown to directly bind the AXL promoter in GBM cells, resulting in increased proliferation and invasion (Yu et al., 2018).

Since, the human *MERTK* promoter has not yet been completely characterized, most transcriptional regulators have been described for mouse *Mertk* gene which shares considerable homology with its human ortholog. Wong *et al* identified sp1, sp3 and E2F as transcription factors essential in regulating *Mertk* promoter activity (Wong and Lee, 2002). Liver C receptor (LXR) is another transcription factor described to be important for the direct induction of *Mertk* transcription activity in mouse macrophages and promoting clearance of apoptotic cells (N et al., 2009).

Very little is known about transcription regulation of TYRO3 in human or in mouse. TYRO3 and AXL have been described as transcriptional targets for CXCR4/SDF-1 (CXCL12) and the expression of AXL and TYRO3 corelate with CXCRL4 expression in thyroid carcinoma cell-line (Avilla et al., 2011).

1.6.3.3 Epigenetic Regulation

DNA methylation is an important epigenetic regulation known for its role in cell-cycle control, tumour suppression and embryonic development. Endogenous AXL gene expression is correlated to CpG methylation within the *AXL* promoter. A lower AXL-expressing CRC cell-line had partially methylated CpG sites compared to a high AXL-expressing CRC cell-line where no such methylated CpG sites were observed (Mudduluru and Allgayer, 2008). Consistent with these results, another separate study also corelated promoter hypomethylation with increased AXL expression in Kaposi's sarcoma (Liu et al., 2010). Histone modification has also been linked to altered gene expression of AXL. In H1299 lung cancer cells, histone acetylation of the AXL promoter region increased the promoter activity likely by enhancing interaction of the transcription factors p300, CREB,

and E2F1 with their consensus binding sites on the *AXL* promoter (Vaughan et al., 2012). No such epigenetic regulation for MERTK and TYRO3 has reported.

1.6.3.4 Post-transcriptional regulation

MicroRNAs (miRNAs) are short non-coding RNA molecules which negatively regulate messenger RNA (mRNA) translation to protein. miRNA-34a and miRNA-155 have been shown to decrease the expression of AXL in blood monocytes (Kurowska-Stolarska et al., 2010). Another team also found that the expression of AXL is negatively regulated by miRNA-34a and miRNA-199a/b (Mudduluru et al., 2011). Although the exact mechanism of this regulation is not known, AXL has recently been shown to be autoregulated in a negative feedback loop by miRNA. AXL overexpression causes upregulation of miRNA-34a via the JNK/ELK1 signaling pathway and upregulated miRNA-34a in return, inhibits AXL expression by binding to the 3'UTR region within the AXL promoter. Malfunction of this regulatory loop is thought to contribute in resistance to apoptosis and metastatic invasion of lung cancer cells (Cho et al., 2016).

Loss of miRNA-335 expression is responsible for an increase in metastatic invasion in breast cancer cells. A search for putative metastatic genes regulated by miRNA-335, found that the 3'UTR promoter region of MERTK is the direct target of miRNA-335. However, the study didn't asses the direct effect of miRNA-335 modification on the level of MERTK protein expression (Tavazoie et al., 2008). miRNA-335 is the only miRNA discovered so far that is able to regulate the expression of MERTK.

Finally, miRNA-7 has been recognized as direct regulator of TYRO3 gene expression. Overexpression of miRNA-7 in HCC and CRC, reduced the expression of TYRO3 at mRNA and protein levels and resulted in decreased proliferation, migration and invasiveness of cancer cells (Kabir et al., 2018, Qin and Qian, 2018).

1.6.4   Ligands for the TAM receptors

Gas6 and Protein S are well characterized vitamin K-dependent ligands of the TAM family receptors that share ~40% sequence similarity and have similar domain organization. Both ligands comprise of 11 γ-carboxyglutamic acid residues (Gla), a loop region, which contains disulphide-bridged ring structure and four EGF-like repeats in N-terminal region and sex hormone binding globulin (SHBG)-like structure composed of two globular laminin G (LG)-like domains in the C-terminal region (Figure-1.10 A). The N-terminal region of the Gla domain is formed after post-translation modification of glutamate residues in the endoplasmic reticulum by γ-glutamyl carboxylase enzyme, requiring the presence vitamin K as a co-factor. Negatively charged glutamic acid (Gla) residues mediate binding to negatively charged phospholipid membranes such as phosphatidylserine (PS) on apoptotic cells through calcium binding. On the other hand, laminin G (LG) domains in C-terminal region promote binding of the ligand to TAM receptors thus promoting phagocytosis of targeted bodies by receptors (Figure-1.10 B) (Hafizi and Dahlback, 2006).

A thrombin sensitive cleavage site in the loop region of proteins S, separates it from Gas6 and is responsible for the characteristic of protein S as negative regulator of blood coagulation. Despite similarities in structure and activity, both ligands; Gas6 and Protein S, have different affinities for different TAM receptors. Gas6 can bind to all three receptors but has the highest affinity to AXL compared to TYRO3 and MERTK (AXL>TYRO3>MERTK). Whereas, Protein S specifically binds to TYRO3 and MERTK but not AXL (TYRO3>MERTK). Protein S is primarily produced and secreted by the liver. In contrast, Gas6 is locally produced in many tissues and expressed by many cells including capillary endothelial cells, vascular smooth muscle cells, and bone marrow cells but is absent from liver cells. Normal human plasma concentration of Gas6 is in the sub

nanomolar range of 0.16–0.28 nM which is 1000-fold lower than that of protein S plasma concentration. Interestingly, only ~40% of Proteins S circulates as free protein in blood plasma that can act as ligand for TAM receptors, ~60% is present as a bound complex with C4 binding protein (C4BP) and cannot activate TAM receptors (Hafizi and Dahlback, 2006, Balogh et al., 2005).

Tubby and tubby like protein-1 (Tulp-1), members of tubby protein family, have recently emerged as novel ligands for the TAM family receptors. Like Gas6 and Protein S, Tubby and Tulp-1 have different affinity for TAM receptors. Tulp-1 interacts with all three members of TAM receptors while Tubby specifically binds to MERTK. The levels of circulating Tubby and Tulp-1 have not been quantified yet but their expression have been shown to be restricted to in adult retina and neuronal tissues. In 2012, the same team that established Tubby and Tulp-1 as ligands for TAM receptors, showed that MERTK induce phagocytosis of apoptotic cells and cellular debris via binding to Galectin-3 and added one more protein in the list of novel ligands for TAM receptors. However, affinity of Galectin-3 for AXL and TRYO3 has not yet been defined (Caberoy et al., 2010, Caberoy et al., 2012).
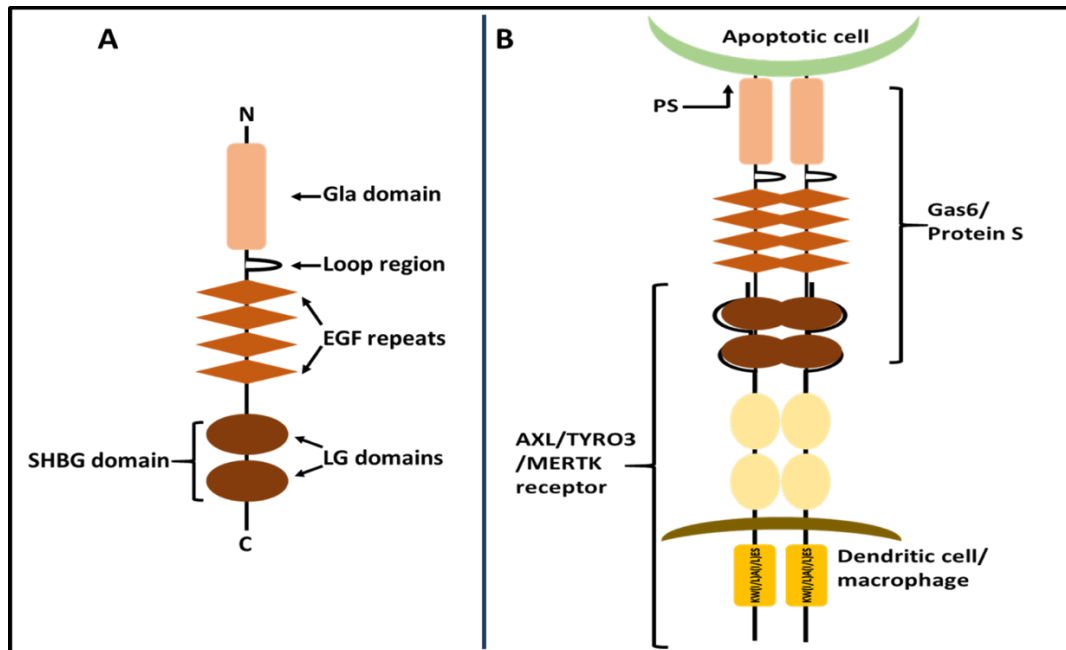
Figure 1. 10- The structure of TAM ligands; Gas6/Protein S and their binding to TAM receptor to mediate phagocytosis. The N-terminal consists of a Gla domain, followed by loop region, four EGF repeats and finally a C-terminal SHBG domain that consist of two LG repeats **A)**; SHBG domain in C-terminal of ligand Gas6/Protein S mediated binding to N-terminal Ig domain of TAM receptor present on immune cells like dendritic cells and macrophages. N-terminal Gla domain of the ligand binds to PS that is presented by outer plasma membrane of apoptotic cells **B)**. (Gla- glutamic acid; EGF- epidermal growth factor; LG- laminin G; SHBG-sex hormone binding globulin) (Adapted from (Axelrod and Pienta, 2014, Lemke and Rothlin, 2008)).

1.6.5   Activation and deactivation of TAM receptors

1.6.5.1 Ligand dependent activation of TAM receptors

The typical activation of RTK involves, ligand binding to the extra-cellular region of the RTK, receptor dimerization and trans-autophosphorylation of tyrosine residues in the intra-cellular kinase domain (Figure-1.11 A). Following autophosphorylation, the activated RTK either leads to phosphorylation/activation of other substrates or recruits signaling molecules to the docking site thus creating macromolecular signaling complex (Linger et al., 2008).

For the MERTK receptor, Y-749, Y-753 and Y-754 are the primary sites of autophosphorylation. For the full activation of the receptors, phosphorylation at all three

tyrosine residues in the kinase domain is essential with Y-749 being the preferred site of autophosphorylation (Ling et al., 1996). Y-749, Y-753 and Y-754 sequence of MERTK receptor are conserved among all three members of TAM receptors, corresponding to 698, 702, 703 residues of AXL and 681, 685, 686 residues of TYRO3 kinase but there is no evidence implicating their role in autophosphorylation (Linger et al., 2008). Residues Y-779, Y-821, and Y-866 that mediate the AXL receptor interaction with signaling molecules phospholipase C (PLC), phosphatidyl inositol 3 kinase (PI3K), and Grb2 (Braunger et al., 1997) are thought to be the potential autophosphorylation site of AXL. However, *in vivo* study of mutant AXL without Y-821 showed normal Gas6 stimulated phosphorylation of the receptor, conflicting the results from *in vitro* study (Fridell et al., 1996). Gas6 stimulation leads to phosphorylation of the residues Y702 and Y703 in AXL kinase domain (Pao-Chun et al., 2009), but further study is required to investigate signaling molecules that bind to these sites for AXL activation.

1.6.5.2 Ligand independent activation of TAM receptors

In addition to the conventional ligand-dependent activation, atypical ligand-independent activation of TAM receptors has also been reported. TAMs can be activated by ligand independent homophilic dimerization of receptor monomers on neighboring cells or on the same cell (Figure-1.11 B and Figure-1.11 C) and by receptor heterodimerization with other RTKs or with other members of TAM family (Figure-1.11 D and Figure-1.11 E).

Overexpression of AXL causes cell-aggregation and ligand-independent receptor activation, via homophilic binding of the receptor on a neighboring cell. Moreover, cell-aggregation and homophilic dimerization of the receptor was independent of tyrosine kinase activity (Bellosta et al., 1995). Another team also reported that over-expression of

TYRO3 was sufficient to induce phosphorylation and activation of the receptor in absence of the ligand (Taylor et al., 1995). Further evidence of ligand-independent receptor dimerization come from the crystal structure of TYRO3, further supporting the previous reports (Heiring et al., 2004).

TAM family receptors can crosstalk with other receptors by forming heterotypic dimers. AXL has been reported to physically interact with RTK EGFR in glioblastoma multiforme (GBM) cell-line in a ligand independent manner. The treatment of GBM cells with EGF lead to trans-activation of the AXL receptor and activation of down-stream signaling pathways (Vouri et al., 2016). Although such heterotypic dimers for TYRO3 and MERTK have not been reported, indirect molecular cross-talk between αvβ5 integrin and MERTK is reported to be essential for promoting phagocytosis of apoptotic cells (Wu et al., 2005).

Heteromeric complex have also been reported among TAM family members. Co-immunoprecipitation experiments in GnRH neuronal cells have showed that AXL and TYRO3 are closely related and can form complex irrespective of the presence of their ligand Gas6 (Pierce et al., 2008). A physical interaction between TYRO3 and AXL has also been reported in Rat2 fibroblast cells, where ectopic expression of TYRO3 but not 'kinase dead' TYRO3 (kdTYRO3) enhanced Gas6-mediated activation of AXL. Similarly, overexpression of AXL induced the phosphorylation of kdTYRO3 receptor (Brown et al., 2012). Indeed, blocking Gas6-mediated phosphorylation of AXL also decreased the activation of TYRO3 in GBM cell-line (Vouri et al., 2015). One study has clearly demonstrated that Gas6-stimulated activation of any one TAM receptor requires the presence of one or both of remaining TAM receptors, further supporting the notion that TAM receptors co-operate in their activation response (Angelillo-Scherrer et al., 2005).
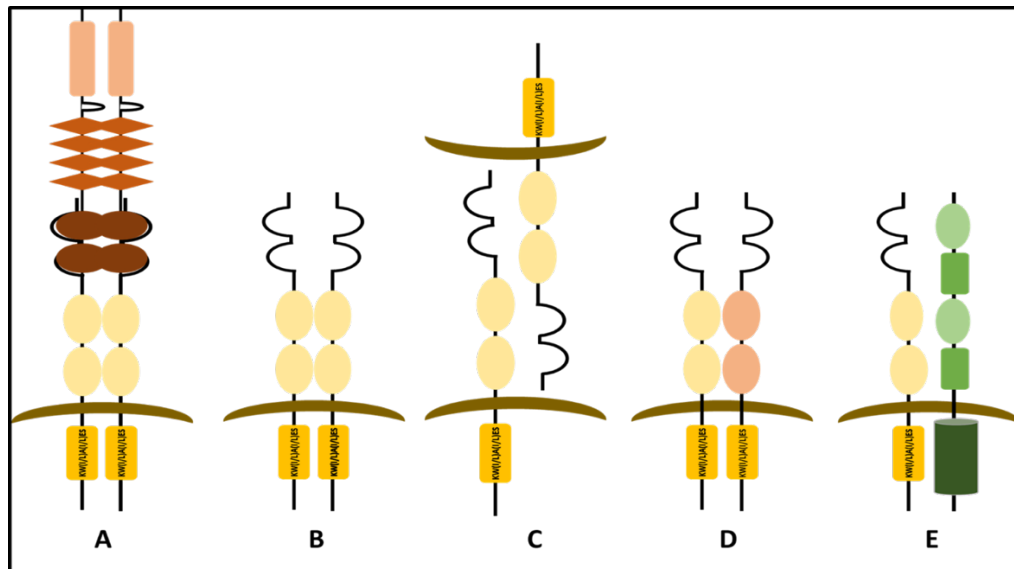
Figure 1. 11- Mechanisms of TAM receptor activation. Gas6-induced dimerization and activation of TAM receptor **A)**; A ligand independent homophilic dimerization of receptors **B)**; Ligand-independent homophilic binding of two receptors on neighboring cells **C)**; Ligand-independent dimerization of two different TAM receptors **D)**; Ligand-independent dimerization of TAM receptor with non-TAM receptor **E)** (adapted from (Korshunov, 2012)).

1.6.5.3 Mechanisms of deactivation of TAM receptors

RTKs maintain normal physiological response by the tight regulation of mechanisms for receptor activation and deactivation. The attenuation and termination of RTK signaling may be induced by antagonistic ligands, hetero-oligomerization with receptor mutant, dephosphorylation by tyrosine phosphatase and by receptor endocytosis and degradation. Impaired RTK deactivation may lead to many pathological conditions including cancer (Schlessinger, 2000). Studies evaluting the mechanisms for TAM receptor deactivation are limited.

Overexpression of C1 domain-containing phosphatase and TENsin homologue (C1-TEN) inhibited HEK-293 proliferation, migration and increased apoptosis of the cells in culture (Hafizi et al., 2005). C1-TEN has been shown to dephosphorylate Y612 of insulin receptor substrate 1 (IRS-1) and accelerate its degradation (Koh et al., 2013). AXL kinase domain has also been shown to bind to (C1-TEN) (Hafizi et al., 2002). This binding may

lead to dephosphorylation of the AXL receptor, however there is no direct evidence demonstrating C1-TEN mediated dephosphorylation of AXL. Protein tyrosine phosphatase receptor type G (PTPG) has recently emerged as tyrosine phosphatase for AXL. A novel mechanism involving Gas6-mediated inactivation of AXL in the presence of tumour suppressor - opioid-binding protein/cell adhesion molecule-like (OPCML) was described. The study shows that OPCML enhances interaction between AXL and phosphatase PTPG which ultimately causes AXL dephosphorylation and inactivation (Antony et al., 2018).

1.6.6   TAM receptor's signaling in cancer

TAM family receptors were originally cloned from cancer cells which manifests their oncogenic potential. All three members of the TAM receptor kinases are overexpressed in a broad spectrum of human cancers including schwannomas and their aberrant activation is related to cancer progression, metastasis and resistance to targeted therapies. Ligand-induced or ligand-independent phosphorylation of TAM intracellular kinase domain promotes a cascade of signaling molecules that subsequently leads to proliferation, survival and migration of the cells. Three important signaling pathways downstream of TAM family receptors involve MAPK, PI3K and PLCγ pathway (Figure-1.12, Figure-1.13 and Figure-1.14) (Linger et al., 2008, Ammoun et al., 2014).

All three receptors promote cell proliferation via the classical MAPK pathway. Ligand-stimulated phosphorylation of AXL and MERTK lead to a cascade of Shc, GrB2, Ras, Raf, MEK1 and ERK1/2 signaling molecules. GrB2 can be activated by direct binding to AXL and MERTK kinase domain or indirectly by binding to Shc which is phosphorylated by activated AXL and MERTK (Linger et al., 2008). While the role of AXL and MERTK

is well defined in mediating the MAPK pathway, data indicating regulation of this pathway by TYRO3 are limited. However, ectopic expression of TYRO3 in Rat2 cells induced phosphorylation of MAPK (Brown et al., 2012). Similarly, TYRO3 was found to be responsible for the activation of ERK in breast cancer and hepatocellular carcinoma (HCC) cell-lines which was reversed upon genetic knock-down of TYRO3 (Ekyalongo et al., 2014, Duan et al., 2016).

The intracellular phosphorylated kinase domains of AXL, TYRO3, and MERTK can directly interact with PI3K to promote cell survival via activation of multiple signaling pathways downstream of AKT. AXL and MERTK both have shown to activate classical AKT/S6K and AKT/NFkB pathways to promote cell survival. Additionally, AXL mediates survival of the cells by activating anti-apoptotic proteins such as Bad, Bcl-2, and Bcl-xL and by inhibiting pro-apoptotic proteins like caspase-3, downstream of AKT. The Gas6-AXL axis is also involved in AKT mediated activation of the JNK signaling pathway to enhance cell survival (Linger et al., 2008). AKT downstream of TYRO3 has also been reported to phosphorylate Bcl-2 associated death promoter (BAD) to promote the survival of neuronal cells (Guo et al., 2011). In Rat2 cells, TYRO3 mediated activation of AKT leads to phosphorylation of mTOR and ribosomal protein S6 kinase beta-1 (P70S6K) (Brown et al., 2012).

In addition to PI3K and GrB2, phospholipase C gamma (PLCγ) can also directly bind to the AXL and MERTK kinase domains, resulting in increased migration of cells. Alternative cell migration signaling pathways involve AXL-mediated Ras, Rac, p38 MAPK, MAPKAP kinase 2, and HSP25 pathways downstream of AKT and; Vav-1, Rac1 and cdc42 pathway directly downstream of MERTK. AXL and MERTK have also been shown to stimulate Src-mediated phosphorylation of FAK, leading to cell migration. Although these are signaling pathways known to sit downstream of the TAM family, the

ultimate downstream targets of signaling pathways may differ depending on cell-type and

tissue microenvironment (Linger et al., 2008, Ammoun et al., 2014).
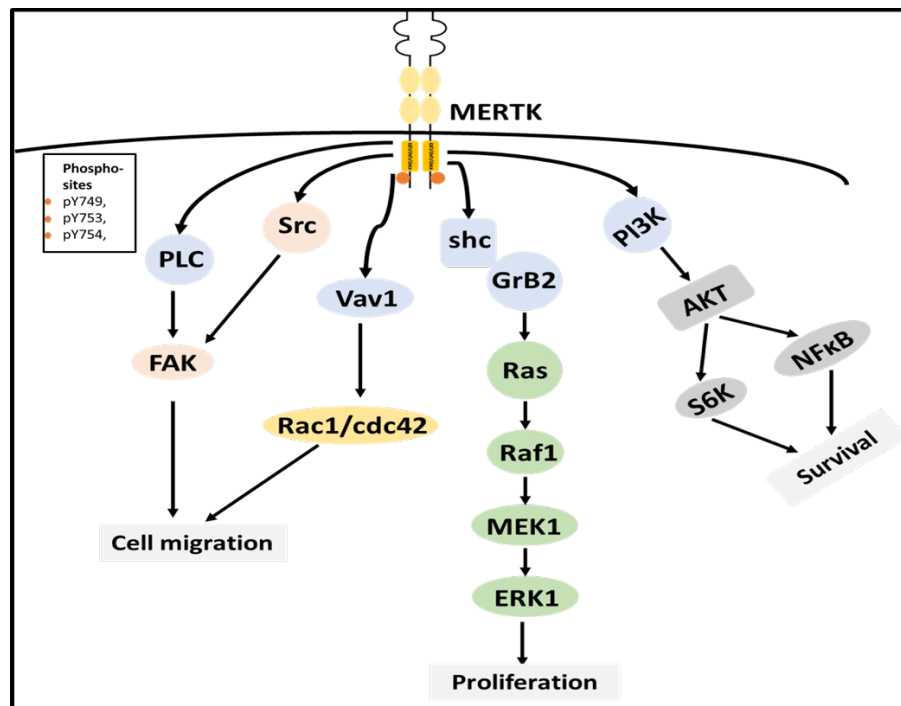
Figure 1. 12- Important oncogenic signaling pathways downstream of MERTK. Molecules in blue; PLC, Vav1, shc, Grb2 and PI3K, can directly or indirectly interact with phosphorylated MERTK kinase. Ras/ERK pathway- green, AKT pathway- grey, Rac1- yellow and FAK/Src pathway- in pink leads to cell proliferation, survival and migration. Phospho sites (dark orange circles) are mentioned at the side in a box (adapted from (Linger et al., 2008)).
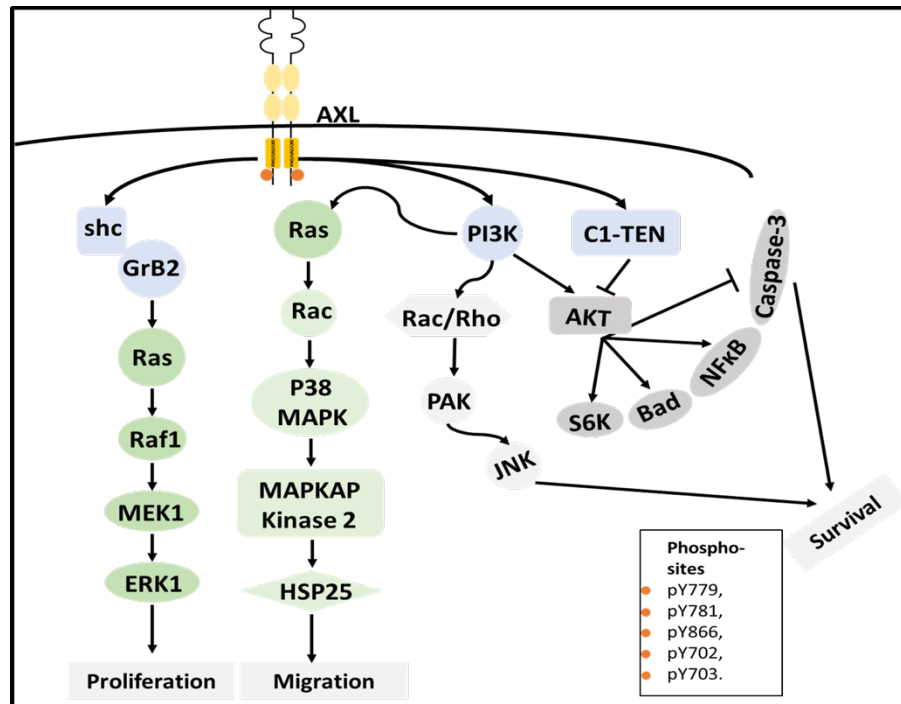
Figure 1. 13- Important oncogenic signaling pathways downstream of AXL. Molecules in blue can directly or indirectly interact with phosphorylated AXL kinase. Ras/ERK pathway- dark green, Ras/HSP25- light green, PI3K/AKT pathway- dark grey, PI3K/JNK pathway light grey leads to cell proliferation, survival and migration. Phospho sites (orange circle) are mentioned at the side in a box (adapted from (Linger et al., 2008)).
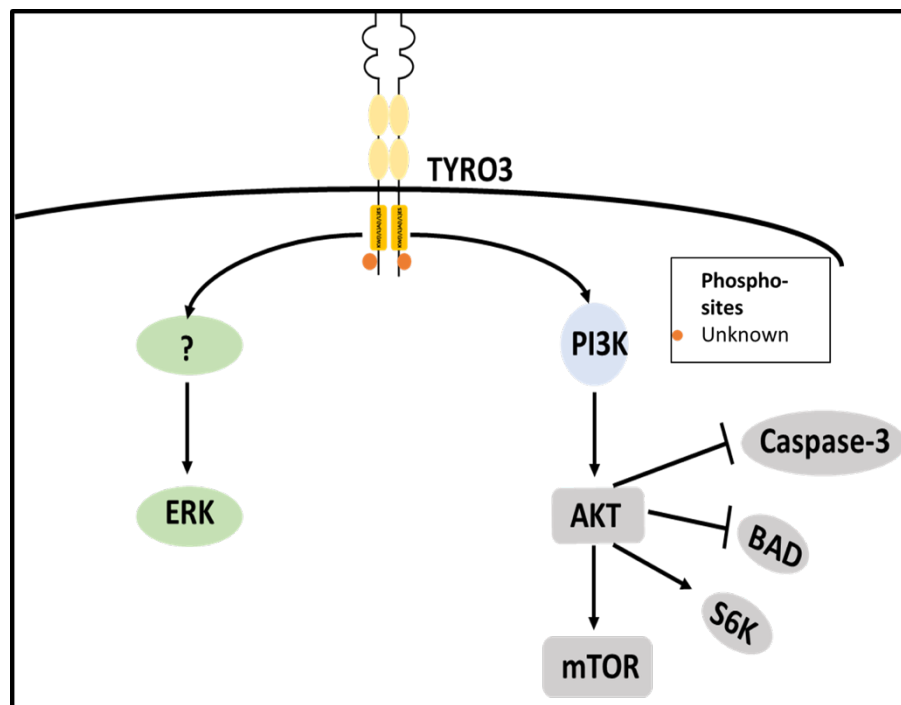
Figure 1. 14- Important oncogenic signaling pathways downstream of TYRO3. Molecules in blue can directly or indirectly interact with phosphorylated TYRO3 kinase. ERK pathway- green, PI3K/AKT pathway- grey leads to cell proliferation, survival and migration. Specific phospho sites (orange circles) for TYRO3 are not known (adapted from (Linger et al., 2008)).

1.6.7 TAM family of receptors in drug resistance

A large body of evidences suggests that activation of TAM family receptors is associated with resistance to conventional and targeted therapies in several cancers (Schoumacher and Burbridge, 2017). As previously described, TAMs can cross-talk, not only with the members of their own family but can also dimerize with non-TAM receptors to bypass the inhibitory effect of targeted kinase inhibitors (Meyer et al., 2013). Activation of TAMs promotes resistance to therapeutic agents and favors tumour growth by maintaining downstream signaling of targeted receptors by an alternative effector or by switching to alternate signaling pathway (Schoumacher and Burbridge, 2017).

Acquired resistance to drugs targeting EGFR such as gefitinib and erlotinib in lung cancer (Bae et al., 2015, Zhang et al., 2012) and lapatinib and erlotinib in breast cancer is common due to AXL overexpression and activation (Meyer et al., 2013). Activation of AXL limits the response to EGFR-tyrosine kinase inhibitor in these cancers by compensating or amplifying downstream signaling of EGFR through association with and/or transactivation of other members of the EGFR family (Tian et al., 2016, Meyer et al., 2013). Increased AXL expression has also shown to be responsible for resistance to imatinib in gastrointestinal stromal tumours, and resistance to imatinib and nilotinib in CML cells (Mahadevan et al., 2007, Dufies et al., 2011). In acute myeloid leukemia (AML) cell-line, AXL mediates resistance to conventional chemotherapeutic drugs; doxorubicin, VP16 and cisplatin by activating compensatory survival signaling to favor tumour growth (Hong et al., 2008). Very recently, MERTK has also been reported to mediate resistance to EGFR inhibitors in non-small cell lung cancer (NSCLC) and to AXL kinase inhibitor in head and neck squamous cell carcinoma (HNSCC), triple-negative breast cancer (TNBC) and NSCLC (Yan et al., 2018, McDaniel et al., 2018).

These studies highlight that TAMs could be attractive therapeutic target in cancer and drug resistance.

Additionally, TAMs role as an immunosuppressor favors their oncogenic potential. Activation of TAM receptors dampen the inflammatory response by promoting activation of M2 state macrophages which secrete anti-inflammatory cytokines and limits expansion of CD8+ T cells. This immunosuppressive environment aids tumour growth by blocking the anti-tumour activity of cytotoxic T cells thus, potentially limiting the effectiveness of anticancer treatment (Cook et al., 2013). Indeed, in metastatic melanomas intrinsic resistance to programmed cell death protein 1 (PD-1) therapy has been demonstrated to be due to overexpression of AXL (Hugo et al., 2016). These reports further emphasize the importance of TAMs as therapeutic target in combination with immunotherapy.

1.6.8 TAM receptors as therapeutic target

Overexpression of TAM receptors in many cancers and the role of TAM family members in promoting cancer cell proliferation, survival, migration and drug resistance makes them an attractive therapeutic target in cancer. Due to advances in the understanding of their biology, several kinase inhibitors targeting TAM receptors have recently been developed and tested in a clinical setting. Below is the summary of TAM inhibitors that are in pre-clinical or in clinical trials (Table-1.3).

Cabozantinib is a multi-kinase inhibitor with strong affinity for AXL. It has recently been approved by the FDA for the treatment of medullary thyroid cancer and renal cell carcinoma (Weitzman and Cabanillas, 2015, Grassi et al., 2016). Currently, it is in clinical trials for the treatment of multiple cancers including non-small cell lung cancer (NSCLC) (phase-II studies-NCT01639508, NCT02132598, NCT00596648, NCT01708954 and NCT01866410), breast cancer (phase-II NCT02260531, NCT03316586), ovarian cancer

(NCT02315430), metastatic melanoma (phase-II NCT01835145) and pancreatic cancer (phase-I NCT01663272, phase-II NCT01466036) as a monotherapy or in combination with other drugs. BPI-9016M is a dual kinase inhibitor with strong activity against c-MET and AXL. BPI-9016M inhibits proliferation, migration and invasion of lung adenocarcinoma cells by disrupting kinase activity of c-MET and AXL and their downstream signaling pathways *in vitro* and *in vivo* (Zhang et al., 2018). BPI-9016M is now being tested in phase-I clinical trial for patients with advanced solid tumours to assess the maximum tolerated dose (MTD) and dose-limiting toxicity (DLT) of the drug (NCT02478866).

BMS-777607 is another small kinase inhibitor with activity against AXL (IC_{50}-1.1 nM), MERTK (IC_{50}-14 nM), TYRO3 (IC_{50}-4.0 nM) as well as inhibitory activity towards RON, MET, FLT3, Aurora B, Lck and VEGFR2. BMS777607 has showed an excellent oral bioavailability, tissue distribution, long half-life (4.5 hours in mouse, 4.8 hours in rat and 4.9 hours in dog) and low systemic clearance. It completely inhibited tumour growth in a Met-dependent gastric cancer xenograft model at 50 mg/kg (C_{max} 43.7 μM) (Schroeder et al., 2009). Due to excellent *in vivo* pharmacokinetic properties and anti-tumour efficacy, BMS777607 was tested in a phase-I multiple-dose escalation study for multiple advanced solid tumours (NCT01721148). The drug demonstrated an excellent safety profile and resulted in a partial response or stabilization of disease condition in a subset of tumour types (Roohullah et al., 2018).

BGB324 (R428) is the first small molecule tyrosine kinase inhibitor developed for its potent activity against AXL (IC_{50}-14nM) and it has >50 and >100-fold selectivity against AXL over MERTK and TYRO3 respectively. It successfully inhibited phosphorylation of AXL and downstream AKT signaling pathway with low nanomolar concentration *in vitro* (IC_{50} 14 nM) and in vivo (IC_{50} 0.1-1.0 μM). The drug showed a long plasma half-

life in mice of 4 hours and 13 hours at 25 mg/kg and 75 mg/kg respectively. A twice daily dose of 25 mg/kg, 75 mg/kg and 100 mg/kg of BGB324 resulted in Cmax of 2.4, 6.8 and 9.0 µM respectively and 7 mg/kg dose was sufficient to increase the survival of mice from 52 days in vehicle-treated animals to >80 days in mice treated with BGB324. BGB324 was well tolerated at all doses in mice and no significant compound-related weight loss, mortality or other adverse clinical signs were observed during the experiment (Hector et al., 2010, Holland et al., 2010). A phase-I clinical trial of BGB324 in acute myeloid leukemia (AML) patients showed that the drug is well-tolerated (Ben-Batalla et al., 2017). Based on pre-clinical and clinical data, BGB324 is currently undergoing phase-Ib trials for AML patients as a single agent or in the combination with chemotherapy drugs cytarabine or decitabine (NCT02488408). Two separate Phase-II trials of BGB324 have also been planned for NSCLC patients. One study is currently testing BGB324 in combination with erlotinib (NCT02424617) in stage III and IV NSCLC patients and another is testing BGB324 in combination with humanized PD-1 antibody-pembrolizumab in advanced NSCLC patients (NCT03184571). Moreover, BGB324 has shown good tolerance in healthy volunteers at up to 1.5 g daily dose (Bergenbio, 2014, April 09).

Moreover, a series of quinolone antibiotic derivatives have recently been developed with the aim of developing a new AXL-specific inhibitor. Of all designed compounds, 8i (nadifloxacin) was found to tightly bind to AXL with binding constant (K_d) value of 1.1 nM and inhibit the kinase activity of AXL with IC$_{50}$ of 26 nM, thought to be the most selective AXL inhibitor to date. The kinase inhibitory assay against a panel of 468 kinases at 1 µM (the concentration ~900 times higher than its K_d value against AXL) displayed excellent target selectivity of compound 8i for AXL except for FLT3, which was inhibited with IC$_{50}$ of 50 nM. In addition, the compound also showed convincing pharmacological

properties in rats. A single oral dose of compound 8i of 25 mg/kg resulted in C_{max} of 2386.9 μg/L (3.6 μM) following 4.0 hours of dose administration which was 138 times higher than its IC_{50} values against AXL kinase and half-life of the compound was 5.68 hours. The compound was well-tolerated, and no obvious toxicity was observed following 200 mg/kg, 400 mg/kg or 800 mg/kg of doses (Tan et al., 2019). Other small molecule kinase inhibitors such as DP3975 and NA80xl- specifically targeting AXL, NPS-1034- targeting AXL and MET and LDC-1267 targeting all three members of the TAM family have also shown great pre-clinical activity and have the potential to be further tested in clinical trials (Ou et al., 2011, Rho et al., 2014, Paolino et al., 2014).

In contrast to AXL, few MERTK-targeted small molecule inhibitors have advanced to clinical trials. One of the first reported MERTK-specific inhibitors is UNC569. Although efficient in reducing tumour growth and increasing sensitivity to chemotherapy drugs in acute lymphocytic leukemia (ALL), UNC569 failed in clinical trials due to its high off-target activity towards human ether-a-go-go-related gene potassium channel (hERG) and suboptimal inhibitory activity towards MERTK (Christoph et al., 2013, Liu et al., 2013). Since then, a number of subsequent derivatives of UNC569 such as UNC1062, UNC1666, and UNC2025 have been developed to have increase potency against MERTK. Out of all three, UNC2025 is the most effective against MERTK (IC_{50}- 2.7 nM) and it has almost equal potency against FLT3 (IC_{50}-14.0 nM) in cell-based assays. A single oral dose of 3 mg/kg UNC2025 in leukemia xenograft mice model effectively decreased phosphorylation of MERTK by 90% and yielded C_{max} of 1.6 μM with half life of 3.8 hours in mice. The compound was well tolerated with minimal side effects in the mice model (Zhang et al., 2014). Additionally, treatment with UNC2025 induced apoptosis, reduced colony-formation and suppressed proliferation in MERTK expressing ALL cell-lines (DeRyckere et al., 2017). A final derivative of this family, MRX-2843

which is an analogue of UNC2025 with a minor side chain substitution, similar PK properties and toxicity profile has recently entered in phase-I clinical trials for relapsed advanced metastatic tumours (NCT03510104). Like UNC2025, MRX-2843 induced apoptosis and inhibited colony formation of MERTK-expressing leukemia cells and both compounds were ~10 times more effective against patient derived AML cells compared to normal human cells, indicating MRX2843's specificity to cancer cells as well as its therapeutic potential (DeRyckere et al., 2017, Minson et al., 2016).

Additionally, other novel approaches to specifically target TAM receptors are in development. These include; the use of monoclonal antibody, antibody-drug conjugate (ADC) and aptamer. An AXL specific monoclonal antibody YW327.6S2 was tested in NSCLC and breast cancer xenograft model and showed successful attenuation of tumour growth via inhibition of Gas/AXL binding, thus downregulating expression and activation of both AXL and its downstream signaling pathways (Ye et al., 2010). In 2016, a phase-I/II clinical trial began recruiting a mixed population of patients with solid tumours to assess the safety and tolerance of a novel AXL specific antibody drug conjugate- HuMax-AXL-ADC (NCT02988817). A high affinity short nucleic acid aptamer that binds to the extra-cellular region of AXL. HuMax-AXL-ADC has been tested pre-clinically in NSCLC where it inhibited AXL activity and decreased tumour cell proliferation, migration and invasion in xenograft model (Cerchia et al., 2012).

Monoclonal antibodies that bind to and inhibit MERTK and TYRO3 have also been developed. A novel MER590 monoclonal antibody reduced the cell surface and total MERTK expression by almost 90% and decreased colony-forming potential and chemoresistance in a NSCLC cell-line (Cummings et al., 2014). A TYRO3-specific monoclonal antibody was able to block TYRO3 and inhibited TYRO3-dependent survival signaling in a melanoma cell-line (Demarest et al., 2013).

A second generation high-affinity AXL decoy receptor, MYD1-72 Fc with an apparent affinity of 93 femtomolar (fm) to Gas6 has also been designed. MYD1-72 Fc specifically blocks AXL signaling at low concentrations and reduces tumour volume in AML mice with almost no toxicity described to-date (Kariolis et al., 2017). These novel strategies widen the therapeutic window of TAM inhibitors and show the potential of further clinical development of these novel molecules. All novel therapeutic strategies targeting TAM receptors that are undergoing clinical development are summarized in Table 1.3.

Drug (code name)	Primary target	TAM inhibition	Phase of development
Foretinib (XL880, GSK1363089)	MET, VEGFR2, AXL, RON	AXL: IC_{50} (in vitro) = 11 nM AXL: IC_{50} (in cells) <100nM	Phase II, active, not recruiting
Cabozantinib (XL184, BMS-907351, marketed as Cometriq)	VEGFR2, MET, MEK, KIT, RET, AXL	AXL: IC_{50} (in vitro) = 7 nM AXL: IC_{50} (in cells) = 42 nM	Approved for medullary thyroid cancer Phase II and III for different solid tumours
Merestinib (LY2801653)	MET, MST1R, DDR1, TIE1, MER, TYRO3, AXL	AXL: IC_{50} (in cells) = 2 nM MERTK: IC_{50} (in cells) = 10 nM TYRO3: IC_{50} (in cells) = 28 nM	Phase I, active, recruiting
MGCD265	MET, AXL, VEGFR2,	Data for AXL not reported	Phase I, active, recruiting
ASLAN002 (BMS-777607)	AXL, RON, MET, TYRO3, MER, FLT3	AXL: IC_{50} (in vitro) = 1.1 nM MERTK: IC_{50} (in cells) = 14 nM TYRO3: IC_{50} (in cells) = 4.3 nM	Phase I, active, not recruiting
NPS-1034	AXL, DDR1, FLT3, KIT, MEK, MET, ROS1, and TIE1	AXL: IC_{50} (in vitro) = 10nM AXL: IC_{50} (in cells) < 0.5 µM	Preclinical
LDC1267	MET, AXL, TYRO3	AXL: IC_{50} (in cells) = 19 nM	Preclinical
Bosutinib (SKI-606, marketed as Bosulif)	BCR-ABL, ABL, SRC, YES, MEK, AXL, BMX	AXL: IC_{50} (in vitro) = 0.56 µM AXL: IC_{50} (in cells) =0.34–1.65 µM	Approved for CML with resistance to treatment Phase II and III for different CML stages
Gilteritinib (ASP2215)	FLT3 and mutants, ALK, AXL	AXL: IC_{50} (in vitro) < 1 µM	Phase I/II, active, recruiting
SGI-7079	MET, MER, YES, RET, FLT3, AXL	AXL: IC_{50} (in vitro) = 58 nM AXL: IC_{50} (in cells) < 1 µM	Preclinical
TP-0903	Aurora A and B, JAK2, ALK, ABL, AXL, MER	AXL: IC_{50} (in vitro) = 27 nM AXL: IC_{50} (in cells) = 222 nM	Preclinical
Crizotinib (PF-02341066, marketed as Xalkori)	ALK, MET, RON, AXL	AXL: IC_{50} (in vitro) = 294 nM	Approved for NSCLC Phase II/III for different solid tumours
Amuvatinib (MP470)	KIT, PDGFR1, FLT3, RET, AXL	AXL: IC_{50} (in cells) < 1 µM	Phase II, development discontinued
UNC2025	MERTK, FLT3, AXL, TYRO3	MERTK: IC_{50} (in vitro) =0.46 nM AXL: IC_{50} (in vitro) = 1.6 nM TYRO3: IC_{50} (in vitro) = 5.8 nM	Preclinical
S49076	MET and mutants, AXL, MERTK, FGFRs	AXL: IC_{50} (in vitro) = 7 nM AXL: IC_{50} (in cells) = 56 nM	Phase I, active, recruiting
Sunitinib (SU11248, marketed as Sutent)	KIT, FLT3, PDGFR, VEGFR2, AXL	AXL: IC_{50} (in vitro) = 9 nM	Approved for renal cell carcinoma, imatinib-resistant gastrointestinal stromal tumour, and metastatic pancreatic neuroendocrine tumours Phase II/III for different solid tumours
BGB324 (R428)	AXL (selective)	AXL: IC_{50} (in vitro) = 14 nM AXL: IC_{50} (in cells) < 30 nM	Phase I/II, active, recruiting
MRX2843	MERTK, FLT3, AXL	MERTK: IC_{50} (in vitro) = 1.3 nM AXL: IC_{50} (in vitro) = 15 nM	Phase I, active, recruiting
HuMax-AXL-ADC	AXL	Data for AXL not reported	Phase I/II, active, recruiting
BPI-9016M	AXL, MET	Data for AXL not reported	Phase I, active, not recruiting
Compound 8i (Nadifloxacin)	AXL and FLT3	AXL: IC_{50} (in vitro) = 26 nM	Preclinical
DP3975	AXL	AXL: IC_{50} (in vitro) = 100 nM	Preclinical
NA80xl	AXL	AXL: IC_{50} (in vitro) < 3 µM	Preclinical
NPS-1034	AXL, Met	AXL: IC_{50} (in vitro) = 10.3 nM	Preclinical
YW327.6S2	AXL	Data for AXL not reported	Preclinical
MER590	MERTK	Data for MERTK not reported	Preclinical
MYD1-72 Fc	AXL	Data for AXL not reported	Preclinical

Table 1. 3- TAM inhibitors in clinical development. A summary of the drug candidates that are in clinical development for AXL, MERTK and TYRO3 receptors with their known IC_{50} values (adapted from(Myers et al., 2016)).

1.7   Project significance/Aims

Our group has previously demonstrated that all three members of TAM family receptors; AXL, MERTK and TYRO3, as well as their ligand Gas6, are overexpressed in schwannomas and have recognized the role of AXL in mediating schwannoma cell proliferation, adhesion and survival (Ammoun et al., 2014). The overall aim of this project is to investigate, possible involvement of the other TAM family members; TYRO3 and MERTK in schwannoma pathology and all three TAM members in meningioma development and progression. The objectives of the research project are as follow;

Firstly, to investigate the expression profile of AXL, MERTK, TYRO3 and their ligand Gas6 in Merlin-deficient human meningioma tissues and primary cells compared to normal controls.

Secondly, to investigate the physical or functional interaction among AXL, MERTK and TYRO3 receptors in human schwannoma and meningioma tissues and primary cells.

Thirdly, to investigate the role of TAM family members in pathological proliferation and survival of human primary schwannoma and meningioma cells via key signaling pathways that are already known to be involved in the tumours development.

Finally, to test different drug candidates targeting TAM kinase receptors such as BGB324 (R428)-AXL inhibitor, UNC2025-MERTK inhibitor and BMS777607-pan-TAM inhibitor to decide the best therapeutic target to take forward in a clinical study.

Chapter 2.0 – Materials and methods

2.1 Cell-culture

2.1.1 Tissue collection and ethics

The sporadic or NF2-associated schwannoma and meningiomas used in this study were obtained with patient's informed consent. The majority of schwannoma and meningioma samples used in this project were collected under 'Molecular Target (MOT) identification' project from Derriford Hospital, Plymouth (NHS Trust: R&D No: 14/P/056) and Bristol Southmead Hospital (NHS Trust: R&D No: 3458) following national ethical approvals (Research ethics committee (REC) No: 14/SW/0119; IRAS project ID: 153351) and received a unique MN numbers. J and SS specimen were collected via Brain archieve and information network (BRAIN UK) under ethical approval (REC No: 14/SC/0098; IRAS project ID: 143874, BRAIN UK Ref: 15/011). The project is also granted approval by Faculty Research Ethics and Integrity Committee (FREIC number for MOT project is 14/15-401 and for BRAIN UK, 14/15-450) Two normal meninges used in this project were obtained from Analytical Biological Services Inc. as frozen tissues and one was purchased as human brain cerebral meninges whole tissue lysate from Novus Biologicals® (NB820-59183; lot B105014).

2.1.2 Cell culture

Schwannoma and meningioma tumour samples were transported from the operation theatre to the laboratory in DMEM (Thermofischer Scientific, MA, USA), 10% FBS (Sigma-Aldrich, MO, USA), 500U/ml Pen/Strep (Thermofischer Scientific, MA, USA) and 2.5 μg Amphotericin B (Sigma- Aldrich, MO, USA). Upon arrival, a small tumour piece was cut and snap frozen in liquid nitrogen before transferring to -80°C for later use. The remaining tumour was incubated for 24 hours in petri dish containing DMEM supplemented with 10% FBS, 500U/ml Penicillin/Streptomycin, and 2.5 μg Amphotericin B in a 37°C and 5% CO_2.

On the next day, incubation media was replaced by digestion medium, containing DMEM, 10% FBS, 500U/ml pen/strep; 1.25 U/ml dispase and 160U/ml collagenase type – I for schwannomas and DMEM, 10% FBS, 100U/ml pen/strep and 40U/ml collagenase type – III for meningiomas. After overnight incubation in digestion medium, tumour samples were further mechanically dissociated with glass pipettes of decreasing diameter until a single-cell suspension was formed. The suspension was transferred to 50 ml falcon tubes and centrifuged for 5 minutes at 1200 rpm. The pellet was resuspended in respective media; DMEM, 10% FBS, 100U/ml pen/strep, 0.5 μM Forskolin (Tocris, Bristol, UK), 2.5 μg/ml Amphotericin (Sigma- Aldrich, MO, USA), 2.5 μg/ml insulin (Thermofischer scientific, MA, USA) and 10 nM β1- heregulin and 0.5 mM 3-isobutyl-1-methylxanthine (IBMX-BioTechne, MN, USA) for schwannomas and seeded into PLL (10 mg/ml) and LA coated 6-well plates (Greiner, USA). Meningiomas cells were cultured in 10% FBS, 1% glutamine, 1% pen/strep and 1% glucose medium. The characteristics of clinical samples used in this study has been provided in supplementary chapter 7.5, table-S1.

Ben-Men-I is a grade-I meningioma cell-line, originally created by Püttmann S et al via hTERT immortalization of meningioma cells derived from meningothelial meningioma attached to parietal falx of a 68-year old female (Puttmann et al., 2005). The cell-line was cultured in 10% FBS, 1% glutamine, 1% pen/strep and 1% glucose medium. A cryopreserved foetal derived human meningeal cells (HMCs), isolated from human leptomeninges, were bought from ScienCell™ at P0 and was cultured in the manufacturer's recommended media, meningeal cell media, ScienCell™.

2.1.2 Passaging and freezing down of cells

Primary cells and cell-lines were cultured in proliferation growth medium until confluent before being passaged. For passaging, cells were washed once in phosphate buffered saline (PBS) (Thermofischer Scientific, MA, USA) and then incubated with

trypsin/EDTA (Thermofischer Scientific, MA, USA) for 2 minutes at 37°C in incubator. Once the cells were detached, trypsin was neutralized with complete growth medium. Cells were collected and centrifuged for 5 minutes at 1200 rpm. The pellet was resuspended in an appropriate volume of culture medium and seeded in fresh flask/6-well plate.
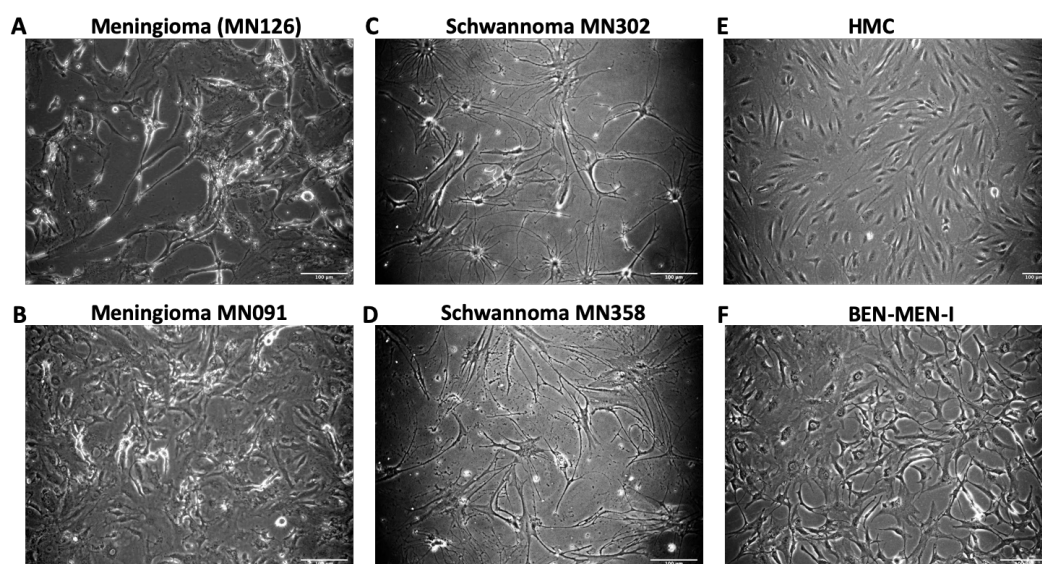
Figure 2. 1- Morphological appearances of the cells used in the project. Representative phase-contrast microscopy images of meningioma primary cells **A), B);** schwannoma primary cells **C), D)**; HMC **E)** and meningioma cell-line Ben-Men-I **F)**. Scale bar 100 μM

To freeze down the cells, pellet was resuspended in 1 ml of freezing medium (450 μl of complete media+450 μl of FBS and 100 μl of dimethyl sulphoxide (DMSO)). The resuspended cells were transferred to cryovial and stored at -80°C overnight in 'Mr Frosty' (Thermofischer Scientific, MA, USA) before transferring to the liquid nitrogen tank for long term storage.

2.1.3 Recovery of cryopreserved cells

The cryovial containing frozen cells were rapidly defrosted in 37°C water-bath by gentle swirling until small ice crystal remain in vial. The content of the whole vial was transferred gently to the bottom of 50ml sterile tube and then 11 ml of pre-warmed complete medium was added in a drop-wise manner to avoid any osmotic shock to the

cells. The cells were then seeded into a T75 flask. Media was changed next day with fresh medium to remove remaining DMSO.

2.1.4 Cell counting

To count the cells, pelleted cells were resuspended in 1 ml of media. 10 μl of cell-suspension was loaded to a hemocytometer counting chamber. Cells in 4 sets of 16 squares were counted under light microscope on 10X objective. Only the cells set within a square counted. The cell concentration was determined by diving total cell number by 4 and multiplying with 10^4 to derive final cells per millilitre.

2.2   Cell-treatments

2.2.1   Detection of cell-death and viability using the CytoTox-Glo™ assay

The CytoTox-Glo™ assay (Promega, Southampton, UK) is based on detection of the distinct intracellular protease activity which is released when cell-membrane is compromised. The membrane compromised 'dead cell-protease' cleaves a luminogenic peptide substrate - alanyl-alanylphenylalanyl-aminoluciferin (AAF) and produce a luminescence signal. Since the AAF substrate cannot cross the intact membrane of live cells and does not produce any appreciable signal from live and healthy cells, the amount of luminescence signal corresponds to the percentage of the cells undergoing cytotoxic stress.

All reagents were thawed at 37°C in water bath and mixed properly to ensure the homogeneity before an experiment. CytoTox-Glo™ cytotoxicity assay reagent was prepared by transferring the content of one bottle of assay buffer to the CytoTox-Glo™ substrate bottle and the lysis reagent was prepared by transferring 33 μl of digitonin to the 5 ml of assay buffer.

For the assay the cells were seeded into a white, flat, clear-bottomed 96 well plate at the desired number (2500 for schwannoma and meningioma primary cells, 1500 for Ben-

Men-I cell-line) in at least triplicates. The following day, cells were treated with the desired drug concentrations plus a vehicle control (DMSO/EtOH) at a final volume of 100 μl/well. Cells were incubated for either 72 hours or seven days before undergoing the Cyto Tox-Glo™ assay. Cyto Tox-Glo™ assay reagents were prepared as per manufacturer's instructions. 50 μl of AAF-Cyto Tox-Glo™ substrate mix was added per well, incubated 15 minutes at room temperature in the dark before quantifying luminescence corresponding to dead cell numbers with a microplate reader (BMG Labtech, Buckinghamshire, UK). 50 μl of prepared cell lysis digitonin mix was then applied to the wells before a further incubation of 15 minutes at room temperature in the dark. A second luminescence reading was taken corresponding to total cell numbers. Data was analyzed in Microsoft Excel. Total cell luminescence was determined as a percentage of control. Dead cells were determined as a percentage of total cells then as a percentage of control.

2.3   Quantifying Gas6 release from cells using enzyme-linked immunosorbent assay (ELISA)

HMC, Ben-Men-I and primary meningioma cells were cultured for seven days or until fully confluent in complete growth medium. Following that, medium was collected and centrifuged at 1500 rpm for 10 minutes at 4°C and concentrated 10x using Amicon ultra centrifugal filters (Millipore, Feltham, UK). Concentrated media samples were aliquoted and stored at -80°C until required. 100 μl of concentrated media samples or standards were loaded into each well (in duplicates) of Gas6 Enzyme-linked immune sorbent assay (ELISA) kit (RayBiotech- Catalog NO: ELH-GAS6) and incubated for 2.5 hours at room temperature with gentle shaking. Following that the wells were washed four times with 1X wash buffer (provided in the kit) before incubating with biotinylated antibody for one

hour at room temperature. The wells were washed once again and 100 μl of Streptavidin solution was added for 45 minutes and incubated at room temperature. Following final wash with 1x wash buffer, 100 μl of TMB one-step Substrate reagent was added to each well and incubated for 30 minutes in dark. Finally, 50 μl of stop solution added to each well and absorbance was read immediately at 450 nm using a microplate reader in order to gauge Gas6 concentration.

2.4 Lentivirus production and infection

2.4.1 Plasmid preparation

Lentiviral vectors pGIPZ and PLKO.1 containing TYRO3 (TYRO3 shRNA438; Clone ID- V2LHS_56438 and TYRO3 shRNA476; Clone ID- V3LHS_637476) and MERTK shRNA sequences (MERTK shRNA62; Clone ID - TRCN0000000862 and MERTK shRNA65; Clone ID- TRCN0000000865) were obtained as bacterial cultures of *E.Coli* (DH5α) in 2x LB-Lennox broth (low salt) medium with 8% glycerol and 100 μg/ml carbenicillin on dry ice from GE Healthcare (Dharmacon, IL, USA). To prepare the plasmid DNA, a loopful of glycerol stock was streaked onto LB agar plate containing 100 μg/ml carbenicillin (Sigma-Aldrich, MO, USA). Plates were incubated overnight in bacterial incubator at 37°C for the growth of antibiotic resistant colonies. The next day, single colony was picked from LB agar plate and amplified in 5 ml of LB broth containing 100 μg/ml carbenicillin and incubated at 37ºC with shaking at 200-250 rpm for 12-16 hours. Plasmid DNA was isolated from bacterial cells using Miniprep kit (Thermo scientific, MA, USA). Lentivirus particles containing a scrambled shRNA sequence were obtained from Dharmacon (RHS4348).

2.4.2 Plasmid DNA isolation: Miniprep

The GeneJET Plasmid Miniprep Kit (Thermo Scientific, MA, USA) was used for rapid preparation of high-quality plasmid DNA. The plasmid DNA was isolated and purified

using manufacturer's instructions. In short, the 5 ml of bacterial culture was centrifuged at 8000 rpm for 2 minutes at room temperature and the pelleted cells were resuspended in 250 μl of the Resuspension Solution. The cells were lysed by adding 250 μl of Lysis Solution and neutralized by adding 350 μl of Neutralization Solution. Following that the lysate was centrifuged for 5 minutes to pellet cell debris and chromosomal DNA. The supernatant containing plasmid DNA was transferred to the supplied GeneJET spin column and the column was centrifuged for 1 minute, followed by 2-3 more washes of column with Wash Solution. In the end, flow-through was discarded and column was centrifuged for additional 1 minute to remove any residual ethanol from plasmid preparation. Finally, plasmid DNA was eluted by adding 50 μl of Elution Buffer to the centre of GeneJET column. All centrifugation steps in the protocol were carried out at 12000 rpm, unless mentioned. The quantity and quality of isolated DNA was assessed using a Nano-drop (Thermo Scientific, MA,USA).

2.4.3   Lentivirus packaging

Both TYRO3 and MERTK shRNA constructs were packaged using second generation packaging plasmid. Low passage human embryonic kidney (HEK) 293FT cells (Thermofischer Scientific) were plated at a density around $2.5*10^6$ and incubated at 37°C and 5% CO_2 overnight in complete medium containing DMEM, 10% FBS, 500U/ml pen/strep; to achieve ~70-80% confluency on the day of transfection. HEK-293 cell-line is derived from human embryonic kidney (HEK) cells. 293FT cells are fast growing variant of 293 cell-line that contains SV-40 large T-antigen which allows the episomal replication of transfected plasmids containing the SV40 origin of replication (Oka et al., 2010). 5 μg of pLenti-shRNA constructs (TYRO3/MERTK) and 6 μg of packaging mix (Dharmacon- TLP4606) were added into 500 μl of Opti-MEM (reduced serum media – Thermofischer scientific). In a separate labelled tube, 44 μl of MegaTran 1.0 (Origene,

MD, USA) transfection reagent was added into 500 μl of Opti-MEM (Thermo Fischer Scientific, MA, USA). The content of both vials was mixed, vortexed and incubated 15-30 minutes at room temperature. Finally, the mixture of DNA and MegaTran were added directly to the 10cm dish of 293FT cells. After 12-18 hours of transfection, media was changed to reduced serum medium (complete growth medium containing 5% FBS). Viral particles were collected after 48 hours of medium change, centrifuged at 3000rpm to remove cellular debris, aliquoted and stored at -80°C until further use.

The titer of home-made TYRO3 shRNA438 was calculated to $7.9*10^5$ TU/ml and TYRO3 shRNA476 was calculated to $8.5*10^5$ TU/ml. Titration was performed by Dr Emmanuel Maze. The schwannoma cells were infected with multiplicity of infection (MOI of 10) in each case. Viral titer was unable to be determined for the home made MERTK shRNA (construct 862 and 865) lenti-viruses due to absence of GFP but 2 ml unconcentrated viral particles was sufficient for 80% knock-down of primary cells.

2.4.4 Pre-made MERTK, AXL and TYRO3 shRNA lentivirus particles

For infecting meningioma primary cells, I used commercially available MERTK shRNA1643 (clone-ID: V2LHS_1643), MERTK shRNA202 (clone ID: V3LHS_372202), MERTK shRNA205 (clone ID: V3LHS_372205), AXL shRNA030 (clone-ID: V3LHS_404030), AXL shRNA652 (clone ID: V3LHS_329652), AXL shRNA653 (clone ID: V3LHS_329653) and TYRO3 shRNA438 (clone ID: V2LHS_56438) and TYRO3 shRNA476 (clone ID: V3LHS_637476) constructs from GE Dharmacon. The titre of each lentivirus particles was $1x10^8$ TU/mL. I used 10 μl of pre-made lenti-virus particles (MOI-10) to infect cells in a 6-well plate. MOI was calculated by following formula; Number of virus particles (TU)/number of cells.

2.4.5　Lentivirus infection

Schwannoma and meningioma primary cells were split into 6-well plates (80,000 cells/well) the day before infection. The wells were coated with Poly L lysine (PLL-Sigma-Aldrich, MO, USA) and laminin (LA-Thermofischer Scientific, MA, USA) for schwannoma cells. Cells were infected with shRNA viral particles targeting AXL, MERTK and TYRO3 in the presence of 8 μg/ml protamine sulphate (Sigma-Aldrich, MO, USA)- polycation. Control cells were infected with non-targeted control or scrambled shRNA in the same manner. After infection cells were incubated at 10% CO_2 for 72 hours after which they were selected with puromycin (10 mg/ml-Sigma-Aldrich, MO, USA). All experiments included a 'non-infected' control well, in order to monitor the cell death upon puromycin selection. After selection, cells were lysed to extract protein and run on sodium dodecyl sulfate polyacrylamide gel electrophoresis (SDS-PAGE) to investigate the target gene knock-down.

2.5　Adenovirus infection

Human primary meningioma cells were plated a day before infection in 6-well plates according to an experiment. Cells were infected with either control GFP adenovirus or adenovirus expressing wild-type Merlin for 72 hours as described in (Ammoun et al., 2014), followed by cells-lysis using RIPA lysis buffer. The lysates were run on SDS-PAGE electrophoresis. Merlin (NF2) wild type (recombinant adenovirus AdNF2) and control GFP-containing vector adenoviruses were a kind gift from J. Testa (Xu and Gutmann, 1998).

2.6　Western blot

2.6.1　Protein extraction and quantification

Cultured cells were washed with ice-cold PBS before the addition of radioimmunoprecipitation assay buffer (RIPA) lysis buffer (150 mM NaCl, 0.5% sodium

deoxycholate, 0.1% SDS, 1% NP40, 50nM tris-HCl; pH-8), containing 1% complete protease inhibitor (Thermo-Scientific, MA, USA) and, 1% phosphatase inhibitor cocktail B and 1% phosphatase cocktail inhibitor C (SantaCruz Biotechnology, TX, USA) on ice. The lysate was collected and incubated on ice for 5 minutes before centrifuging at 13,000 rpm for 15 minutes at 4°C to remove cell debris. Following the centrifugation, the supernatant was transferred to a clean and labelled 1.5 ml Eppendorf tube and stored at -80°C until requierd. Pierce bicinchoninic acid (BCA) assay kit (Thermo Scientific, MA, USA) was used to quantify total protein concentration. The concentration of unknown protein was determined with reference to the standard concentration of Bovine Serum Albumin (BSA–2mg/ml), provided in the kit. The content of one Albumin Standard (BSA) ampule (2mg/ml) used to create various stock concentrations of 0, 25, 125, 250, 500, 750, 1000, 1500, 2000 μg/ml by diluting it into lysis reagent (RIPA/ low salt Triton X-100). The whole protein lysates were diluted to 1:5 and 12 μl of the standard and unknown protein samples were pipetted in duplicates into 96-well plate. 100 μl of working reagent (50:1, reagent A: B) was applied to each well containing sample or standard. Plate was briefly mixed on plate shaker for 30 seconds and incubated at 37°C for 30 minutes. The plate was allowed to cool at room temperature and absorbance was measured at 562 nM on microplate reader (BMG, Buckinghamshire, UK). The absorbance value (at 562 nM) of blank standard replicate was subtracted from the absorbance values of all other standard and unknown sample replicates. The average blank corrected values of the absorbance were used to plot the standard curve for each BSA standard concentration, and the protein concentration of an unknown sample was determined using the linear equation based on standard curve using Micorsoft Excel.

2.6.2 Sodium dodecyl sulphate- polyacrylamide gel electrophoresis (SDS-PAGE)

The proteins were separated according to size by an electrophoresis using discontinuous polyacrylamide gel system. A stacking gel of 4% (Table-2.1) and a resolving gel of 8% or 10% (Table-2.2) were used, throughout the experiments depending on the size of protein of interest. Spacer plate (1.5 mm) and short plate were fixed into the casting frame and placed into casting stand (Bio-Rad, Watford, UK). Firstly, the resolving gel was prepared and poured between the glass plates and layered with 50% isopropanol. Once the gel polymerised, isopropanol was removed, and gel surface was rinsed with distilled water before layering the stacking gel on top of the resolving gel. Comb was placed and allowed the gel to polymerise.

20 μg of total protein per sample was mixed with 4X loading buffer (250 mM Tris-HCl (pH-6.8), 8% SDS, 40% glycerol, 200mM DTT and 0.4% bromophenol blue (all Sigma-Aldrich, MO, USA) and boiled at 95°C for 5 minutes. The samples were allowed to cool at room temperature before loading into the gel and run at 120V for 100 minutes in 1X running buffer (200 ml 10X running buffer (Table-2.3) in 800ml of distilled water). 10 μl of precision plus prestained dual color protein ladder (Bio-Rad, Watford, UK) was loaded with samples as a standard size of protein.

10 ml	4%
H$_2$O	7.5 ml
Tris HCl 1.5M (pH 6.8)	1.25 ml
40% Acrylamide	1.0 ml
10% SDS	100 µl
10% APS	100 µl
TEMED	10 µl

Table 2. 1- Recipe for stacking gel.

10 ml	5% (100-250) KDa	10% (30-150) KDa
H$_2$O	5.9 ml	4.8 ml
Tris HCl 1.5M (pH 8.8)	2.8 ml	2.5 ml
40% Acrylamide	1.25 ml	2.5 ml
10% SDS	100 µl	100 µl
10% APS	75 µl	75 µl
TEMED	10 µl	10 µl

Table 2. 2- Recipe for resolving gel.

	Running buffer 5X	Transfer buffer 10X
Trizma base	22.7 g	45.5 g
Glycine	108 g	108 g
SDS	7.5 g	-
Distilled water	Up to 1.5 L	Up to 1.5 L

Table 2. 3- Recipe for Running buffers and Transfer buffer stock

2.6.3   Protein transfer and immunodetection

Separated proteins were transferred onto the activated polyvinylidene fluoride (PVDF)

membrane (Bio-Rad, Watford, UK) at 250 mA for 90 minutes in 1X transfer buffer

(100ml of 10X transfer buffer (Table 2.3) into 700ml of distilled water and 200ml of methanol) along with ice packs at 4°C. The membrane was then blocked for 1 hour with either 5% blocking milk (5% skim milk powder/ tris-buffered saline with 0.1% tween (TBST)) for total proteins or 5% BSA/TBST for phospho proteins. Following blocking, membrane was incubated with primary antibody (Table 2.4) of interest in 5% BSA/TBST at 4°C overnight on shaker. The following day, the membrane was washed three times for 10 minutes in TBST and incubated with corresponding secondary antibody (Table-2.5) for one hour at room temperature. The membrane was again washed 3-4 times for 15 minutes before detecting the protein bound antibody using enhanced chemical luminescence (ECL) detection system. In short, Pierce ECL western blotting substrate (Thermo- Scientific, MA, USA) or Pierce ECL Plus western blotting substrate (Thermo-Scientific, MA, USA) was poured onto membrane in the dark. After 3- 5 minutes, excess of ECL reagent was removed and the protein bands were detected using ECL hyper film (GE Healthcare, IL, USA) by exposing the films from few seconds to several minutes onto the membrane. ECL hyper films were developed using Xenograph compact X4 X-ray film processor (Thermofischer scientific, MA, USA).

Primary antibody	Species	Company	Catalogue NO	Dilution
AXL (C89E7)	Rabbit	CST, MA, USA	#8661	1:1000
TYRO3 (D38C6)	Rabbit	CST, MA, USA	#5585	1:500
MERTK (D21F11)	Rabbit	CST, MA, USA	#4319	1:500
Phospho AXL(Tyr702) (D12B2)	Rabbit	CST, MA, USA	#5724	1:500
Phospho TYRO3(Tyr681)	Rabbit	Biorbyt, Cambridge, UK	orb186274	1:500
Gas6 (D3A3G)	Rabbit	CST, MA, USA	#67202	1:500
Phospho MERTK	Rabbit	Fabgennix, TX, USA	PMKT-140AP	1:500

Merlin (D1D8)	Rabbit	CST, MA, USA	#6995	1:1000
Phospho Merlin (Ser518)	Rabbit	CST, MA, USA	#9163	1:500
GAPDH	Mouse	Millipore, Feltham, UK	MAB374	1:10,000
Anti-alpha Tubulin [DM1A]	Rabbit	Abcam, Cambridge, UK	ab7291	1:5000
Phospho-p44/42 MAPK (Erk1/2) (Thr202/Tyr204)	Rabbit	CST, MA, USA	#9101	1:1000
p44/42 MAPK (Erk1/2) (137F5)	Rabbit	CST, MA, USA	#4695	1:1000
Phospho AKT (Ser473) (D9E)	Rabbit	CST, MA, USA	#4060	1:1000
AKT (pan) (C67E7)	Rabbit	CST, MA, USA	#4691	1:1000
Phospho-SAPK/JNK (Thr183/Tyr185)	Rabbit	CST, MA, USA	#9251	1:1000
SAPK/JNK	Rabbit	CST, MA, USA	#9252	1:1000
Phospho FAK (Tyr397) (D20B1)	Rabbit	CST, MA, USA	#8556	1:1000
Total FAK	Rabbit	CST, MA, USA	#3285	1:1000
Cyclin-D1 (92G2)	Rabbit	CST, MA, USA	#2978	1:1000

Table 2. 4- Primary antibodies used to detect protein of interest in Western blot

Secondary antibodies	Type	Company	Catalogue NO	Dilution
Goat anti-Rabbit	HRP-conjugated	BioRad, Watford, UK	#170-6516	1:10,000
Goat anti-mouse	HRP-conjugated	BioRad, Watford, UK	#172-1019	1:10,000

Table 2. 5- Secondary antibodies used to detect primary antibodies in Western blot

2.6.4 Densitometry method

Films were scanned to create a digital image and Image-J software was used for densitometry quantification of protein band (Schneider et al., 2012). Blots were inverted prior to density measurement so that bands appear white on a black background. To take the measurments, rectangle tool was selected from Image J and adjusted to contain the whole of the largest band and was subsequently used to take densities of all other bands

across the row. The same frame was used to take the background measurement and was later substracted from each individual protein band measurement to get the net value of protein band of interest. All bands at the correct molecular weight ± approximately 5 kDa were measured for the target protein (uncropped Western blot images in chapter 7.4, Figure- S5). Any visible overlapping bands in this region were measured to ensure that the level of background signal substraction is appropriate to the background noise in the membrane and is not artificially affected by detected signal. Any other non-specific bands at different molecular weight was excluded. The same measurments were taken for loading control bands and their backgrounds correspond to each protein band. Finally, data normalization was performed by dividing the net value of target protein to the net value of loading control of that lane.

2.7 Co-immunoprecipitation (CO-IP)

2.7.1 Tissue homogenization

Schwannoma and meningioma tumour tissues as well as Ben-Men-I cell-line, were used for co-immunoprecipitation experiments instead of primary cells due to the large amount of proteins requirement. On receiving, larger piece of frozen schwannoma tissue was cut into small pieces whilst keeping it on dry ice. Smaller pieces were transferred into cold and fresh 1.5 ml Eppendorf tubes and stored at -80°C until further use. To homogenize the tissue pieces, 500 μl of ice-cold low salt Triton X-100 lysis buffer was used (30 mM Tris (pH 8.0), 75mM NaCl, 10% glycerol and 1% Triton X-100) for approximately 10-20 mg of tissue. The schwannoma tissue was added to pre-chilled homogenizer containing the low salt triton X-100 lysis buffer (supplemented with 1% complete protease inhibitor and 1% phosphatase cocktail B and phosphatase cocktail C and homogenized using up-down strokes of pestle on ice. Ben-Men-I cells were lysed using low salt triton X-100 as described in chapter-2.6.1. The tissue lysate was transferred to

fresh pre-chilled 1.5 ml eppendorf tube and centrifuged at 3000 rpm for 10 minutes at 4°C to remove any cell-debris. The supernatant was collected in pre-chilled 1.5 ml eppendorf tube and protein concentration was determined using BCA assay or aliquoted and stored at -80°C until further use.

2.7.2   Pre-IP bead washes and CO-IP incubation

To each 1.5 ml eppendorf tubes, 20 μl of protein G Sepharose beads (GE Healthcare, IL, USA) were added to a tube and washed 3-4 times with 1 ml of low salt Triton X-100 lysis buffer at 2000 rpm for 2 minutes at 4°C. To the washed beads tissue lysate (1 mg/ml) and antibody (Table-2.6) was added, tubes were sealed with parafilm and incubated at 4°C overnight on rotor. IgG (1 μg) antibody of the same species as IP-antibody was used as a negative control.

2.7.3   Post-IP bead washes and eluting the protein complex

The next day, beads were washed again for 6-7 times with 1 ml of low salt Triton X-100 lysis buffer at 2000 rpm for 2 minutes at 4°C to remove non-specific binding to beads other than IP-antibody/protein complex. The protein complex was eluted by boiling the beads at 95°C for 5 minutes in 40 μl 2X reducing sample buffer. The samples were allowed to cool at room temperature and finally centrifuged at 13000 rpm for 2 minutes to pellet the beads and supernatant was transferred to a fresh 1.5 ml of eppendorf tube. Samples were run using SDS-PAGE to detect the protein.

IP	Antibody	Species	Company	Catalogue NO	Dilution
AXL-IP	AXL	Rabbit	CST, MA, USA	#8661	1 μg/mg of lysate
TYRO3-IP	TYRO3	Rabbit	CST, MA, USA	#5585	5 μg/mg of lysate
MERTK-IP	MERTK	Rabbit	CST, MA, USA	#4319	1 μg/mg of lysate
IgG-IP	IgG	Rabbit	CST, MA, USA	#2729	1 μg/mg of lysate

Table 2. 6- List of primary antibodies used for co-immunoprecipitation

2.8   Immunohistochemistry (IHC)

Formalin fixed paraffin embedded (FFPE) thin tissue sections (4 μm) were cut and sections were baked at 60ºC for 10 minutes by the Department of Cellular and Anatomical Pathology at University Hospitals Plymouth. Sections were dewaxed and rehydrated by washing slides two times for five minutes in xylene (Thermo Fisher Scientific, MA, USA) and 100% ethanol (VWR®, PA, USA) respectively followed by wasing in running water for five minutes. The endogenous peroxidase activity is blocked by incubating slides in 3% hydrogen peroxide in methanol for 30 minutes at RT. The slides were washed in running tap water for 10 minutes before antigen retrieval by boiling slides in citrate buffer (pH 6.0) or EDTA buffer (pH 9.0) for 30 minutes. Following that slides were slides were quilibriated by washing them in TBST for five minuets and then blocked using 1% normal horse serum for 30 minutes before applying primary antibodies overnight.

The next day slides were washed two times for five minutes and biotinylated secondary and tertiary antibodies applied according to manufacturer's instructions (Vectastain Universal Elite ABC kit (Vector Laboratories Ltd, CA, USA). Slides were washed in TBST twice for five minutes and then 3,3'-diaminobenzidine (DAB (Sigma-Aldrich, MO, USA) solution was applied for five minutes. Slides were washed again in running tap water for five minutes before counterstained with Mayers Haemaatoxylin (Sigma-Aldrich, MO, USA) for two minutes and excess of solution was removed washing slides in running tap water for 10 minutes. Finally, the slides were washed twice in 100% ethanol and xylene before mounting with DPX (Sigma-Aldrich, MO, USA). Images were acquired by Leica DMRB and the scoring of staining intensity was performed with the help of consultant neuropathologist, Dr David Hilton (Department of Cellular and Anatomical Pathology at University Hospitals Plymouth).

Antibody	Species	Company	Catalogue NO	Dilution
AXL	Rabbit	Abnova, Taipei, Taiwan	PAB2999	1:100
pAXL (Y779)	Rabbit	R&D system, MN, USA	AF2228	1:500
MERTK	Rabbit	Abcam, Cambridge, UK	ab52968	1:1000
pMERTK	Rabbit	FabGennix, TX, USA	PMKT-140AP	1:250
TYRO3	Rabbit	ATLAS, Stockholm, Sweden	HPA071245	1:500

Table 2. 7- List of primary antibodies used for IHC

2.9   Immunocytochemistry/immunofluorescence (ICC/IF)

Schwannoma and meningioma primary cells were seeded on 8 chambered microscopic slides (Lab-Tek-Thermofischer scientific, MA, USA) until confluent in complete growth medium. To perform immunofluorescence staining, culture media was aspirated, and cells were washed with 1X PBS before fixing the cells with 4% paraformaldehyde (PFA) for 10 minutes at room temperature. Cells were permeabilized with 0.2% Triton X-100 for 5 minutes at room temperature. Cells were again washed three times for 5 minutes at room temperature with PBS, followed by blocking using 10% normal goat serum (NGS) in 1% BSA for 60 minutes at room temperature to block non-specific binding of antibodies. After an hour cells were again washed once with PBS and incubated overnight with primary antibody (Table-2.8). The following day, any unbound primary antibody was removed by washing the cells three times with PBS for five minutes and then the cells were incubated with corresponding secondary antibodies (Table-2.9) in 1% BSA and nuclear stain DAPI at concentration of 1:500 for 1 hour in the dark at room temperature. Lab-Tek chamber was removed and coverslip was applied to cells using vectashield antifade mounting media and slides were sealed using nail vanish to prevent drying and movement under microscope. Slides were imagined using 20X or 40X

magnification with Zeiss confocal microscope LSM510 and images were taken with

built-in CCD camera for digital imaging with LSM image software.

Primary antibody	Species	Company	Catalogue NO	Dilution
Ki67 (MIB-1)	Mouse	Agilent Technologies Ltd, CA, USA	M7240	1:100
Cleaved Caspase-3 (Asp175)	Rabbit	CST, MA, USA	#9661	1:100
AXL (C89E7)	Rabbit	CST, MA, USA	#8661	1:100
TYRO3	Mouse	Biorbyt, Cambridge, UK	orb167076	1:50
AXL (7E10)	Mouse	Thermofischer Scientific, MA, USA	MA5-15504	1:100
MERTK (D21F11)	Rabbit	CST, MA, USA	#4319	1:100

Table 2. 8- Primary antibodies used to detect protein of interest in ICC

Secondary antibodies	Type	Company	Catalogue NO	Dilution
Goat anti-rabbit	488	Thermofisher scientific, MA, USA	A11008	1:500
Goat anti-mouse	594	Thermofisher scientific, MA, USA	A11005	1:500

Table 2. 8- Secondary antibodies used to detect protein of interest in ICC

2.10 Data analysis

GraphPad Prism data analysis software was used throughout the project to calculate statistical significance in each experiment. Experiments were performed at least in triplicates unless otherwise mentioned. For statistical analysis Mann-Whitney test (for comparison of two columns) and Kruskal-Wallis test (for comparison of more than two columns) with Dunn's multiple comparison (to compare mean rank of each column to mean rank of every other column) or ANOVA with Dunnett's multiple comparison test (to compare mean of every column to mean of control column) was used. The p value was used to determine the significance of the results where ns= non-significant >0.05, *=$p<0.05$, **=$p<0.01$ and ***=$p<0.001$.

Chapter 3 – Results

3a – Expression and interaction of TAM receptors in Merlin-deficient tumours

3a.1 Characterize the expression of TAM receptors and their ligand Gas6 in meningiomas

<u>Introduction</u>

As previously mentioned, meningiomas are the most common intracranial brain tumours, responsible for ~30-40% of all cases. Meningiomas can exhibit wide variety of genetic alterations but interestingly all NF2-related meningiomas and ~50-60% of spontaneous meningiomas are linked to mutation in *NF2* and loss of protein Merlin (Riemenschneider et al., 2006). The large percentage of meningiomas, carrying *NF2* mutations provides an ideal opportunity to identify a novel candidate that is deregulated in all Merlin-deficient tumours and hence can be used as a common therapeutic target for treatment of all *NF2*-mutated tumours.

TAM receptors and their agonist Gas6 are overexpressed in several cancers including Merlin-deficient schwannomas as well as mesotheliomas, gliomas, melanomas, breast, colorectal and prostate cancer (Ammoun et al., 2014, Pinato et al., 2013, Pierce and Keating, 2014, Schwartz and Assoian, 2001, Holland et al., 2010, Schmitz et al., 2016, Wu et al., 2004, Jung et al., 2016). All three TAMs and their ligand Gas6 are known to be overexpressed and aberrantly regulated in human schwannoma primary cells and tissues. Moreover, expression of Gas6 and AXL was correlated with pathological proliferation, adhesion and survival of schwannoma cells (Ammoun et al., 2014). By performing IHC, our team previously showed higher expression of AXL, MERTK, pAXL and Gas6 in meningioma tissues compared to control tissues (Hilton et al., 2016). However, detailed investigation of the role of AXL or any other TAM members in pathophysiology of meningioma was not carried out at that point and authors warranted further investigation to examine the role of these receptors in meningioma development.

The aim of this chapter is to characterize the expression and activation of TAM receptors as well as their ligand Gas6 in Merlin-deficient meningioma tissues, primary cells and a cell-line using Western blotting. The status of *NF2* or Merlin expression was determined for each sample (including tissue and meningioma primary cell) by either *NF2* sequencing at the Manchester Centre for Genomic Medicine, Mangen (Manchester Department of clinical genetics) or by a Western blotting in the laboratory. Detail of *NF2* status and Merlin expression of all meningioma samples used in this chapter is described in supplementary section (supplementary chapter 7.5; table S1 and table S2).

3a.1.1 TAM receptors are highly expressed and activated in meningiomas

Firstly, I performed Western blot analysis to investigate the expression of total as well as phosphorylated form of AXL, TYRO3 and MERTK in Merlin-negative G (grade)-I, II and III meningioma tissues compared to normal meningeal tissue (NMT) as a control.

Notably, Western blot analysis showed an increased expression and phosphorylation of AXL and MERTK in all three meningioma grades with significant increases observed in the expression and phosphorylation of AXL in G-I and in phosphorylation of MERTK in G-II compared to NMT. There was no striking change in the levels of either phosphorylated or total AXL and MERTK between different meningioma grades. Variable expression and phosphorylation of TYRO3 was also observed in all three meningioma grades with no significant difference compared to NMT or between the different grades (Figure - 3.1 A and Figure - 3.1 B).
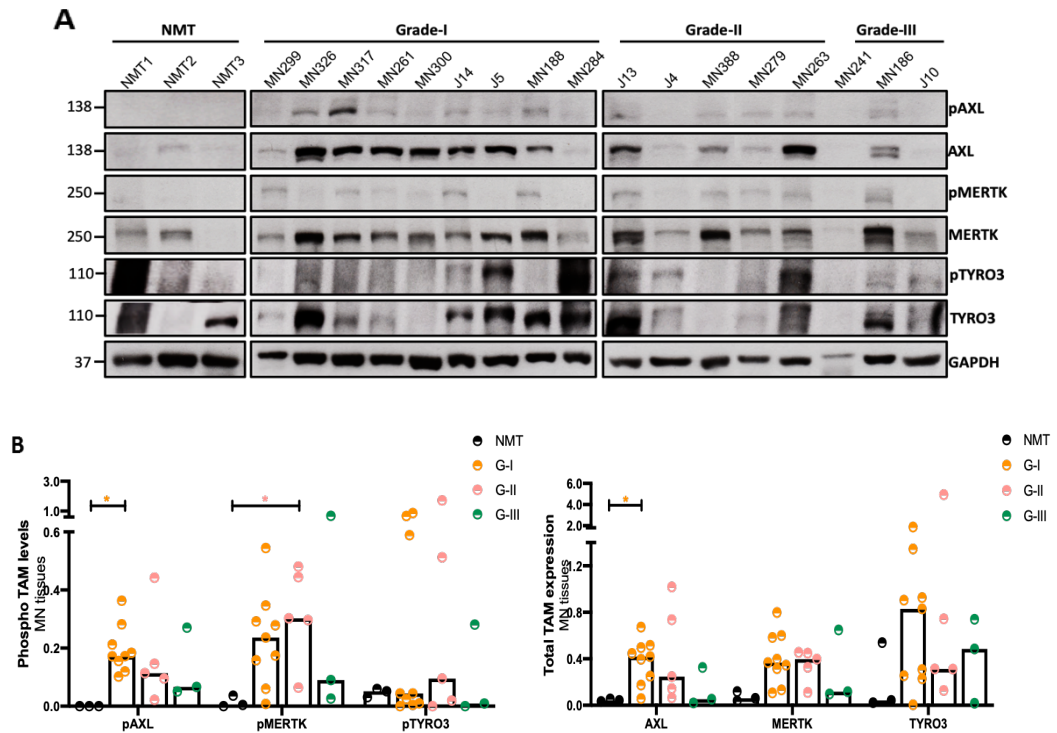
Figure 3. 1- AXL, MERTK and TYRO3 are highly expressed and activated in human Merlin-negative meningioma tissues. Western blot panel shows the expression and phosphorylation of AXL, MERTK and TYRO3 in different grades of Merlin-deficient meningioma tissues and NMT as a control. GAPDH was used as a loading control **A)**; A scatter plot shows the level of phosphorylated (left) and total (right) AXL, MERTK and TYRO3 in NMT (n=3), G-I (n=9), G-II (n=5) and G-III (n=3) meningioma tissues **B)**. Each dot in a scatter plot represents the data for an individual patient; the bar represents median value of phospho and total AXL, MERTK and TYRO3. Statistical difference was calculated using Kruskal-Wallis test followed by Dunn's multiple comparision test; * = p <0.05. NMT= normal meningeal tissue, G-I= grade I, G-II= grade II and G-III= grade-III. Membranes were firstly probed with phospho TAM antibodies and developed with ECL plus followed by reprobing with total TAM antibodies and developed with normal ECL or ECL plus. Phospho antibodies required much longer exposure time compared to total.

Additionally, I also examined the expression and phosphorylation status of TAM receptors in Merlin-negative, G-I meningioma primary cells and Ben-Men-I cell-line against normal human meningeal cells (HMC) as a positive control. HMCs are primary human meningeal cells, derived from healthy leptomeninges of foetus and Ben-Men-I is *NF2* mutated, WHO G-I cell-line, developed by retrovirally transducing primary cells derived from meningothelial meningiomas to surpass cellular senescence (Puttmann et al., 2005). Cryopreserved HMC and Ben-Men-I cells at passage 0 (P0) were bought from

Science cell research laboratories (Carlsbad, CA, USA) and DSMZ (Brunswick, Germany) company respectively.

Consistent with the results of tumour tissues, Merlin-negative G-I meningioma primary cells and a cell-line, Ben-Men-I displayed variable expression and phosphorylation of AXL, MERTK and TYRO3 receptors. Moreover, Merlin-deficient meningioma primary cells showed significantly higher phosphorylation of AXL and MERTK compared to Merlin-positive HMCs, whereas the Merlin-deficient meningioma cell-line, Ben-Men-I, showed prominently higher phosphorylation of these two proteins. However, this difference was statistically insignificant (Figure-3.2 A). There was no remarkable difference in the expression of AXL, MERTK and TYRO3 (Figure-3.2 B) or phosphorylation of TYRO3 (Figure-3.2 A) in Ben-Men-I and meningioma primary cells compared to HMC (Explanation of possible reasons in chapter-3.1.4).
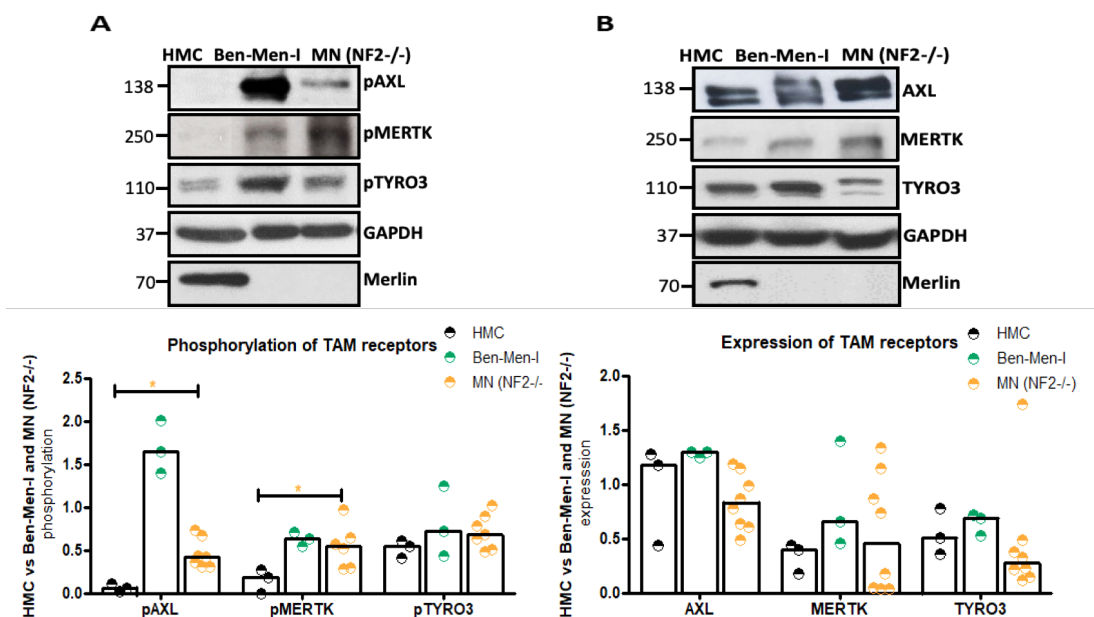
Figure 3. 2- Expression and phosphorylation of AXL, MERTK and TYRO3 in Merlin-negative (NF2-/-) human meningioma cells. Western blot of normal human meningeal cells (HMC, n=3) as a positive control, Merlin- negative meningioma cell-line, Ben-Men-I (n=3) and Merlin-negative meningioma primary cells (MN (NF2-/-), n=6 to n=8) showing **A)** the phosphorylation of AXL, MERTK and TYRO3; and **B)** the expression of AXL, MERTK and TYRO3. Merlin status of the samples were detected using a Western blot. Scatter graphs were plotted using GraphPad Prism software and it represents the data of each sample as an individual dot; the bar represents median value of phospho and total AXL, MERTK and TYRO3. Statistical difference for HMC vs Ben-Men-I and MN (NF2-/-) was calculated using Mann-Whitney test; * = p <0.05. GAPDH was used as a loading control.

3a.1.2 Gas6 is overexpressed and released from meningioma cells

Since Gas6 is highly expressed and released from Merlin-negative human schwannoma primary cells, I wanted to investigate whether this is also the case for Merlin-negative human meningioma cells and tissues. Western blot analysis showed variable expression of Gas6 in all three grades of meningiomas as well as NMT. However, the expression of Gas6 was slightly higher in G-I compared to NMT, G-II and G-III (Figure-3.3 A). Due to heterogeneity of meningiomas, the number of tumour tissues analyzed for Gas6 expression needs to be increased before drawing any conclusions.

Consistent with this finding, remarkably higher expression of Gas6 was also observed in G-I Merlin-negative meningioma primary cells and a cell-line, Ben-Men-I compared to HMCs (Figure-3.3 B).
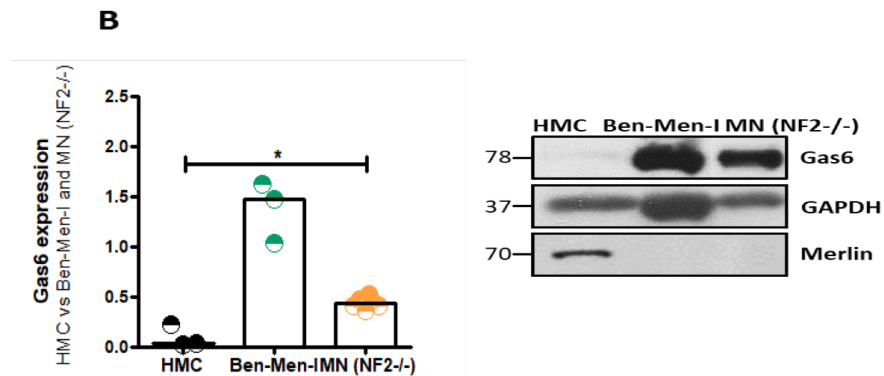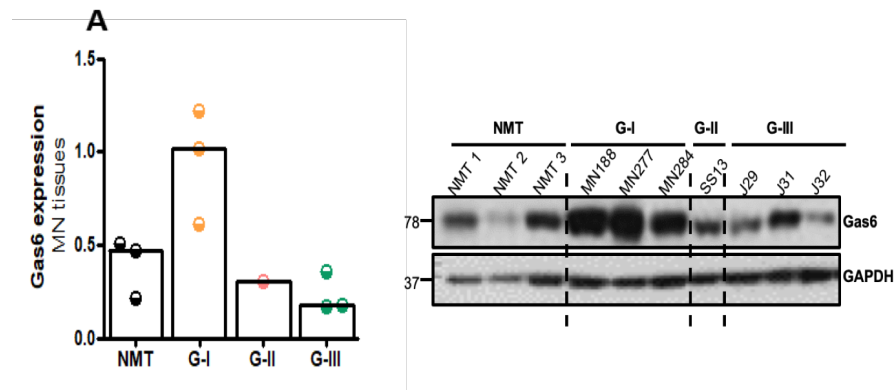
Figure 3. 3- Gas6 expression in meningioma tissues and cells. Western blot shows Gas6 expression in **A)** G-I (n=3), G-II (n=1) and G-III (n=3) Merlin-negative meningioma tissues compared to NMT (n=3); and **B)** Ben-Men-I (n=3) and Merlin-negative meningioma primary cells (n=6) compared to Merlin-positive HMC (n=3) as a positive control. Graphs are the quantification of band density, measured using Image J. Data were normalized to GAPDH. Bars represents the median value and statistical difference was calculated using Kruskal-Wallis and Dunn's multiple comparision post-hoc test (G-II, Gas6 expression was not included in statistical test) or Mann-Whitney test; * = p <0.05,

Next, I performed a Gas6 ELISA on cell-culture supernatant of HMCs, Ben-Men-I and meningioma primary cells to check whether Gas6 is released into cell-culture media. The results showed higher release of Gas6 from meningioma primary cells and Ben-Men-I cells compared to HMC cells, although this difference was statistically non-significant (Figure-3.4).
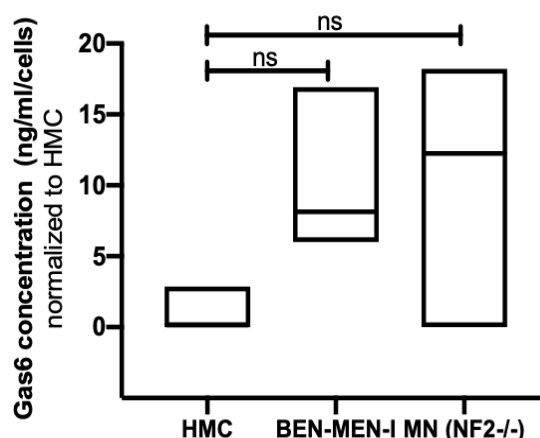
Figure 3. 4 - Gas6 release from meningioma cells. The graph shows the release of Gas6 from HMC (n=3) control, Ben-Men-I (n=3) and meningioma primary cells (n=5) by ELISA. Statistical difference for HMC vs Ben-Men-I and meningioma primary cells (MN (NF2-/-)) was calculated using Mann-Whitney test; ns=not significant.

3a.1.3 Overexpression of AXL, MERTK and TYRO3 but not Gas6 is Merlin-dependent in meningiomas

Overexpression of AXL, TYRO3 and Gas6 were due to loss of Merlin in schwannoma primary cells (Ammoun et al., 2014). Hence, I looked whether the expression of TAMs and their ligand Gas6 are also under negative regulation of Merlin in meningioma cells. In order to investigate this, I reintroduced Merlin using adenovirus to Merlin-negative meningioma primary cells. Merlin overexpression in these cells decreased the expression of AXL, TYRO3 and MERTK nevertheless, the expression of Gas6 remain unaffected (Figure-3.5 A and Figure-3.5 B). Successful reintroduction of Merlin was tested in each experiment by probing the membrane with anti-Merlin (NF2) antibody.
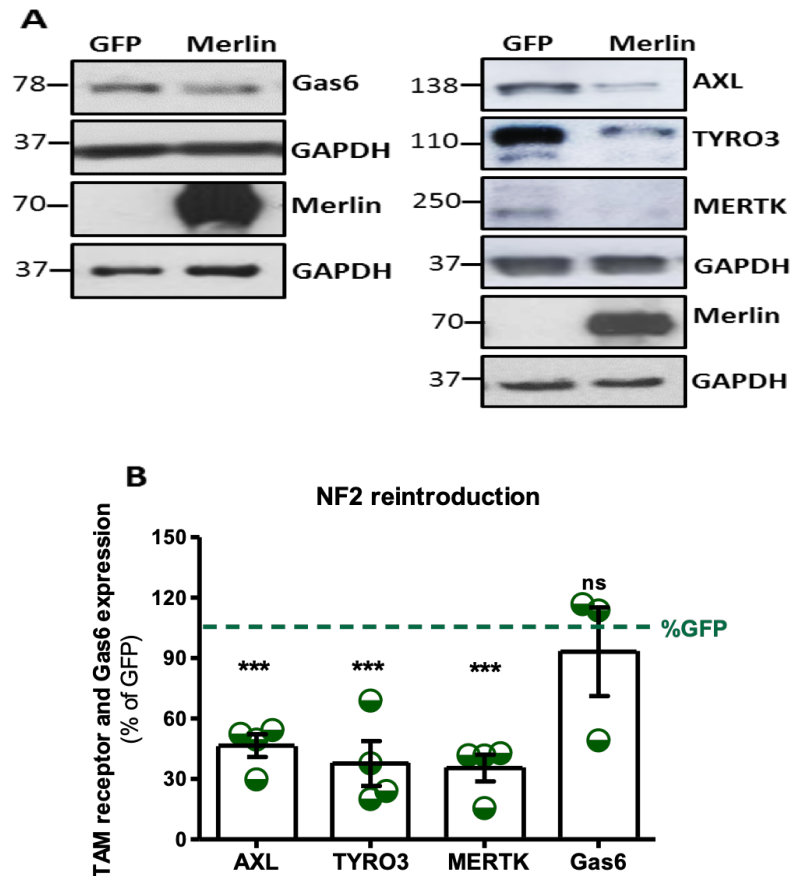
Figure 3. 5- Overexpression of AXL, TYRO3 and MERTK but not Gas6 is dependent on Merlin in Merlin-negative meningioma primary cells. Adenovirus containing GFP or NF2 constructs were used to infect Merlin-negative meningioma primary cells. Cells were infected for three days before lysis. Proteins were separated then, transferred to PVDF membrane and probed with AXL, TYRO3, MERTK and Gas6 antibodies. Merlin reintroduction was checked each time by probing the membrane with a Merlin (NF2) antibody. **A)** A representative Western blot images of AXL, TYRO3, MERTK and Gas6 on Merlin-reintroduction. GAPDH was used as a loading control; **B)** Scatter plots shows significant reduction in expression of AXL (n=4), TYRO3 (n=4) and MERTK (n=4) but not of Gas6 (n=3) on Merlin reintroduction. Data are represented as mean ± standard error of mean. Statistical calculations were carried out using ANOVA with Dunnett's multiple comparison test; *** = p <0.001 and ns=non-significant.

3a.1.4 Discussion

Like other cancers, high expression and activation of multiple growth factor receptors and their downstream signaling pathways is a signature event in the pathogenesis of meningiomas. Overexpression of TAM receptors and Gas6 has been associated with increased proliferation, survival, migration and multiple drug resistance in several cancers (Petrilli and Fernandez-Valle, 2016). The contribution of AXL in promoting pathogenesis of schwannomas has been previously established by our group, whereby, AXL, TYRO3, MERTK and Gas6 are all overexpressed and activated. The study also confirmed that the expression of AXL, TYRO3 and Gas6 but not MERTK, are under negative regulation of Merlin (Ammoun et al., 2014). Since, *NF2* mutations leading to Merlin loss is also the cause of all NF2-related meningiomas and 50-60% of spontaneous meningiomas (Hilton et al., 2016), I investigated whether this family of receptors and their ligand are also aberrantly regulated in Merlin-deficient meningiomas just as in schwannomas.

In search for growth factors and their receptors responsible for the development of meningiomas, Hilton *et al* broadly assessed the expression of several proteins in different grades of meningiomas and non-neoplastic meninges by performing immunohistochemistry (IHC). Interestingly, the authors found noteworthy differences in the staining of AXL, MERTK, Gas6 and pAXL between neoplastic and non-neoplastic meninges along with several other proteins (Hilton et al., 2016) and suggested further investigation of this important family receptors in meningioma pathogenesis. By performing Western blot analysis on different grades of meningioma tissues, I further verified the results of IHC and showed the higher expression and constitutional activation of all three TAM receptors as well as their ligand Gas6 in Merlin-deficient meningioma tissues compared to NMT (Figure-3.1 and Figure-3.3 A).

I further assessed the expression and phosphorylation of TAMs and Gas6 in Merlin-negative G-I meningioma cell-line; Ben-Men-I and in meningioma primary cells and found a wide spread expression of AXL, MERTK, TYRO3 and Gas6 in all primary meningioma samples and in Ben-Men-I (Figure-3.2 B and Figure-3.3 B). However, there was no significant difference in their expression except of Gas6, compared to HMCs. Of note, HMCs are derived from fetal leptomeninges and therefore may not recapitulate the real scenario of adult human tissue. Even though HMCs are not an ideal control for our adult primary meningioma cells, it was the only closest choice available during this project. Interestingly, further evaluation of phosphorylation status of TAMs in HMCs and meningioma cells revealed that TAMs, particularly AXL and MERTK, are present in an unphosphorylated form in HMC cells (Figure-3.2 A). Since the phosphorylation of RTKs is the major determinant of their activity compared to their expression, it can be concluded that all three TAM receptors are expressed and activated in Ben-Men-I and meningioma primary cells.

Increased basal activation of TAM receptors in meningioma tissues and cells may attribute to higher expression and release of Gas6 from these cells (Figure-3.4). Gas6 is a universal ligand that can bind and phosphorylate to all three TAM receptors with different affinity and has been shown to be highly expressed in tumour cells of gastric cancer, ovarian cancer and GBM (Sawabu et al., 2007, Sun et al., 2004, Hutterer et al., 2008). In addition, Gas6 is also highly expressed in tumour-associated cells such as macrophages. In fact, in human colorectal cancer, Gas6 has been shown to be mostly expressed and secreted by tumour-associated macrophages and communicate with tumour cells to act on TAM receptors (Schmitz et al., 2016, Loges et al., 2010). High infiltration of macrophages has also been described as the big phenomenon of schwannoma and meningioma tumours (de Vries et al., 2013, Domingues et al., 2013). Therefore, it is safe

to say that Gas6 released by tumour cells or by tumour micro-environment may have a role in activating TAM receptors in an autocrine or in a paracrine manner.

Again, the activation of TAM receptors is not exclusively due to only ligand Gas6. But proteins S, tubby, tulp-1, Galectin-3 have also been described to activate TAM receptors and their role in NF2-related tumours is completely unexplored (Caberoy et al., 2010, Caberoy et al., 2012). Alternatively, the possibility of ligand-independent activation of TAMs in NF2 tumours cannot be denied as many growth factors receptors such as EGFR, PDGFR, c-MET, HER2 with which TAMs have been shown to physically interact and trans-activate in a ligand-independent manner, are also over-expressed in schwannoma and meningioma tumours (Hilton et al., 2016, Hanemann, 2008).

Furthermore, there is little research available on the mechanisms responsible for TAMs and Gas6 overexpression in cancer in general. However, the reduction in expression of AXL, MERTK and TYRO3 in Merin-deficient meningioma primary cells upon Merlin re-introduction (Figure-3.5), suggest that Merlin may directly or indirectly regulate the expression of this family of receptors in Merlin-deficient tumours. Similarly, Merlin re-introduction also reduced the expression of AXL, TYRO3 and Gas6 in schwannoma primary cells but not of MERTK (Ammoun et al., 2014). In contrast, I found the expression of MERTK but not Gas6 is under negative regulation of Merlin in meningioma cells.

In summary, this is the first study reporting the levels of all three members of TAM receptors, their ligand Gas6, and the potential link to Merlin in meningiomas. Although much more future work is needed to understand the factors/mechanisms behind the overexpression and activation of TAM family receptors in this group of tumours, this data shows that TAMs are highly expressed and activated, and their expression at least partially is regulated by Merlin in meningioma, just as in schwannomas. Because this

family of receptors are also overexpressed in variety of other *NF2*-mutated tumours as described before (Pinato et al., 2013, Pierce and Keating, 2014, Schlegel et al., 2013, Holland et al., 2010, Schmitz et al., 2016, Wu et al., 2004, Jung et al., 2016), it is likely that TAM overexpression in these tumours may also be linked directly to Merlin loss.
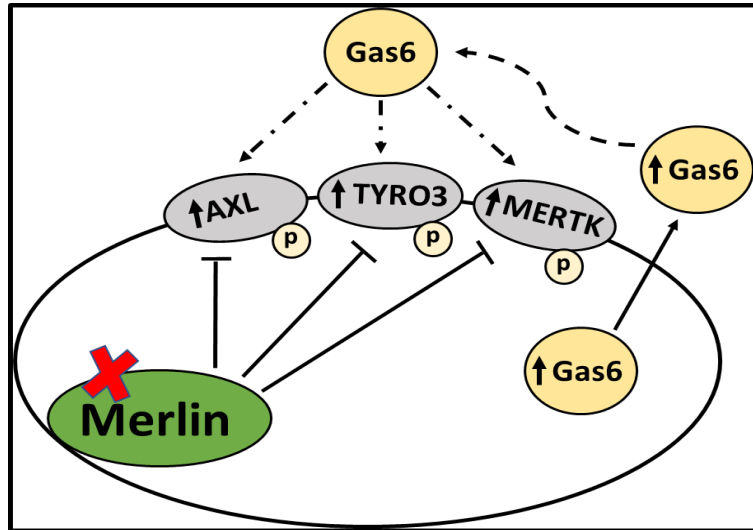
Figure 3. 6- Overexpression of TAM receptors and Gas6 in Merlin-deficient meningiomas. AXL, TYRO3, MERTK and Gas6 are highly expressed and activated in Merlin-deficient meningioma cells and tissues. Merlin (directly or indirectly) regulates the expression of AXL, MERTK and TYRO3 but not of Gas6. Highly expressed Gas6 is released by meningioma tumour cells or from the tumour microenvironment which can potentially activate TAM family receptors in an autocrine or in a paracrine manner.

3a.2 Interaction among TAM family receptors

Introduction

RTKs are a class of cell-surface receptors that transduce signal across cell-membrane and are essential for normal cellular processes. Nevertheless, aberrant regulation of RTKs is the cause of many pathological conditions including cancer. When overexpressed, RTKs can form homo or hetero-dimers in a ligand-dependent or in an independent manner. Such hetero-dimeric interactions among RTKs may influence the down-stream signaling of a target molecule by modifying the kinetic properties of enzymes, altering the specificity of a protein for its substrate or by creating a new binding site for small effector molecule and/or by directly inactivating/suppressing the target proteins. All these alterations may have a direct impact on the success of a targeted drug therapy (Rao et al., 2014).

Depending on the expression levels and membrane localization, TAM receptors have been shown to dimerize with non-TAM receptors. For example, AXL has been shown to physically interact with ErbB family members such as EGFR, HER2 and HER3 in several cancers including breast cancer, ovarian cancer, squamous cell-carcinoma and glioblastoma multiforme (Scaltriti et al., 2016, Vouri et al., 2016). Additionally, AXL is also reported to form a complex with other RTKs such as MET and PDGFR (Meyer et al., 2013). Through these physical interactions, AXL can amplify the down-stream signaling of its target protein or activate an alternate pathway to sustain tumour growth even in the presence of other tyrosine kinase inhibitors and thus may result in resistance to targeted drug therapy. Identifying protein-protein interaction and cross-talk among RTKs can therefore help deciding the suitable drug target or successfully predicting a combination drug therapy for patients.

Although physical complex among TAM family receptors has long been assumed, evidences showing such interaction among TAMs are lacking in cancer. AXL and

TYRO3 were found in complex in a human gonadotropin releasing hormone (GnRH) neuronal cell-line and have been shown to be important for promoting survival of neuronal cells (Pierce et al., 2008). Moreover, two separate studies reported that Gas6-mediated phosphorylation/activation of a TAM receptor requires the presence of one or both of the other TAM family members and that the surface expression of AXL is dramatically reduced in TYRO3 or MERTK knock-out platelet cells (Angelillo-Scherrer et al., 2005, Seitz et al., 2007). These evidences hint at the collaborative nature of TAM family receptors which appear to perform their actions as a team rather than working strictly individually.

As all three members of the TAM family and their ligand Gas6 are overexpressed in meningiomas and in schwannomas, I decided to investigate whether collaborative cross-talk among TAM family members exist in these tumours. This section explores the possibility of physical or functional dependency of TAMs on one another.

3a.2.1 MERTK forms a complex with TYRO3 in schwannoma and meningioma tissues

To investigate, whether there is physical interaction among TAM family receptors in Merlin-deficient tumours, I performed co-immunoprecipitation (CO-IP) experiments on Merlin-deficient schwannoma and meningioma tissue lysates as well as on the meningioma cell-line, Ben-Men-I. CO-IP experiments revealed the physical interaction between TYRO3 and MERTK (Figure-3.7 A) but not between AXL and MERTK (Figure 3.7 B) or AXL and TYRO3 (Figure 3.7 C) in schwannoma tissues
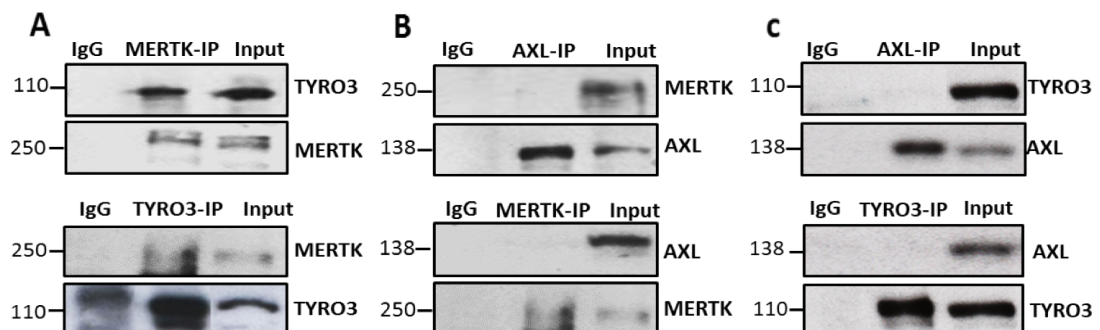
Figure 3. 7– Physical interaction among TAM receptors in schwannomas. Western blot analysis of immunoprecipitated schwannoma tumour lysates shows physical interaction between **A)** MERTK (upper) and TYRO3 (lower) (n=6); but not between **B)** AXL (upper) and MERTK (lower) (n=7) or **C)** AXL (upper) and TYRO3 (lower) (n=5).

TYRO3-MERTK complex was also confirmed in G-I, Merlin-deficient meningioma tissues (Figure-3.8 A) but not in Ben-Men-I cell-line (Figure-3.8 a), despite successful pull-down of the proteins. In addition, AXL and MERTK, as well as AXL and TYRO3, were also not in complex in either meningioma tissue lysates (Figure-3.8 B and Figure-3.8 C) or in meningioma cell-line Ben-Men-I (Figure-3.8 b and Figure-3.8 c).
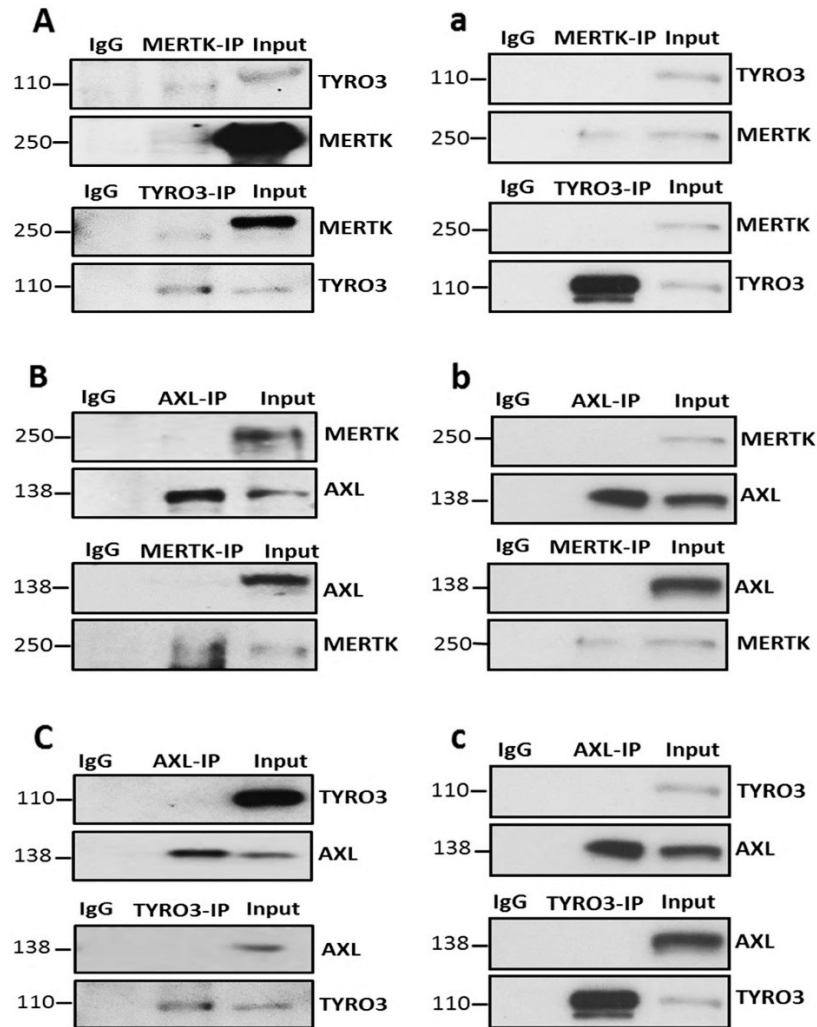
Figure 3. 8- Physical interaction among TAM receptors in meningiomas. Western blot analysis of immunoprecipitated Merlin-negative meningioma tumour lysates showed physical interaction between **A)** TYRO3 and MERTK but not between **B)** AXL-MERTK and **C)** AXL-TYRO3. No physical interaction between **a)** MERTK-TYRO3, **b)** AXL-MERTK or **c)** AXL-TYRO3 was observed in Ben-Men-I cell-line (n=3).

3a.2.2 Crosstalk among TAM family receptors

After confirming the physical interaction between TYRO3 and MERTK, I decided to further investigate the functional interaction among TAM family receptors. Since reports suggest that TAM receptors work in co-operation and require the presence of one or both of its TAM family members to function (Angelillo-Scherrer et al., 2005, Seitz et al., 2007), I checked whether the absence of one TAM receptor affects the expression of other TAMs in schwannoma and meningioma primary cells. To do so, I used home-made or commercially available lentivirus particles to knock-down the expression of a specific TAM receptor in primary cultured schwannoma and meningioma cells and analyzed the effect of knock-down on other TAM family members using a Western blot.

3a.2.2.1 MERTK knock-down decreases the expression of AXL and TYRO3 in schwannoma and meningioma primary cells

Using home-made lentivirus particles with two different MERTK shRNA constructs (Dharmacon, Inc), I successfully knocked-down the expression of MERTK protein compared to control scrambled (scr) shRNA in primary schwannoma cells (Figure-3.9 A and B). Interestingly, *MERTK* knock-down also significantly reduced the expression of AXL and TYRO3 in the same samples (Figure-3.9 A and Figure-3.9 B).
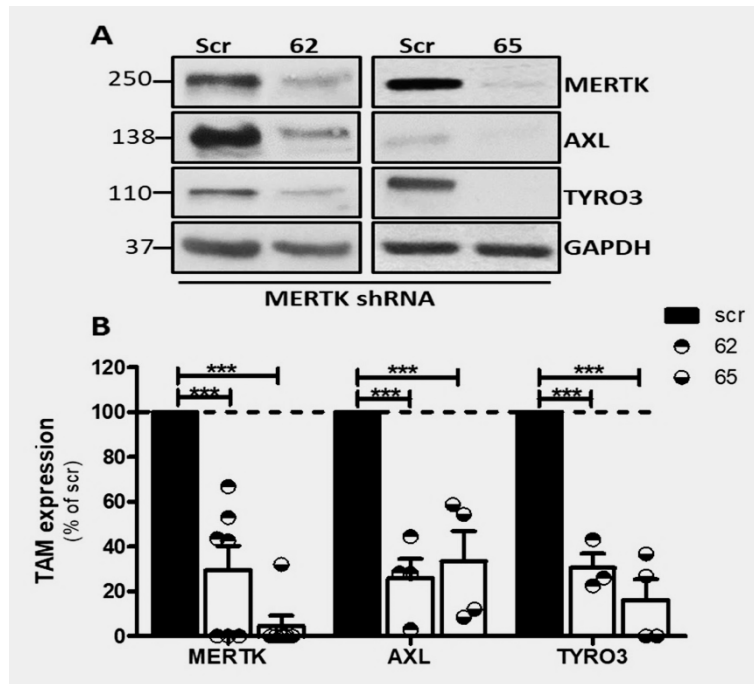
Figure 3. 9– *MERTK* Knock-down significantly decreases the expression of AXL and TYRO3 in schwannoma primary cells. Western blot analysis of schwannoma primary cells infected with scramble shRNA (scr- negative control) and MERTK shRNA (construct 62 and 65). **A)** Representative immunoblot shows the expression of MERTK (top panel), AXL (second panel) and TYRO3 (third panel) upon MERTK knock-down. GAPDH was used as a loading control; **B)** Scatter plot shows the relative expression of MERTK (n=7), AXL (n=4) and TYRO3 (n=3 or 4) in MERTK shRNA cells (construct 62 and 65) compared to scr shRNA. Data were normalized to scr and each dot in scatter graph represents an individual patient's knock-down data. Statistical calculations were performed with GraphPad Prism software using ANOVA with Dunnett's multiple comparison test. ***p<0.001.

To check whether this is the case also in meningiomas, I infected four different meningioma primary cells to knock-down MERTK expression. I used ready-made-lentiviral particles with two different MERTK shRNA (Dharmacon, Inc) constructs for the experiment due to time constraints to produce more home-made viruses. Unfortunately, out of four only two meningioma primary cells survived puromycin selection. Western blot analysis of two successfully infected meningioma samples revealed effective knock-down in MERTK expression with only one shRNA construct (Figure-3.10). Interestingly, prominent decrease in the expression of AXL and partial decrease in the expression of TYRO3 was consistent with a reduction in the expression of MERTK (Figure-3.10) as seen in schwannoma primary cells. Therefore, it is reasonable to suggest that the levels of AXL and TYRO3 in schwannoma and meningioma cells depend on MERTK expression.
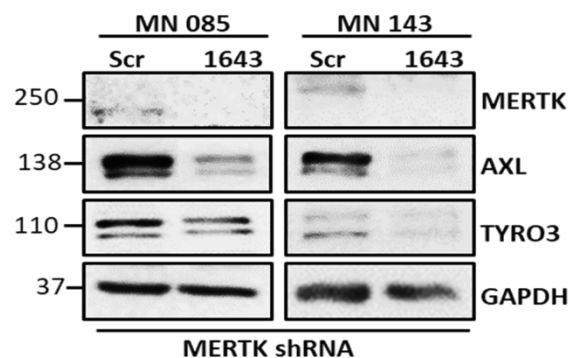
Figure 3. 10- *MERTK* **knock-down decreases the expression of AXL and TYRO3 in meningioma primary cells.** Western blot analysis shows a decrease in the expression of MERTK in two different meningioma primary cells using MERTK shRNA construct-1643 compared to Scr shRNA (top panel). MERTK shRNA also decreased the expression of AXL and TYRO3 (second and third panel respectively n=2). GAPDH was used as a loading control. The statistics was not performed due to small sample size.

3a.2.2.2 **TYRO3 and AXL knock-down does not affect the expression of other TAM members in schwannoma and meningioma primary cells**

Since MERTK and TYRO3 form a physical complex (Figure-3.7 A and Figure-3.8 A) and MERTK shRNA in schwannoma and meningioma cells decreased the expression of TYRO3 and AXL (Figure-3.9 and Figure-3.10), I decided to knock-down the expression of TYRO3 and of AXL to check whether this effect is reciprocal.

Western blot analysis of schwannoma primary cells infected with two different constructs (438 and 476) of TYRO3 shRNA confirmed prominent decrease in the expression of TYRO3 but reducing TYRO3 expression did not influence the expression of either AXL or MERTK (Figure-3.11).
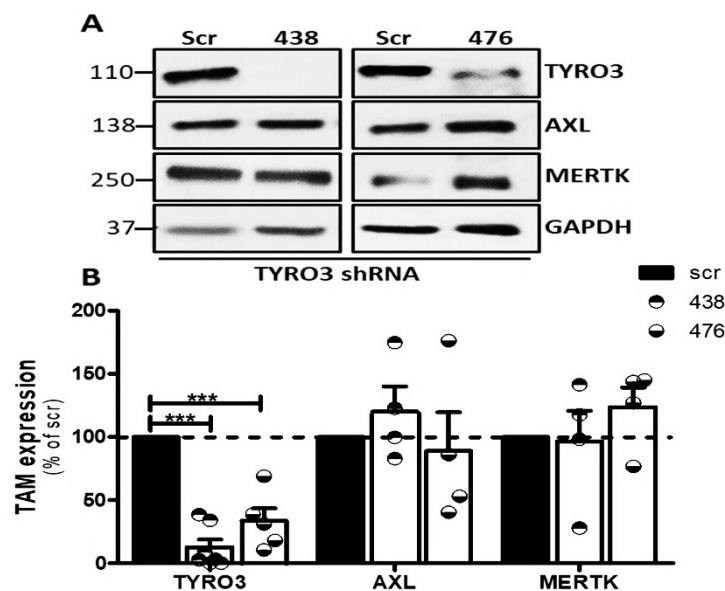
Figure 3. 11- *TYRO3* **knock-down does not affect the expression of AXL and MERTK in schwannoma primary cells.** Schwannoma primary cells were infected with scramble shRNA (scr-negative control) and TYRO3 shRNA (constructs 438 and 476) for 72 hrs or until all cells were GFP-positive. Cells were lysed and run on an 8% SDS-PAGE. **A)** Immunoblot showing the expression of TYRO3 (top panel), AXL (second panel) and MERTK (third panel) upon TYRO3 KD. GAPDH was used as a loading control; **B)** Scatter plot shows successful knock-down of TYRO3 (n=7 for 438 or n=5 for 476) and unaffected expression of AXL (n=4) and MERTK (n=4) upon TYRO3 knock-down. Each dot in scatter graph represents the knock-down data of an individual patient. Data were normalized to scr. ANOVA with Dunnett's multiple comparison test was performed using GraphPad Prism software. ***p<0.001.

Like MERTK shRNA in meningiomas, similar difficulty was faced when I tried to knock-down *TYRO3* and *AXL* in meningioma primary cells using two different shRNA constructs. Out of four different meningioma primary cells infected with TYRO3 and AXL shRNA, only one (MN 085) showed successful infection and knock-down of AXL and two (MN 085 and MN 143) gave efficient reduction in TYRO3 expression.

In accordance with schwannoma primary cells, both TYRO3 shRNA constructs (438 and 476) successfully knocked down the expression of TYRO3 in two different meningioma primary cells but did not influence the expression of either AXL or MERTK (Figure-3.12).
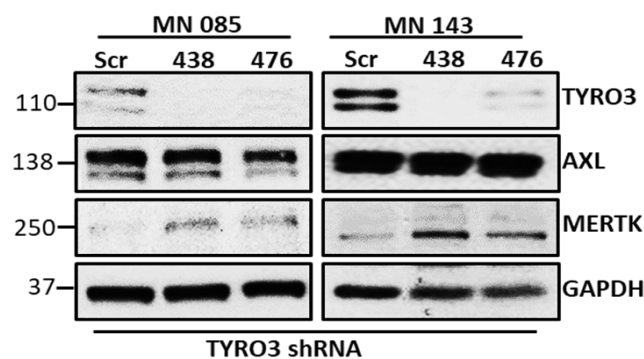
Figure 3. 12- ***TYRO3*** **knock-down does not affect the expression of AXL or MERTK in meningioma primary cells.** Infection of TYRO3 shRNA (438 and 476) in two different meningioma primary cells successfully decreased the expression of TYRO3 (top panel) compared to scr shRNA. Reducing TYRO3 expression did not influence the expression of either AXL (second panel) or MERTK (third panel), (n=2). GAPDH was used as a loading control. The statistics was not performed due to small sample size.

AXL shRNA specifically reduced the expression of AXL in meningioma primary cell without affecting total TYRO3 or MERTK expression levels (Figure-3.13). This was in accordance with AXL shRNA data from schwannoma primary cells (Ammoun et al., 2014).
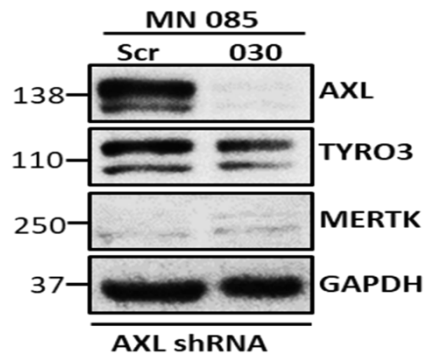
Figure 3. 13- *AXL* **knock-down does not affect the expression of TYRO3 or MERTK in meningioma primary cells.** Western blot of meningioma primary cells infected with scr and AXL shRNA (construct 030, n=1). AXL knock-down reduces the expression of AXL (top panel) but does not affect the expression of TYRO3 (second panel) and MERTK (third panel). GAPDH was used as a loading control.

3a.2.3 Discussion

Crosstalk among cell-surface receptors and their role in modulating extra-cellular stimuli to co-ordinate intrinsic cell response has been well documented in both physiological and pathological conditions. TAMs can communicate directly or indirectly with neighboring receptors and can be trans-activated by an alternate receptor in a ligand-dependent or independent manner to favor the tumour growth and survival. TAM family receptors are frequently involved in causing drug resistance by compensating the oncogenic signaling of a targeted receptor molecule in several cancers. In fact, AXL expression has been suggested as a strong predictor of resistance to ErbB family inhibitors (Meyer et al., 2013). Due to the established role of AXL in multiple drug resistance, most of the crosstalk studies have often centered around this TAM family member, whereas the role of TYRO3 and MERTK has remained widely unexplored.

When co-expressed in GnRH neuronal cells, AXL and TYRO3 coordinate their action to promote neuronal cell survival, migration and proliferation by forming a physical complex (Pierce et al., 2008). TYRO3 overexpression in Rat2 fibroblast cell-line resulted in AXL-TYRO3 dimerization and increased Gas6-mediated phosphorylation of AXL kinase (Brown et al., 2012). Despite of strong evidence in several systems suggesting a co-operative nature and an extensive crosstalk among TAM family members for normal physiological functions (Angelillo-Scherrer et al., 2005, Seitz et al., 2007), it is surprising that not many reports have paid attention at the crosstalk among TAM family members in cancer.

All three TAM receptors and their ligand Gas6 are highly expressed in Merlin-deficient schwannomas (Ammoun et al., 2014) and meningiomas (Figure-3.1, Figure-3.2 and Figure-3.3). In schwannomas, Ammoun *et al* showed the importance of AXL in mediating pathological proliferation and survival of the tumour cells but also anticipated

the involvement of other two members of this family in carrying out this action (Ammoun et al., 2014). Based on the previous data from our laboratory and from others, interaction or cross-talks among TAM members in schwannomas and menigniomas was suspected.

I performed co-immunoprecipitation (CO-IP) to unravel any potential physical interaction among TAMs in schwannomas and meningiomas. As CO-IP experiments require a large concentration of proteins to begin with, I chose to use a small piece of tumour tissue over precious primary cells which can grow only up-to limited number of passages. Moreover, using tumour tissue provides the advantage of studying endogenous protein-protein associations in their native form (Mohammed and Carroll, 2013).

CO-IP revealed a physical interaction between TYRO3 and MERTK in schwannoma and meningioma tissues. This is the first time that complex between TYRO3 and MERTK has been reported (Figure-3.7 A and Figure-3.8 A). In contrast to Merlin-deficient schwannoma and meningioma tissues, Merlin-deficient Ben-Men-I cell-line did not show physical interaction between TYRO3 and MERTK despite successful pull-down of both proteins (Figure-3.8 a). These differences may attribute to the tumour micro-environment. Schwannoma and meningioma tumours show significant infiltration by macrophages and to a lesser extent by lymphocytes, particularly T cells, NK cells and rarely B cells. In fact, macrophage infiltration is known to be pronounced in Merlin-deficient meningiomas compared to Merlin-positive (Domingues et al., 2016, de Vries et al., 2013). Infiltration of M2-polarized macrophages have also been confirmed in this study and showed that MERTK but not AXL or TYRO3 are highly expressed by M2-macrophages in meningiomas (supplementary chapter 7.3, Figure S3). The upregulation of MERTK, but not of AXL or TYRO3, has also been observed previously in tissue macrophages compared to circulating monocytes (Malawista et al., 2016).Therefore, it is highly likely that MERTK located on tissue macrophages and on tumour cells (supplementary chapter

7.3, Figure-S3) may physically interact with TYRO3 present mostly on tumour cells (supplementary chapter 7.3, Figure-S3) in schwannoma and meningioma tissues. Since cell-line cultures are generally devoid of immune cells such as macrophages, it may not necessarily always replicate the *in vivo* scenario. Ideally, CO-IP experiment should be performed on schwannoma and meningioma primary cells at lower passages which represent the closer view of tumour micro-environment. However, the limited availability of the primary cells made this difficult.

In addition, it has been reported that the physical interaction of endogenously expressed TYRO3 and AXL receptors is enhanced by stimulation of cells with Gas6 in glioblastoma multiforme (GBM) (Vouri et al., 2016). Since Gas6 is strongly expressed in both schwannoma (Ammoun et al., 2014) and meningioma tissues (Figure-3.3) it can potentially enhance TYRO3-MERTK complex formation in tissues, therefore, to prove this hypothesis the CO-IP in Ben-Men-I cells would need to be repeated in the presence of exogenously added Gas6.

Next, to address the functional importance of TYRO3/MERTK physical interaction in schwannoma and meningioma cells, firstly I knocked down the expression of MERTK using MERTK shRNA and found that reducing MERTK expression compromised the expression of TYRO3 and AXL (Figure-3.9 and Figure-3.10). To ensure MERTK shRNA mediated reduction in AXL and TYRO3 expression was not due to an off-target effect, three different MERTK shRNA constructs (TRCN0000000862, TRCN0000000865 and V2LHS_1643) were used. The specificity of the shRNA sequence was also confirmed by the providing company. Moreover, knock-down of MERTK using two of the same MERTK shRNA constructs, TRCN0000000862 and TRCN0000000865, by a different group in A549 NSCLC cells did not affect the expression of AXL (Linger R et al., 2013). Contrarily, lack of MERTK receptor has been shown to reduce the expression of AXL

on the surface of platelets (Angelillo-Scherrer et al., 2005) and TYRO3 in ratinal pigment epithelium (RPE) cells (Prasad et al., 2006), suggesting that the interdependent expression pattern of TAM receptors could be cell-specific.

MERTK shRNA-mediated decreases in AXL and TYRO3 levels that have been observed in this study could be either due to the involvement of MERTK in maintaining the stability of AXL and TYRO3 or due to MERTK-mediated transcriptional regulation of AXL and TYRO3 in schwannoma and meningioma cells. Firstly, to investigate if MERTK is involved in mediating the accumulation of AXL and TYRO3 at the plasma membrane, a surface biotinylating assay can be performed, a simple method to quantify total amount of cell-surface receptors (Arancibia-Carcamo et al., 2006). To examine the role of MERTK in maintaining the stability of these proteins cycloheximide chase assay can be done on MERTK knock-out and MERTK-expressing cells. Cycloheximide chase assay assess protein stability by blocking protein synthesis using cycloheximide and measuring the changes in the level of a protein of interest at different time points (Buchanan et al., 2016). Alternatively, the control and MERTK knock-out cells can be treated with proteasomal degradation inhibitor MG132 followed by Western blotting to examine whether MERTK inhibits proteasomal degradation of AXL and TYRO3.

To investigate if MERTK regulates the transcription of AXL and TYRO3, qPCR would need to be performed on cells infected with MERTK shRNA or control shRNA. Although there is no direct evidence suggesting an involvement of MERTK in regulating transcription of AXL and TYRO3, MERTK has been shown to phosphorylate transcription factor, cAMP response element-binding protein (CREB) and phosphorylated CREB has, in turn, been shown to regulate the transcription of AXL and TYRO3 by binding to their promoter (Linger et al., 2013, Kokkinaki et al., 2013, Schulz et al., 1993). Additionally, the presence of MERTK in nucleus of leukemia cells has been

reported recently, further raising the possibility of an undiscovered role of MERTK as a transcription factor (Migdall-Wilson et al., 2012). Therefore, I would like to study the possibility of above mentioned both mechanisms to get further insight into phenomenon observed in this study.

In contrast to MERTK knock-down, reducing TYRO3 and AXL levels did not affect either the expression of MERTK or of each other in both schwannoma and meningioma cells (Figure-3.11, Figure-3.12 and Figure-3.13). Similarly, macrophages lacking AXL or TYRO3 had no effect on the expression of MERTK, but instead diminished MERTK phosphorylation (Seitz et al., 2007). In addition, when in complex, TAM receptors have been shown to cross-phosphorylate each other (Brown et al., 2012). Therefore, the role of AXL and TYRO3 in promoting the phosphorylation of MERTK as well as cross-phosphorylation of each other in schwannoma and meningioma cells cannot be excluded. Next, it will be important to check the level of pMERTK in the absence of AXL and TYRO3; and the level of pAXL and pTYRO3 when the cells are infected with TYRO3 shRNA and AXL shRNA respectively (Figure-3.14 b and c).

Although this study did not explore the above-mentioned possibilities due to time and technical limitations, the results emphasize the co-operative nature of TAMs in schwannoma and meningioma tumours and highlight the need for future work in this area to unravel the crosstalk among TAMs and therefore gain a better understanding of their role in tumour biology.
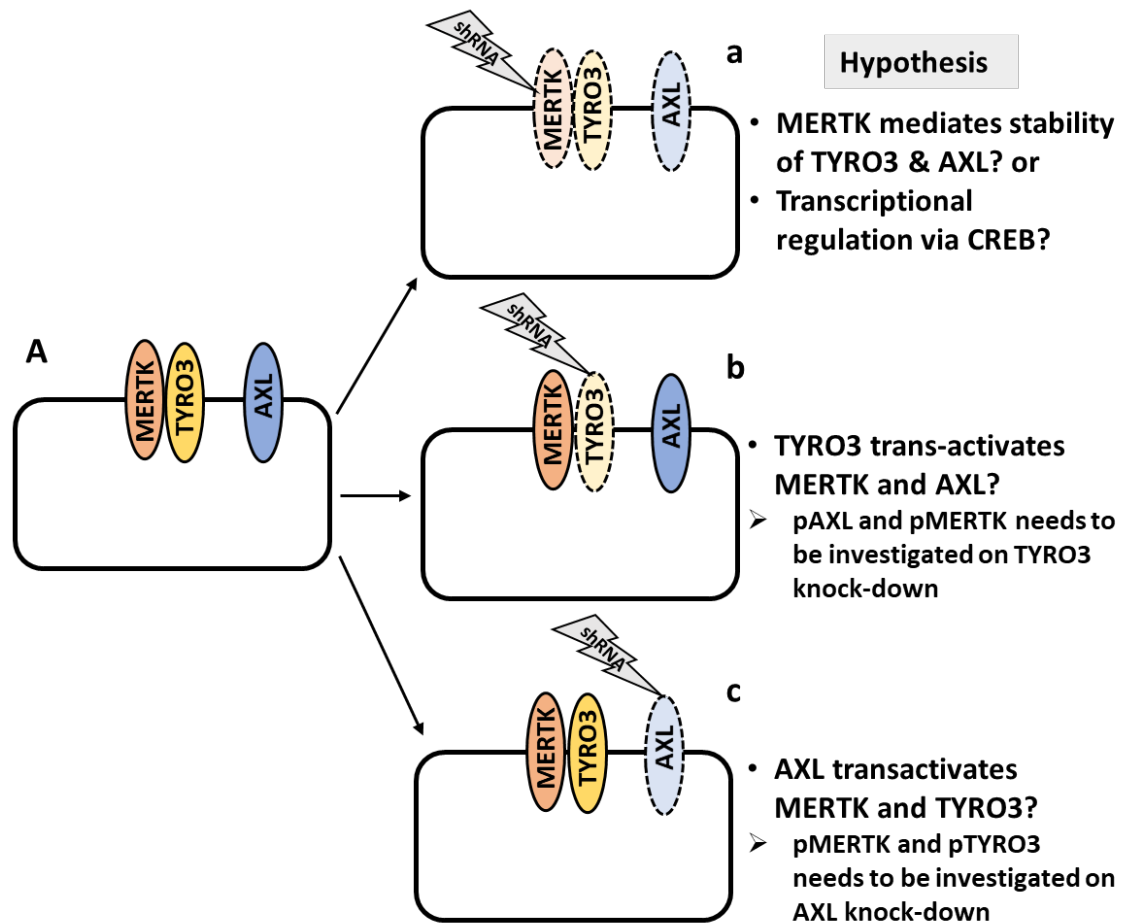
Figure 3. 14 Interaction and crosstalk among TAM family receptors. Results showed that TYRO3 and MERTK form a complex **A);** Knock-down of MERTK decreases the expression of TYRO3 and AXL **a);** TYRO3 knock-down did not have effect on expression of either AXL or MERTK **b**); Expression of TYRO3 and MERTK remained unaffected upon AXL knock-down **c).** Dashed lines indicate reduced expression of the protein**.**

Chapter 3b – Targeting TAM receptors in Merlin-deficient tumours

3b.1 The role of TAM receptors in schwannoma and meningioma pathophysiology

<u>Introduction</u>

By reducing AXL expression using AXL shRNA, our group has previously shown its positive effect on reducing schwannoma cell growth *in vitro* (Ammoun et al., 2014). Here I wanted to investigate the role of remaining two members of the TAM family in schwannoma tumorigenesis and all three members in meningioma tumorigenesis. To determine the role of MERTK, AXL and TYRO3 in schwannoma and meningioma pathogenesis, firstly I specifically depleted each TAM receptor using lentivirus-mediated knock-down and looked for changes in proliferation of cells by detecting the expression of cyclin-D1 compared to control cells.

Cyclin-D1 plays a central role in the regulation of proliferation via promoting the cell-cycle progression through the G1/S phase. Merlin has been reported to exert its anti-proliferative effect partly by repressing cyclin-D1 and causing cell-cycle arrest. Loss of Merlin has been shown to be responsible for increases cyclin-D1 expression and increased S-phase entry in mesothelioma cells (Xiao et al., 2005). Cyclin-D1 has thought to promote the proliferation and differentiation of breast cancer cells by shortening the G1/S phase transition (Colozza et al., 2005). Overexpression of cyclin-D1 has been also linked to Merlin-deficient schwannomas (Colozza et al., 2005, Zhou et al., 2011). However, the expression of cyclin-D1 is not clear in G-I Merlin-deficient meningiomas and therefore, firstly I checked the expression of cyclin-D1 in Merlin-deficient G-I meningioma cells compared to HMCs.

3b.1.1 Cyclin-D1 is highly expressed in G-I Merlin-deficient meningioma primary cells and Ben-Men-I cell-line

Western blot analysis revealed a prominent increase in cyclin-D1 levels in Merlin-deficient meningioma primary cells and Ben-Men-I cells compared to Merlin-positive HMC cells (Figure-3.15).
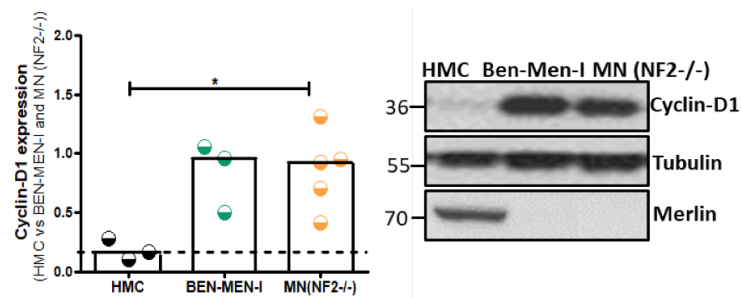
Figure 3. 15- Expression of Cyclin-D1 in meningioma cells. Western blot analysis showed higher expression of cyclin-D1 in Ben-Men-I (n=3) and meningioma primary cells (n=5) compared to HMCs (n=3) as a control. Tubulin was used as a loading control. Bars represents the median value and statistical difference was calculated using Mann-Whitney test, *p<0.05

3b.1.2 Knock-down of MERTK and AXL but not TYRO3 decrease cyclin-D1 levels in schwannoma and meningioma primary cells.

Western blot analysis showed that reducing the expression of MERTK using MERTK shRNA in primary schwannoma cells (Figure-3.16 A) and primary meningioma cells (Figure-3.16 B) led to a substantial reduction in cyclin-D1 expression.
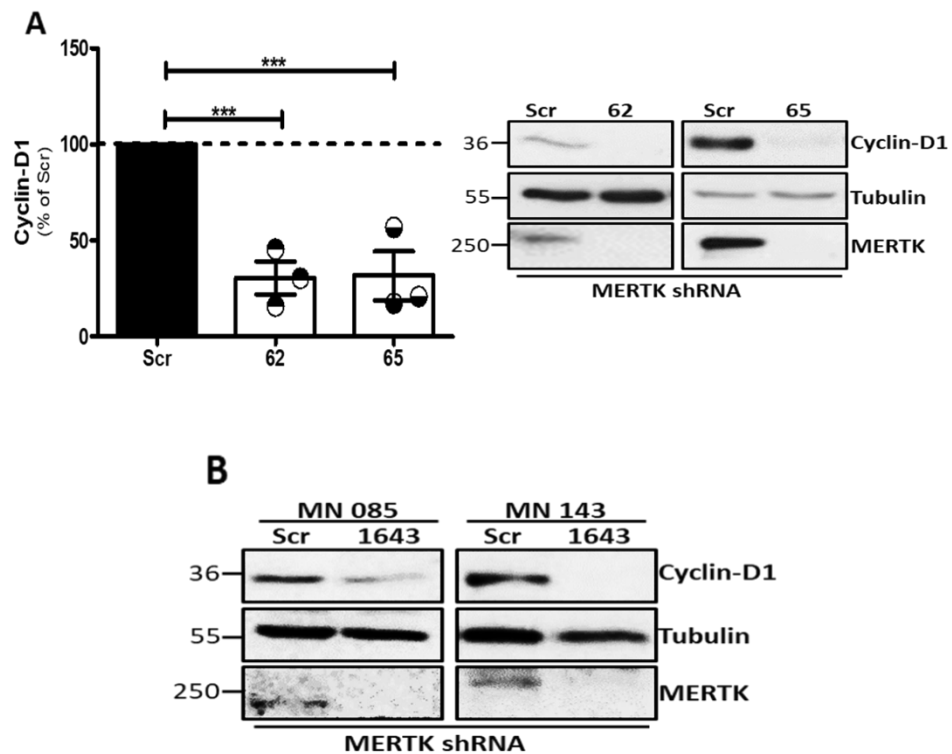
Figure 3. 16- Reducing MERTK expression decreases cyclin-D1 expression in schwannoma and meningioma primary cells. Representative Western blot showing knock-down of *MERTK* with MERTK shRNA (constructs 62, 65 and 1643) in schwannoma (n=3) A); and meningioma primary cells (n=2) **B)**, resulted in decreases in cyclin-D1 levels. The successful knock-down of MERTK was achieved in all experiments (bottom panels). scramble (scr) was used as a negative control and tubulin as a loading control. Statistical significance for schwannoma primary cells were calculated by ANOVA with Dunnett's multiple comparison test using GraphPad Prism analysis software, ***p<0.001 A); Statistical calculations were not carried out for meningioma primary cells due to small sample size B).

A successful AXL knock-down in meningioma primary cells using AXL shRNA (construct 030) also efficiently decreased the cyclin-D1 levels compared to control (Figure-3.17). This result was in accordance with AXL knock-down results in schwannomas although more repeats are required in meningioma cells before a firm conclusion can be drawn (Ammoun et al., 2014).
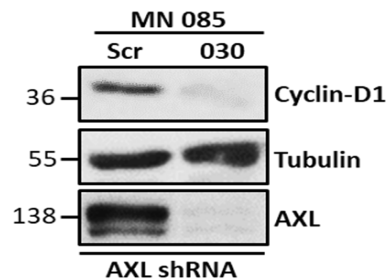
Figure 3. 17- Reducing AXL expression decreases cyclin-D1 expression in meningioma cells. Western blot analysis shows that successful knock-down of AXL expression (shRNA construct 30) in meningioma primary cells (bottom panel, n=1) led to decreased expression of cyclin-D1 (top panel). Tubulin was used as a loading control (central panel). Statistical analysis was not possible due to the low sample size.

In contrast to MERTK and AXL, TYRO3 knock-down did not affect the cyclin-D1 levels in either schwannoma (Figure-3.18 A) or meningioma primary cells (Figure-3.18 B).
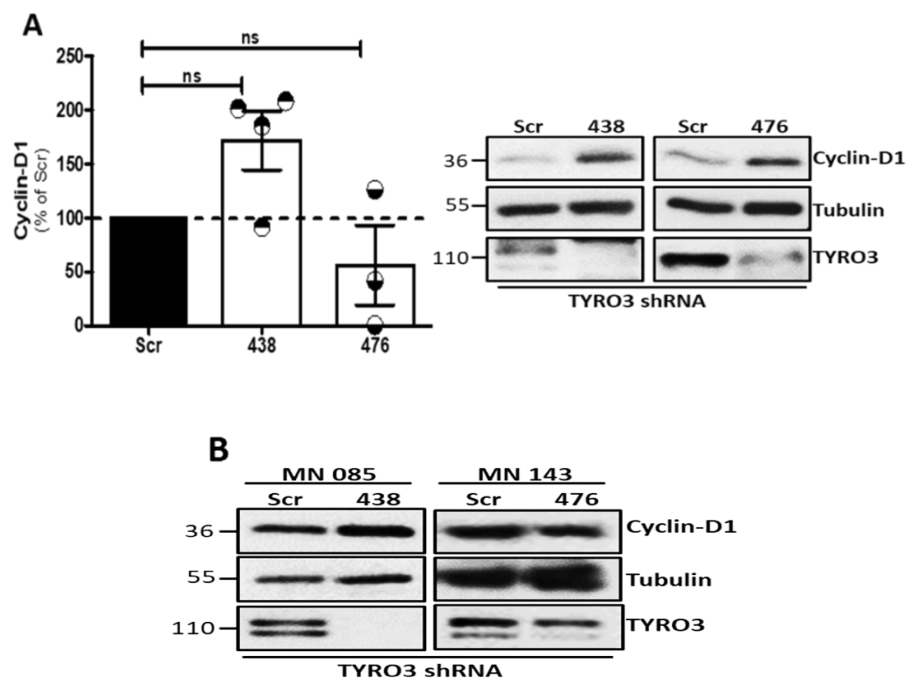
Figure 3. 18- Reducing TYRO3 expression did not have any effect on cyclin-D1 expression in schwannoma and meningioma primary cells. TYRO3 shRNA (construct 438 and 476) decreased TYRO3 expression in schwannoma primary cells (bottom panels, n=3 for 476 or n=4 for 438) **A)** and meningioma primary cells (bottom panels, n=2) **B)**, with no effect on the expression of cyclin-D1 (A and B, top panels). Tubulin was used as a loading control (A and B, central panels). ANOVA with Dunnett's multiple comparison test was used to assess statistical significance for schwannoma primary cells, ns=non-significant (A); sample size was small to calculate statistical significance in meningioms (B).

3b.1.3 TAM inhibition by small molecule inhibitors decrease proliferation and survival of schwannoma and meningioma primary cells.

Genetic knock-down of TAM receptors proposed that both MERTK and AXL are involved in the increased proliferation of schwannoma and meningioma primary cells via cyclin-D1 (Figure-3.16 and Figure-3.17), suggesting that both receptors may be potential therapeutic targets in these tumours. Therefore, I further tested the effect of MERTK/FLT3 inhibitor UNC2025, AXL specific inhibitor BGB324 and pan-TAM inhibitor BMS777607 on proliferation and survival of schwannoma and meningioma primary cells as well meningioma Ben-Men-I cell-line.

3b.1.3.1   Cytotoxicity assay

I performed high throughput screening (HTS) for UNC2025, BGB324 and BMS777607 using Cyto-Tox Glo^{TM} (Promega) assay to assess the effectiveness of these compounds in Merlin-deficient schwannoma and meningioma primary cells as well as cell-line, Ben-Men-I. The assay measures the number of dead cells and total cells following an exposure to a test compound.

3b.1.3.1.1 UNC2025

UNC2025 significantly inhibited schwannoma cell growth by 50% at 3.96 μM with a concomitant increase in number of dead cells following 72 hrs of treatment. Prolonged treatment of schwannoma primary cells with UNC2025 for 7 days further slightly decreased the number of total cells with IC_{50} of 3.09 μM with no additional cytotoxicity (Figure-3.19 A and Figure-3.19 a).

UNC2025 was more effective at inhibiting meningioma cell growth compared to schwannoma. It potently reduced Ben-Men-I and meningioma primary total cell number with IC_{50} of 1.95 μM and 1.45 μM respectively, which was almost half the concentration required to inhibit schwannoma cell numbers by 50% after 72 hrs. Interestingly, after 72

hrs, the drug did not induce cell-death in meningioma primary cells but only in Ben-Men-I cells which showed significant increase in dead cells at 3 μM, suggesting that UNC2025 is cytostatic to meningioma primary cells at shorter time period. UNC2025 was cytotoxic to both Ben-Men-I and meningioma primary cells at higher concentrations after 7 days and led to further decreases in total cell numbers (IC_{50} Ben-Men-I- 1.08 μM and IC_{50} meningioma primary cells- 0.47 μM) (Figure-3.19 B and b) (Figure-3.19 C and c).
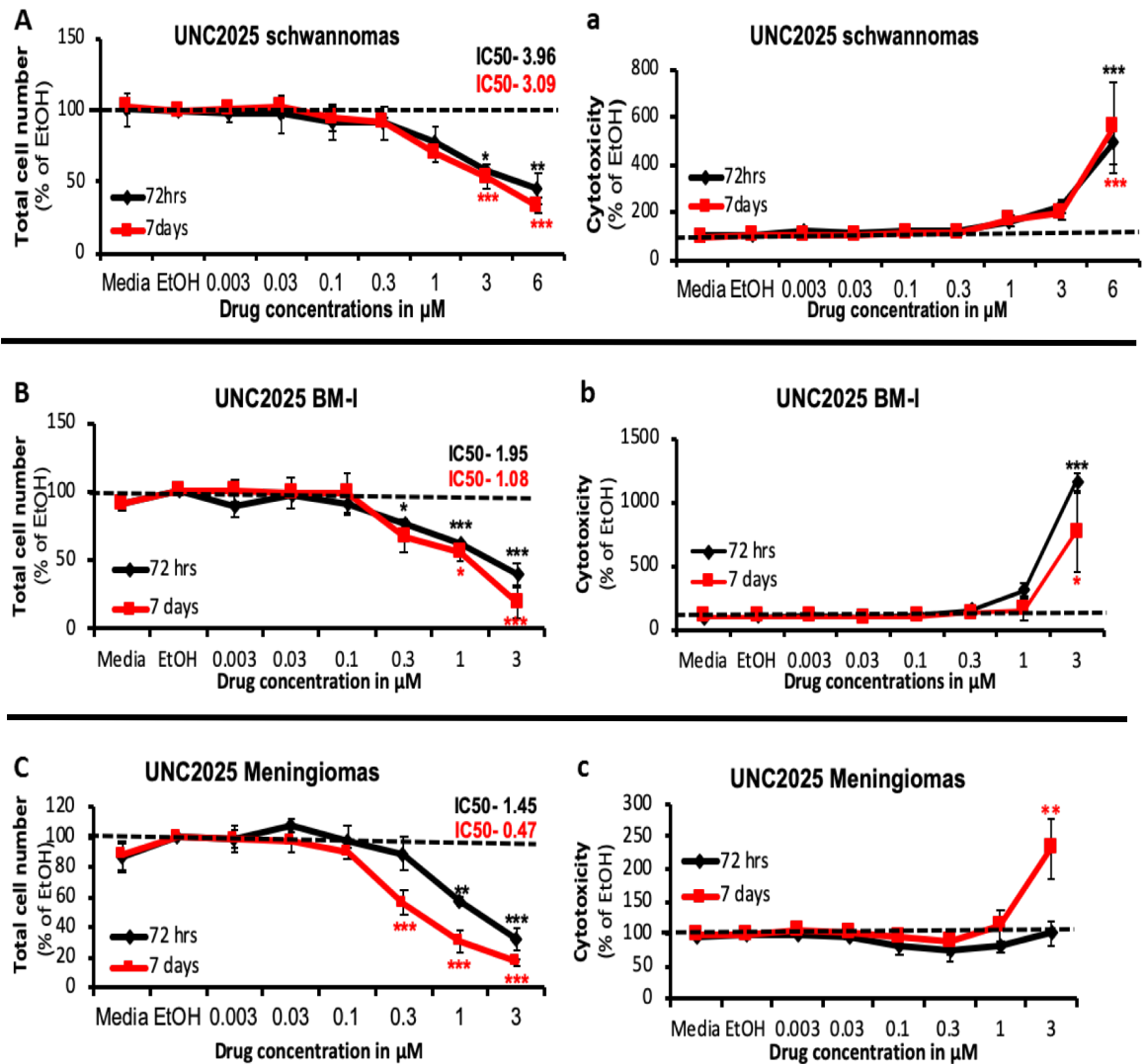
Figure 3. 19- Characterization of sensitivity of schwannoma and meningioma cells to MERTK inhibitor UNC2025. The tumour cells were treated with a single dose of UNC2025 at the indicated concentrations for 72 hrs (black) and 7 days (red). Reduction in total cell numbers for schwannomas **A)**, Ben-Men-I (BM-I) **B)** and meningioma primary cells **C)** and an increase in dead cell numbers for schwannomas **a)**, BM-I **b)** and meningioma primary cells **c)**; were reported using CytoTox-Glo[TM] assay. Tumour cells cultured in media only were used as a negative control and ethanol (EtOH) used as a vehicle control. The error bar indicates the standard error of mean for schwannoma primary cells (n=4), BM-I cell-line (n=3) and meningioma primary cells (n=4) performed in triplicates. ANOVA with Dunnett's multiple comparison test was used to calculate statistical significance; *$p<0.05$, **$p<0.01$ and ***$p<0.001$. IC_{50} was calculated using GraphPad Prism analysis software.

3b.1.3.1.2 BGB324

Incubation of schwannoma primary cells with BGB324 for 72 hrs resulted in a decrease in total cell number from 0.3 μM with significant reduction observed at 1 μM. However, higher concentrations of the drug had only negligible additional effect on cell growth and the highest concentration of 10 μM failed to decrease total cells by 50%. A treatment of schwannoma primary cells for 7 days with BGB324 (IC_{50}-14.30 μM) did not have a much additional effect on reducing schwannoma total cell numbers. BGB324 caused a dose-dependent increase in cytotoxicity and led to significant schwannoma cell-death at 10 μM after both time points (Figure-3.20 A and Figure-3.20 a).

The treatment of Ben-Men-I and meningioma primary cells with 0.3 μM of BGB324 decreased cell growth only a little, while the concentrations ≥1.0 μM strongly diminished the number of total cells after 72 hrs. The IC_{50} of BGB324 for Ben-Men-I and meningioma primary cells were calculated to 2.35 μM and 3.70 μM respectively after 72 hrs. BGB324 was even more effective following 7 days of treatment and reduced Ben-Men-I and meningioma primary total cell number with an IC_{50} of 0.03 μM and 0.13 μM respectively. The concentration of 5 μM nearly completely abolished the cell growth after 7 days of drug treatment in both cell-types. Strikingly, despite significant reduction in total cell number at 1 μM, neither Ben-Men-I nor meningioma primary cells showed increase in cell death at this concentration after 72 hrs of drug treatment. A dose-dependent increase in cell death was observed from 3 μM which was stronger in Ben-Men-I compared to meningioma primary cells. BGB324 was moderately cytotoxic at all concentration to meningioma primary cells and Ben-Men-I cells after 7 days (Figure-3.20 B and b) (Figure-3.20 C and c).
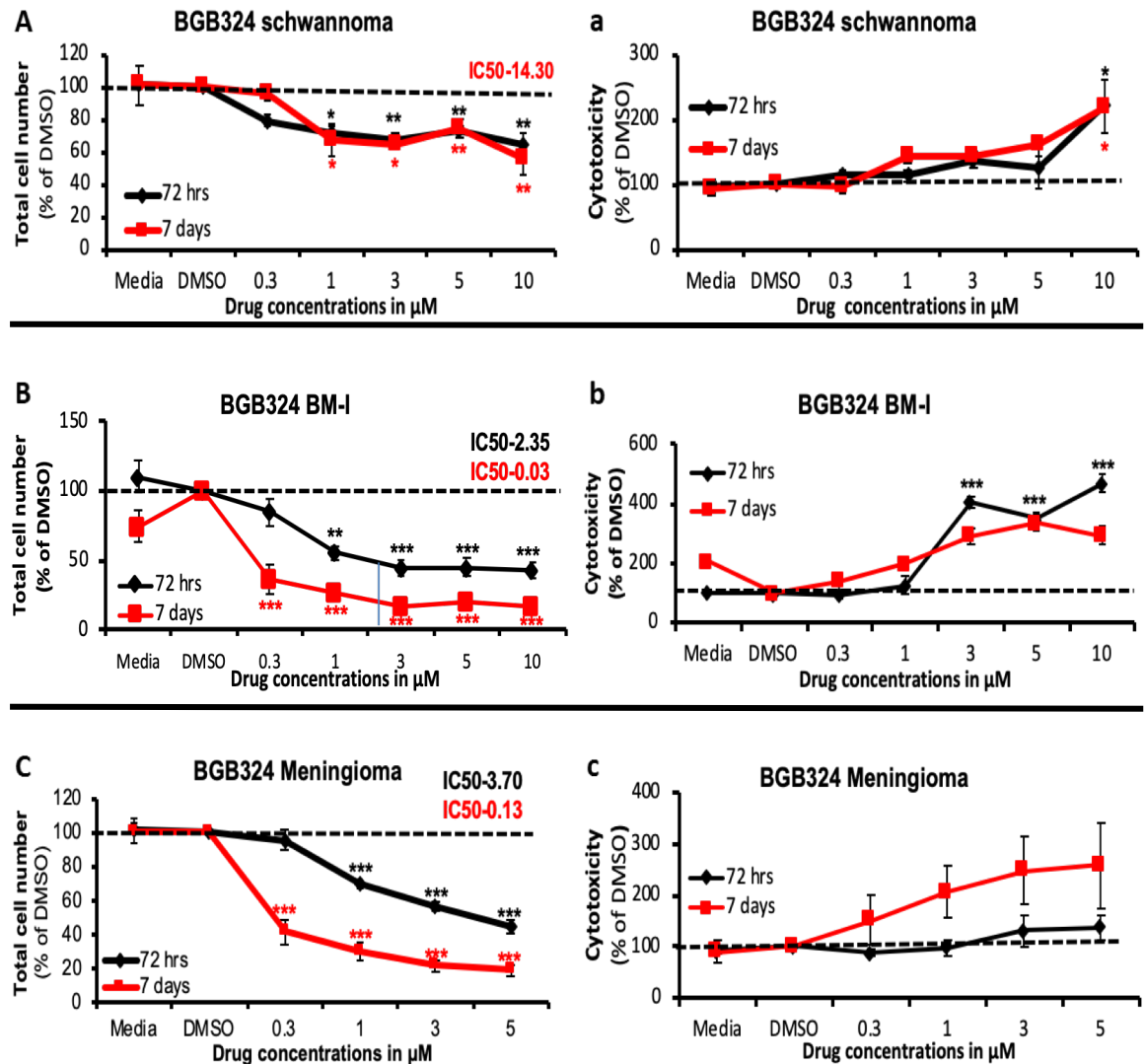
Figure 3. 20- Characterization of sensitivity of schwannoma and meningioma cells to AXL specific inhibitor BGB324. AXL inhibitor BGB324 decreased the total cell numbers of schwannoma primary cells **A)**, BM-I **B)** and meningioma primary cells **C)**; with concomitant increase in dead cells **a), b)** and **c)** shown by Cyto-Tox glo[TM] cytotoxicity assay. DMSO was used as a vehicle control and cells with media as a negative control. The tumour cells were treated with a single dose of BGB324 in technical triplicates for 72 hrs (black) and 7 days (red). Error bars indicates standard error of mean (schwannomas-72 hrs and 7 days (n=4); BM-I- 72 hrs and 7 days (n=3) and meningioma primary cells- 72 hrs and 7 days (n=4)). IC_{50} was calculated using GraphPad Prism analysis software. ANOVA with Dunnett's multiple comparison was used for statistical evaluation; *$p<0.05$, **$p<0.01$ and ***$p<0.001$.

3b.1.3.1.3 BMS777607

The highest concentration of BMS777607 (100 µM) was insufficient to decrease schwannoma total cell number by half following 72 hrs of treatment. Additional 7 days treatment of schwannoma primary cells with BMS777607 did not further reduce total cell number. The approximate IC_{50} of BMS777607 was calculated to be 127 µM for schwannoma primary cells following 7 days treatment (Figure-3.21 A and Figure-3.21 a). BMS777607-mediated increase in dead cells and decrease in total cell number was apparent only from 80 µM in Ben-Men-I (Figure-3.21 B and Figure-3.21 b) and meningioma cells (Figure-3.21 C and Figure-3.21 c) following 72 hrs treatment. Further, 7 days treatment of meningioma primary cells with BMS777607 had only a slight additional reduction in the total cell number with IC_{50} of 63.85 µM.
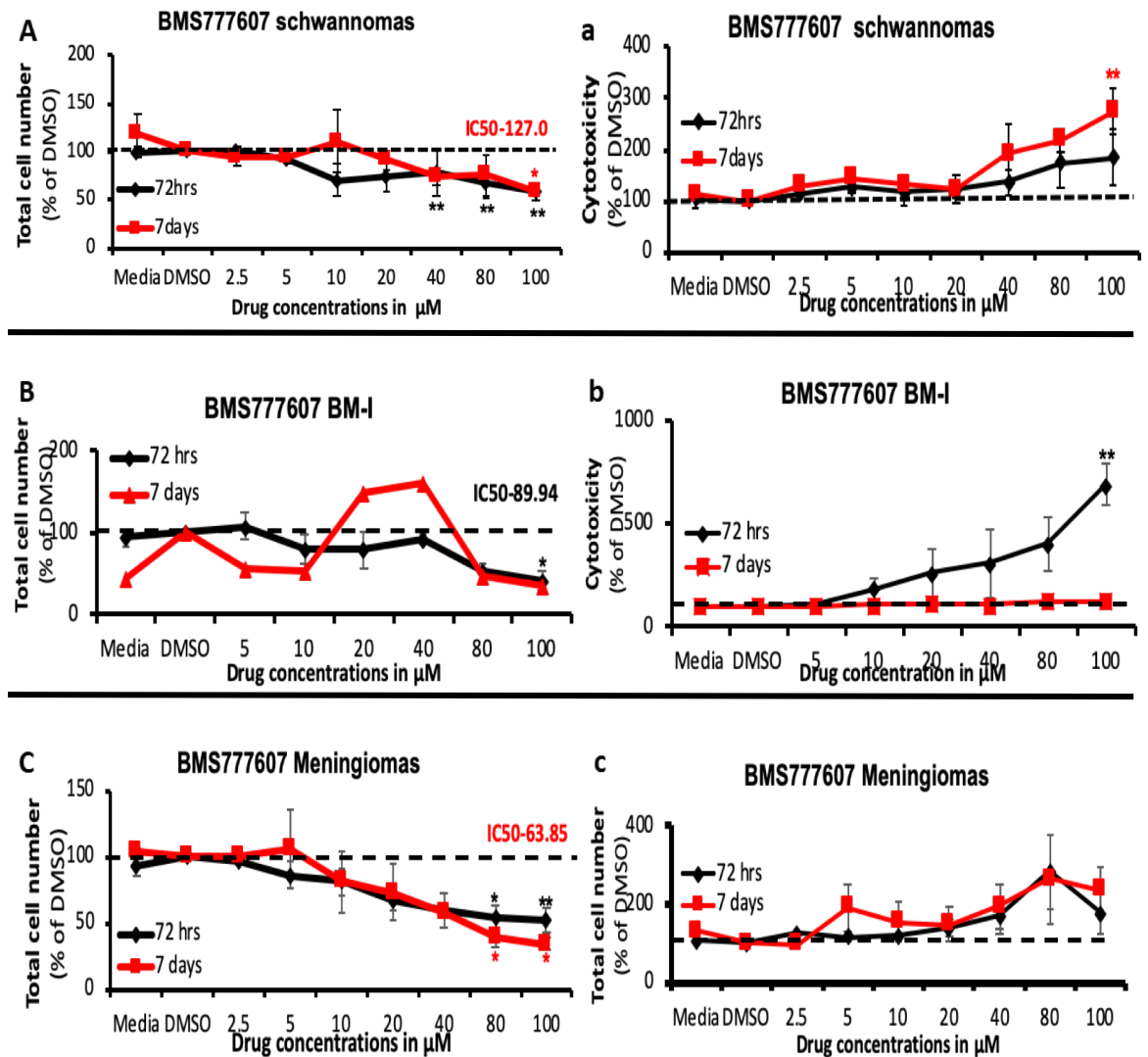
Figure 3. 21- Characterization of sensitivity of schwannoma and meningioma cells to pan-TAM inhibitor BMS777607. Schwannoma primary cells **A), a)**; BM-I **B), b)**; and meningioma primary cells **C), c)** were treated with a single dose of BMS777607 for 72 hrs (black) and 7 days (red). The graphs represent the effect of BMS777607 on total cell number A), B), C) and dead cells a), b) and c) evaluated by Cyto-Tox Glo^{TM} assay compared to DMSO (vehicle control). Cells with media was used as a negative control. ANOVA with Dunnett's multiple comparison test was used to calculate statistical significance; *p<0.05, **p<0.01 and ***p<0.001. IC$_{50}$ was calculated using GraphPad Prism analysis software. (Schwannomas- 72 hrs and 7 days (n=3); BM-I- 72 hrs (n=3) and 7 days (n=1); meningioma primary cells- 72 hrs and 7 days (n=3)).

3b.1.3.2   Ki67 and Caspase-3 staining

Ki67 is a nuclear protein that is present in all proliferating cells but is absent from quiescent or resting cells, making it a good marker of cell proliferation (Jurikova et al., 2016). The active form of caspase-3, cleaved caspase-3, is associated with initiation of a programmed cell death cascade and has been used as an apoptosis marker. The evaluation of cleaved caspase-3 levels is used to determine the cytotoxic effectiveness and strength of therapeutic agents (Jelinek et al., 2015).

To support the results of cyclin-D1 achieved following shRNA knock-down of TAM receptors and the results of cytotoxicity assay obtained after treatment with TAM kinase inhibitors, I performed Ki67 and cleaved caspase-3 staining to assess the proliferative and apoptotic status of schwannoma and meningioma primary cells before and after treatment with anti-TAM drugs.

3b.1.3.2.1 UNC2025

Schwannoma primary cells treated with various concentration of UNC2025 for 72 hrs led to a dose-dependent decrease in proliferation, as reflected from decline in Ki67-positive (red) (IC_{50}-0.17 μM) cells as well as an increase in apoptosis as demonstrated by increase in cleaved caspsase-3-positive (green) cells at higher concentrations of the drug (Figure-3.22).
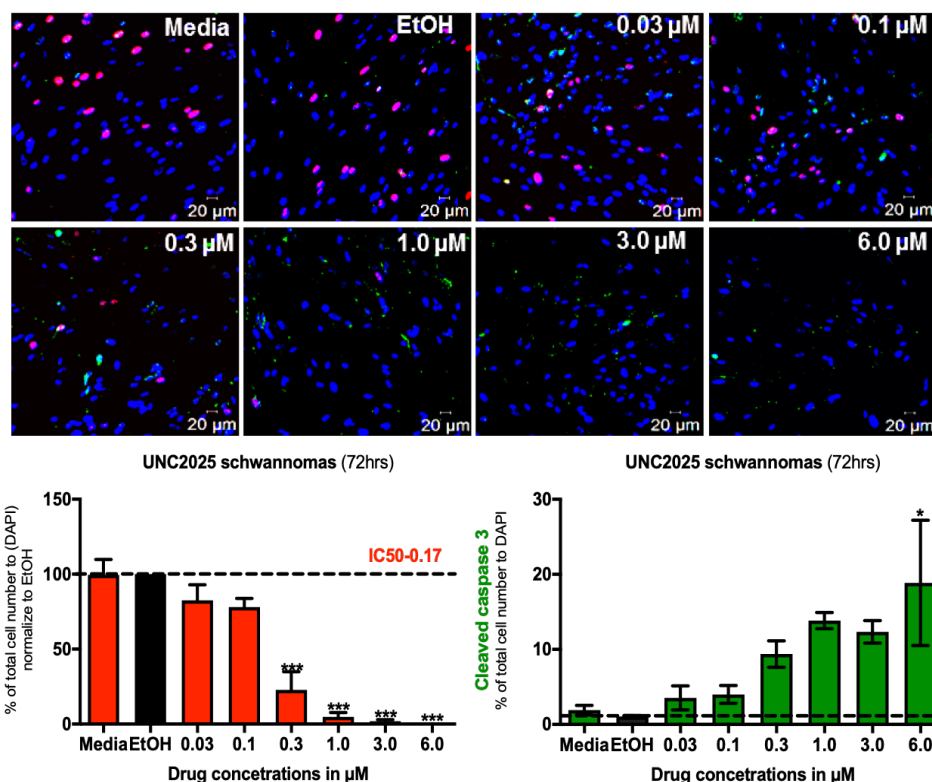
Figure 3. 22- UNC2025 decreases proliferation and induces apoptosis of schwannoma primary cells. Schwannoma primary cells were treated with EtOH (vehicle control) or indicated concentrations of UNC2025 (0.03-6.0 μM) for 72 hrs. Following that cells were fixed and stained with primary antibodies Ki67 (red) and cleaved caspase-3 (green). The percentage of proliferating and apoptotic cells were calculated by dividing Ki67 and cleaved caspase-3 positive cells to total number of cells (DAPI-blue). Graphs represent mean ± standard error of mean of three individual experiments (n=3). Statistical significance was calculated using ANOVA with Dunnett's multiple comparison test, *p<0.05 and ***p<0.001. IC_{50} was calculated using GraphPad Prism analysis software.

A dose-dependent decrease in proliferation was also observed in meningioma primary cells after treatment of the cells with UNC2025, again measured by Ki67 (IC_{50}-0.19 μM) as well as by cyclin-D1 (IC_{50}-0.31 μM) detected by Western blotting after 72 hrs. UNC2025 induced apoptosis demonstrated by increased cleaved caspase-3 positive cells compared to vehicle (EtOH). However, this increase was non-significant (Figure-3.23 A and Figure-3.23 B).
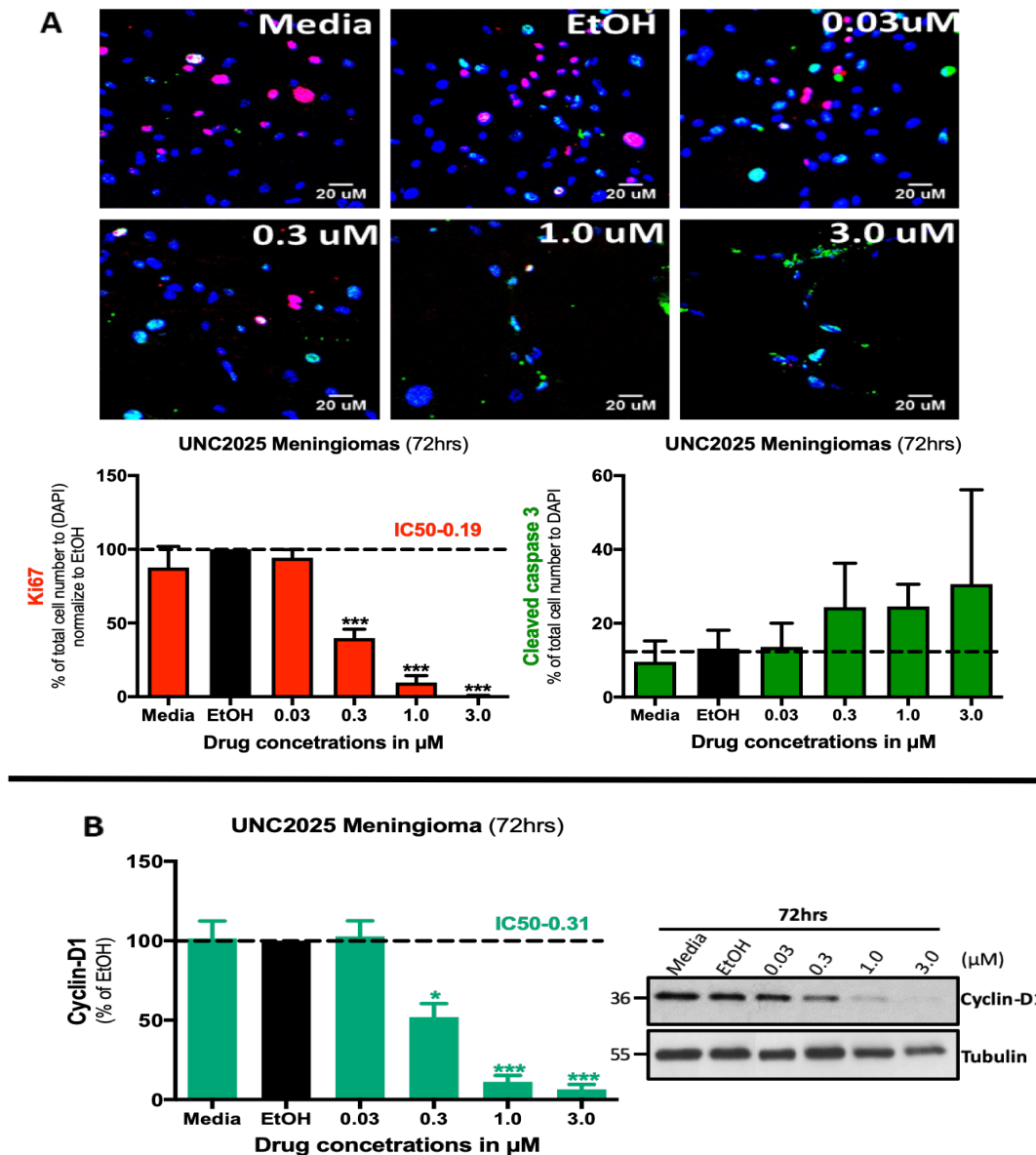
Figure 3. 23- UNC2025 decreases proliferation and induces apoptosis of meningioma primary cells. Meningioma primary cells were treated with EtOH (vehicle control) or indicated concentrations of UNC2025 (0.03-3.0 μM) for 72 hrs. Following that cells were fixed and stained with primary antibodies Ki67 (red) and cleaved caspase-3 (green). Immunofluorescence staining shows a dose-dependent decrease in proliferating cells by Ki67 staining (red) and increase in apoptotic cells by cleaved caspase-3 staining (green) after 72 hrs incubation of meningioma primary cells with UNC2025 (n=3). DAPI (blue) was used as a nuclear stain **A)**; Western blot analysis further confirmed a significant decrease in expression of cyclin-D1 levels compared to EtOH (vehicle control) and media (negative control) (n=3). Tubulin was used as a loading control **B)**. Graphs represent mean ± standard error of mean. IC_{50} and statistical calculations were performed by GraphPad Prism analysis software. ANOVA with Dunnett's multiple comparison test; *$p<0.05$ and ***$p<0.001$.

3b.1.3.2.2 BGB324

BGB324 significantly inhibited fast dividing Ki67-positive schwannoma primary cells

with an IC_{50} of 0.48 μM and showed dose-dependent increase in cleaved caspase-3

positive apoptotic cells following 72 hrs of drug treatment (Figure-3.24).
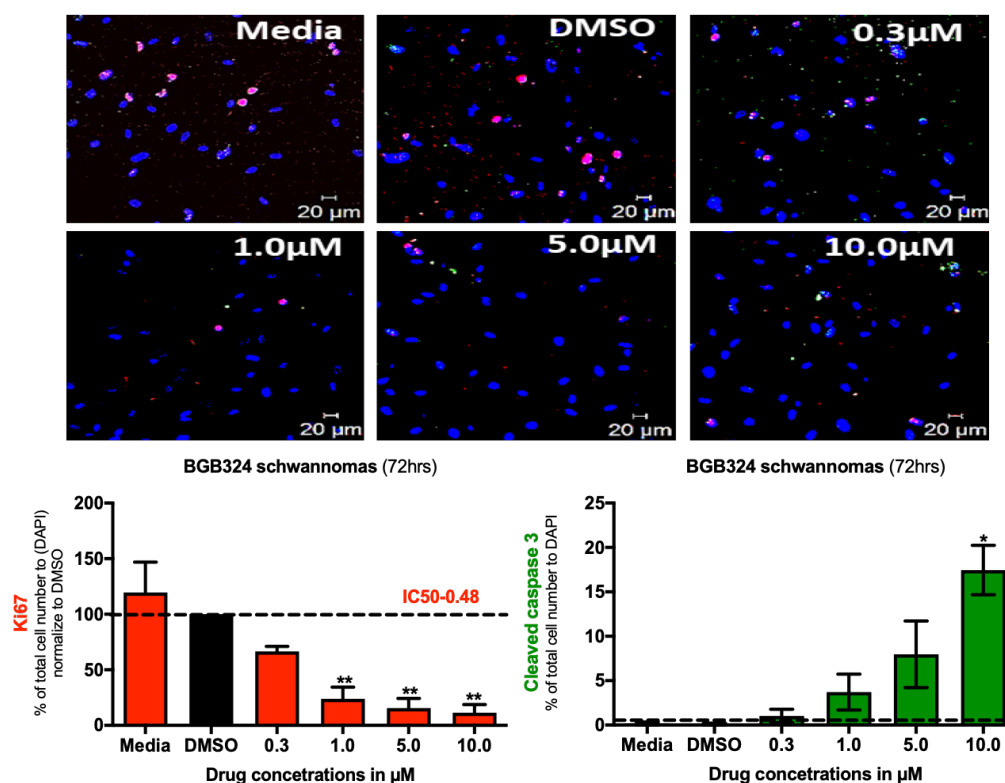
Figure 3. 24- BGB324 decreases proliferation and increases apoptosis of schwannoma primary cells. Ki67 (red) is significantly reduced and cleaved caspase-3 (green) is increased in a dose-dependent manner compared to DMSO (vehicle control) and cells containing only media (negative control) upon treatment of schwannoma primary cells with BGB324 (0.3-10.0 μM) for 72 hrs. DAPI (blue) was used as a nuclear stain. Graphs represent mean ± standard error of mean of three individual experiments (n=3). IC_{50} and statistical calculations were performed using GraphPad Prism analysis software, ANOVA with Dunnett's multiple comparison test *p<0.05 and **p<0.01.

BGB324 also successfully inhibited proliferation of meningioma primary cells by

inducing cytotoxicity as seen from dose-dependent decreases in Ki67 staining (IC_{50}-0.42

μM) and cyclin-D1 (IC_{50}-1.41 μM) and increase in apoptotic cells as measured by cleaved

caspase-3 positive cells after 72 hrs treatment (Figure-3.25 A and Figure-3.25 B).
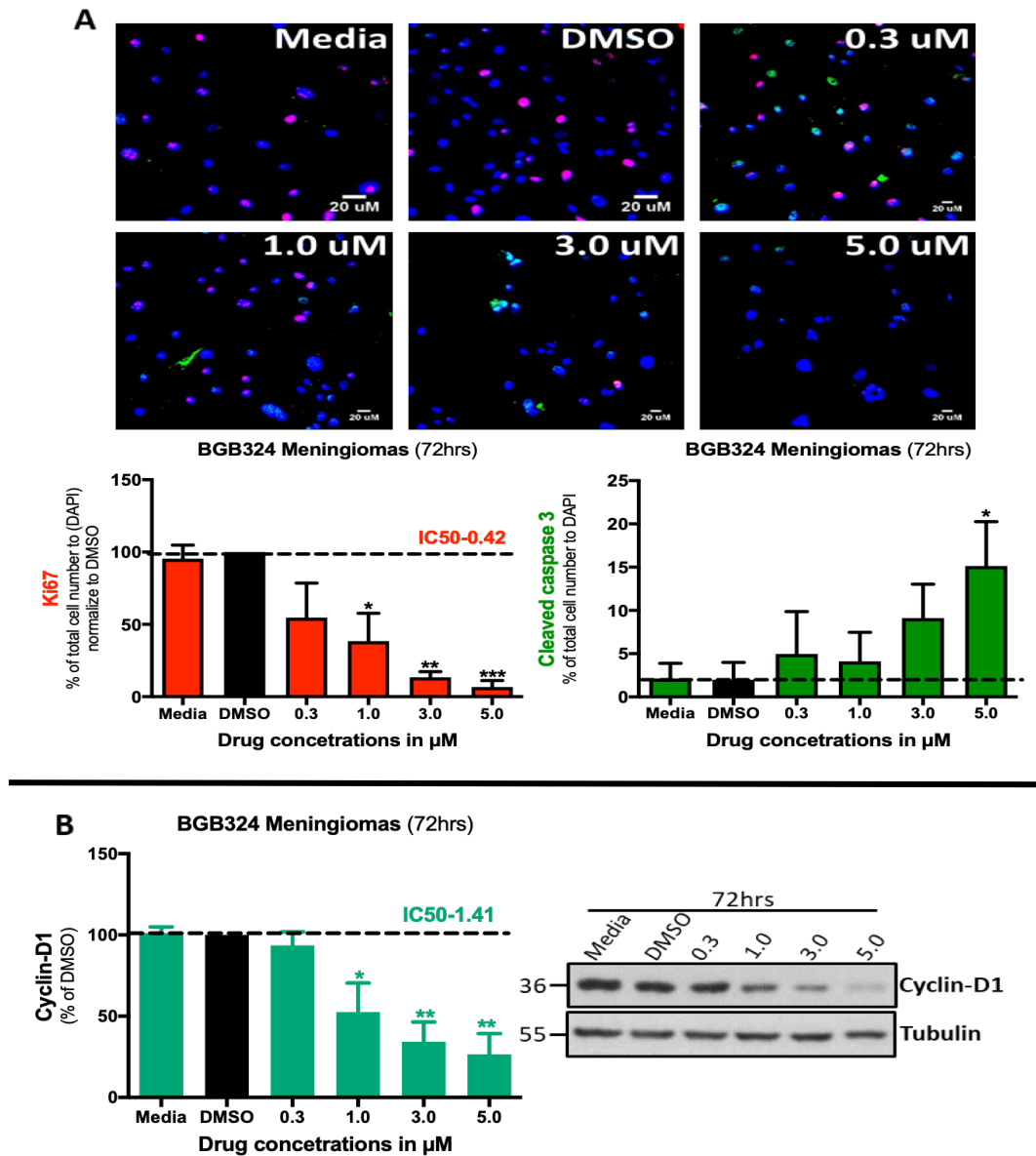
Figure 3. 25- BGB324 decreases proliferation and induces apoptosis of meningioma primary cells. Meningioma primary cells treated with AXL inhibitor BGB324 with indicated concentrations (0.3-5.0 μM) or DMSO (vehicle) showed concentration-dependent decrease in proliferation of cells assessed by Ki67 (red) and increase in apoptotic cells measured by cleaved caspase-3 (green). DAPI was used as a nuclear stain (n=3) **A)**; Reduction in proliferation was also confirmed using Western blot by measuring cyclin-D1 levels compared to vehicle and media (n=4). Tubulin was used as a loading control **B)**. Graphs represent mean ± standard error of mean. Calculations for IC_{50} and statistical significance were carried out using GraphPad Prism analysis software. ANOVA with Dunnett's multiple comparison test $*p < 0.05$, $**p < 0.01$ and $***p < 0.001$.

3b.1.3.2.3 BMS777607

Treatment of schwannoma primary cells with pan-TAM inhibitor BMS777607 for 72 hrs significantly decreased the number of Ki67-positive cells with an IC_{50} of 10.62 μM and increased Cleaved caspase-3 positive cells from 40 μM (Figure-3.26)
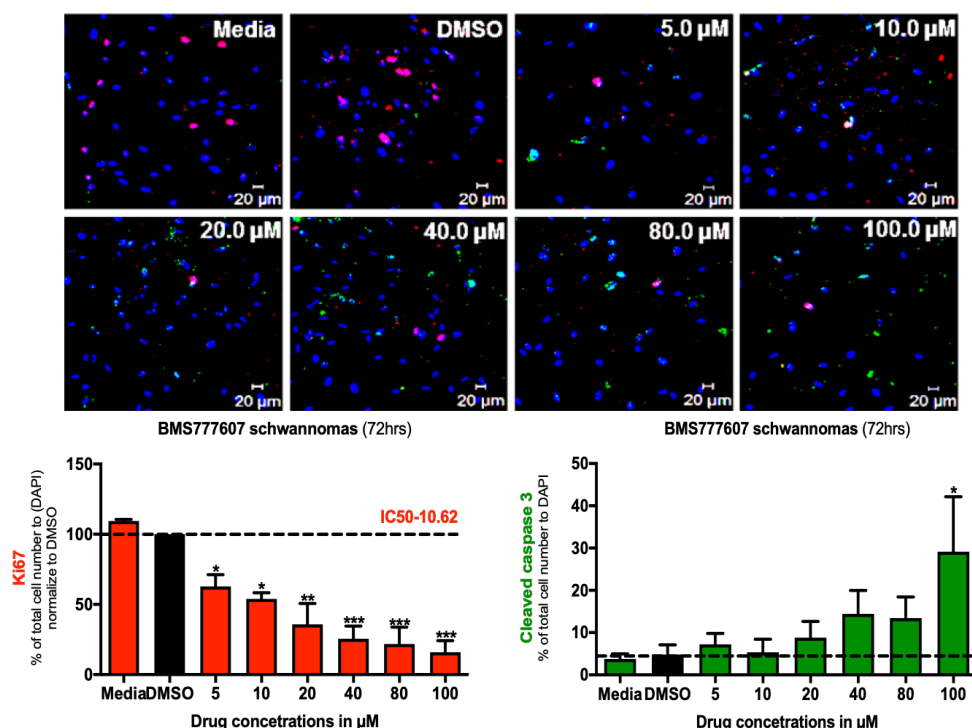
Figure 3. 26- BMS777607 decreases proliferation and increases apoptosis of schwannoma primary cells. Incubation of schwannoma primary cells with BMS777607 (5.0-100.0 μM) for 72 hrs led to a significant decrease in Ki67 positive (red) cells and an increase in cleaved caspase-3 positive (green) cells in a dose-dependent manner. DMSO was used as a vehicle control and cells with media only as a negative control. DAPI (blue) was used as a nuclear stain. Graphs represent mean ± standard error of mean of three individual experiments (n=3). Calculations for IC_{50} and statistical significance were carried out using GraphPad Prism analysis software. ANOVA with Dunnett's multiple comparison test *p<0.05, **p<0.01 and ***p<0.001.

The treatment of meningioma primary cells with BMS777607 caused dose dependent decrease in Ki67-positive cells with a concomitant increase in cleaved caspase-3 positive apoptotic cells from 40 μM (Figure-3.29 A). In aggrement with this, Western blot analysis showed a significant decrease in Cyclin-D1 expression from 40 μM with an IC_{50} of 78.73 μM (Figure-3.27 B).
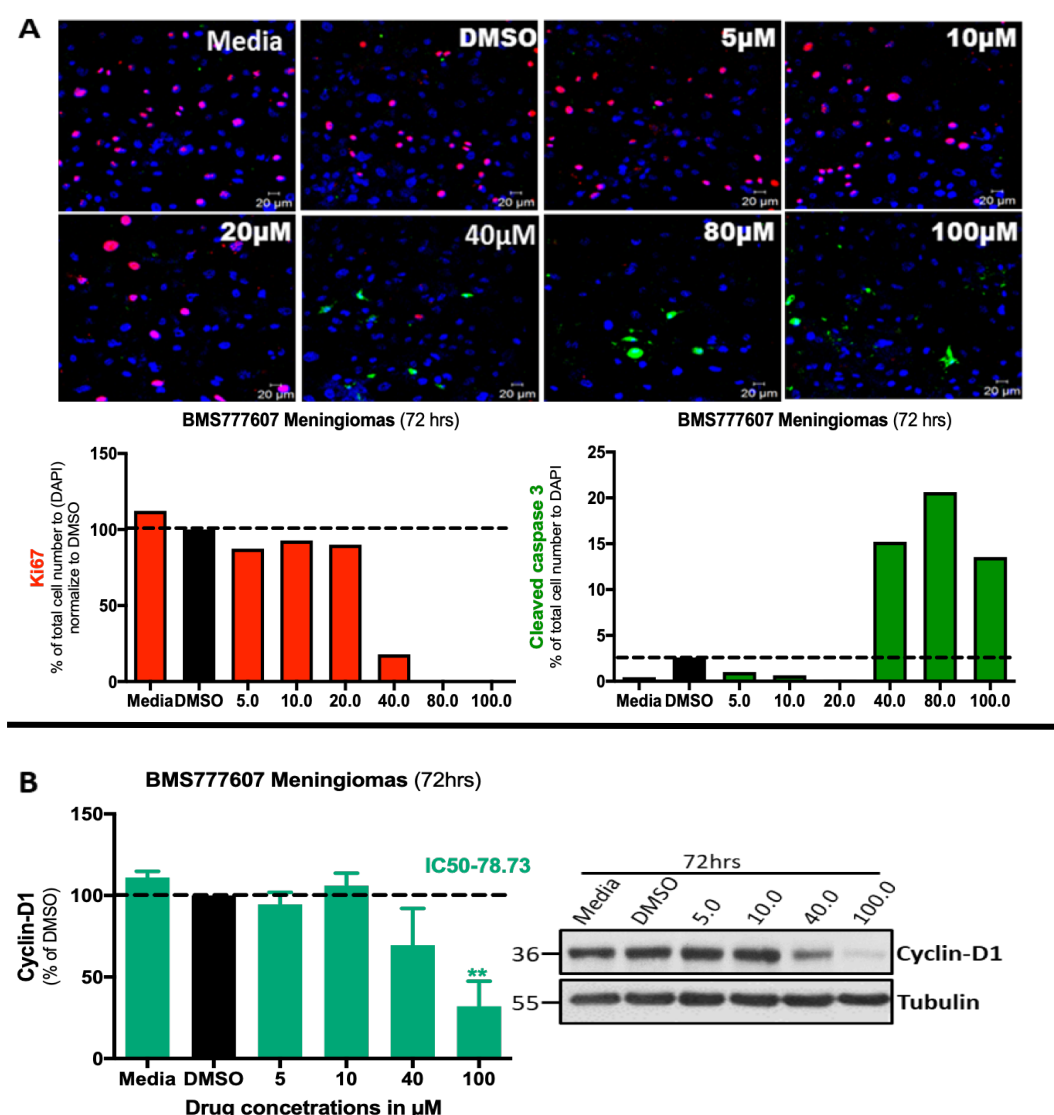
Figure 3. 27- BMS777607 decreases proliferation and increases apoptosis of meningioma primary cells. Incubation of meningioma primary cells with various concentrations of BMS777607 (5.0 μM – 100 μM) reduced the numbers of Ki67-positive cells (red) and increased the numbers of apoptotic cells (cleaved caspase-3, green) in a concentration-dependent manner. DMSO was used as a vehicle. Meningioma primary cells with complete growth factor media was used as a negative control. DAPI (blue) was used as a nuclear stain (n=1) **A);** A representative Western blot shows that BMS77607 also decreased the expression of cyclin-D1 in a concentration-dependent manner. Tubulin was used as a negative control. Graphs represent mean ± standard error of mean of three individual experiments (n=3) **B)**. ANOVA with Dunnett's multiple comparison test was used to calculate the statistical significance. **p<0.01.

3b.1.4 Comparative efficacy of TAM inhibitors for inhibition of TAM receptors in schwannoma and meningioma primary cells.

UNC2025, BGB324 and BMS777607 can dephosphorylate their respective kinases and inhibit downstream signaling pathways *in vitro,* showing effects from within a few minutes to up an hour (Zhang et al., 2014, Oien et al., 2017). Therefore, most published studies have reported the effect of these inhibitors against their respective kinases only at a shorter time period while their long-term effects on related kinases or on total protein levels remain unrecorded.

Schwannomas and meningiomas are mostly benign tumours and patients may need to be treated for a prolonged period of time, sometimes for years. Therefore, a better understanding of kinase inhibitor's long-term effects on other related kinases or on the total protein levels *in vitro* may possibly help in preventing compensatory activation of alternate signaling pathways or inhibitor-mediated unwanted effects. TAM receptors share a high structural homology and demonstrate an extensive cross-talk in both schwannomas and meningiomas, therefore I compared the efficacy of TAM inhibitors for inhibition of all three TAM receptors.

I treated meningioma primary cells with different concentrations of MERTK inhibitor UNC2025, AXL inhibitor BGB324 and pan-TAM inhibitor BMS777607 for two time points; 1 hr (shorter) and 72 hrs (longer). The limited availability of primary schwannoma cell material meant that I was restricted to just one timepoint of one-hour as this timepoint is well documented in literature.

3b.1.4.1   UNC2025 inhibits MERTK activity in schwannoma and meningioma primary cells

Incubation of schwannoma primary cells with UNC2025 for one-hour led to successful inhibition of MERTK phosphorylation from 3 μM with IC_{50} of 3.19 μM (Figure-3.28 A). Interestingly, UNC2025 also inhibited the phosphorylation of AXL with similar potency as of MERTK with IC_{50} of 3.96 μM (Figure-3.28 B) but had no effect on the phosphorylation of TYRO3 (Figure-3.28 C). In addition, the total levels of MERTK, AXL and TYRO3 also remain unaffected by UNC2025 after one-hour of treatment (Figure-3.28 A, Figure-3.28 B and Figure-3.28 C).
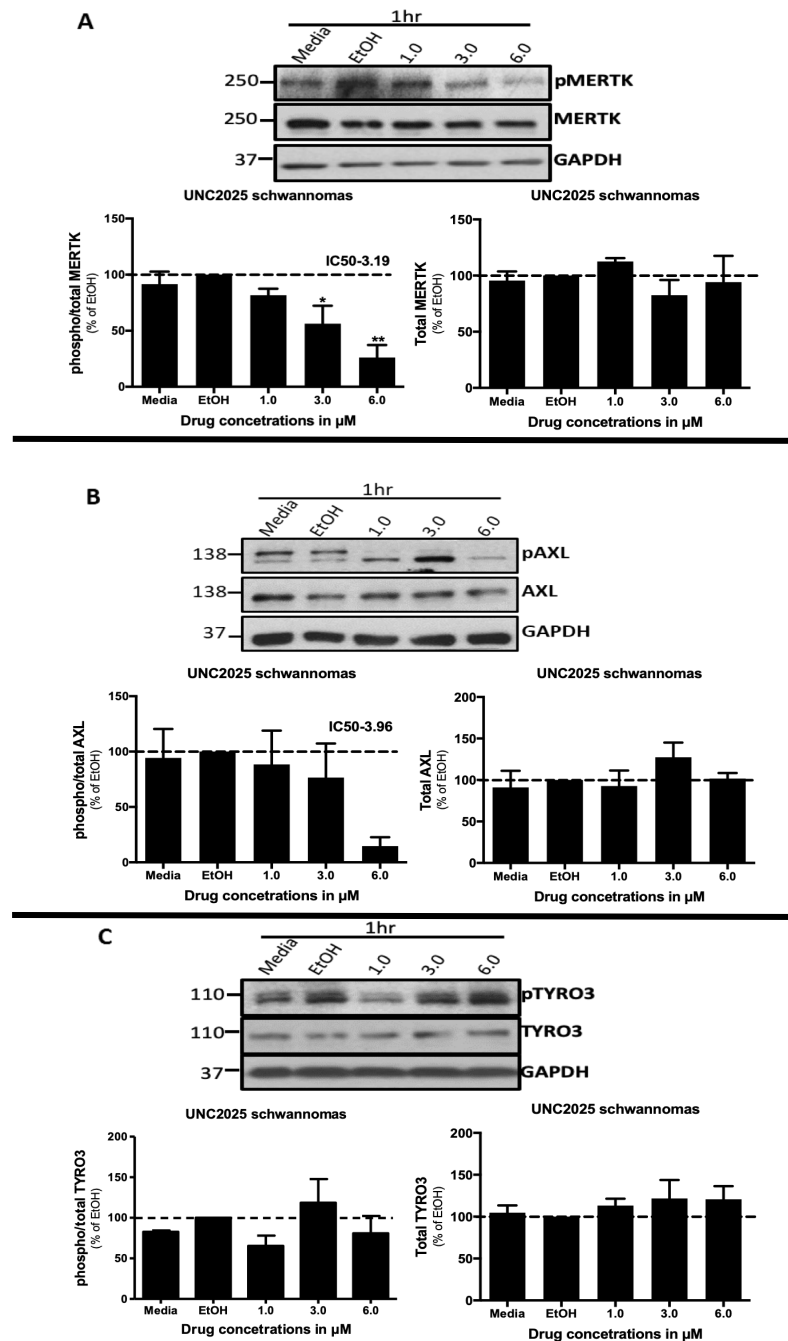
Figure 3. 28- Comparative efficacy of UNC2025 for inhibition of TAM receptors in schwannoma primary cells. Western blot of phosphorylated and total MERTK **A)**, AXL **B)** and TYRO3 **C)** in schwannoma primary cells following one-hour UNC2025 treatment with indicated (1.0-6.0 μM) concentrations. EtOH was used as a vehicle control and cells with media as a negative control. GAPDH was used as a loading control. Densitometry of Western blot of pMERTK/MERTK and MERTK/GAPDH (n=4); pAXL/AXL and AXL/GAPDH (n=3); pTYRO3/TYRO3 and TYRO3/GAPDH (n=3), graphs represent mean ±standard error of mean of individual schwannoma primary cells. ANOVA with Dunnett's multiple comparison test was performed to calculate statistical significance *$p < 0.05$ and **$p < 0.01$. IC_{50} was calculated using Graphpad Prism analysis software.

UNC2025 successfully inhibited the phosphorylation of MERTK with IC_{50} of 0.93 μM but did not affect the expression following one-hour of treatment in meningioma primary cells. Further incubation of meningioma primary cells with UNC2025 for 72 hrs led to prominent decrease in the levels of phospho-MERTK (IC_{50}-2.81) as well as total MERTK; however, there was no statistically significant difference in the ratio of phosphorylated MERTK *vs* total MERTK (Figure-3.29 A). There was no significant difference in phospho-AXL or total AXL expression levels compared to control following one-hour of UNC2025 treatment. However, a significant increase in relative phosphorylation of AXL was observed following 72 hrs of treatment (Figure-3.29 B). No remarkable changes in the phosphorylation and expression of total TYRO3 observed at either time points following incubation of meningioma primary cells with UNC2025 (Figure-3.29 C).
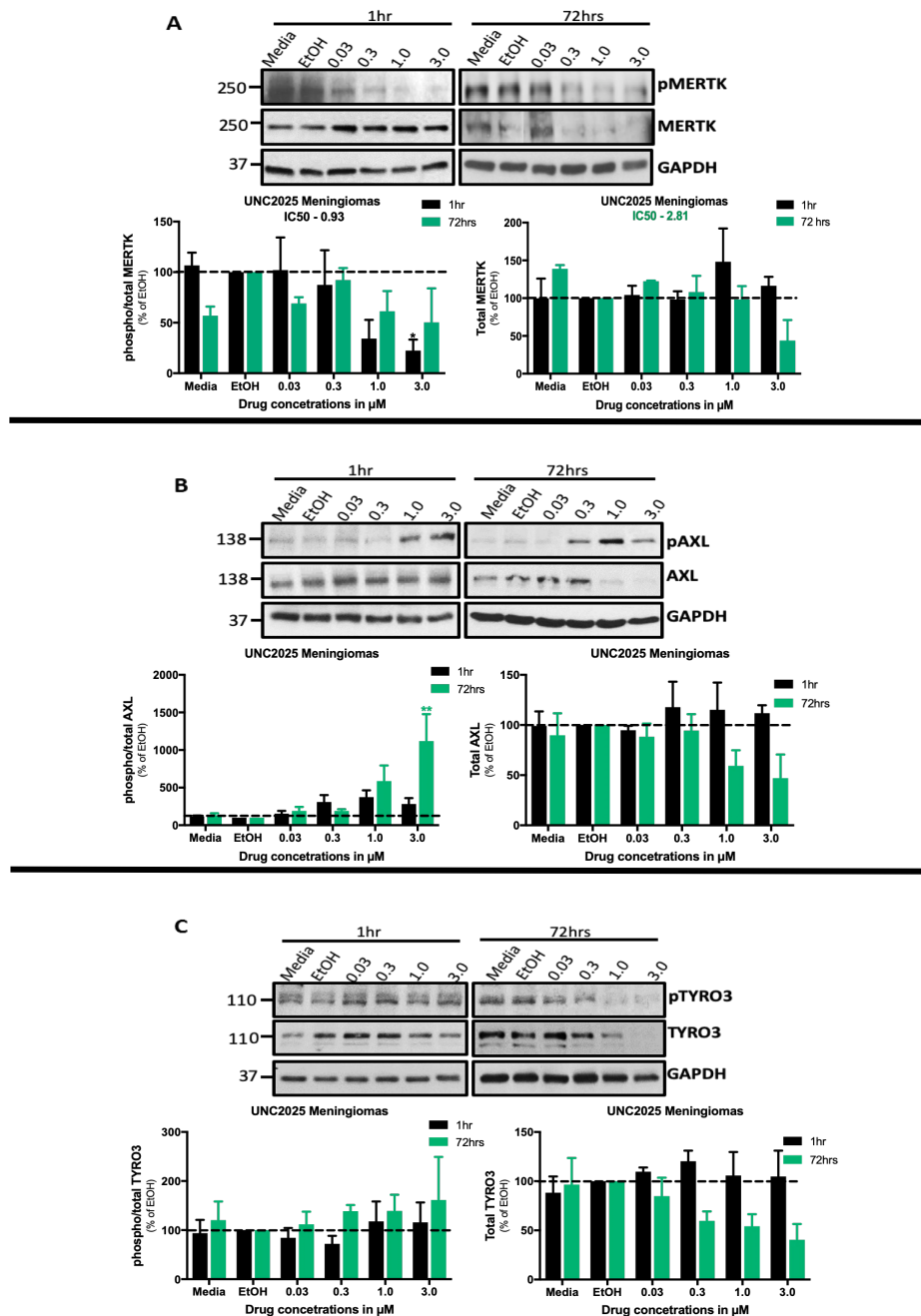
Figure 3. 29- Comparative efficacy of UNC2025 for inhibition of TAM receptors in meningioma primary cells. Western blot of phosphorylated and total MERTK **A)**, AXL **B)** and TYRO3 **C)** in meningioma primary cells following 1 hr and 72 hrs treatments of UNC2025 with indicated concentrations (0.03- 3.0 μM). EtOH was used as vehicle control and cells with media as a negative control. GAPDH was used as a loading control. Densitometry of Western blot of pMERTK/MERTK and MERTK/GAPDH (1hr and 72 hrs- n=3); pAXL/AXL and AXL/GAPDH (1 hr and 72 hrs-n=3); pTYRO3/TYRO3 and TYRO3/GAPDH (1 hr and 72 hrs-n=3), graphs represent mean ±standard error of mean of individual meningioma primary cells. ANOVA with Dunnett's multiple comparison test was performed to calculate statistical significance *p<0.05 and **p<0.01. IC$_{50}$ was calculated using Graphpad Prism analysis software.

3b.1.4.2 BGB324 inhibits AXL activity in meningioma primary cells

Unlike UNC2025 in schwannomas (Figure-3.28), one-hour treatment of BGB324 was not enough to inhibit the activation of AXL and even up to 40 μM concentration of the kinase inhibitor failed to successfully inhibit phospho-AXL (Figure-3.30 A). In addition, BGB324 did not have any effect on either phospho-MERTK (Figure-3.30 B) or phospho-TYRO3 (Figure-3.30 C) at this time point. Since 72 hrs treatment of schwannoma primary cells with BGB324 significantly reduced the total cell numbers (Figure-3.20 A) and decreased the proliferation by inducing apoptosis (Figure-3.24), the inhibitory effect of BGB324 was checked on phosphorylation of AXL at this time-point. Western blot analysis showed that while BGB324 failed to decrease levels of phospho-AXL at one-hour, it remarkably inhibited phosphorylation of AXL at 72 hrs (Supplementary figure S2-top panel).
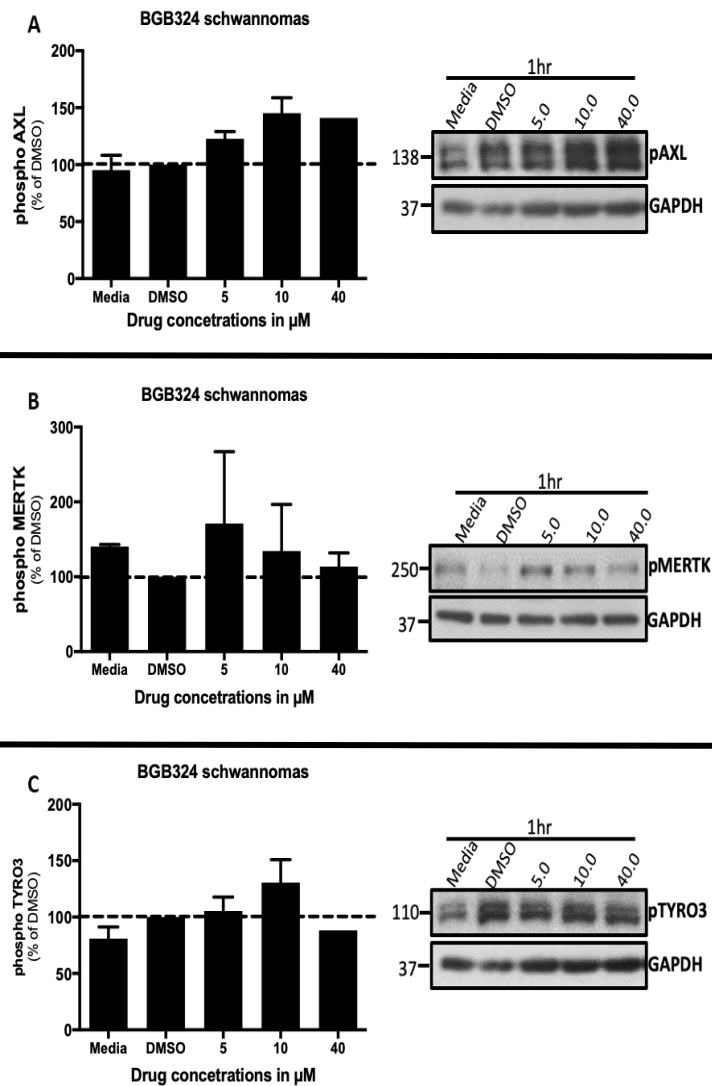
Figure 3. 30C- Comparative efficacy of BGB324 for inhibition of TAM receptors in schwannoma primary cells. AXL inhibitor BGB324 (5.0-40.0 μM) did not inhibit the activity/phosphorylation of AXL **A)**, TYRO3 **B)**, or MERTK **C)** following one-hour treatment of schwannoma primary cells. DMSO was used as a vehicle control and cells with media as a negative control. GAPDH was used as a loading control. Graphs represent mean ± standard error of mean of three individual schwannoma primary cells (n=3). ANOVA with Dunnett's multiple comparison test was performed to calculate statistical significance difference (See supplementary figure S2 for BGB324 mediated inhibition of pAXL at 72 hrs).

One-hour treatment of meningioma primary cells with BGB324 proficiently decreased the levels of phosphorylated AXL with an IC_{50} of 2.98 µM but did not affect the expression of total AXL. Further 72 hrs treatment of the cells with BGB324 led to dose-dependent decrease in the expression of both total-AXL (IC_{50}-0.28) and phospho-AXL but the ratio of phospho/total AXL remain unchanged (Figure-3.31 A). No changes were observed in the levels of either phosphorylated or total MERTK and TYRO3 following one-hour of BGB324 treatment. Moreover, there was no difference in the ratio of phosphorylated *vs* total MERTK and TYRO3 following 72 hrs of treatment but BGB324 prominently decreased the expression of both total MERTK (IC_{50} – 1.04) and TYRO3 (IC_{50} – 0.43) following 72 hrs of BGB324 treatment (Figure-3.31 B and Figure-3.31 C).
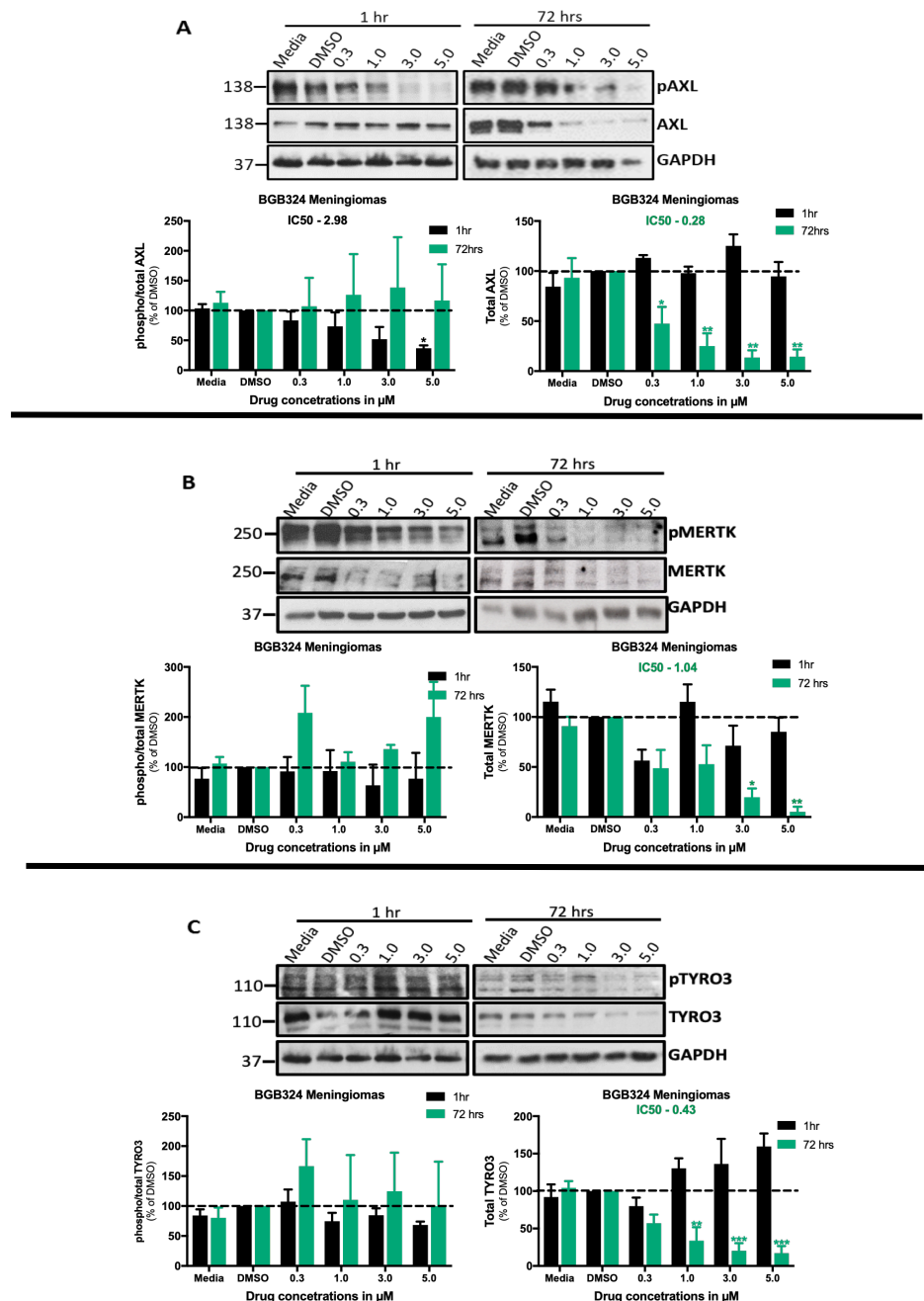
Figure 3. 31- Comparative efficacy of BGB324 for inhibition of TAM receptors in meningioma primary cells. Representative Western blot of phosphorylated and total AXL **A)**, MERTK **B)** and TYRO3 **C)** in meningioma primary cells following 1 hr and 72 hrs treatments of BGB324 (0.3-5.0 µM). DMSO was used as a vehicle control. Media with cells was used as a negative control. Densitometry of Western blot of pAXL/AXL and AXL/GAPDH (1hr and 72 hrs- n=3); pMERTK/MERTK and MERTK/GAPDH (1 hr and 72 hrs- n=3); pTYRO3/TYRO3 and TYRO3/GAPDH (1hr and 72 hrs- n=3), graphs represent mean ± standard error of mean of individual meningioma primary cells. ANOVA with Dunnett's multiple comparison test was performed to calculate statistical significance *$p<0.05$, **$p<0.01$ and ***$p<0.001$. IC_{50} was calculated using Graphpad Prism analysis software.

3b.1.4.3 BMS777607 inhibits AXL activity in schwannoma and meningioma primary cells.

BMS777607 treatment of schwannoma primary cells for one-hour reduced relative phosphorylation of AXL by 50% at 0.84 μM and nearly abolished activity of the receptor at 10 μM without affecting its expression level (Figure-3.32 A). There was no difference in the ratio of phosphorylated MERTK to total MERTK or phosphorylated TYRO3 to total TYRO3 between BMS777607 treated and vehicle (DMSO) treated or media only schwannoma cells, but the expression of total MERTK and TYRO3 were decreased in dose-dependent manner (Figure-3.32 B and Figure-3.32 C).
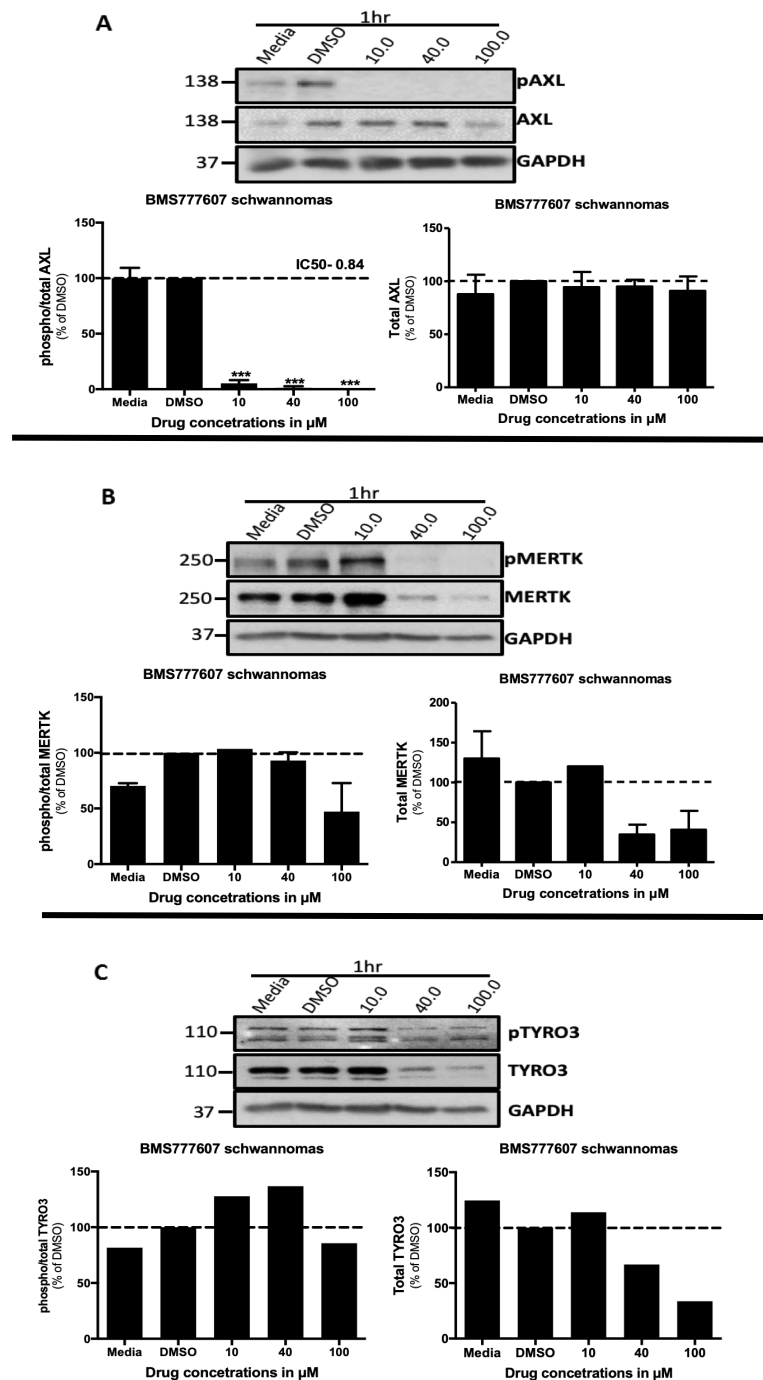
Figure 3. 32- Comparative efficacy of BMS777607 for inhibition of TAM receptors in schwannoma primary cells. Schwannoma primary cells were incubated with BMS777607 (10.0-100.0 μM) or DMSO (vehicle) for 1 hr before cells were lysed and lysates were run on. 8% SDS-PAGE. Membranes were probed with phospho and total AXL **A)**; MERTK **B)**, and TYRO3 **C)** antibodies. GAPDH was used as a loading control. Densitometry of Western blot of phospho/total AXL and AXL/GAPDH (n=3); phospho/total MERTK and MERTK/GAPDH (n=2); phospho/total TYRO3 and TYRO3/GAPDH (n=1), graphs represent mean ± standard error of mean of individual schwannoma primary cells. IC_{50} and statistical calculations were carried out using GraphPad Prism analysis software. ANOVA with Dunnett's multiple comparison test was used to determine statistical significance, ***$p<0.001$.

Meningioma primary cells treated with BMS777607 demonstrated a strong inhibition in the levels of phosphorylated AXL at very low concentrations with IC_{50} of 0.09 μM after one-hour of treatment. Surprisingly, the level of phospho-AXL raised back to basal following 72 hrs of BMS777607 treatment which again started dropping from 40 μM, increasing the IC_{50} value from 0.09 μM to 23.78 μM. BMS777607 did not affect the expression of total AXL at either time points (Figure-3.33 A). There were no apparent change in relative phosphorylation and expression of MERTK at either time-points of BMS777607 treatment (Figure-3.33 B). Moreover, BMS777607 did not affect the relative phosphorylation of TYRO3 following one-hour of treatment but decrease in phospho TYRO3/TYRO3 was apparent following 72 hrs of treatment (and Figure-3.33 C). More experiments would need to be performed for TYRO3 and MERTK at both time-points to conclude as to whether these changes are significant.
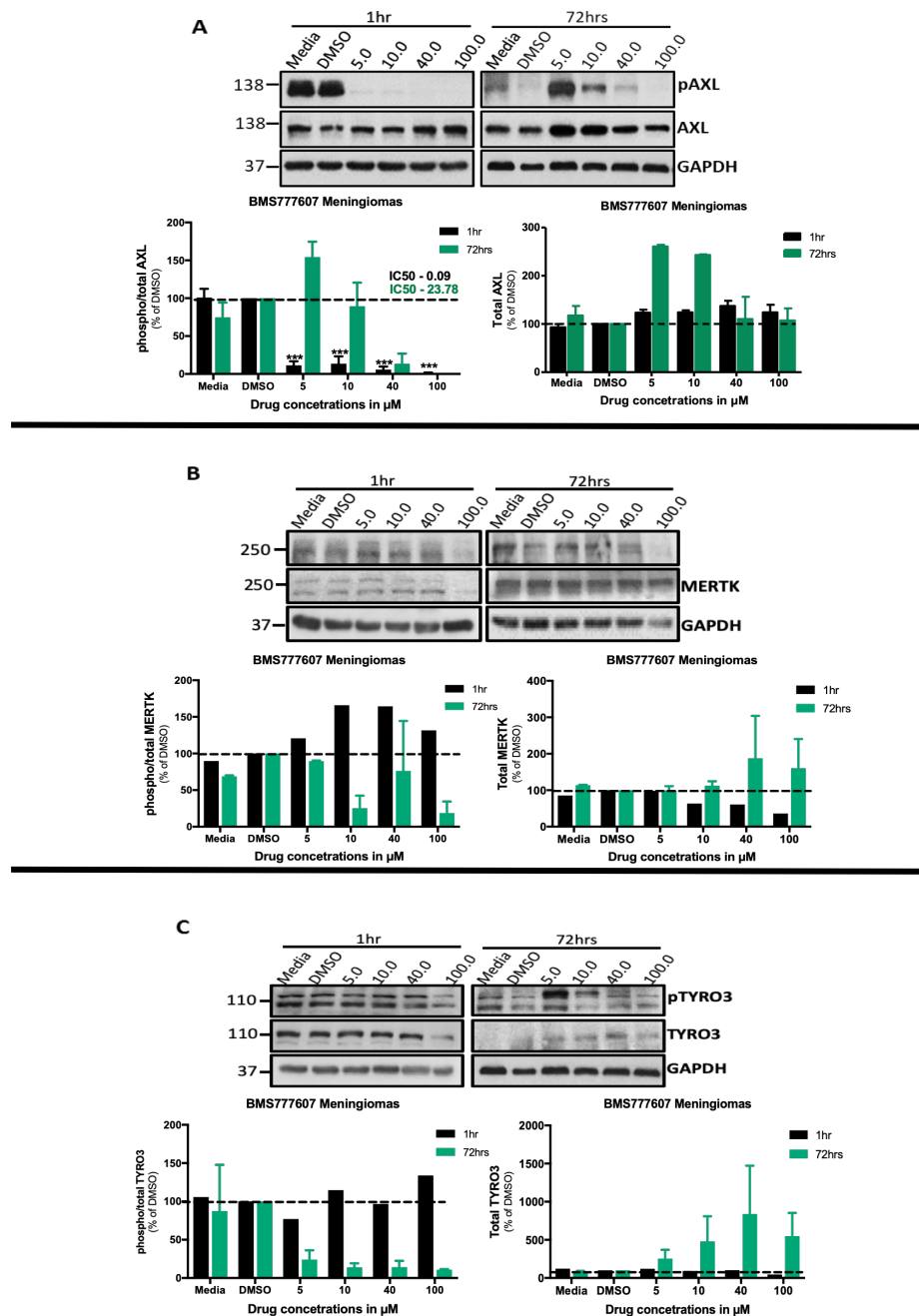
Figure 3. 33- Comparative efficacy of BMS777607 for inhibition of TAM receptors in meningioma primary cells. Western blot of phosphorylated and total levels of AXL **A)**; MERTK **B)**; and TYRO3 **C)** in meningioma primary cells, treated with BMS777607 (5.0-100.0 μM) at two different time points; 1 hr (black bars) and 72 hrs (green bars). GAPDH was used as a loading control and cells with media only as a negative control. Densitometry of Western blot of phospho/total AXL (1hr- n=3, 72 hrs- n=2); phospho/total MERTK (1hr- n=1, 72 hrs- n=2); phospho/total TYRO3 (1hr- n=1, 72hrs- n=2), graphs represent mean ± standard error of mean of individual meningioma primary cells. ANOVA with Dunnett's multiple comparison test was used to calculate statistical significance, ***$p < 0.001$.

3b.1.5 Discussion

Increased expression and activation of TAM receptors has been linked to increase cell growth and resistance to apoptosis in several cancers (Linger et al., 2008) which are also the key features of both schwannomas and meningiomas. TAM receptors are highly expressed and activated in these Merlin-deficient tumours; and in schwannomas, Gas6-mediated activation of AXL has been shown to be responsible for pathological proliferation and survival of the tumour cells (Ammoun et al., 2014). Here I further investigated the role of TAM family receptors in the pathogenesis of schwannomas and meningiomas by using shRNA-mediated gene knock-down and TAM kinase inhibitors. MERTK inhibitor UNC2025, AXL inhibitor BGB324 and pan-TAM inhibitor BMS777607 have already proved their antitumorigenic potency in clinical or pre-clinical trials for other cancers (Zhang et al., 2014, Holland et al., 2010, Roohullah et al., 2018). I tested the effectiveness of UNC2025, BGB324 and BMS777607 in regulating schwannoma and meningioma cell growth *in vitro* firstly by using CytoTox-Glo^{TM} cytotoxicity assay. As described before, CytoTox-Glo^{TM} counts dead cells and total cell numbers in culture media by measuring the proteases released from membrane compromised cells. In addition, live cells can be calculated by subtracting dead cells from total cell numbers and hence allowing an opportunity to measure live cells and dead cells in the same well. The data from the experiment therefore provides the valuable information on if the test compound has an effect on cell growth/proliferation or induce direct cytotoxic effect that leads eventually to cell death (Niles et al., 2009).

UNC2025 (IC_{50} 3.96 μM- 72 hrs and IC_{50} 3.09 μM- 7 days for schwannoma; IC_{50} 1.45 μM- 72 hrs and IC_{50} 0.47 μM- 7 days for meningioma) and BGB324 (IC_{50} 14.30 μM- 7 days for schwannoma and IC50 3.70 μM- 72 hrs and 0.13 μM- 7 days for meningioma) both successfully inhibited their respective kinase and reduced the total cell number of

schwannoma and meningioma cells in culture (Figure-3.19 A and C and Figure-3.20 A and C, Figure-3.28, Figure-3.29, Figure-S2 and Figure-3.31). However, BGB324 was more effective in reducing meningioma cell numbers as compared to schwannoma cells, whereas UNC2025 effectively inhibited the oncogenic growth of both schwannoma and meningioma cells *in vitro* (see table-3.1 for IC_{50} comparison). Of note, in contrast to schwannoma, meningioma cells demonstrated that the inhibitory effect of UNC2025 and BGB324 was more cytostatic rather than cytotoxic at shorter time point (72 hrs) and significant increases in dead cells were observed only after prolonged treatment of meningioma cells for 7 days (Figure-3.19 a and c; Figure-3.20 a and c). BMS777607 (IC_{50} 127 μM – 7 days for schwannoma and IC_{50} 63.85 μM – 7 days for meningioma) was the least effective kinase inhibitor out of all three tested inhibitors in both schwannoma and meningioma cells (Figure-3.21).

While the cytotoxicity assay gives a general overview on the effect of the test molecule on cell proliferation and survival in a quick and reliable manner, it is not a standard technique to measure the cell proliferation. Therefore, I further assessed the effect of UNC2025, BGB324 and BMS777607 on proliferation of schwannoma and meningioma cells by performing Ki67 staining. Indeed, UNC2025 (IC_{50}-0.17 μM for schwannoma and IC_{50}-0.19 μM for meningioma) and BGB324 (IC_{50}-0.48 μM for schwannoma and IC_{50} 0.43 μM for meningioma) successfully inhibited fast dividing Ki67 positive cells following 72 hrs treatment (Figure-3.22, Figure-3.23, Figure-3.24 and Figure-3.25). However, BMS777607 required ~62-fold higher concentration than UNC2025 and ~22-fold higher concentration than BGB324 to inhibit proliferating schwannoma cell by 50% (Figure-3.26) (see table-3.1 for IC_{50}).

One mechanism by which tumour cells sustain continuous proliferation is by altering the expression and/or activity of cell cycle-related proteins such as cyclin-D1. Cyclin-D1 is

an important regulator of cell-cycle progression through G1 to S phase. In normal conditions, its level is regulated by ubiquitin-dependent proteasomal degradation. Inefficient degradation or genetic upregulation leads to overexpression of cyclin-D1 in several cancers including breast, esophagus, bladder and lung cancer. In breast cancer, overexpression of cyclin-D1 has also linked to development of resistance to endocrine therapy targeting estrogen receptor (ER) (Alao, 2007).

Aberrant expression of cyclin-D1 has also been reported in schwannoma primary cells compared to normal Schwann cells (Zhou et al., 2011) which can be reversed by knocking-down the expression of AXL (Ammoun et al., 2014). Here, I again demonstrated increased level of cyclin-D1 in meningioma cells compared to normal human meningeal cells (Figure-3.15). In addition, reducing MERTK and AXL expression (Figure-3.16 and Figure-3.17) but not TYRO3 expression (Figure-3.18) using shRNA led to a significant decrease in cyclin-D1 levels in both schwannoma and meningioma cells. Knock-down results were further supported by MERTK inhibitor UNC2025 (IC_{50}-0.31 μM) and AXL inhibitor BGB324 (IC_{50}-1.41 μM) in meningioma, both of which showed a successful reduction in cyclin-D1 levels (Figure-3.23 B and Figure-3.25 B). Consistent with cytotoxicity assay data, the pan-TAM inhibitor- BMS777607 (IC_{50}-78.73 μM) was the least effective in decreasing cyclin-D1 levels (Figure-3.27 B).

While BMS777607 inhibited the kinase activity of AXL by 50% in both tumour cell-types with minimal concentrations of 0.84 μM or below after one-hour, it had a negligible effect on TYRO3 and MERTK kinase activity even at 100 μM (Figure-3.32 and Figure-3.33). Importantly, reduced phospho-AXL levels following one-hour incubation of meningioma cells with BMS777607 returned to basal levels or even increased at lower concentration (5.0 μM) following 72 hrs treatment and with the IC_{50} of BMS777607 for AXL inhibition increased to 23.78 μM (Figure-3.33 A). This could potentially be due to

acquired resistance to the drug, possiebly by feedback activation of an alternative receptor or signaling pathway. Similar results have been reported recently whereupon BMS777607-mediated inhibition of pMET following 24 hours treatment of triple-negative breast cancer (TNBC) and non-small cell lung cancer (NSCLC) cells led, in turn, to increase in pAXL levels with concomitant increase in total AXL, TYRO3, MERTK and Gas6 expression (Baumann et al., 2017).

Furthermore, in breast cancer cells, BMS777607 has been shown to increase the resistance to cytotoxic agents including doxorubicin, bleomycin, paclitaxel, and methotrexate by inducing a polyploidy. Polyploidy is the presence of more than two copies of a single gene that has been linked to pathologies including drug resistance in cancer by inducing division in senescent cells (Sharma et al., 2013, Mosieniak and Sikora, 2010). BMS777607 was also shown to only partially decrease tumour growth *in vivo* at the dose of 6.25 mg/kg (Cmax- 4.5 μM), further increases in dose up to 50 mg/kg (C$_{max}$-43.7 μM) was required for complete inhibition of tumour growth (Schroeder et al., 2009). Consistent with these reports, even 100 μM concentration of the inhibitor failed to reduce schwannoma total cell numbers by 50% and concentration of over 60 μM was required to decrease meningioma cell numbers by half after seven days (Figure-3.21 A and C). Taking published reports and our *in vitro* data into consideration, BMS777607 does not seem to be an ideal candidate to take forward for the treatment of schwannomas and meningiomas.

In addition to increased proliferation, increased resistance to apoptosis is another hallmark feature of both schwannomas and meningiomas. Schwannoma cells cultured in serum-free media for five days, only showed negligible cell death. Moreover, Gas6-mediated activation of TAM receptors further decreased cell death by activation of survivin (Ammoun et al., 2014). My results showed that treatment of schwannoma and

meningioma cells with MERTK and AXL small molecule inhibitors decreases the survival of tumour cells by increasing the levels of pro-apoptotic protein, cleaved caspase-3 (Figure-3.22, Figure-3.23, Figure-3.24, Figure-3.25, Figure-3.26 and Figure-3.27).

Of note, genetic knock-down of *MERTK* in schwannoma and meningioma primary cells reduced the expression of AXL (Figure-3.9 and Figure-3.10) and treatment with MERTK inhibitor UNC2025 led to decrease in the phosphorylation of AXL after one-hour in schwannoma primary cells (Figure-3.28 B). Similarly, incubation of meningioma primary cells with BGB324 for 72 hrs concomitantly reduced the expression of TYRO3 and MERTK along with AXL (Figure-3.31). Although it has yet remained to determine whether these observed effects are due to a cross-talk among these receptors, there are evidences suggesting that TAM receptors can cross-phosphorylate each other and that the absence of one receptor may adversely affect the activity of remaining TAM members (Angelillo-Scherrer et al., 2005, Brown et al., 2012). In addition, direct evidence comes from GBM, where inhibition of phosphorylated AXL by BGB324 also reduced the activity of TYRO3 (Vouri et al., 2015). In short, due to an extensive cross-talk among TAM family members it is difficult to identify the role of individual TAM receptors in promoting tumorigenesis, but I can conclude from my data that AXL and MERTK work together and play a concerted role in promoting the proliferation and survival of schwannoma and meningioma cells *in vitro* which can be successfully inhibited using UNC2025 and BGB324.

Interestingly, meningioma cells were overall more sensitive to all three tested inhibitors compared to schwannoma cells (Table-3.1). The limited efficacy of most drug treatments in schwannoma primary cells could be attributed to the intrinsic drug resistance mediated by multiple drug resistance proteins such as p-glycoprotein (p-gp). P-gp is a cell-membrane protein responsible for causing an efflux of many important anti-cancer drugs

and develop resistance in many cancers. Merlin-deficient schwannoma cells reported to have an endogenous high level of p-gp compared to Schwann cells (Provenzano, 2018). The p-gp inhibitor PSC833 (Valspodar) has been shown to have a beneficial effect in combination with anti-cancer drugs in several cancers by reversing the effect of p-gp (Baekelandt et al., 2001, Fracasso et al., 2005). It remains to be seen whether a combination treatment of TAM inhibitors with PSC833 would have an additional beneficial effect in reducing schwannoma growth.

Importantly, when cells were treated with UNC2025 and BGB324 for a prolonged period (72 hrs), reduction in total MERTK, AXL and TYRO3 levels were observed but not at the shorter treatment (one-hour) (Figure-3.29 and Figure-3.31). Therefore, a question remains whether this reduction is due to inhibitor-mediated dephosphorylation or inhibitor-mediated conformation changes leading to receptor internalization and degradation, or both. Since kinase inhibitors induce the dephosphorylation of their respective kinase within short time frame (up to 60 minutes), not many reports have studied the effect of kinase inhibitors at longer time periods. Recently emerging studies show that degradation of RTKs is a better therapeutic strategy as it provides complete blockage of downstream signaling compared to only inhibition of the kinase activity where receptor can still act as scaffold for cross-talk with another receptor (Bae et al., 2015, Burslem et al., 2018). In this context, it is essential to understand whether the UNC2025- and BGB324-induced reduction in total TAM protein levels is of beneficial rather an unwanted effect in these tumours before pursuing these drugs as a therapeutic strategy. Future experiments should be conducted by incubating schwannoma and meningioma cells with proteasome inhibitor such as MG132 or lysosomal inhibitor chloroquine along with TAM kinase inhibitors UNC2025 and BGB324 to get further insight into the mechanism by which these drugs act to reduce protein levels.

In conclusion, this is the first report describing the therapeutic importance of TAM receptors in schwannomas and meningiomas by successfully targeting them with novel tyrosine kinase inhibitors, UNC2025 and BGB324. Blocking the expression and activation of MERTK and AXL reduces the proliferation of schwannoma and meningioma primary cells probably by cell-cycle arrest at G1 phase as well as inducing apoptosis. In addition, this report highlights the importance of not drawing conclusions of the anti-tumor effect of a specific TAM tyrosine kinase inhibitor at longer treatment (24 hrs, 48 hrs or 72 hrs) while studying their specificity only on a shorter time period (few minutes to an hour), especially when the TAM receptors are co-expressed in the cells of interest.

IC$_{50}$(μM)	UNC2025			BGB324			BMS777607		
	Sc	MN	BM-I	Sc	MN	BM-I	Sc	MN	BM-I
Total cells - 72 hrs	3.96	1.45	1.95	-	3.70	2.35	-	-	89.94
Total cells - 7 days	3.09	0.47	1.08	14.30	0.13	0.03	127.0	63.85	-
Ki67 -72 hrs	0.17	0.19	-	0.48	0.42	-	10.62	-	-
Cyclin-D1 - 72 hrs	-	0.31	-	-	1.41	-	-	78.73	-
pMERTK - 1hr	3.19	0.93	-	-	-	-	-	-	-
MERTK - 1hr	-	-	-	-	-	-	-	-	-
pMERTK - 72 hrs	-	-	-	-	-	-	-	-	-
MERTK - 72 hrs	-	2.81	-	-	1.04	-	-	-	-
pAXL - 1hr	3.96	-	-	-	2.98	-	0.84	0.09	-
AXL - 1hr	-	-	-	-	-	-	-	-	-
pAXL - 72 hrs	-	-	-	-	-	-	-	23.78	-
AXL - 72 hrs	-	-	-	-	0.28	-	-	-	-
pTYRO3 - 1hr	-	-	-	-	-	-	-	-	-
TYRO3 - 1hr	-	-	-	-	-	-	-	-	-
pTYRO3 - 72 hrs	-	-	-	-	-	-	-	-	-
TYRO3 - 72 hrs	-	-	-	-	0.43	-	-	-	-

Table 3.1- Summary of IC$_{50}$ values of UNC2025, BGB324 and BMS777607. IC$_{50}$ values were calculated by inserting values into a non-linear regression curve using GraphPad Prism analysis software.

3b.2   TAM down-stream signaling pathways

Introduction

I further investigated the role of MERTK, AXL and TYRO3 in schwannoma and meningioma cell proliferation and survival by dissecting their relevant down-stream signaling pathways. TAM family receptors signal via multiple pathways to mediate their oncogenic effect on target cell/tissues. Nevertheless, Ras/Raf/MEK/ERK, PI3K/AKT, Rac/PAK/JNK and Src/FAK pathways have repeatedly been described down-stream of TAM receptors in multiple cancers (Linger et al., 2008). Interestingly, all these pathways are highly activated and have shown to be important for both schwannoma and meningioma development (Ammoun et al., 2008, Hilton et al., 2016). In addition, the stimulation of Merlin-deficient schwannoma primary cells with Gas6 strongly activated pERK, pAKT, pJNK, pFAK and pSrc within five minutes (Ammoun et al., 2014).

ERK-1/2 is a protein serine-threonine kinase which, when activated, phosphorylates other protein kinases and transcription factors to promote multiple cellular processes such as cell-cycle progression, proliferation, adhesion, migration, survival and differentiation (Roskoski, 2012). In schwannomas and meningiomas, strong nuclear expression of pMEK and pERK1/2 is associated with increased cell proliferation (Ammoun et al., 2008, Hilton et al., 2009, Hilton et al., 2016). The c-Jun N-termianal kinase (JNK) is also a member of MAPK family. JNK can act as either a tumour promoter or a tumour suppressor depending on the tissue and cell type. However, persistent activation of JNK has been reported to play a pro-tumorigenic role in several cancers including brain tumour, GBM (Bubici and Papa, 2014). The hyper-phosphorylated form of JNK has also been detected in the nucleus of schwannoma and meningioma primary cells where, in schwannoma, it was shown to promote Schwann cell de-differentiation (Kaempchen et al., 2003, Parkinson et al., 2004, Hilton et al., 2016).

Another two important molecules regulated by Merlin are AKT and focal adhesion kinase (FAK). The aberrant activity of both signaling molecules in schwannoma and meningioma is evident from their high expression and phosphorylation and presence in the nucleus (Jacob et al., 2008, Hilton et al., 2016, Ammoun et al., 2012, Wang et al., 2012). Nuclear AKT and FAK provides a proliferation and survival advantage to schwannoma cells by inducing degradation of the tumour supperessor protein p53 (Ammoun et al., 2015).

I investigated the role of TAM family receptors in mediating the signaling of the above-mentioned pathways in schwannomas and meningiomas using kinase specific inhibitors or shRNA-mediated genetic knock-down. As explained above, due to time constraints and difficulty in achieving successful knock-down in meningioma primary cells, only the results of one or two successful knock-down are presented here.

3b.2.1 The role of MERTK in the regulation of downstream oncogenic signaling in schwannoma and meningioma primary cells

MERTK knock-down in schwannoma and meningioma primary cells (Figure-3.9 and Figure-3.10), which also strongly reduced AXL and TYRO3 in both cell types, profoundly decreased pAKT, pJNK and pFAK levels in schwannoma primary cells (Figure-3.34 A) and pJNK and pFAK levels in meningioma primary cells (Figure-3.34 B). Interestingly, MERTK shRNA65 construct was less effective in inhibiting pJNK levels compared to MERTK shRNA62 in schwannoma cells (Figure-3.34 A).
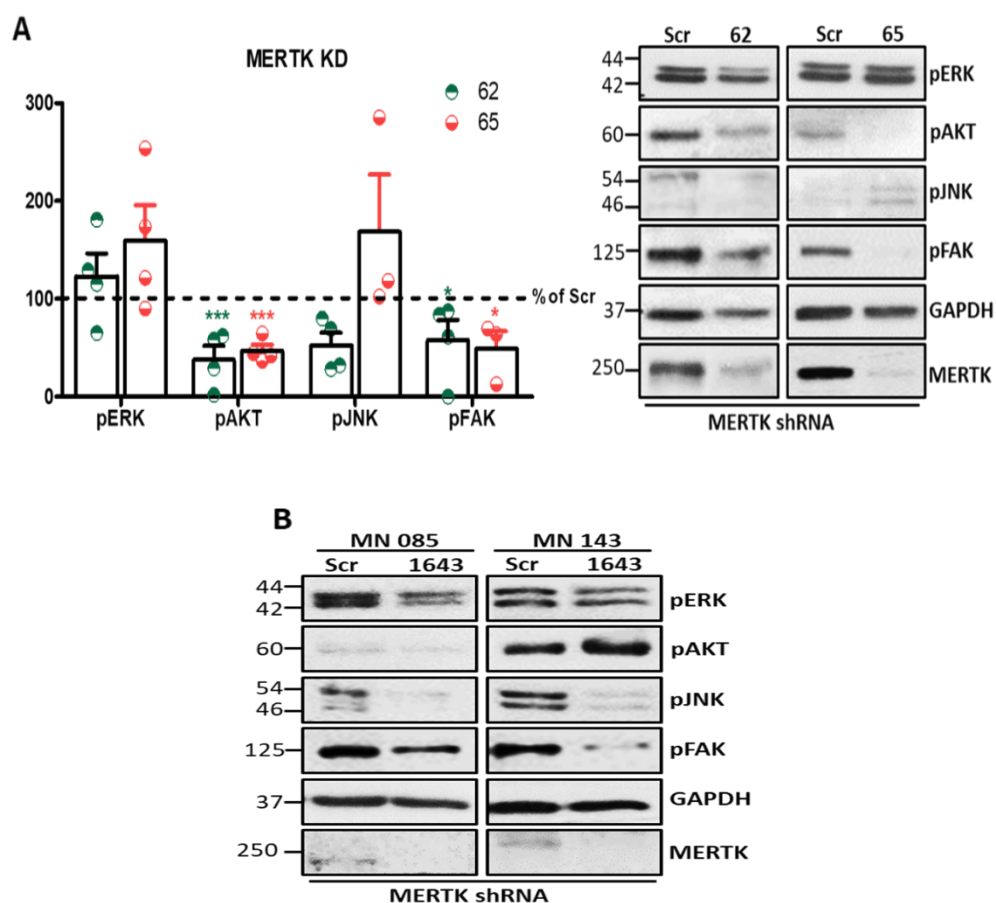
Figure 3. 34- The effect of *MERTK* knock-down on downstream oncogenic signaling in schwannoma and meningioma primary cells . *MERTK* knock-down decreased the levels of pAKT (n=4 for 62 and 65), pJNK (construct-62) (n=4 for 62 and n=3 for 65) and pFAK (n=4 for 62 and n=3 for 65) but not of pERK (n=4 for 62 and 65) in schwannoma primary cells. Error bar indicates the standard error of mean of individual experiments, each dot in a scatter plot represents an individual data set. ANOVA with Dunnett's multiple comparison test was used to calculate statistical difference, *p<0.05 and ***p<0.0001 **A)**. MERTK shRNA decreased the levels of pJNK and pFAK in two different meningioma cells but not pERK and pAKT (n=2) **B)**. GAPDH was used as a loading control.

Treatment of schwannoma and meningioma primary cells with MERTK inhibitor UNC2025 for one-hour caused a dose-dependent decrease in phosphorylated ERK and AKT but does not affect the expression of either total ERK or AKT. UNC2025 decreased the levels of total JNK in both cell-types following one-hour of treatment. A decrease in phospho JNK/total JNK ratio was also observed in both cell-types; however, this difference was not statistically significant. UNC2025 did not affect phospho-FAK signaling in either cell-types following one-hour of treatment (Figure-3.35 A and Figure-3.35 B).
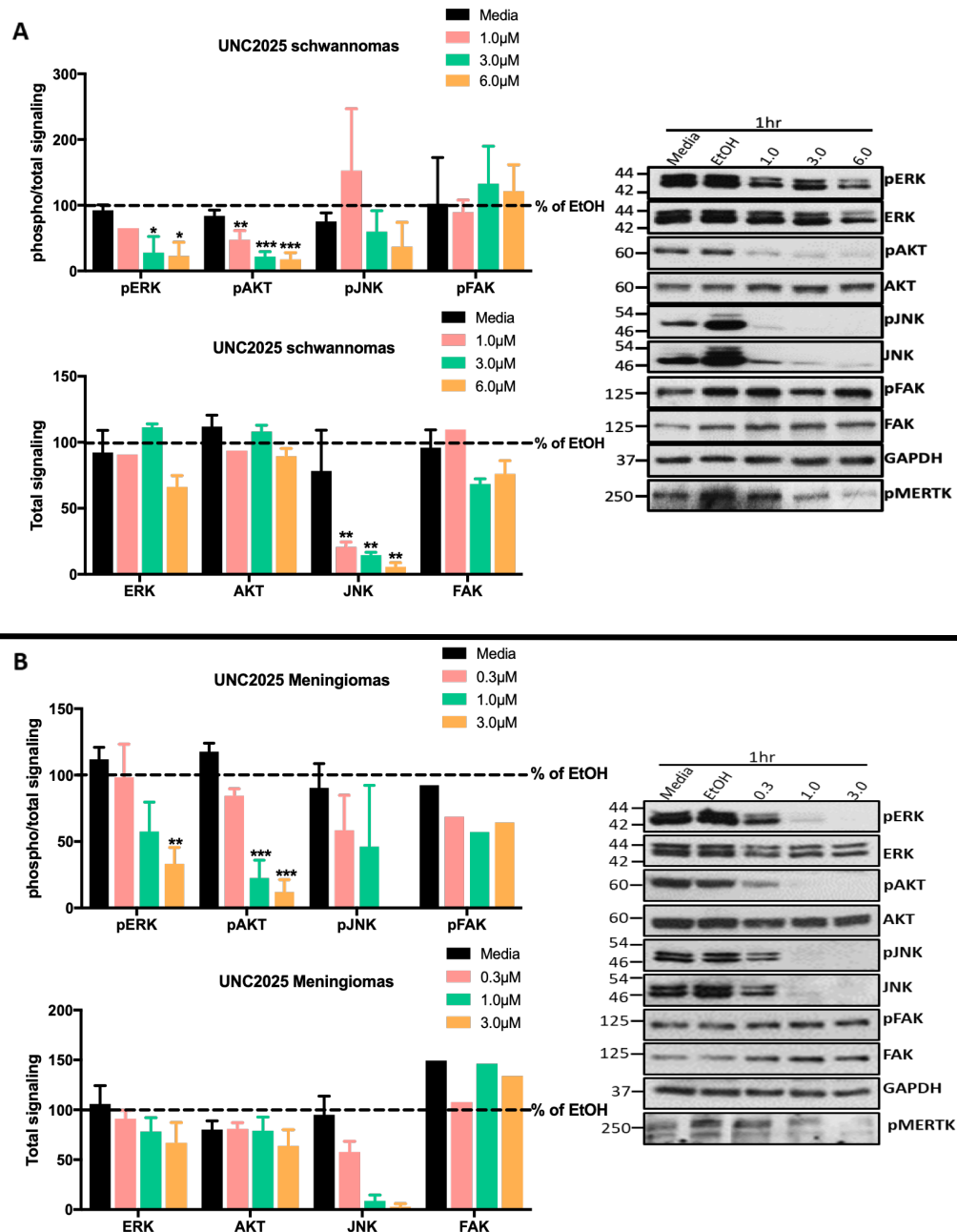
Figure 3. 35- The effect of MERTK inhibition by UNC2025 on downstream signaling molecules responsible for schwannoma and meningioma development. Representative Western blot of phosphorylated and total ERK, AKT, JNK and FAK in schwannoma **A)** and meningioma **B)** primary cells following one-hour of UNC2025 treatment. GAPDH was used as a loading control. Densitometry of Western blot of pERK/ERK and ERK/GAPDH (n=4-schwannomas; n=5-meningiomas); pAKT/AKT and AKT/GAPDH (n=3-schwannoma; n=4-meningiomas); pJNK/JNK and JNK/GAPDH (n=3-schwannomas; n=2-meningiomas); pFAK/FAK and FAK/GAPDH (n=2-schwannomas; n=1 meningiomas). Data were normalized to EtOH (vehicle) and media (cells containing normal growth medium) was used as a negative control, graphs represent mean ±SEM. ANOVA with Dunnett's multiple comparison test was performed using GraphPad Prism analysis software to calculate statistical significance; *p<0.05, **p<0.01 and ***p<0.001.

3b.2.2 The role of AXL in the regulation of downstream oncogenic signaling in meningioma primary cells

Genetic knock-down of *AXL*, which did not affect the expression of MERTK and TYRO3 in either schwannoma (Ammoun et al., 2014) or meningioma primary cells (Figure-3.13), impeded phospho-FAK signaling in schwannoma primary cells (Ammoun et al., 2014). A partial decrease in pFAK levels were also observed in meningioma primary cells on *AXL* knock-down. In addition, AXL shRNA also reduced pAKT levels in meningioma primary cells (Figure-3.36).
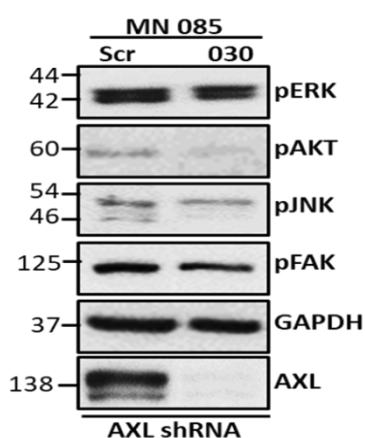
Figure 3. 36- The effect of *AXL* knock-down on downstream oncogenic signaling in schwannoma and meningioma primary cells. Western blot analysis shows that *AXL* knock-down in meningioma primary cells led to clear decrease in levels of pAKT and slight decrease in pFAK but has no effect on pERK levels (n=1). GAPDH was used as a loading control.

Incubation of meningioma primary cells with BGB324 for one-hour caused dose-dependent decrease in the relative phosphorylation of ERK, AKT and JNK signaling molecules in meningioma primary cells (Figure-3.37). BGB324 also slightly reduced total JNK levels in meningioma primary cells compared to vehicle; however, this difference was non-significant. BGB324 did not inhibit phospho-FAK and total FAK exprssion levels after one-hour of treatment (Figure-3.37).
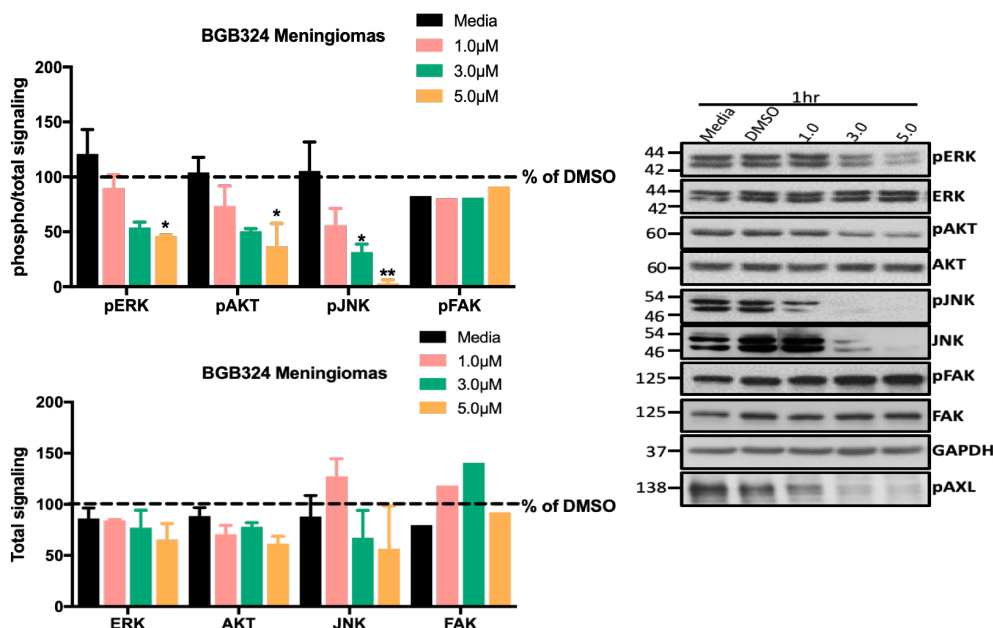
Figure 3. 37- The effect of AXL inhibition by BGB324 on downstream oncogenic signaling in meningioma primary cells. Representative Western blots of phosphorylated and total ERK, AKT, JNK and FAK following one-hour treatment of meningioma primary cells with BGB324. GAPDH was used as a loading control. Densitometry of Western blot of pERK/ERK and ERK/GAPDH (n=3); pAKT/AKT and AKT/GAPDH (n=3); pJNK/JNK and JNK/GAPDH (n=3); pFAK/FAK and FAK/GAPDH (n=1); graphs represent mean ±SEM. Data were normalized to DMSO (vehicle) and media (cells containing normal growth medium) was used as a negative control. GraphPad Prism analysis software was used to calculate statistical significance using ANOVA with Dunnett's multiple comparison test, *p<0.05 and **p<0.01.

Whilst BGB324 failed to effectively reduce phospho-AXL levels in schwannoma primary cells following one-hour treatment (Figure-3.30 A), BMS777607 almost completely abolished phospho-AXL in schwannoma primary cells at 10 μM after one-hour of treatment (Figure-3.32 A). Therefore, I decided to use BMS777607 to dissect downstream signaling of AXL receptor in schwannoma primary cells. BMS777607 mediated dose-dependent decrease in phospho-AKT levels from 10 μM. BMS777607 also led to dose-dependent decrease in the expression and phosphorylation of JNK; however, there was no noticeable difference in phospho JNK/JNK ratio compared to vehicle. BMS777607 did not affect either phosphorylated or total levels of ERK and FAK signaling molecules in schwannoma primary cells following one-hour of drug treatment (Figure-3.38). More repeats of this experiment will need to be performed to firmly conclude any data.
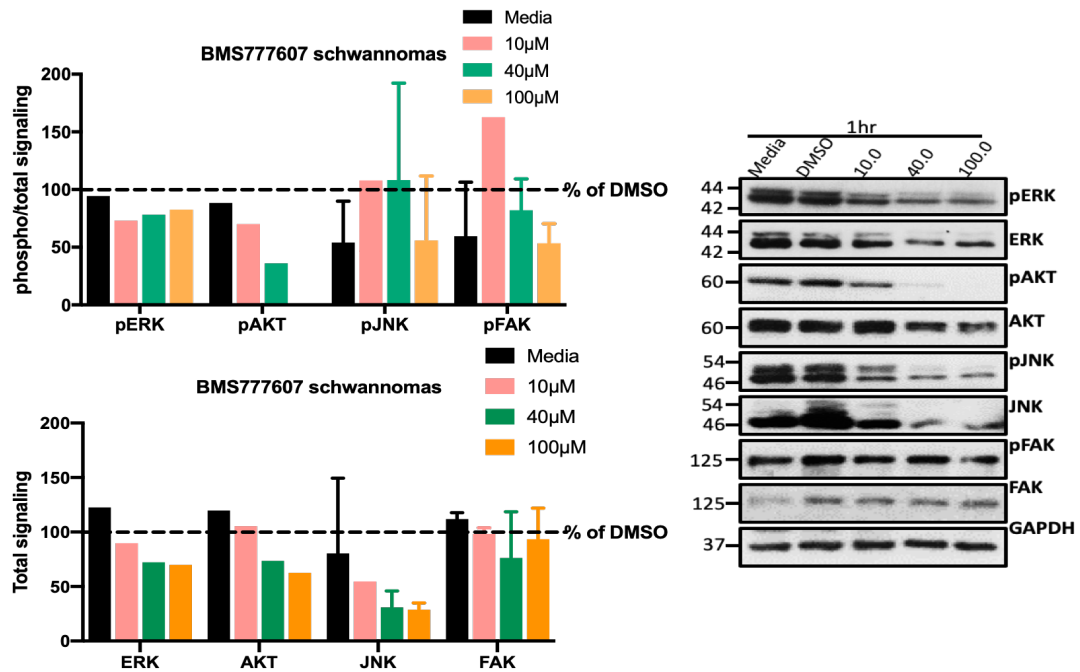
Figure 3. 38- The effect of AXL inhibition by BMS777607 on downstream oncogenic signaling in schwannoma primary cells. Representative Western blot of phosphorylated and total ERK, AKT, JNK and FAK following one-hour treatement of schwannoma primary cells with BMS77760. Schwannoma primary cells were treated with increasing concentration of BMS777607 (10.0-100.0 μM) or DMSO (vehicle control) for one-hour. GAPDH was used as a loading control. Densitometry of Western blot of pERK/ERK and ERK/GAPDH (n=1); pAKT/AKT and AKT/GAPDH (n=1); pJNK/JNK and JNK/GAPDH (n=2); pFAK/FAK and FAK/GAPDH (n=2), graphs represent mean ±SEM. Statistical calculation was not performed due to a small sample size.

3b.2.3 The role of TYRO3 in the regulation of downstream oncogenic signaling in schwannoma and meningioma primary cells

Although TYRO3 knock-down did not decrease the levels of cyclin-D1 in either schwannoma or meningioma primary cells (Figure - 3.18), strong expression and activation of the protein was previously observed in schwannoma primary cells (Ammoun et al., 2014) and in meningioma tissues and cells (Figure - 3.1 and Figure - 3.2). Hence, I decided to further explore an oncogenic potential of the receptor in these tumours using knock-down approach.

Indeed, a lentivirus mediated knock-down of *TYRO3* in schwannoma primary cells led to significant reduction of phospho-AKT and phospho-JNK levels and partial decrease in phospho-ERK levels (Figure-3.39 A). Conversely, in meningioma primary cells, TYRO3 reduction showed very inconclusive results and no consistent change in any downstream signaling pathways were detected (Figure-3.39 B).
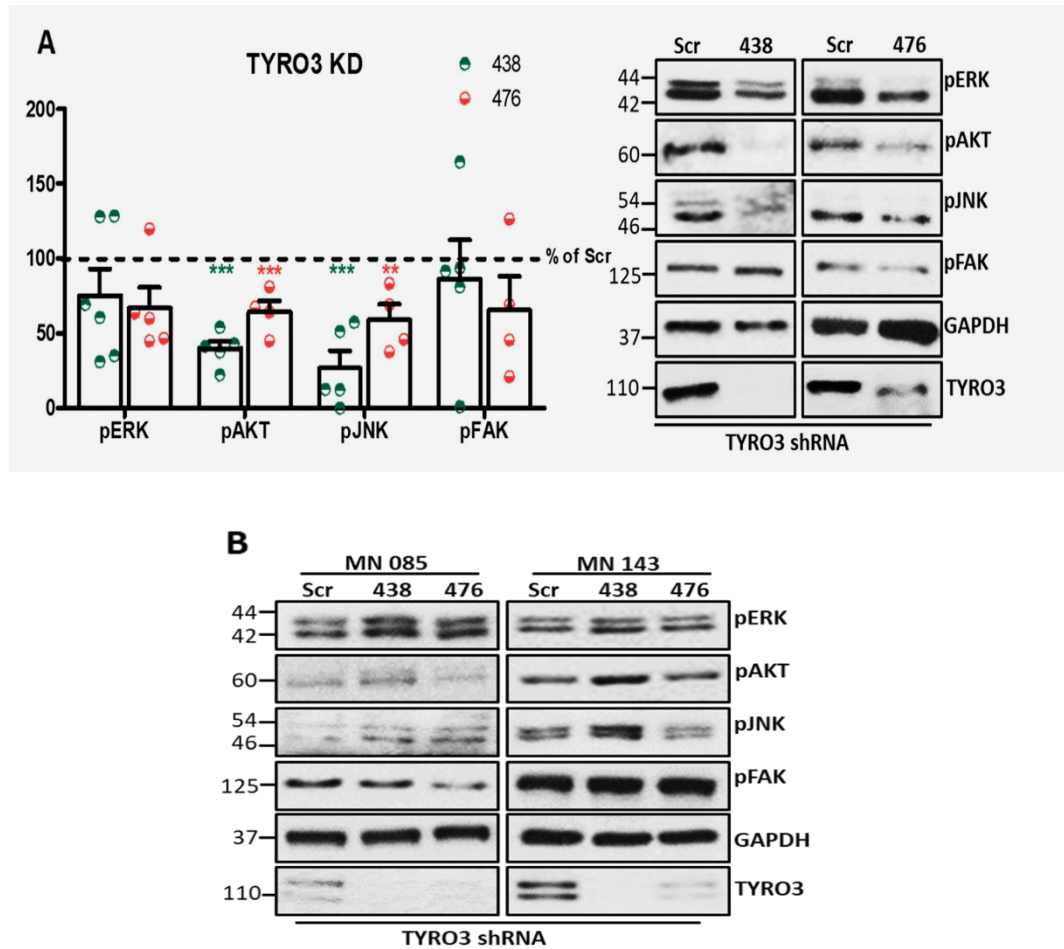
Figure 3. 39- The effect of *TYRO3* **knock-down on downstream oncogenic signaling in schwannoma and meningioma primary cells.** Knock-down of *TYRO3* using two shRNA constructs, 438 and 476, in schwannoma cells lead to a significant decrease in the levels of pAKT (n=4 for 438 and 476) and pJNK (n=5 for 438 and n=4 for 476). A partial decrease in the levels of pERK (n=6 for 438 and n=5 for 476) was observed but the levels of pFAK were not affected (n=5 for 438 and n=4 for 476). ANOVA with Dunnett's multiple comparison test was used to calculate statistical significance; *p<0.05, **p<0.01 and ***p<0.001 **A)**. No change in the levels of pERK pAKT, pJNK or pFAK was seen in Western blots of meningioma cells infected with TYRO3 shRNA (n=2) **B)**. GAPDH was used as a loading control.

3b.2.4 Discussion

The co-operative nature of TAM family members poses a challenge for dissecting the role of individual TAM receptor in promoting tumour development. A genetic knock-down of MERTK decreased total levels of AXL and TYRO3 in both schwannoma and meningioma primary cells (Figure-3.9 and Figure-3.11) but TYRO3 and AXL shRNA did not affect either expression of MERTK or of each other (Figure-3.11, Figure-3.12 and Figure-3.13). In schwannoma primary cells, UNC2025 decreased pAXL along with pMERTK after one-hour (Figure-3.28) but it was specific to pMERTK inhibition in meningioma cells (Figure-3.29). In addition, while BGB324 failed to inhibit pAXL after one-hour of treatment in schwannoma cells (Figure-3.31), it specifically inhibited pAXL in meningioma cells at the same time point (Figure-3.32). Capitalizing on the discrepancies between the modes of action of shRNA-mediated knock-down and kinase inhibitors, I looked at the role of TAM receptors on the activation of key downstream signaling pathways in schwannoma and meningioma primary cells as an individual entity or in a concert.

I previously determined that reducing the expression and activation of MERTK and AXL, by shRNA knock-down and kinase inhibitors, decreases proliferation of schwannoma and meningioma primary cells in culture via reducing cyclin-D1 (Figure-3.16 to Figure-3.17 and Figure-3.23 B, Figure-3.25 B). In prostate cancer, MEK/ERK specific inhibitor, PD098059 reduced cyclin-D1 levels by decreasing MEK/ERK/Jun pathway (Lee et al., 2016), signifying that ERK is upstream of cyclin-D1. Consistent with this finding, I showed that the inhibition of MERTK and AXL phosphorylation by UNC2025 and BGB324 in schwannoma and meningioma cells reduced pERK levels in a dose-dependent manner (Figure-3.35 and Figure-3.37), suggesting that a similar mechanism may play a role in decreasing cyclin-D1 levels downstream of ERK in schwannoma and meningioma

cells. Other studies have also demonstrated that treatments with UNC2025 and BGB324 lead to significant reductions in pERK-mediated proliferation in leukemia cells and NSCLC *in vitro* (DeRyckere et al., 2017, Cummings et al., 2015, Ben-Batalla et al., 2017). However, genetic knock-down of MERTK and AXL did not affect pERK levels in either cell-types (Figure-3.34 and Figure-3.36). These results suggest that an ERK-independent mechanism could be driving MERTK and AXL-mediated proliferation in schwannomas and meningiomas. Comparable results have also been reported previously in head and neck cancer where pERK levels were efficiently reduced by MERTK inhibitor UNC1062 but remain completely unaffected upon *MERTK* genetic knock-down (von Massenhausen et al., 2016). Similarly, in liposarcomas *AXL* genetic knock-down decreased the cell proliferation but did not affect pERK levels (May et al., 2015). However, in many other tumour cell-types MERTK and AXL shRNA decreased pERK levels (Martinelli et al., 2015, Keating et al., 2010), pointing towards differences in MERTK and AXL-induced signaling depending on the cell-type and tumour microenvironment.

Fms-like tyrosine kinase 3 (FLT3) is a type-III, RTK with familiar oncogenic role in hematopoietic malignancies. In AML, it activates the classical Ras/Raf/Mek/ERK1/2 signaling pathway to promote cell proliferation (Takahashi, 2011). A relatively high abundance of FLT3 has also been reported in meningiomas and astrocytic tumours such as GBM (Essbach et al., 2013). However, the importance of this receptor has not been further studied in these tumours. To recall that UNC2025 is a dual kinase inhibitor with equal potency against FLT3 and MERTK (Zhang et al., 2014). Moreover, BGB324 which has been considered as an AXL specific kinase inhibitor, has recently been shown to inhibit FLT3 with equivalent potency (Myers et al., 2018). Preliminary Western blots performed to check the effect of UNC2025 and BGB324 on pFLT3 showed successful inhibition of this kinase by both kinase inhibitors in these tumour cells (supplementary

figure-S1 and S2). Therefore, the involvement of FLT3 in debilitating pERK1/2 signaling by UNC2025 and BGB324 in schwannoma and meningioma primary cells cannot be dismissed. A detailed assessment of the role of the FLT3 receptor in tumour biology of schwannoma and meningioma is requied before either UNC2025 or BGB324 can be considered for the treatment of these tumours.

In addition to Ras/Raf/MEK/ERK pathway, Rac/PAK/JNK and PI3K/AKT cascades are also responsible for enhancing proliferation and survival of Merlin-deficient schwannoma and meningioma cells by inhibiting caspase-dependent apoptosis (Petrilli and Fernandez-Valle, 2016). I earlier showed that the inhibition of MERTK and AXL phosphorylation by UNC2025 and BGB324 in schwannomas and meningiomas increases the levels of cleaved caspase-3 and thus promotes apoptotic cell death (Figure-3.22 to Figure-3.25) which likely occurs via inhibition of pJNK and pAKT signaling molecules (Figure-3.35 and Figure-3.37).

JNK has been shown to play a vital role in both cell proliferation and apoptosis depending on the cell-type and a stimulus. In schwannoma primary cells, increased JNK/Jun signaling has been associated with Schwann cells de-differentiation and proliferation (Hilton et al., 2009). JNK can phosphorylate the transcription factor c-Jun, leading to increases in cyclin-D1 levels and subsequently to increased cell proliferation. JNK also enhances the survival of schwannoma cells by preventing the accumulation of reactive oxygen species (ROS) and inhibiting JNK confers sensitivity to γ-irradiation and increases apoptosis (Yue et al., 2013). Reducing MERTK expression in both schwannomas and meningiomas (Figure-3.34) and AXL expression in meningiomas (Figure-3.36) using MERTK shRNA and AXL shRNA respectively decreases pJNK levels. A dose-dependent decrease in pJNK was also observed upon treatment of schwannoma and meningioma primary cells with UNC2025 (Figure-3.35) and BGB324

(Figure-3.37), suggesting that UNC2025 and BGB324 blocks pJNK signaling by inhibiting pMERTK, pAXL and likely also pFLT3 as pFLT3 has also been shown to signal via pJNK in other cancers (Hartman et al., 2006).

PI3K/AKT signaling also plays an important role in promoting cell survival and cell proliferation by directly inhibiting apoptosis or by an indirect interaction with key mediators of proliferation such as *cyclin-D1*. In several cancers, activated MERTK and AXL bind to PI3K and phosphorylate AKT to protect cells from apoptotic cell death via various mechanisms (Cummings et al., 2013, Hasanbasic et al., 2004, Goruppi et al., 1997). AKT inhibits the pro-apoptotic protein caspase-3 and phosphorylates nuclear factor kappa-light-chain-enhancer of activated B cells (NF-kB) which in turn can activate anti-apoptotic proteins such as B-cell lymphoma 2 (Bcl-2) and B-cell lymphoma extra-large (Bcl-xL) (Hasanbasic et al., 2004). In NSCLC, UNC2025-mediated inhibition of pMERTK blocks basal and Gas6-induced phosphorylation of AKT and induces apoptotic cell death (Cummings et al., 2015). Similarly, genetic knock-down of MERTK and AXL reduced the survival of astrocytoma and melanoma cells by blocking the activation of AKT and its downstream effector mTOR (Keating et al., 2010, Tworkoski et al., 2013). In accordance with these reports, blocking the expression and activation of MERTK and AXL in schwannoma primary cells successfully inhibited pAKT signaling (Figure-3.34 A, Figure-3.35 A). Inhibition of pAKT was also observed in meningioma cells after genetic knock-down of AXL as well as after treatment with BGB324 (Figure-3.36 and Figure-3.37). Again, since MERTK does not engage pAKT signaling in meningioma cells, decreases in pAKT level after treatment with UNC2025 in meningioma could be due to FLT3 (Brandts et al., 2005).

FAK is another important signaling molecule in schwannoma and meningioma development. It plays a significant role in cell-matrix adhesion but when translocate to

nucleus, it can also regulate the cell proliferation by inhibiting the tumour suppressor activity of p53 in schwannoma cells (Ammoun et al., 2012). AXL receptor has been shown to signal via Src and FAK in schwannoma cells, when stimulated with Gas6 (Ammoun et al., 2014). In anaplastic meningioma cells, increased expression and phosphorylation of FAK facilitates cell migration (Wang et al., 2012). In melanoma cells, Gas6-induced activation of MERTK increased the phosphorylation of FAK and reducing the expression of MERTK impaired the migration and invasion of the tumour cells (Schlegel et al., 2013, Tworkoski et al., 2013). In head and neck cancer, inhibition of MERTK using UNC1062 decreased pFAK levels and reduced migration and invasion of the tumour cells (von Massenhausen et al., 2016). Similarly, my data shows that the genetic knock-down of MERTK and AXL disrupts the phosphorylation/activation of FAK in both schwannoma and meningioma primary cells (Figure-3.34 and Figure-3.36). However, all three TAM inhibitors failed to reduce pFAK levels following one-hour treatment of schwannoma and meningioma cells (Figure-3.35, Figure-3.37 and Figure-3.38). I would like to perform all signaling pathway experiments also at 72 hrs to see the long-term effect of kinase inhibitor on downstream signaling.

Out of three TAM members, TYRO3 is the least studied RTK in cancer. Only very recently, few publications have recognized the transforming potential of TYRO3 in promoting breast, colon, melanoma, and ovarian cancer (Chien et al., 2016, Ekyalongo et al., 2014, Kim et al., 2015, Smart et al., 2018). This is likely the reason that there have been only few efforts to develop TYRO3-specific inhibitor yet. Regardless of no change in cyclin-D1 levels (Figure-3.18), a genetic knock-down of TYRO3 caused a small but clear decrease in pERK and a significant decrease in pJNK levels in schwannoma cells (Figure-3.39). Since elevated activity of JNK is also related to higher cell-matrix adhesion and the fact that AXL has previously been shown to be responsible for increased cell-

matrix adhesion of schwannoma primary cells, I would like to investigate if TYRO3 is also involved in pathological cell-matrix adhesion of Merlin negative schwannoma cells via JNK signaling by performing adhesion assay as previously described in (Ammoun et al., 2014). In addition, a role of TYRO3 in promoting apoptosis also needs to be investigated further by performing cleaved caspase-3 staining on TYRO3 knock-down cells. Knock-down of TYRO3 in a melanoma cell-line has been shown to induce apoptosis in cells treated with TYRO3 shRNA cells compared to control shRNA (Demarest et al., 2013). Similarly, thyroid cells also showed enhanced apoptosis on siTYRO3 exposure (Avilla et al., 2011). Another group showed increased apoptosis in colorectal cancer cell-line and colorectal cancer patient cells upon treatment with a neutralizing TYRO3 antibody (Chien et al., 2016). In this regard, it is possible that TYRO3 may be important for increased cell survival and cell-matrix adhesion rather than proliferation in at least schwannoma cells as no consistent change in pJNK levels were observed on TYRO3 knock-down in meningioma cells.

Furthermore, genetic knock-down of *TYRO3* also reduced pAKT in schwannoma primary cells (Figure-3.39). Likewise, activation of PI3K/AKT signaling has been shown to be interrupted in platelets from TYRO3-/- mice (Angelillo-Scherrer et al., 2005). Importantly, phosphorylation of AXL was also inhibited in this TYRO3-/- mice and therefore it is difficult to say if inhibition of pAKT is due to TYRO3-/- or due to pAXL inhibition or both. Although ectopic expression TYRO3 in Rat2 cells led to enhanced activation of the AKT/mammalian target of rapamycin (mTOR)/ribosomal protein S6 kinase beta-1 (P70S6K) cascade suggesting that PI3K/AKT signaling is downstream of TYRO3 (Brown et al., 2012). Moreover, in rat hippocampal neurons, AKT phosphorylation was corelated with TYRO3 expression and was inhibited in TYRO3-/- mice (Guo et al., 2011, Zhong et al., 2010).

In summary, in meningioma primary cells, MERTK engages pJNK and pFAK whereas AXL engages pAKT, pJNK and pFAK signaling molecules. In schwannoma primary cells MERTK acts via pAKT, pJNK and pFAK; AXL acts via pSrc and pFAK (Ammoun et al., 2014); and TYRO3 acts via pERK, pAKT and pJNK. Both AXL and MERTK contribute to increased proliferation and survival of schwannoma and meningioma primary cells. The contribution of TYRO3 is yet to be determined for both tumour types. TAM receptor-mediated signaling can be successfully reversed using AXL inhibitor BGB324 and MERTK inhibitor UNC2025.

	UNC2025 (1 hr)		BGB324 (1 hr)		BMS777607 (1 hr)		MERTK shRNA		AXL shRNA		TYRO3 shRNA	
	Sch	MN	Sch	MN	Sch	MN	Sch	MN	Sch	MN	Sch	MN
pERK	✓	✓	-	✓	✓	-	✗	✗	-	✗	✓	✗
ERK	✗	✗	-	✗	✓	-	-	-	-	✗	-	-
pAKT	✓	✓	-	✓	✓	-	✓	✗	✓	✓	✓	✗
AKT	✗	✗	-	✗	✗	-	-	-	-	-	-	-
pJNK	✗	✗	-	✓	✗	-	✓	✓	-	✓	✓	✗
JNK	✓	✓	-	✓	✓	-	-	-	-	-	-	-
pFAK	✗	✗	-	✗	✗	-	✓	✓	✓	✓	✗	✗
FAK	✗	✗	-	✗	✗	-	✗	✗	-	-	-	-
pAXL	✓	✗	✗	✓	✓	✓	-	-	-	-	-	-
AXL	✗	✗	-	✗	✗	✗	✓	✓	-	✓	✗	✗
pMERTK	✓	✓	✗	✗	✗	✗	-	-	-	-	-	-
MERTK	✗	✗	-	✗	✓	✓	✓	✓	-	✗	✗	✗
pTYRO3	✗	✗	✗	✗	✗	✗	-	-	-	-	-	-
TYRO3	✗	✗	✗	✗	✓	✓	✓	✓	-	✗	✗	✗
pFLT3	-	✓	✓	✓	-	-	-	-	-	-	-	-

Table 3.2- A summary of shRNA and kinase inhibitor mediated inhibition of TAM receptors and their downsteam signaling effectors.

Chapter 4.0 - Conclusions

Conclusions

- MERTK, AXL and TYRO3 receptors and their ligand Gas6 are highly expressed and activated in Merlin-deficient meningioma tissues compared to normal control.

- Although there was no significant difference in the expression of TAM receptors in Merlin-deficient G-I meningioma cell-line Ben-Men-I and meningioma primary cells compared to HMCs, these receptors (except TYRO3) were highly phosphorylated in meningioma cells.

- The expression of all three TAM receptors were Merlin-dependent but Gas6 expression was not.

- MERTK and TYRO3 form a complex in schwannoma and meningioma tissues but not in Ben-Men-I cell-line and the expression of TYRO3 is dependent on the expression of MERTK in both tumour types.

- Although AXL and MERTK are not in complex either in schwannomas or meningiomas, expression of AXL is dependent on MERTK in both tumours.

- In meningioma cells, MERTK signals via pJNK and pFAK; AXL signals via pAKT, pJNK and pFAK.

- In schwannoma cells, MERTK signals via pAKT, pJNK and pFAK; TYRO3 activates pERK, pAKT and pJNK.

- UNC2025 is the most effective TAM family inhibitor tested in inhibiting the cell growth of both tumours and has the potential to be used as a common drug for treating schwannomas and meningiomas.

- BGB324 effectively inhibits meningioma cell growth at low concentrations but comparatively higher concentrations were required in order to have the same effect on schwannoma cell growth *in vitro.*

- *In vitro* BMS777607 was the least effective at inhibiting schwannoma and meningioma tumour cell growth and should not be considered for a further clinical development for either of the tumours studied in this report.

Chapter 5.0 – General discussion and future work

5.1 TAMs in schwannomas and meningiomas

TAM family receptors have been implicated in several cancers including but not limited to leukemia, colorectal cancer, gliomas, breast cancer, hepatocellular carcinoma and prostate cancer (Lemke, 2013). Our group has previously reported an elevated expression and activation of TYRO3, AXL and MERTK as well as their ligand Gas6 in Merlin-deficient schwannoma cells and tissues. Gas6-mediated activation of AXL receptor has been shown to play a role in the pathological proliferation, cell-matrix adhesion and survival of schwannoma cells (Ammoun et al., 2014). However, a role of the rest of the TAM family members has not been previously investigated. Moreover, IHC staining in search for differences in the expression and activation of growth factors, growth factor receptors and downstream signaling pathways between meningioma tissues and non-neoplastic meninges revealed significantly stronger staining of AXL, MERTK, Gas6 and pAXL along with multiple other molecules in meningioma tissues (Hilton et al., 2016). To my knowledge, no previous detailed studies have been carried out to understand the role of this family receptors in meningioma pathology. In this project, I have focused on Merlin-negative schwannoma and meningioma tumours since our previous results demonstrated a strong link between Merlin deficiency and the expression of TAMs and their agonist Gas6 in schwannoma (Ammoun et al., 2014). Here, I evaluated the expression and activation of AXL, MERTK and TYRO3 as well as their ligand Gas6 in Merlin-negative meningioma tissues and cells using Western blot. I also investigated the interaction and a cross-talk among TAM family members as well as their potential role as therapeutic targets by performing *in vitro* inhibition and knock-down experiments in both schwannoma and meningioma primary cells.

By analyzing protein expression and phosphorylation of AXL, MERTK and TYRO3 across meningioma tissues, I found an overexpression and activation of all three TAM

receptors and Gas6 in Merlin-deficient meningioma tissues (Figure-3.1 and Figure-3.3 A). To prove whether this upregulation is at the transcription level, I could have further performed qPCR. However, kinase inhibitors target protein itself and protein expression is more important to determine the therapeutic response (von Massenhausen et al., 2016), I only investigated protein levels of these receptors in this study due to time restraints and limited materials. Moreover, increased basal activation of TAM receptors were also detected in G-I Merlin-deficient meningioma primary cells and Ben-Men-I cell line which could be due to either paracrine/autocrine activation by released Gas6, or Gas6-dependent and/or independent complex formation with other types of receptors such as EGFR or PDGFR (Meyer et al., 2016, Vouri et al., 2016)

Although the exact mechanism of overexpression of these receptors is not yet clear, their expression seems to be partly regulated by the *NF2* gene since ectopic expression of Merlin significantly decreased TAM family expression levels in meningioma cells as was seen previously in schwannomas (Ammoun et al., 2014). However, not all TAM overexpressing tumours are Merlin-deficient i.e gastric cancer, head and neck cancer. Moreover, only a partial reduction (~50%) in the expression of AXL, MERTK and TYRO3 was achieved upon Merlin reintroduction and therefore an involvement of other regulatory genes or mechanisms in governing the expression of these receptors cannot be denied. Probably this is likely the reason why there was no significant difference in pAXL levels between Merlin-deficient and Merlin-expressing meningiomas (Hilton et al., 2016).

Ammoun *et al* previously established the importance of AXL in mediating schwannoma cell proliferation, survival and cell-matrix adhesion (Ammoun et al., 2014). By using *in vitro* knock-down and kinase inhibition experiments, here I further showed that not only AXL but also MERTK plays a vital role in mediating proliferation and survival of

schwannoma and meningioma cells. BGB324-mediated AXL and UNC2025-mediated MERTK inhibition represent novel therapeutic approaches in NF2-related tumours which have also been shown to enhance the efficacy of standard anti-cancer treatments in several other tumours including glioblastoma multiforme, non-small cell lung cancer, and breast cancer (Vouri et al., 2015, Sufit et al., 2016, Okimoto and Bivona, 2015, Li et al., 2009). Recently, TYRO3 has also emerged as an important modulator of tumorigenesis and many literatures have shown a benificial effect of targeting TYRO3 receptor (Smart et al., 2018). Although TYRO3 was not directly involved in mediating proliferation of schwannomas and meningioma cells, reducing TYRO3 expression in schwannoma significantly decreased pAKT and pJNK signaling. Therefore, the role of TYRO3 in promoting survival, cell-matrix adhesion and migration of these tumour should be further investigated in future.

An important finding of this study is the identification of the endogenous complex between TYRO3 and MERTK in schwannoma and meningioma tissues (Figure-3.7 A and Figure-3.8 A). Although physical interaction between AXL and TYRO3 has been reported in Rat2 cells, GnRH expressing neuronal cell-line and GBM cell-line (Brown et al., 2012, Vouri et al., 2016), this is the first study to report a complex between TYRO3 and MERTK. This interaction between TYRO3 and MERTK could be ligand dependent or independent. In GBM cell-line, endogenous interaction between AXL and TYRO3 was slightly enhanced upon stimulation of cells with Gas6 (Vouri et al., 2016). Although, this effect was deemed negligible. Moreover, structural studies revealed that TYRO3 can form a homo or heterocomplex in the absence of a ligand (Heiring et al., 2004). I show higher expression and release of Gas6 in meningioma cells as well in as Ben-Men-I cell-line. However, the physical interaction was only detected in schwannoma and meningioma tissue samples but not in the cell-line, suggesting that Gas6 may or may not

be important in complying TYRO3-MERTK complex formation in these tumours. As mentioned previously, CO-IP experiments of Ben-Men-I cells in culture both in the presence and absence of Gas6 would need to be carried out for this to be fully elucidated. Although the importance of TYRO3-MERTK complex in these tumours is not clear yet, it seems that MERTK, AXL and TYRO3 all co-operate and signal via multiple cascades such as AKT, JNK, FAK and cyclin-D1 to enhance schwannoma and meningioma cells proliferation and survival. Therefore, inhibitors of common downstream signaling pathways, as described in previous studies by our research group and by others, in schwannomas and meningiomas could also be used as therapeutic target for these tumours (Ammoun et al., 2008, Ammoun et al., 2010, Ammoun et al., 2011, Ammoun et al., 2012). Since RAS-RAF-MEK pathway and PI3K-AKT-mTOR pathway are two major pathways downstream of multiple RTKs, many inhibitors targeting these pathways have been developed and are currently in clinical trials (Tan et al., 2017). However, compensatory activation of alternative signaling cascades leading to drug resistance to targeted therapy has remained the main obstacle in the success of these kinds of treatments. For instance, in breast cancer, a highly specific MEK inhibitor-PD0325901, in addition to inhibiting the MEK/ERK pathway, caused an upregulation of PI3K pathway to sustain the oncogenic signaling (Hoeflich et al., 2009). In addition, inhibition of AKT or MEK in breast cancer cell-lines, was responsible for increased transcription and phosphorylation of multiple RTKs by alleviating feedback loop inhibition in cancer cells (Duncan et al., 2012, Chandarlapaty et al., 2011). Therefore, targeting a single molecule may not be an effective strategy also in schwannomas and meningiomas, instead a combination therapy that targets the RTK as well as downstream targets could be a more logical approach to inhibit schwannoma and meningioma growth.

Fascinatingly, UNC2025 and BGB324 successfully inhibited not only their respective kinases but also down-stream signaling molecules such as ERK, AKT and JNK. These signaling pathways are not only downstream of TAM receptors but also of several other receptors such as PDGFR, EGFR, IGFR1, VEGFR and integrins which all are highly expressed and activated in both schwannoma and meningioma tumours (Ammoun et al., 2014, Hilton et al., 2016). These results further emphasize the importance of targeting TAM family receptors in schwannoma and meningioma tumours. However, experiments investigating the effect of these drugs on signaling pathway inhibition must be performed for longer incubations (72 hrs or more) to see whether there is any risk of compensatory mechanisms.

5.2   Is it wise to target Gas6 in Merlin-deficient schwannoma and meningioma tumours?

In addition to directly targeting TAM kinases, more of an indirect approach of inhibiting TAM receptors by targeting their ligand has been gaining an attention recently. In pancreatic ductal carcinoma cells, Gas6 neutralizing antibody GMAB1 and GMAB2 successfully blocked Gas6-mediated autocrine activation of AXL (Moody et al., 2016). Anti-coagulant factor warfarin has also recently shown the efficiency in reducing metastatic growth of lung and pancreatic cancer by inhibiting Gas6-mediated activation of TAM receptors through blocking y-carboxylation of Gas6 (Paolino and Penninger, 2016, Kirane et al., 2015). Since schwannomas and meningiomas overexpress and release Gas6 (Figure-3.3 and Figure-3.4) that can activate TAM signaling in an autocrine or in a paracrine loop, targeting Gas6 in these tumours could be an interesting therapeutic approach. However, so far very few studies have used this approach to successfully target Gas6 in cancer and none of the aforementioned therapies have been successful enough to enter into clinical trials. In addition, there is adequate evidence of ligand-independent

activation of TAM receptors as well as the discovery of several new ligands for TAM receptors would further complicate any therapies targeting just one TAM family ligand (Caberoy et al., 2010, Caberoy et al., 2012, Bellosta et al., 1995, Heiring et al., 2004). Hence, rather than targeting a single ligand, I still believe that directly targeting TAM receptors is a much better strategy, at least for Merlin-negative schwannoma and meningioma tumours.

5.3 The best drug candidate for Merlin-negative schwannoma and meningioma tumours.

When comparing the effectiveness of UNC2025 and BGB324 in inhibiting schwannoma and meningioma cell growth, BGB324 was less effective at inhibiting AXL kinase and reducing total cell number (IC_{50}-14.30 µM-7 days) of schwannoma cells. However, BGB324 potently inhibited meningioma cell growth (IC_{50}-3.70 µM; 72 hrs and IC_{50}-0.13 µM; 7 days) at lower concentrations with minimum toxicity. On the other hand, UNC2025 was effective reducing oncogenic growth of both schwannoma (IC_{50}- 3.96 µM; 72 hrs and IC_{50}-3.09 µM; 7 days) and meningioma cells (IC_{50}- 1.45 µM; 72hrs and IC_{50}-0.47 µM; 7days) at lower concentrations. Whereas BGB324 makes an ideal candidate for Merlin-deficient sporadic meningioma patients, NF2 patients- suffering from multiple schwannomas and meningiomas, often require treatment for both tumour types. In this context, for NF2 patients with schwannomas and meningiomas, UNC2025 is the most potent candidate. Originally designed as type-II pan-TAM inhibitor, BMS-777607 unfortunately failed to reduce both schwannoma and meningioma cell growth at concentrations below 100 µM and therefore is not an ideal candidate to take forward in a clinical trial for NF2-related tumours.

Importantly, UNC2025 is a MERTK/FLT3 dual kinase inhibitor (Zhang et al., 2014). In addition, an elegant study published last year established that BGB324, which has long

been believed as an AXL-specific kinase inhibitor, also targets FLT3 with an equal potency (Myers et al., 2018). Whereas developing a highly specific kinase inhibitor has often remained a priority, most of the inhibitors involve a certain degree of cross-reactivity with other protein kinases, especially RTKs due to high homology within the kinase domain. TAM family receptors share a striking similarity in kinase domain not just among each other but also with other RTK families such as FLT3, RON, MET and Aurora A/B, In AML, AXL and FLT3 co-immunoprecipitate and AXL siRNA or soluble AXL chimeric protein (AXL-Fc) diminishes FLT3 phosphorylation (Park et al., 2013). The role of FLT3 is not well researched in brain tumours, however, a preliminary study carried out by Eßbach *et al* showed the expression of FLT3 at mRNA level in 87% of astrocytic tumours and in GBM (Essbach et al., 2013). The expression of FLT3 was also confirmed in all grades of meningiomas (Andrae et al., 2012). BGB324 and UNC2025 both successfully inhibited phosphorylation of FLT3 (supplementary figure S1 and S2) along with AXL and MERTK respectively. In this case, it is highly likely that the anti-tumour activity of these inhibitors in reducing schwannoma and meningioma cell growth may have been enhanced due to their effect on this additional kinase.

5.4   Potential use of TAM inhibitors as immune-modulators in Merlin-negative schwannoma and meningioma tumours

There has been a growing recognition of a complex cross-talk between tumour cells and stromal immune cells. Tumour cells can modulate stromal cells to facilitate the growth and development of tumours (Loges et al., 2010) and TAM receptors may play an important role in mediating this cross-talk. As previously described, TAM receptors are also expressed by tumour-infiltrating leukocytes such as macrophages and dendritic cells and, more importantly, expression of AXL and MERTK is restricted to anti-inflammatory M2 type macrophages (Chiu et al., 2015, Zizzo et al., 2012). Strong staining of MERTK

and the presence of AXL in M2 macrophages was also observed in this study (Supplimentary chapter 7.3, Figure- S3). TAM signaling is known to play a vital role in suppressing the production of pro-inflammatory cytokines such as IL-12 therefore, inhibiting the anti-tumour immune response by macrophages and dendritic cells (Cook et al., 2013). Moreover, there is evidence that TAM-overexpressing tumour cells can instruct macrophages to overexpress and secret elevated levels of Gas6 within the tumour microenvironment. This enhances TAM receptor signaling and create a positive feedback loop, further enhancing tumour growth (Loges et al., 2010). Secretion of Gas6 from the tumour microenvironment has been shown to be responsible for enhanced tumorigenic growth of GBM, breast cancer and colon cancer (Schoumacher and Burbridge, 2017). Targeting the immuno-suppressive effect of TAM receptors provides an excellent opportunity to enhance the effectiveness of anti-cancer treatment. One study reported increased serological levels of pro-inflammatory cytokines and higher numbers of CD8$^+$ T lymphocytes in MERTK-/- mice compared to wild type (Cook et al., 2013). Additional studies suggest a role of MERTK in regulating immune checkpoint signaling through PD-L1 and PD-L2. PD-L1 and PD-L2 bind to PD-1 on tumour-infiltrating T cells, rendering them inactive and inducing apoptosis of tumour-reactive T cells therefore, suppressing anti-tumour immune response (Dong et al., 2002, Blank et al., 2004). Expression of PDL-1, PDL-2 and/or PD-1 is a prognostic factor in several cancers (Konishi et al., 2004, Yamamoto et al., 2008). Constitutively activated MERTK increased the expression of PD-L1 and PD-L2 in epithelial cells and genetic knock-down of MERTK in the aggressive breast cancer cell-line MDA-MB 231 reduced the expression of PD-L1 compared to control (Nguyen et al., 2014). Although the exact mechanism of how MERTK inhibits PD-L1 and PD-L2 signaling is not known yet, recent study also showed that inhibition of MERTK using the small molecule MERTK inhibitor MRX-2843,

decreased the expression of PD-1 on CD4$^+$ and CD8$^+$ T cells as well as T$_{reg}$ cells in leukemia (Lee-Sherick et al., 2018).

Similarly, inhibition of AXL by BGB324 in prostate cancer reduced the activity of tank-binding kinase 1 (TBK1) that resulted in decrease of immunosuppressor chemokines CCL11, IL-7, IL-1β, and IL-6 as well as tumour-associated macrophages (Ludwig et al., 2018). In the mammary adenocarcinoma 4T1/Balb/C syngeneic mouse model, treatment of BGB324 (50 mg/kg bid) enhanced the responsiveness to anti-CTLA-4/anti-PD-1 treatment (10 mg/kg of each, 4 doses) by increasing CD8+ T cell tumor infiltration (Research, 2016 January). Moreover, two out of four -AML patients treated with BGB324 for three weeks in a clinical trial showed enhanced T cell clonal population and anti-tumour immune response (Sonja, 2016).

In addition, another study reported the potential of targeting TAM receptors to enhance ani-tumour response by activation of NK cells. The authors showed that all three TAM receptors are expressed by natural killer (NK) cells *in vitro* and binding of TAM receptors to Gas6 inhibits the proliferation of NK cells and production of interferon gamma (IFN-y). The inhibition of TAM receptors using TAM specific inhibitor LDC1267 *in vivo* resulted in release of NK cells and killing of tumour cells (Paolino et al., 2014, Sonja, 2016). These results are encouraging for future research into TAM receptors and their link to immunological signaling as targeting TAM receptors may promote anti-tumour immunity in cancer treatments.

Since schwannomas and meningiomas also show high infiltration of macrophages, targeting TAM receptors in these tumours may enhance anti-tumour immune response. Very preliminary work carried out in this project also showed a correlation between level of MERTK and macrophage infiltration in meningiomas (Supplementary chapter 7.3, Figure S4). However, so far little is known about the mechanism and importance of

macrophages in NF2-related tumours, furthermore, the effect of TAM signaling in mediating immune cell–tumour cell interaction may be tumour specific. Future experiments should be conducted to study the importance of high MERTK level in macrophages along with on tumour cells and to study the effect of MERTK inhibition on anti-tumour immune response and to compare the effectiveness of MERTK inhibition in tumours with high and low macrophage infiltration.

5.5   Concerns of using TAM inhibitors

While the role of TAM receptors as oncogenes and immune suppressors in several cancers makes the inhibition of TAM receptors an impressive strategy on one side, counterproductive results of TAM inhibition in other systems present a paradox regarding the use of TAM inhibitors. Li Q and colleagues showed that TAM triple knock-out mice developed systemic autoimmunity which resulted in an increased production of proinflammatory cytokines such as TNF-α and disruption of the blood brain barrier (BBB). Moreover, increased neuronal cell death in these mice, probably due to increased neuroinflammation, raises concerns for the development of neurodegenerative disorders such as Alzimer's and Parkinson's disease in long term (Li et al., 2013). Interestingly, TAM receptors and their ligand Gas6 seem to play a tumour suppressor role in colitis-colorectal cancer as opposed to the usual oncogenic role demonstrated in many other cancers. Chronic inflammation caused by colitis increases the risk of colorectal cancer and TAMs appear to reduce the inflammatory immune response in this condition, therefore helping to prevent the onset of related cancer. Indeed, two separate studies showed that Gas6-/- and AXL-/-MERTK-/- mice had larger tumour volume and decreased overall survival (Bosurgi et al., 2013, Akitake-Kawano et al., 2013).

The contradictory role of TAM receptors and Gas6 emphasizes a real need to think thoroughly about the potential long-term effects of TAM inactivation since chronic

inflammation has long been associated with increased risk of cancer. In order to deal with this problem Bosurgi *et al* suggested to develop a therapeutic strategy that spare the macrophages population involved in regulation of local inflammation and tissue homeostasis from TAM inhibition (Bosurgi et al., 2013). While this approach can be of use for inflammation-driven cancer like the colitis-colorectal cancer mentioned previously, I believe that it could be little biased as activating innate immune response has a protective role in several other cancers. A better understanding of the cell-type and the tumour-type specific role of TAM signaling in inflammation setting would help in deciding upon the therapeutic suitability of targeting TAMs in specific cancers.

Again, while removal of all three TAM receptors lead to development of systemic immunity in TAM triple knock-out mice, strikingly it did not reduce the life expectancy and the effects of autoimmunity were also appeared to be well-tolerated (Li et al., 2013). Moreover, it was complete depletion of TAMs that lead to excess immunity in these mice, therefore partial inhibition of TAMs or reducing TAM levels only to basal physiological level may provide therapeutic benefits without inducing unnecessary toxicity. AXL inhibitor BGB324 has proved its effectiveness at low, physiologically-safe doses in healthy volunteers and showed its potential to be used as a cancer immunotherapy in future without inducing a toxicity (Wnuk-Lipinska et al., 2014). Consistent with this UNC2025 has also shown promising results in pre-clinical trials and an analogue of the drug, MRX2843, has just entered into phase-I clinical trial (NCT03510104). Although there is skepticism about long-term effects of these kinase inhibitors on patient's immunity, in immediate setting BGB324 and particularly UNC2025 appear to be promising small molecules for the treatment of NF2 patients.

In conclusion, the development of TAM therapies for the treatment of meningioma and schwannomas are promising but futher investigations are required to ensure anti-

tumourgenic effects do not have long term consequences on normal tissue maintenance and development.

6.0 <u>References</u>

AAVIKKO, M., LI, S. P., SAARINEN, S., ALHOPURO, P., KAASINEN, E., MORGUNOVA, E., LI, Y., VESANEN, K., SMITH, M. J., EVANS, D. G., POYHONEN, M., KIURU, A., AUVINEN, A., AALTONEN, L. A., TAIPALE, J. & VAHTERISTO, P. 2012. Loss of SUFU function in familial multiple meningioma. *Am J Hum Genet,* 91**,** 520-6.

ABEDALTHAGAFI, M., BI, W. L., AIZER, A. A., MERRILL, P. H., BREWSTER, R., AGARWALLA, P. K., LISTEWNIK, M. L., DIAS-SANTAGATA, D., THORNER, A. R., VAN HUMMELEN, P., BRASTIANOS, P. K., REARDON, D. A., WEN, P. Y., AL-MEFTY, O., RAMKISSOON, S. H., FOLKERTH, R. D., LIGON, K. L., LIGON, A. H., ALEXANDER, B. M., DUNN, I. F., BEROUKHIM, R. & SANTAGATA, S. 2016. Oncogenic PI3K mutations are as common as AKT1 and SMO mutations in meningioma. *Neuro Oncol,* 18**,** 649-55.

ABEDALTHAGAFI, M. S., MERRILL, P. H., BI, W. L., JONES, R. T., LISTEWNIK, M. L., RAMKISSOON, S. H., THORNER, A. R., DUNN, I. F., BEROUKHIM, R., ALEXANDER, B. M., BRASTIANOS, P. K., FRANCIS, J. M., FOLKERTH, R. D., LIGON, K. L., VAN HUMMELEN, P., LIGON, A. H. & SANTAGATA, S. 2014. Angiomatous meningiomas have a distinct genetic profile with multiple chromosomal polysomies including polysomy of chromosome 5. *Oncotarget,* 5**,** 10596-606.

AGARWAL, R., LIEBE, S., TURSKI, M. L., VIDWANS, S. J., JANKU, F., GARRIDO-LAGUNA, I., MUNOZ, J., SCHWAB, R., RODON, J., KURZROCK, R., SUBBIAH, V. & PAN-CANCER WORKING, G. 2014. Targeted therapy for hereditary cancer syndromes: neurofibromatosis type 1, neurofibromatosis type 2, and Gorlin syndrome. *Discov Med,* 18**,** 323-30.

AGNIHOTRI, S., JALALI, S., WILSON, M. R., DANESH, A., LI, M., KLIRONOMOS, G., KRIEGER, J. R., MANSOURI, A., KHAN, O., MAMATJAN, Y., LANDON-BRACE, N., TUNG, T., DOWAR, M., LI, T., BRUCE, J. P., BURRELL, K. E., TONGE, P. D., ALAMSAHEBPOUR, A., KRISCHEK, B., AGARWALLA, P. K., BI, W. L., DUNN, I. F., BEROUKHIM, R., FEHLINGS, M. G., BRIL, V., PAGNOTTA, S. M., IAVARONE, A., PUGH, T. J., ALDAPE, K. D. & ZADEH, G. 2016. The genomic landscape of schwannoma. *Nat Genet,* 48**,** 1339-1348.

AKITAKE-KAWANO, R., SENO, H., NAKATSUJI, M., KIMURA, Y., NAKANISHI, Y., YOSHIOKA, T., KANDA, K., KAWADA, M., KAWADA, K., SAKAI, Y. & CHIBA, T. 2013. Inhibitory role of Gas6 in intestinal tumorigenesis. *Carcinogenesis,* 34**,** 1567-74.

AKKERMANN, R., APRICO, A., PERERA, A. A., BUJALKA, H., COLE, A. E., XIAO, J., FIELD, J., KILPATRICK, T. J. & BINDER, M. D. 2017. The TAM receptor Tyro3 regulates myelination in the central nervous system. *Glia,* 65**,** 581-591.

ALAHMADI, H. & CROUL, S. E. 2011. Pathology and genetics of meningiomas. *Semin Diagn Pathol,* 28**,** 314-24.

ALANIN, M. C., KLAUSEN, C., CAYE-THOMASEN, P., THOMSEN, C., FUGLEHOLM, K., POULSGAARD, L., LASSEN, U., MAU-SORENSEN, M. & HOFLAND, K. F. 2015. The effect of bevacizumab on vestibular schwannoma tumour size and hearing in patients with neurofibromatosis type 2. *Eur Arch Otorhinolaryngol,* 272**,** 3627-33.

ALAO, J. P. 2007. The regulation of cyclin D1 degradation: roles in cancer development and the potential for therapeutic invention. *Mol Cancer,* 6**,** 24.

ALLEN, M. P., LINSEMAN, D. A., UDO, H., XU, M., SCHAACK, J. B., VARNUM, B., KANDEL, E. R., HEIDENREICH, K. A. & WIERMAN, M. E. 2002. Novel mechanism for gonadotropin-releasing hormone neuronal migration involving Gas6/Ark signaling to p38 mitogen-activated protein kinase. *Mol Cell Biol,* 22**,** 599-613.

AMMOUN, S., CUNLIFFE, C. H., ALLEN, J. C., CHIRIBOGA, L., GIANCOTTI, F. G., ZAGZAG, D., HANEMANN, C. O. & KARAJANNIS, M. A. 2010. ErbB/HER receptor activation and preclinical efficacy of lapatinib in vestibular schwannoma. *Neuro Oncol,* 12**,** 834-43.

AMMOUN, S., EVANS, D. G., HILTON, D. A., STREETER, A., HAYWARD, C. & HANEMANN, C. O. 2019. Phase 0 trial investigating the intratumoural concentration and activity of sorafenib in neurofibromatosis type 2. *J Neurol Neurosurg Psychiatry.*

AMMOUN, S., FLAIZ, C., RISTIC, N., SCHULDT, J. & HANEMANN, C. O. 2008. Dissecting and targeting the growth factor-dependent and growth factor-independent extracellular signal-regulated kinase pathway in human schwannoma. *Cancer Res,* 68**,** 5236-45.

AMMOUN, S., PROVENZANO, L., ZHOU, L., BARCZYK, M., EVANS, K., HILTON, D. A., HAFIZI, S. & HANEMANN, C. O. 2014. Axl/Gas6/NFkappaB signalling in schwannoma pathological proliferation, adhesion and survival. *Oncogene,* 33**,** 336-46.

AMMOUN, S., SCHMID, M. C., TRINER, J., MANLEY, P. & HANEMANN, C. O. 2011. Nilotinib alone or in combination with selumetinib is a drug candidate for neurofibromatosis type 2. *Neuro Oncol,* 13**,** 759-66.

AMMOUN, S., SCHMID, M. C., ZHOU, L., HILTON, D. A., BARCZYK, M. & HANEMANN, C. O. 2015. The p53/mouse double minute 2 homolog complex deregulation in merlin-deficient tumours. *Mol Oncol,* 9**,** 236-48.

AMMOUN, S., SCHMID, M. C., ZHOU, L., RISTIC, N., ERCOLANO, E., HILTON, D. A., PERKS, C. M. & HANEMANN, C. O. 2012. Insulin-like growth factor-binding protein-1 (IGFBP-1) regulates human schwannoma proliferation, adhesion and survival. *Oncogene,* 31**,** 1710-22.

ANDRAE, N., KIRCHES, E., HARTIG, R., HAASE, D., KEILHOFF, G., KALINSKI, T. & MAWRIN, C. 2012. Sunitinib targets PDGF-receptor and Flt3 and reduces survival and migration of human meningioma cells. *Eur J Cancer,* 48**,** 1831-41.

ANGELILLO-SCHERRER, A., BURNIER, L., FLORES, N., SAVI, P., DEMOL, M., SCHAEFFER, P., HERBERT, J. M., LEMKE, G., GOFF, S. P., MATSUSHIMA, G. K., EARP, H. S., VESIN, C., HOYLAERTS, M. F., PLAISANCE, S., COLLEN, D., CONWAY, E. M., WEHRLE-HALLER, B. & CARMELIET, P. 2005. Role of Gas6 receptors in platelet signaling during thrombus stabilization and implications for antithrombotic therapy. *J Clin Invest,* 115**,** 237-46.

ANTONY, J., ZANINI, E., KELLY, Z., TAN, T. Z., KARALI, E., ALOMARY, M., JUNG, Y., NIXON, K., CUNNEA, P., FOTOPOULOU, C., PATERSON, A., ROY-NAWATHE, S., MILLS, G. B., HUANG, R. Y., THIERY, J. P., GABRA, H. & RECCHI, C. 2018. The tumour suppressor OPCML promotes AXL inactivation by the phosphatase PTPRG in ovarian cancer. *EMBO Rep,* 19.

APRA, C., PEYRE, M. & KALAMARIDES, M. 2018. Current treatment options for meningioma. *Expert Rev Neurother,* 18**,** 241-249.

ARANCIBIA-CARCAMO, I. L., FAIRFAX, B. P., MOSS, S. J. & KITTLER, J. T. 2006. Studying the Localization, Surface Stability and Endocytosis of Neurotransmitter Receptors by Antibody Labeling and Biotinylation Approaches. *In:* KITTLER, J. T. & MOSS, S. J. (eds.) *The Dynamic Synapse: Molecular Methods in Ionotropic Receptor Biology.* Boca Raton (FL).

AVILLA, E., GUARINO, V., VISCIANO, C., LIOTTI, F., SVELTO, M., KRISHNAMOORTHY, G., FRANCO, R. & MELILLO, R. M. 2011. Activation of TYRO3/AXL tyrosine kinase receptors in thyroid cancer. *Cancer Res,* 71**,** 1792-804.

AXELROD, H. & PIENTA, K. J. 2014. Axl as a mediator of cellular growth and survival. *Oncotarget,* 5**,** 8818-52.

BAE, S. Y., HONG, J. Y., LEE, H. J., PARK, H. J. & LEE, S. K. 2015. Targeting the degradation of AXL receptor tyrosine kinase to overcome resistance in gefitinib-resistant non-small cell lung cancer. *Oncotarget,* 6**,** 10146-60.

BAEKELANDT, M., LEHNE, G., TROPE, C. G., SZANTO, I., PFEIFFER, P., GUSTAVSSSON, B. & KRISTENSEN, G. B. 2001. Phase I/II trial of the multidrug-resistance modulator valspodar combined with cisplatin and doxorubicin in refractory ovarian cancer. *J Clin Oncol,* 19**,** 2983-93.

BALOGH, I., HAFIZI, S., STENHOFF, J., HANSSON, K. & DAHLBACK, B. 2005. Analysis of Gas6 in human platelets and plasma. *Arterioscler Thromb Vasc Biol,* 25**,** 1280-6.

BASER, M. E., FRIEDMAN, J. M., JOE, H., SHENTON, A., WALLACE, A. J., RAMSDEN, R. T. & EVANS, D. G. 2011. Empirical development of improved diagnostic criteria for neurofibromatosis 2. *Genet Med,* 13**,** 576-81.

BASU, B., DEAN, E., PUGLISI, M., GREYSTOKE, A., ONG, M., BURKE, W., CAVALLIN, M., BIGLEY, G., WOMACK, C., HARRINGTON, E. A., GREEN, S., OELMANN, E., DE BONO, J. S., RANSON, M. & BANERJI, U. 2015. First-in-Human Pharmacokinetic and Pharmacodynamic Study of the Dual m-TORC 1/2 Inhibitor AZD2014. *Clin Cancer Res,* 21**,** 3412-9.

BAUMANN, C., ULLRICH, A. & TORKA, R. 2017. GAS6-expressing and self-sustaining cancer cells in 3D spheroids activate the PDK-RSK-mTOR pathway for survival and drug resistance. *Mol Oncol,* 11**,** 1430-1447.

BEAUCHAMP, R. L., JAMES, M. F., DESOUZA, P. A., WAGH, V., ZHAO, W. N., JORDAN, J. T., STEMMER-RACHAMIMOV, A., PLOTKIN, S. R., GUSELLA, J. F., HAGGARTY, S. J. & RAMESH, V. 2015. A high-throughput kinome screen reveals serum/glucocorticoid-regulated kinase 1 as a therapeutic target for NF2-deficient meningiomas. *Oncotarget,* 6**,** 16981-97.

BELLOSTA, P., COSTA, M., LIN, D. A. & BASILICO, C. 1995. The receptor tyrosine kinase ARK mediates cell aggregation by homophilic binding. *Mol Cell Biol,* 15**,** 614-25.

BEN-BATALLA, I., ERDMANN, R., JORGENSEN, H., MITCHELL, R., ERNST, T., VON AMSBERG, G., SCHAFHAUSEN, P., VELTHAUS, J. L., RANKIN, S., CLARK, R. E., KOSCHMIEDER, S., SCHULTZE, A., MITRA, S., VANDENBERGHE, P., BRUMMENDORF, T. H., CARMELIET, P., HOCHHAUS, A., PANTEL, K., BOKEMEYER, C., HELGASON, G. V., HOLYOAKE, T. L. & LOGES, S. 2017. Axl Blockade by BGB324 Inhibits BCR-ABL Tyrosine Kinase Inhibitor-Sensitive and -Resistant Chronic Myeloid Leukemia. *Clin Cancer Res,* 23**,** 2289-2300.

BENTZIEN, F., ZUZOW, M., HEALD, N., GIBSON, A., SHI, Y., GOON, L., YU, P., ENGST, S., ZHANG, W., HUANG, D., ZHAO, L., VYSOTSKAIA, V., CHU, F., BAUTISTA, R., CANCILLA, B., LAMB, P., JOLY, A. H. & YAKES, F. M. 2013. In vitro and in vivo activity of cabozantinib (XL184), an inhibitor of RET, MET, and VEGFR2, in a model of medullary thyroid cancer. *Thyroid,* 23**,** 1569-77.

BERGENBIO. 2014, April 09. *Bergenbio presents positive phase ia data on bgb324 at aacr* [Online]. Available: h[ttps://www.bergenbio.com/bergenbio-presents-positive-phase-ia-data-on-bgb324-at-aacr/](https://www.bergenbio.com/bergenbio-presents-positive-phase-ia-data-on-bgb324-at-aacr/) [Accessed].

BERTOTTI, A., BRACCO, C., GIROLAMI, F., TORTI, D., GASTALDI, S., GALIMI, F., MEDICO, E., ELVIN, P., COMOGLIO, P. M. & TRUSOLINO, L. 2010. Inhibition of Src impairs the growth of met-addicted gastric tumors. *Clin Cancer Res,* 16**,** 3933-43.

BI, W. L., ABEDALTHAGAFI, M., HOROWITZ, P., AGARWALLA, P. K., MEI, Y., AIZER, A. A., BREWSTER, R., DUNN, G. P., AL-MEFTY, O., ALEXANDER, B. M., SANTAGATA, S., BEROUKHIM, R. & DUNN, I. F. 2016. Genomic landscape of intracranial meningiomas. *J Neurosurg,* 125**,** 525-35.

BIJLSMA, E. K., BROUWER-MLADIN, R., BOSCH, D. A., WESTERVELD, A. & HULSEBOS, T. J. 1992. Molecular characterization of chromosome 22 deletions in schwannomas. *Genes Chromosomes Cancer,* 5**,** 201-5.

BINDER, M. D., CATE, H. S., PRIETO, A. L., KEMPER, D., BUTZKUEVEN, H., GRESLE, M. M., CIPRIANI, T., JOKUBAITIS, V. G., CARMELIET, P. & KILPATRICK, T. J. 2008. Gas6 deficiency increases oligodendrocyte loss and microglial activation in response to cuprizone-induced demyelination. *J Neurosci,* 28**,** 5195-206.

BINDER, M. D. & KILPATRICK, T. J. 2009. TAM Receptor Signalling and Demyelination. *Neurosignals,* 17**,** 277-287.

BLAKELEY, J. O. & PLOTKIN, S. R. 2016. Therapeutic advances for the tumors associated with neurofibromatosis type 1, type 2, and schwannomatosis. *Neuro Oncol,* 18**,** 624-38.

BLANK, C., BROWN, I., PETERSON, A. C., SPIOTTO, M., IWAI, Y., HONJO, T. & GAJEWSKI, T. F. 2004. PD-L1/B7H-1 inhibits the effector phase of tumor rejection by T cell receptor (TCR) transgenic CD8+ T cells. *Cancer Res,* 64**,** 1140-5.

BOLLAG, G., CLAPP, D. W., SHIH, S., ADLER, F., ZHANG, Y. Y., THOMPSON, P., LANGE, B. J., FREEDMAN, M. H., MCCORMICK, F., JACKS, T. & SHANNON, K. 1996. Loss of NF1 results in activation of the Ras signaling pathway and leads to aberrant growth in haematopoietic cells. *Nat Genet,* 12**,** 144-8.

BONDY, M. & LIGON, B. L. 1996. Epidemiology and etiology of intracranial meningiomas: a review. *J Neurooncol,* 29**,** 197-205.

BOSURGI, L., BERNINK, J. H., DELGADO CUEVAS, V., GAGLIANI, N., JOANNAS, L., SCHMID, E. T., BOOTH, C. J., GHOSH, S. & ROTHLIN, C. V. 2013. Paradoxical role of the proto-oncogene Axl and Mer receptor tyrosine kinases in colon cancer. *Proc Natl Acad Sci U S A,* 110**,** 13091-6.

BOULAGNON-ROMBI, C., FLEURY, C., FICHEL, C., LEFOUR, S., MARCHAL BRESSENOT, A. & GAUCHOTTE, G. 2017. Immunohistochemical Approach to the Differential Diagnosis of Meningiomas and Their Mimics. *J Neuropathol Exp Neurol,* 76**,** 289-298.

BOYD, K. P., KORF, B. R. & THEOS, A. 2009. Neurofibromatosis type 1. *J Am Acad Dermatol,* 61**,** 1-14; quiz 15-6.

BRANDAO, L., MIGDALL-WILSON, J., EISENMAN, K. & GRAHAM, D. K. 2011. TAM receptors in leukemia: expression, signaling, and therapeutic implications. *Crit Rev Oncog,* 16**,** 47-63.

BRANDTS, C. H., SARGIN, B., RODE, M., BIERMANN, C., LINDTNER, B., SCHWABLE, J., BUERGER, H., MULLER-TIDOW, C., CHOUDHARY, C., MCMAHON, M., BERDEL, W. E. & SERVE, H. 2005. Constitutive activation of Akt by Flt3 internal tandem duplications is necessary for increased survival, proliferation, and myeloid transformation. *Cancer Res,* 65**,** 9643-50.

BRASTIANOS, P. K., HOROWITZ, P. M., SANTAGATA, S., JONES, R. T., MCKENNA, A., GETZ, G., LIGON, K. L., PALESCANDOLO, E., VAN HUMMELEN, P., DUCAR, M. D., RAZA, A., SUNKAVALLI, A., MACCONAILL, L. E., STEMMER-RACHAMIMOV, A. O., LOUIS, D. N., HAHN, W. C., DUNN, I. F. & BEROUKHIM, R. 2013. Genomic sequencing of meningiomas identifies oncogenic SMO and AKT1 mutations. *Nat Genet,* 45**,** 285-9.

BRAUNGER, J., SCHLEITHOFF, L., SCHULZ, A. S., KESSLER, H., LAMMERS, R., ULLRICH, A., BARTRAM, C. R. & JANSSEN, J. W. 1997. Intracellular signaling of the Ufo/Axl receptor tyrosine kinase is mediated mainly by a multi-substrate docking-site. *Oncogene,* 14**,** 2619-31.

BROWN, J. E., KRODEL, M., PAZOS, M., LAI, C. & PRIETO, A. L. 2012. Cross-phosphorylation, signaling and proliferative functions of the Tyro3 and Axl receptors in Rat2 cells. *PloS One,* 7**,** e36800.

BUBICI, C. & PAPA, S. 2014. JNK signalling in cancer: in need of new, smarter therapeutic targets. *Br J Pharmacol,* 171**,** 24-37.

BUCHANAN, B. W., LLOYD, M. E., ENGLE, S. M. & RUBENSTEIN, E. M. 2016. Cycloheximide Chase Analysis of Protein Degradation in Saccharomyces cerevisiae. *J Vis Exp*.

BUETOW, M. P., BUETOW, P. C. & SMIRNIOTOPOULOS, J. G. 1991. Typical, atypical, and misleading features in meningioma. *Radiographics,* 11**,** 1087-106.

BUJKO, M., MACHNICKI, M. M., GRECKA, E., RUSETSKA, N., MATYJA, E., KOBER, P., MANDAT, T., RYDZANICZ, M., PLOSKI, R., KRAJEWSKI, R., BONICKI, W., STOKLOSA, T. & SIEDLECKI, J. A. 2017. Mutational Analysis of Recurrent Meningioma Progressing From Atypical to Rhabdoid Subtype. *World Neurosurg,* 97**,** 754 e1-754 e6.

BURSLEM, G. M., SMITH, B. E., LAI, A. C., JAIME-FIGUEROA, S., MCQUAID, D. C., BONDESON, D. P., TOURE, M., DONG, H., QIAN, Y., WANG, J., CREW, A. P., HINES, J. & CREWS, C. M. 2018. The Advantages of Targeted Protein Degradation Over Inhibition: An RTK Case Study. *Cell Chem Biol,* 25**,** 67-77 e3.

BUSH, M. L., OBLINGER, J., BRENDEL, V., SANTARELLI, G., HUANG, J., AKHMAMETYEVA, E. M., BURNS, S. S., WHEELER, J., DAVIS, J., YATES, C. W., CHAUDHURY, A. R., KULP, S., CHEN, C. S., CHANG, L. S., WELLING, D. B. & JACOB, A. 2011. AR42, a novel histone deacetylase inhibitor, as a potential therapy for vestibular schwannomas and meningiomas. *Neuro Oncol,* 13**,** 983-99.

CABEROY, N. B., ALVARADO, G., BIGCAS, J. L. & LI, W. 2012. Galectin-3 is a new MerTK-specific eat-me signal. *J Cell Physiol,* 227**,** 401-7.

CABEROY, N. B., ZHOU, Y. & LI, W. 2010. Tubby and tubby-like protein 1 are new MerTK ligands for phagocytosis. *EMBO J,* 29**,** 3898-910.

CAI, D. X., BANERJEE, R., SCHEITHAUER, B. W., LOHSE, C. M., KLEINSCHMIDT-DEMASTERS, B. K. & PERRY, A. 2001. Chromosome 1p and 14q FISH analysis in clinicopathologic subsets of meningioma: diagnostic and prognostic implications. *J Neuropathol Exp Neurol,* 60**,** 628-36.

CERCHIA, L., ESPOSITO, C. L., CAMORANI, S., RIENZO, A., STASIO, L., INSABATO, L., AFFUSO, A. & DE FRANCISCIS, V. 2012. Targeting Axl with an high-affinity inhibitory aptamer. *Mol Ther,* 20**,** 2291-303.

CHANDARLAPATY, S., SAWAI, A., SCALTRITI, M., RODRIK-OUTMEZGUINE, V., GRBOVIC-HUEZO, O., SERRA, V., MAJUMDER, P. K., BASELGA, J. & ROSEN, N. 2011. AKT inhibition relieves feedback suppression of receptor tyrosine kinase expression and activity. *Cancer Cell,* 19**,** 58-71.

CHANG, L. S., AKHMAMETYEVA, E. M., WU, Y., ZHU, L. & WELLING, D. B. 2002. Multiple transcription initiation sites, alternative splicing, and differential polyadenylation contribute to the complexity of human neurofibromatosis 2 transcripts. *Genomics,* 79**,** 63-76.

CHEN, H., XUE, L., WANG, H., WANG, Z. & WU, H. 2017. Differential NF2 Gene Status in Sporadic Vestibular Schwannomas and its Prognostic Impact on Tumour Growth Patterns. *Sci Rep,* 7**,** 5470.

CHIEN, C. W., HOU, P. C., WU, H. C., CHANG, Y. L., LIN, S. C., LIN, S. C., LIN, B. W., LEE, J. C., CHANG, Y. J., SUN, H. S. & TSAI, S. J. 2016. Targeting TYRO3 inhibits epithelial-mesenchymal transition and increases drug sensitivity in colon cancer. *Oncogene,* 35**,** 5872-5881.

CHIU, K. C., LEE, C. H., LIU, S. Y., CHOU, Y. T., HUANG, R. Y., HUANG, S. M. & SHIEH, Y. S. 2015. Polarization of tumor-associated macrophages and Gas6/Axl signaling in oral squamous cell carcinoma. *Oral Oncol,* 51**,** 683-9.

CHO, C. Y., HUANG, J. S., SHIAH, S. G., CHUNG, S. Y., LAY, J. D., YANG, Y. Y., LAI, G. M., CHENG, A. L., CHEN, L. T. & CHUANG, S. E. 2016. Negative feedback regulation of AXL by miR-34a modulates apoptosis in lung cancer cells. *RNA,* 22**,** 303-15.

CHOI, W. T., RAMACHANDRAN, R. & KAKAR, S. 2017. Immunohistochemical approach for the diagnosis of a liver mass on small biopsy specimens. *Hum Pathol,* 63**,** 1-13.

CHRISTOPH, S., DERYCKERE, D., SCHLEGEL, J., FRAZER, J. K., BATCHELOR, L. A., TRAKHIMETS, A. Y., SATHER, S., HUNTER, D. M., CUMMINGS, C. T., LIU, J., YANG, C., KIREEV, D., SIMPSON, C., NORRIS-DROUIN, J., HULL-RYDE, E. A., JANZEN, W. P., JOHNSON, G. L., WANG, X., FRYE, S. V., EARP, H. S., 3RD & GRAHAM, D. K. 2013. UNC569, a novel small-molecule mer inhibitor with efficacy against acute lymphoblastic leukemia in vitro and in vivo. *Mol Cancer Ther,* 12**,** 2367-77.

CLARK, V. E., ERSON-OMAY, E. Z., SERIN, A., YIN, J., COTNEY, J., OZDUMAN, K., AVSAR, T., LI, J., MURRAY, P. B., HENEGARIU, O., YILMAZ, S., GUNEL, J. M., CARRION-GRANT, G., YILMAZ, B., GRADY, C., TANRIKULU, B., BAKIRCIOGLU, M., KAYMAKCALAN, H., CAGLAYAN, A. O., SENCAR, L., CEYHUN, E., ATIK, A. F., BAYRI, Y., BAI, H., KOLB, L. E., HEBERT, R. M., OMAY, S. B., MISHRA-GORUR, K., CHOI, M., OVERTON, J. D., HOLLAND, E. C., MANE, S., STATE, M. W., BILGUVAR, K., BAEHRING, J. M., GUTIN, P. H., PIEPMEIER, J. M., VORTMEYER, A., BRENNAN, C. W., PAMIR, M. N., KILIC, T., LIFTON, R. P., NOONAN, J. P., YASUNO, K. & GUNEL, M. 2013. Genomic analysis of non-NF2 meningiomas reveals mutations in TRAF7, KLF4, AKT1, and SMO. *Science,* 339**,** 1077-80.

COLLORD, G., TARPEY, P., KURBATOVA, N., MARTINCORENA, I., MORAN, S., CASTRO, M., NAGY, T., BIGNELL, G., MAURA, F., YOUNG, M. D., BERNA, J., TUBIO, J. M. C., MCMURRAN, C. E., YOUNG, A. M. H., SANDERS, M., NOORANI, I., PRICE, S. J., WATTS, C., LEIPNITZ, E., KIRSCH, M., SCHACKERT, G., PEARSON, D., DEVADASS, A., RAM, Z., COLLINS, V. P., ALLINSON, K., JENKINSON, M. D., ZAKARIA, R., SYED, K., HANEMANN, C. O., DUNN, J., MCDERMOTT, M. W., KIROLLOS, R. W., VASSILIOU, G. S., ESTELLER, M., BEHJATI, S., BRAZMA, A., SANTARIUS, T. & MCDERMOTT, U. 2018. An integrated genomic analysis of anaplastic meningioma identifies prognostic molecular signatures. *Sci Rep,* 8**,** 13537.

COLOZZA, M., AZAMBUJA, E., CARDOSO, F., SOTIRIOU, C., LARSIMONT, D. & PICCART, M. J. 2005. Proliferative markers as prognostic and predictive tools in early breast cancer: where are we now? *Ann Oncol,* 16**,** 1723-39.

CONTI, P., PANSINI, G., MOUCHATY, H., CAPUANO, C. & CONTI, R. 2004. Spinal neurinomas: retrospective analysis and long-term outcome of 179 consecutively operated cases and review of the literature. *Surg Neurol,* 61**,** 34-43; discussion 44.

COOK, R. S., JACOBSEN, K. M., WOFFORD, A. M., DERYCKERE, D., STANFORD, J., PRIETO, A. L., REDENTE, E., SANDAHL, M., HUNTER, D. M., STRUNK, K. E., GRAHAM, D. K. & EARP, H. S., 3RD 2013. MerTK inhibition in tumor leukocytes decreases tumor growth and metastasis. *J Clin Invest,* 123**,** 3231-42.

CORONA, A. P., OLIVEIRA, J. C., SOUZA, F. P., SANTANA, L. V. & REGO, M. A. 2009. Risk factors associated with vestibulocochlear nerve schwannoma: systematic review. *Braz J Otorhinolaryngol,* 75**,** 593-615.

COUCE, M. E., AKER, F. V. & SCHEITHAUER, B. W. 2000. Chordoid meningioma: a clinicopathologic study of 42 cases. *Am J Surg Pathol,* 24**,** 899-905.

CUMMINGS, C. T., DERYCKERE, D., EARP, H. S. & GRAHAM, D. K. 2013. Molecular pathways: MERTK signaling in cancer. *Clin Cancer Res,* 19**,** 5275-80.

CUMMINGS, C. T., LINGER, R. M., COHEN, R. A., SATHER, S., KIRKPATRICK, G. D., DAVIES, K. D., DERYCKERE, D., EARP, H. S. & GRAHAM, D. K. 2014. Mer590, a novel monoclonal antibody targeting MER receptor tyrosine kinase, decreases colony formation and increases chemosensitivity in non-small cell lung cancer. *Oncotarget,* 5**,** 10434-45.

CUMMINGS, C. T., ZHANG, W., DAVIES, K. D., KIRKPATRICK, G. D., ZHANG, D., DERYCKERE, D., WANG, X., FRYE, S. V., EARP, H. S. & GRAHAM, D. K. 2015. Small Molecule Inhibition of MERTK Is Efficacious in Non-Small Cell Lung Cancer Models Independent of Driver Oncogene Status. *Mol Cancer Ther,* 14**,** 2014-22.

CURTO, M., COLE, B. K., LALLEMAND, D., LIU, C. H. & MCCLATCHEY, A. I. 2007. Contact-dependent inhibition of EGFR signaling by Nf2/Merlin. *J Cell Biol,* 177**,** 893-903.

CUSTER, B., LONGSTRETH, W. T., JR., PHILLIPS, L. E., KOEPSELL, T. D. & VAN BELLE, G. 2006. Hormonal exposures and the risk of intracranial meningioma in women: a population-based case-control study. *BMC Cancer,* 6**,** 152.

D'CRUZ, P. M., YASUMURA, D., WEIR, J., MATTHES, M. T., ABDERRAHIM, H., LAVAIL, M. M. & VOLLRATH, D. 2000. Mutation of the receptor tyrosine kinase gene Mertk in the retinal dystrophic RCS rat. *Hum Mol Genet,* 9**,** 645-51.

DE VRIES, M., BRIAIRE-DE BRUIJN, I., MALESSY, M. J., DE BRUINE, S. F., VAN DER MEY, A. G. & HOGENDOORN, P. C. 2013. Tumor-associated macrophages are related to volumetric growth of vestibular schwannomas. *Otol Neurotol,* 34**,** 347-52.

DEMAREST, S. J., GARDNER, J., VENDEL, M. C., AILOR, E., SZAK, S., HUANG, F., DOERN, A., TAN, X., YANG, W., GRUENEBERG, D. A., RICHARDS, E. J., ENDEGE, W. O., HARLOW, E. & KOOPMAN, L. A. 2013. Evaluation of Tyro3 expression, Gas6-mediated Akt phosphorylation, and the impact of anti-Tyro3 antibodies in melanoma cell lines. *Biochemistry,* 52**,** 3102-18.

DERYCKERE, D., LEE-SHERICK, A. B., HUEY, M. G., HILL, A. A., TYNER, J. W., JACOBSEN, K. M., PAGE, L. S., KIRKPATRICK, G. G., ERYILDIZ, F., MONTGOMERY, S. A., ZHANG, W., WANG, X., FRYE, S. V., EARP, H. S. & GRAHAM, D. K. 2017. UNC2025, a MERTK Small-Molecule Inhibitor, Is Therapeutically Effective Alone and in Combination with Methotrexate in Leukemia Models. *Clin Cancer Res,* 23**,** 1481-1492.

DOMINGUES, P., GONZALEZ-TABLAS, M., OTERO, A., PASCUAL, D., MIRANDA, D., RUIZ, L., SOUSA, P., CIUDAD, J., GONCALVES, J. M., LOPES, M. C., ORFAO, A. & TABERNERO, M. D. 2016. Tumor infiltrating immune cells in gliomas and meningiomas. *Brain Behav Immun,* 53**,** 1-15.

DOMINGUES, P. H., TEODOSIO, C., OTERO, A., SOUSA, P., ORTIZ, J., MACIAS MDEL, C., GONCALVES, J. M., NIETO, A. B., LOPES, M. C., DE OLIVEIRA, C., ORFAO, A. & TABERNERO, M. D. 2013. Association between inflammatory infiltrates and isolated monosomy 22/del(22q) in meningiomas. *PLoS One,* 8**,** e74798.

DONG, H., STROME, S. E., SALOMAO, D. R., TAMURA, H., HIRANO, F., FLIES, D. B., ROCHE, P. C., LU, J., ZHU, G., TAMADA, K., LENNON, V. A., CELIS, E. & CHEN, L. 2002. Tumor-associated B7-H1 promotes T-cell apoptosis: a potential mechanism of immune evasion. *Nat Med,* 8**,** 793-800.

DUAN, Y., WONG, W., CHUA, S. C., WEE, H. L., LIM, S. G., CHUA, B. T. & HO, H. K. 2016. Overexpression of Tyro3 and its implications on hepatocellular carcinoma progression. *Int J Oncol,* 48**,** 358-66.

DUFIES, M., JACQUEL, A., BELHACENE, N., ROBERT, G., CLUZEAU, T., LUCIANO, F., CASSUTO, J. P., RAYNAUD, S. & AUBERGER, P. 2011. Mechanisms of AXL overexpression and function in Imatinib-resistant chronic myeloid leukemia cells. *Oncotarget,* 2**,** 874-85.

DUNCAN, J. S., WHITTLE, M. C., NAKAMURA, K., ABELL, A. N., MIDLAND, A. A., ZAWISTOWSKI, J. S., JOHNSON, N. L., GRANGER, D. A., JORDAN, N. V., DARR, D. B., USARY, J., KUAN, P. F., SMALLEY, D. M., MAJOR, B., HE, X., HOADLEY, K. A., ZHOU, B., SHARPLESS, N. E., PEROU, C. M., KIM, W. Y., GOMEZ, S. M., CHEN, X., JIN, J., FRYE, S. V., EARP, H. S., GRAVES, L. M. & JOHNSON, G. L. 2012. Dynamic reprogramming of the kinome in response to targeted MEK inhibition in triple-negative breast cancer. *Cell,* 149**,** 307-21.

EKYALONGO, R. C., MUKOHARA, T., FUNAKOSHI, Y., TOMIOKA, H., KATAOKA, Y., SHIMONO, Y., CHAYAHARA, N., TOYODA, M., KIYOTA, N. & MINAMI, H. 2014. TYRO3 as a potential therapeutic target in breast cancer. *Anticancer Res,* 34**,** 3337-45.

ESSBACH, C., ANDRAE, N., PACHOW, D., WARNKE, J. P., WILISCH-NEUMANN, A., KIRCHES, E. & MAWRIN, C. 2013. Abundance of Flt3 and its ligand in astrocytic tumors. *Onco Targets Ther,* 6**,** 555-61.

EVANS, D. G. 2009. Neurofibromatosis type 2 (NF2): a clinical and molecular review. *Orphanet J Rare Dis,* 4**,** 16.

EVANS, D. G., BIRCH, J. M., RAMSDEN, R. T., SHARIF, S. & BASER, M. E. 2006. Malignant transformation and new primary tumours after therapeutic radiation for benign disease: substantial risks in certain tumour prone syndromes. *J Med Genet,* 43**,** 289-94.

EVANS, D. G., HUSON, S. M., DONNAI, D., NEARY, W., BLAIR, V., NEWTON, V. & HARRIS, R. 1992. A clinical study of type 2 neurofibromatosis. *Q J Med,* 84**,** 603-18.

EVANS, D. G., KING, A. T., BOWERS, N. L., TOBI, S., WALLACE, A. J., PERRY, M., ANUP, R., LLOYD, S. K. L., RUTHERFORD, S. A., HAMMERBECK-WARD, C., PATHMANABAN, O. N., STAPLETON, E., FREEMAN, S. R., KELLETT, M., HALLIDAY, D., PARRY, A., GAIR, J. J., AXON, P., LAITT, R., THOMAS, O., AFRIDI, S., FERNER, R. E., HARKNESS, E. F., SMITH, M. J. & ENGLISH SPECIALIST, N. F. R. G. 2018. Identifying the deficiencies of current diagnostic criteria for neurofibromatosis 2 using databases of 2777 individuals with molecular testing. *Genet Med*.

EVANS, D. G., MORAN, A., KING, A., SAEED, S., GURUSINGHE, N. & RAMSDEN, R. 2005. Incidence of vestibular schwannoma and neurofibromatosis 2 in the North West of England over a 10-year period: higher incidence than previously thought. *Otol Neurotol,* 26**,** 93-7.

FARSCHTSCHI, S., MERKER, V. L., WOLF, D., SCHUHMANN, M., BLAKELEY, J., PLOTKIN, S. R., HAGEL, C. & MAUTNER, V. F. 2016. Bevacizumab treatment for symptomatic spinal ependymomas in neurofibromatosis type 2. *Acta Neurol Scand,* 133**,** 475-80.

FERNANDEZ-VALLE, C., TANG, Y., RICARD, J., RODENAS-RUANO, A., TAYLOR, A., HACKLER, E., BIGGERSTAFF, J. & IACOVELLI, J. 2002. Paxillin binds schwannomin and regulates its density-dependent localization and effect on cell morphology. *Nat Genet,* 31**,** 354-62.

FINE, S. W., MCCLAIN, S. A. & LI, M. 2004. Immunohistochemical staining for calretinin is useful for differentiating schwannomas from neurofibromas. *Am J Clin Pathol,* 122**,** 552-9.

FRACASSO, P. M., BLUM, K. A., MA, M. K., TAN, B. R., WRIGHT, L. P., GOODNER, S. A., FEARS, C. L., HOU, W., ARQUETTE, M. A., PICUS, J., DENES, A., MORTIMER, J. E., RATNER, L., IVY, S. P. & MCLEOD, H. L. 2005. Phase I study of pegylated liposomal doxorubicin and the multidrug-resistance modulator, valspodar. *Br J Cancer,* 93**,** 46-53.

FRIDELL, Y. W., JIN, Y., QUILLIAM, L. A., BURCHERT, A., MCCLOSKEY, P., SPIZZ, G., VARNUM, B., DER, C. & LIU, E. T. 1996. Differential activation of the Ras/extracellular-signal-regulated protein kinase pathway is responsible for the biological consequences induced by the Axl receptor tyrosine kinase. *Mol Cell Biol,* 16**,** 135-45.

FRIEDMAN, J. M. 2002. Neurofibromatosis 1: clinical manifestations and diagnostic criteria. *J Child Neurol,* 17**,** 548-54; discussion 571-2, 646-51.

FUKAMI, S., RIEMENSCHNEIDER, M. J., KOHNO, M. & STEIGER, H. J. 2016. Expression and gene doses changes of the p53-regulator PPM1D in meningiomas: a role in meningioma progression? *Brain Tumor Pathol,* 33**,** 191-9.

FUSE, M. A., PLATI, S. K., BURNS, S. S., DINH, C. T., BRACHO, O., YAN, D., MITTAL, R., SHEN, R., SOULAKOVA, J. N., COPIK, A. J., LIU, X. Z., TELISCHI, F. F., CHANG, L. S., FRANCO, M. C. & FERNANDEZ-VALLE, C. 2017. Combination Therapy with c-Met and Src Inhibitors Induces Caspase-Dependent Apoptosis of Merlin-Deficient Schwann Cells and Suppresses Growth of Schwannoma Cells. *Mol Cancer Ther,* 16**,** 2387-2398.

GARBIN, U., BAGGIO, E., STRANIERI, C., PASINI, A., MANFRO, S., MOZZINI, C., VALLERIO, P., LIPARI, G., MERIGO, F., GUIDI, G., COMINACINI, L. & FRATTA PASINI, A. 2013. Expansion of necrotic core and shedding of Mertk receptor in human carotid plaques: a role for oxidized polyunsaturated fatty acids? *Cardiovasc Res,* 97**,** 125-33.

GERBER, P. A., ANTAL, A. S., NEUMANN, N. J., HOMEY, B., MATUSCHEK, C., PEIPER, M., BUDACH, W. & BOLKE, E. 2009. Neurofibromatosis. *Eur J Med Res,* 14**,** 102-5.

GHISO, E., MIGLIORE, C., CICIRIELLO, V., MORANDO, E., PETRELLI, A., CORSO, S., DE LUCA, E., GATTI, G., VOLANTE, M. & GIORDANO, S. 2017. YAP-Dependent AXL Overexpression Mediates Resistance to EGFR Inhibitors in NSCLC. *Neoplasia,* 19**,** 1012-1021.

GIOVANNINI, M., BONNE, N. X., VITTE, J., CHAREYRE, F., TANAKA, K., ADAMS, R., FISHER, L. M., VALEYRIE-ALLANORE, L., WOLKENSTEIN, P., GOUTAGNY, S. & KALAMARIDES, M. 2014. mTORC1 inhibition delays growth of neurofibromatosis type 2 schwannoma. *Neuro Oncol,* 16**,** 493-504.

GONZALVO, A., FOWLER, A., COOK, R. J., LITTLE, N. S., WHEELER, H., MCDONALD, K. L. & BIGGS, M. T. 2011. Schwannomatosis, sporadic schwannomatosis, and familial schwannomatosis: a surgical series with long-term follow-up. Clinical article. *J Neurosurg,* 114**,** 756-62.

GORUPPI, S., RUARO, E., VARNUM, B. & SCHNEIDER, C. 1997. Requirement of phosphatidylinositol 3-kinase-dependent pathway and Src for Gas6-Axl mitogenic and survival activities in NIH 3T3 fibroblasts. *Mol Cell Biol,* 17**,** 4442-53.

GOUDARZI, S., RIVERA, A., BUTT, A. M. & HAFIZI, S. 2016. Gas6 Promotes Oligodendrogenesis and Myelination in the Adult Central Nervous System and After Lysolecithin-Induced Demyelination. *ASN Neuro,* 8.

GOUTAGNY, S., NAULT, J. C., MALLET, M., HENIN, D., ROSSI, J. Z. & KALAMARIDES, M. 2014. High incidence of activating TERT promoter mutations in meningiomas undergoing malignant progression. *Brain Pathol,* 24**,** 184-9.

GOUTAGNY, S., RAYMOND, E., ESPOSITO-FARESE, M., TRUNET, S., MAWRIN, C., BERNARDESCHI, D., LARROQUE, B., STERKERS, O., GIOVANNINI, M. & KALAMARIDES, M. 2015. Phase II study of mTORC1 inhibition by everolimus in neurofibromatosis type 2 patients with growing vestibular schwannomas. *J Neurooncol,* 122**,** 313-20.

GOUTAGNY, S., RAYMOND, E., STERKERS, O., COLOMBANI, J. M. & KALAMARIDES, M. 2011. Radiographic regression of cranial meningioma in a NF2 patient treated by bevacizumab. *Ann Oncol,* 22**,** 990-1.

GOUTAGNY, S., YANG, H. W., ZUCMAN-ROSSI, J., CHAN, J., DREYFUSS, J. M., PARK, P. J., BLACK, P. M., GIOVANNINI, M., CARROLL, R. S. & KALAMARIDES, M. 2010. Genomic profiling reveals alternative genetic pathways of meningioma malignant progression dependent on the underlying NF2 status. *Clin Cancer Res,* 16**,** 4155-64.

GRAHAM, D. K., DAWSON, T. L., MULLANEY, D. L., SNODGRASS, H. R. & EARP, H. S. 1994. Cloning and mRNA expression analysis of a novel human protooncogene, c-mer. *Cell Growth Differ,* 5**,** 647-57.

GRASSI, P., VERZONI, E., RATTA, R., MENNITTO, A., DE BRAUD, F. & PROCOPIO, G. 2016. Cabozantinib in the treatment of advanced renal cell carcinoma: design,

development, and potential place in the therapy. *Drug Des Devel Ther,* 10**,** 2167-72.

GREEN, T. P., FENNELL, M., WHITTAKER, R., CURWEN, J., JACOBS, V., ALLEN, J., LOGIE, A., HARGREAVES, J., HICKINSON, D. M., WILKINSON, R. W., ELVIN, P., BOYER, B., CARRAGHER, N., PLE, P. A., BERMINGHAM, A., HOLDGATE, G. A., WARD, W. H., HENNEQUIN, L. F., DAVIES, B. R. & COSTELLO, G. F. 2009. Preclinical anticancer activity of the potent, oral Src inhibitor AZD0530. *Mol Oncol,* 3**,** 248-61.

GUO, H., BARRETT, T. M., ZHONG, Z., FERNANDEZ, J. A., GRIFFIN, J. H., FREEMAN, R. S. & ZLOKOVIC, B. V. 2011. Protein S blocks the extrinsic apoptotic cascade in tissue plasminogen activator/N-methyl D-aspartate-treated neurons via Tyro3-Akt-FKHRL1 signaling pathway. *Mol Neurodegener,* 6**,** 13.

GUTMANN, D. H., AYLSWORTH, A., CAREY, J. C., KORF, B., MARKS, J., PYERITZ, R. E., RUBENSTEIN, A. & VISKOCHIL, D. 1997. The diagnostic evaluation and multidisciplinary management of neurofibromatosis 1 and neurofibromatosis 2. *JAMA,* 278**,** 51-57.

HAFIZI, S., ALINDRI, F., KARLSSON, R. & DAHLBACK, B. 2002. Interaction of Axl receptor tyrosine kinase with C1-TEN, a novel C1 domain-containing protein with homology to tensin. *Biochem Biophys Res Commun,* 299, 793-800.

HAFIZI, S. & DAHLBACK, B. 2006. Gas6 and protein S. Vitamin K-dependent ligands for the Axl receptor tyrosine kinase subfamily. *FEBS J,* 273**,** 5231-44.

HAFIZI, S., IBRAIMI, F. & DAHLBACK, B. 2005. C1-TEN is a negative regulator of the Akt/PKB signal transduction pathway and inhibits cell survival, proliferation, and migration. *FASEB J,* 19**,** 971-3.

HALLIDAY, J., RUTHERFORD, S. A., MCCABE, M. G. & EVANS, D. G. 2018. An update on the diagnosis and treatment of vestibular schwannoma. *Expert Rev Neurother,* 18**,** 29-39.

HANEMANN, C. O. 2008. Magic but treatable? Tumours due to loss of merlin. *Brain,* 131**,** 606-15.

HANEMANN, C. O., BARTELT-KIRBACH, B., DIEBOLD, R., KAMPCHEN, K., LANGMESSER, S. & UTERMARK, T. 2006. Differential gene expression between human schwannoma and control Schwann cells. *Neuropathol Appl Neurobiol,* 32**,** 605-14.

HARTMAN, A. D., WILSON-WEEKES, A., SUVANNASANKHA, A., BURGESS, G. S., PHILLIPS, C. A., HINCHER, K. J., CRIPE, L. D. & BOSWELL, H. S. 2006. Constitutive c-jun N-terminal kinase activity in acute myeloid leukemia derives from Flt3 and affects survival and proliferation. *Exp Hematol,* 34**,** 1360-76.

HASANBASIC, I., CUERQUIS, J., VARNUM, B. & BLOSTEIN, M. D. 2004. Intracellular signaling pathways involved in Gas6-Axl-mediated survival of endothelial cells. *Am J Physiol Heart Circ Physiol,* 287**,** H1207-13.

HECTOR, A., MONTGOMERY, E. A., KARIKARI, C., CANTO, M., DUNBAR, K. B., WANG, J. S., FELDMANN, G., HONG, S. M., HAFFNER, M. C., MEEKER, A. K., HOLLAND, S. J., YU, J., HECKRODT, T. J., ZHANG, J., DING, P., GOFF, D., SINGH, R., ROA, J. C., MARIMUTHU, A., RIGGINS, G. J., ESHLEMAN, J. R., NELKIN, B. D., PANDEY, A. & MAITRA, A. 2010. The Axl receptor tyrosine kinase is an adverse prognostic factor and a therapeutic target in esophageal adenocarcinoma. *Cancer Biol Ther,* 10**,** 1009-18.

HEIRING, C., DAHLBACK, B. & MULLER, Y. A. 2004. Ligand recognition and homophilic interactions in Tyro3: structural insights into the Axl/Tyro3 receptor tyrosine kinase family. *J Biol Chem,* 279**,** 6952-8.

HILTON, D. A. & HANEMANN, C. O. 2014. Schwannomas and their pathogenesis. *Brain Pathol,* 24**,** 205-20.

HILTON, D. A., RISTIC, N. & HANEMANN, C. O. 2009. Activation of ERK, AKT and JNK signalling pathways in human schwannomas in situ. *Histopathology,* 55**,** 744-9.

HILTON, D. A., SHIVANE, A., KIRK, L., BASSIRI, K., ENKI, D. G. & HANEMANN, C. O. 2016. Activation of multiple growth factor signalling pathways is frequent in meningiomas. *Neuropathology,* 36**,** 250-61.

HOEFLICH, K. P., O'BRIEN, C., BOYD, Z., CAVET, G., GUERRERO, S., JUNG, K., JANUARIO, T., SAVAGE, H., PUNNOOSE, E., TRUONG, T., ZHOU, W., BERRY, L., MURRAY, L., AMLER, L., BELVIN, M., FRIEDMAN, L. S. & LACKNER, M. R. 2009. In vivo antitumor activity of MEK and phosphatidylinositol 3-kinase inhibitors in basal-like breast cancer models. *Clin Cancer Res,* 15**,** 4649-64.

HOEHN, H. J., KRESS, Y., SOHN, A., BROSNAN, C. F., BOURDON, S. & SHAFIT-ZAGARDO, B. 2008. Axl-/- mice have delayed recovery and prolonged axonal damage following cuprizone toxicity. *Brain Res,* 1240**,** 1-11.

HOLLAND, S. J., PAN, A., FRANCI, C., HU, Y., CHANG, B., LI, W., DUAN, M., TORNEROS, A., YU, J., HECKRODT, T. J., ZHANG, J., DING, P., APATIRA, A., CHUA, J., BRANDT, R., PINE, P., GOFF, D., SINGH, R., PAYAN, D. G. & HITOSHI, Y. 2010. R428, a selective small molecule inhibitor of Axl kinase, blocks tumor spread and prolongs survival in models of metastatic breast cancer. *Cancer Res,* 70**,** 1544-54.

HONG, C. C., LAY, J. D., HUANG, J. S., CHENG, A. L., TANG, J. L., LIN, M. T., LAI, G. M. & CHUANG, S. E. 2008. Receptor tyrosine kinase AXL is induced by chemotherapy drugs and overexpression of AXL confers drug resistance in acute myeloid leukemia. *Cancer Lett,* 268**,** 314-24.

HUGO, W., ZARETSKY, J. M., SUN, L., SONG, C., MORENO, B. H., HU-LIESKOVAN, S., BERENT-MAOZ, B., PANG, J., CHMIELOWSKI, B., CHERRY, G., SEJA, E., LOMELI, S., KONG, X., KELLEY, M. C., SOSMAN, J. A., JOHNSON, D. B., RIBAS, A. & LO, R. S. 2016. Genomic and Transcriptomic Features of Response to Anti-PD-1 Therapy in Metastatic Melanoma. *Cell,* 165**,** 35-44.

HUTTERER, M., KNYAZEV, P., ABATE, A., RESCHKE, M., MAIER, H., STEFANOVA, N., KNYAZEVA, T., BARBIERI, V., REINDL, M., MUIGG, A., KOSTRON, H., STOCKHAMMER, G. & ULLRICH, A. 2008. Axl and growth arrest-specific gene 6 are frequently overexpressed in human gliomas and predict poor prognosis in patients with glioblastoma multiforme. *Clin Cancer Res,* 14**,** 130-8.

IKEDA, T., HASHIMOTO, S., FUKUSHIGE, S., OHMORI, H. & HORII, A. 2005. Comparative genomic hybridization and mutation analyses of sporadic schwannomas. *J Neurooncol,* 72**,** 225-30.

JACOB, A., LEE, T. X., NEFF, B. A., MILLER, S., WELLING, B. & CHANG, L. S. 2008. Phosphatidylinositol 3-kinase/AKT pathway activation in human vestibular schwannoma. *Otol Neurotol,* 29**,** 58-68.

JACOBY, L. B., JONES, D., DAVIS, K., KRONN, D., SHORT, M. P., GUSELLA, J. & MACCOLLIN, M. 1997. Molecular analysis of the NF2 tumor-suppressor gene in schwannomatosis. *Am J Hum Genet,* 61**,** 1293-302.

JAKSCH-BOGENSPERGER, H., HAMMERSCHMID, A., AIGNER, L., TRINKA, E., GEHWOLF, R., EBNER, Y., HUTTERER, M. & COUILLARD-DESPRES, S. 2018. Proseek single-plex protein assay kit system to detect sAxl and Gas6 in serological material of brain tumor patients. *Biotechnol Rep (Amst),* 18**,** e00252.

JAMES, M. F., HAN, S., POLIZZANO, C., PLOTKIN, S. R., MANNING, B. D., STEMMER-RACHAMIMOV, A. O., GUSELLA, J. F. & RAMESH, V. 2009. NF2/merlin is a novel negative regulator of mTOR complex 1, and activation of mTORC1 is associated with meningioma and schwannoma growth. *Mol Cell Biol,* 29**,** 4250-61.

JANSSEN, J. W., SCHULZ, A. S., STEENVOORDEN, A. C., SCHMIDBERGER, M., STREHL, S., AMBROS, P. F. & BARTRAM, C. R. 1991. A novel putative tyrosine kinase receptor with oncogenic potential. *Oncogene,* 6**,** 2113-20.

JELINEK, M., BALUSIKOVA, K., SCHMIEDLOVA, M., NEMCOVA-FURSTOVA, V., SRAMEK, J., STANCIKOVA, J., ZANARDI, I., OJIMA, I. & KOVAR, J. 2015. The

role of individual caspases in cell death induction by taxanes in breast cancer cells. *Cancer Cell Int,* 15**,** 8.

JI, R., MENG, L., JIANG, X., CVM, N. K., DING, J., LI, Q. & LU, Q. 2014. TAM receptors support neural stem cell survival, proliferation and neuronal differentiation. *PLoS One,* 9**,** e115140.

JI, R., TIAN, S., LU, H. J., LU, Q., ZHENG, Y., WANG, X., DING, J., LI, Q. & LU, Q. 2013. TAM receptors affect adult brain neurogenesis by negative regulation of microglial cell activation. *J Immunol,* 191**,** 6165-77.

JINDA, W., POUNGVARIN, N., TAYLOR, T. D., SUZUKI, Y., THONGNOPPAKHUN, W., LIMWONGSE, C., LERTRIT, P., SURIYAPHOL, P. & ATCHANEEYASAKUL, L. O. 2016. A novel start codon mutation of the MERTK gene in a patient with retinitis pigmentosa. *Mol Vis,* 22**,** 342-51.

JOHANSSON, G., PENG, P. C., HUANG, P. Y., CHIEN, H. F., HUA, K. T., KUO, M. L., CHEN, C. T. & LEE, M. J. 2014. Soluble AXL: a possible circulating biomarker for neurofibromatosis type 1 related tumor burden. *PLoS One,* 9**,** e115916.

JOKINEN, C. H., DADRAS, S. S., GOLDBLUM, J. R., VAN DE RIJN, M., WEST, R. B. & RUBIN, B. P. 2008. Diagnostic implications of podoplanin expression in peripheral nerve sheath neoplasms. *Am J Clin Pathol,* 129**,** 886-93.

JUNG, Y., DECKER, A. M., WANG, J., LEE, E., KANA, L. A., YUMOTO, K., CACKOWSKI, F. C., RHEE, J., CARMELIET, P., BUTTITTA, L., MORGAN, T. M. & TAICHMAN, R. S. 2016. Endogenous GAS6 and Mer receptor signaling regulate prostate cancer stem cells in bone marrow. *Oncotarget,* 7**,** 25698-711.

JURIKOVA, M., DANIHEL, L., POLAK, S. & VARGA, I. 2016. Ki67, PCNA, and MCM proteins: Markers of proliferation in the diagnosis of breast cancer. *Acta Histochem,* 118**,** 544-52.

KABIR, T. D., GANDA, C., BROWN, R. M., BEVERIDGE, D. J., RICHARDSON, K. L., CHATURVEDI, V., CANDY, P., EPIS, M., WINTLE, L., KALINOWSKI, F., KOPP, C., STUART, L. M., YEOH, G. C., GEORGE, J. & LEEDMAN, P. J. 2018. A microRNA-7/growth arrest specific 6/TYRO3 axis regulates the growth and invasiveness of sorafenib-resistant cells in human hepatocellular carcinoma. *Hepatology,* 67**,** 216-231.

KAEMPCHEN, K., MIELKE, K., UTERMARK, T., LANGMESSER, S. & HANEMANN, C. O. 2003. Upregulation of the Rac1/JNK signaling pathway in primary human schwannoma cells. *Hum Mol Genet,* 12**,** 1211-21.

KAHN, J., GILLESPIE, A., TSOKOS, M., ONDOS, J., DOMBI, E., CAMPHAUSEN, K., WIDEMANN, B. C. & KAUSHAL, A. 2014. Radiation therapy in management of sporadic and neurofibromatosis type 1-associated malignant peripheral nerve sheath tumors. *Front Oncol,* 4**,** 324.

KARAJANNIS, M. A., LEGAULT, G., HAGIWARA, M., BALLAS, M. S., BROWN, K., NUSBAUM, A. O., HOCHMAN, T., GOLDBERG, J. D., KOCH, K. M., GOLFINOS, J. G., ROLAND, J. T. & ALLEN, J. C. 2012. Phase II trial of lapatinib in adult and pediatric patients with neurofibromatosis type 2 and progressive vestibular schwannomas. *Neuro Oncol,* 14**,** 1163-70.

KARAJANNIS, M. A., LEGAULT, G., HAGIWARA, M., GIANCOTTI, F. G., FILATOV, A., DERMAN, A., HOCHMAN, T., GOLDBERG, J. D., VEGA, E., WISOFF, J. H., GOLFINOS, J. G., MERKELSON, A., ROLAND, J. T. & ALLEN, J. C. 2014. Phase II study of everolimus in children and adults with neurofibromatosis type 2 and progressive vestibular schwannomas. *Neuro Oncol,* 16**,** 292-7.

KARAM, J. A., DEVINE, C. E., URBAUER, D. L., LOZANO, M., MAITY, T., AHRAR, K., TAMBOLI, P., TANNIR, N. M. & WOOD, C. G. 2014. Phase 2 trial of neoadjuvant axitinib in patients with locally advanced nonmetastatic clear cell renal cell carcinoma. *Eur Urol,* 66**,** 874-80.

KARIOLIS, M. S., MIAO, Y. R., DIEP, A., NASH, S. E., OLCINA, M. M., JIANG, D., JONES, D. S., 2ND, KAPUR, S., MATHEWS, II, KOONG, A. C., RANKIN, E. B.,

COCHRAN, J. R. & GIACCIA, A. J. 2017. Inhibition of the GAS6/AXL pathway augments the efficacy of chemotherapies. *J Clin Invest,* 127**,** 183-198.

KAWAHARA, E., ODA, Y., OOI, A., KATSUDA, S., NAKANISHI, I. & UMEDA, S. 1988. Expression of glial fibrillary acidic protein (GFAP) in peripheral nerve sheath tumors. A comparative study of immunoreactivity of GFAP, vimentin, S-100 protein, and neurofilament in 38 schwannomas and 18 neurofibromas. *Am J Surg Pathol,* 12**,** 115-20.

KEATING, A. K., KIM, G. K., JONES, A. E., DONSON, A. M., WARE, K., MULCAHY, J. M., SALZBERG, D. B., FOREMAN, N. K., LIANG, X., THORBURN, A. & GRAHAM, D. K. 2010. Inhibition of Mer and Axl receptor tyrosine kinases in astrocytoma cells leads to increased apoptosis and improved chemosensitivity. *Mol Cancer Ther,* 9**,** 1298-307.

KEPES, J. J., MORAL, L. A., WILKINSON, S. B., ABDULLAH, A. & LLENA, J. F. 1998. Rhabdoid transformation of tumor cells in meningiomas: a histologic indication of increased proliferative activity: report of four cases. *Am J Surg Pathol,* 22**,** 231-8.

KETTER, R., RAHNENFUHRER, J., HENN, W., KIM, Y. J., FEIDEN, W., STEUDEL, W. I., ZANG, K. D. & URBSCHAT, S. 2008. Correspondence of tumor localization with tumor recurrence and cytogenetic progression in meningiomas. *Neurosurgery,* 62**,** 61-9; discussion 69-70.

KIM, N. Y., LEE, H. Y. & LEE, C. 2015. Metformin targets Axl and Tyro3 receptor tyrosine kinases to inhibit cell proliferation and overcome chemoresistance in ovarian cancer cells. *Int J Oncol,* 47**,** 353-60.

KINO, T., TAKESHIMA, H., NAKAO, M., NISHI, T., YAMAMOTO, K., KIMURA, T., SAITO, Y., KOCHI, M., KURATSU, J., SAYA, H. & USHIO, Y. 2001. Identification of the cis-acting region in the NF2 gene promoter as a potential target for mutation and methylation-dependent silencing in schwannoma. *Genes Cells,* 6**,** 441-454.

KIRANE, A., LUDWIG, K. F., SORRELLE, N., HAALAND, G., SANDAL, T., RANAWEERA, R., TOOMBS, J. E., WANG, M., DINEEN, S. P., MICKLEM, D., DELLINGER, M. T., LORENS, J. B. & BREKKEN, R. A. 2015. Warfarin Blocks Gas6-Mediated Axl Activation Required for Pancreatic Cancer Epithelial Plasticity and Metastasis. *Cancer Res,* 75**,** 3699-705.

KOH, A., LEE, M. N., YANG, Y. R., JEONG, H., GHIM, J., NOH, J., KIM, J., RYU, D., PARK, S., SONG, P., KOO, S. H., LESLIE, N. R., BERGGREN, P. O., CHOI, J. H., SUH, P. G. & RYU, S. H. 2013. C1-Ten is a protein tyrosine phosphatase of insulin receptor substrate 1 (IRS-1), regulating IRS-1 stability and muscle atrophy. *Mol Cell Biol,* 33**,** 1608-20.

KOKKINAKI, M., ABU-ASAB, M., GUNAWARDENA, N., AHERN, G., JAVIDNIA, M., YOUNG, J. & GOLESTANEH, N. 2013. Klotho regulates retinal pigment epithelial functions and protects against oxidative stress. *J Neurosci,* 33**,** 16346-59.

KOLIAS, A. G., CHARI, A., SANTARIUS, T. & HUTCHINSON, P. J. 2014. Chronic subdural haematoma: modern management and emerging therapies. *Nat Rev Neurol,* 10**,** 570-8.

KONISHI, J., YAMAZAKI, K., AZUMA, M., KINOSHITA, I., DOSAKA-AKITA, H. & NISHIMURA, M. 2004. B7-H1 expression on non-small cell lung cancer cells and its relationship with tumor-infiltrating lymphocytes and their PD-1 expression. *Clin Cancer Res,* 10**,** 5094-100.

KOONTZ, N. A., WIENS, A. L., AGARWAL, A., HINGTGEN, C. M., EMERSON, R. E. & MOSIER, K. M. 2013. Schwannomatosis: the overlooked neurofibromatosis? *AJR Am J Roentgenol,* 200**,** W646-53.

KORSHUNOV, V. A. 2012. Axl-dependent signalling: a clinical update. *Clin Sci (Lond),* 122**,** 361-8.

KOUTSIMPELAS, D., FELMEDEN, U., MANN, W. J. & BRIEGER, J. 2011. Analysis of cytogenetic aberrations in sporadic vestibular schwannoma by comparative genomic hybridization. *J Neurooncol,* 103**,** 437-43.

L, N. D. A. K. 2019. Vestibular schwannomas: A Review. *Applied Radiology (The Journal of practical medical imaging and management,* 48**,** 22-27.

LAI, C. & LEMKE, G. 1991. An extended family of protein-tyrosine kinase genes differentially expressed in the vertebrate nervous system. *Neuron,* 6**,** 691-704.

LALLEMAND, D., CURTO, M., SAOTOME, I., GIOVANNINI, M. & MCCLATCHEY, A. I. 2003. NF2 deficiency promotes tumorigenesis and metastasis by destabilizing adherens junctions. *Genes Dev,* 17**,** 1090-100.

LALLEMAND, D., MANENT, J., COUVELARD, A., WATILLIAUX, A., SIENA, M., CHAREYRE, F., LAMPIN, A., NIWA-KAWAKITA, M., KALAMARIDES, M. & GIOVANNINI, M. 2009. Merlin regulates transmembrane receptor accumulation and signaling at the plasma membrane in primary mouse Schwann cells and in human schwannomas. *Oncogene,* 28**,** 854-865.

LAM, R. 2016. Acoustic neuroma manifesting as toothache and numbness. *Aust Dent J,* 61**,** 109-112.

LAWS, E. R., JR. & THAPAR, K. 1993. Brain tumors. *CA Cancer J Clin,* 43**,** 263-71.

LEE-SHERICK, A. B., JACOBSEN, K. M., HENRY, C. J., HUEY, M. G., PARKER, R. E., PAGE, L. S., HILL, A. A., WANG, X., FRYE, S. V., EARP, H. S., JORDAN, C. T., DERYCKERE, D. & GRAHAM, D. K. 2018. MERTK inhibition alters the PD-1 axis and promotes anti-leukemia immunity. *JCI Insight,* 3.

LEE, J. D., KWON, T. J., KIM, U. K. & LEE, W. S. 2012. Genetic and epigenetic alterations of the NF2 gene in sporadic vestibular schwannomas. *PLoS One,* 7**,** e30418.

LEE, Y., KO, D., MIN, H. J., KIM, S. B., AHN, H. M., LEE, Y. & KIM, S. 2016. TMPRSS4 induces invasion and proliferation of prostate cancer cells through induction of Slug and cyclin D1. *Oncotarget,* 7**,** 50315-50332.

LEMKE, G. 2013. Biology of the TAM receptors. *Cold Spring Harb Perspect Biol,* 5**,** a009076.

LEMKE, G. & ROTHLIN, C. V. 2008. Immunobiology of the TAM receptors. *Nat Rev Immunol,* 8**,** 327-36.

LEONE, P. E., BELLO, M. J., MENDIOLA, M., KUSAK, M. E., DE CAMPOS, J. M., VAQUERO, J., SARASA, J. L., PESTANA, A. & REY, J. A. 1998. Allelic status of 1p, 14q, and 22q and NF2 gene mutations in sporadic schwannomas. *Int J Mol Med,* 1**,** 889-92.

LI, Q., LU, Q., LU, H., TIAN, S. & LU, Q. 2013. Systemic autoimmunity in TAM triple knockout mice causes inflammatory brain damage and cell death. *PLoS One,* 8**,** e64812.

LI, W., YOU, L., COOPER, J., SCHIAVON, G., PEPE-CAPRIO, A., ZHOU, L., ISHII, R., GIOVANNINI, M., HANEMANN, C. O., LONG, S. B., ERDJUMENT-BROMAGE, H., ZHOU, P., TEMPST, P. & GIANCOTTI, F. G. 2010. Merlin/NF2 Suppresses Tumorigenesis by Inhibiting the E3 Ubiquitin Ligase CRL4(DCAF1) in the Nucleus. *Cell,* 140**,** 477-490.

LI, Y., YE, X., TAN, C., HONGO, J. A., ZHA, J., LIU, J., KALLOP, D., LUDLAM, M. J. & PEI, L. 2009. Axl as a potential therapeutic target in cancer: role of Axl in tumor growth, metastasis and angiogenesis. *Oncogene,* 28**,** 3442-55.

LIANG, R. F., XIU, Y. J., WANG, X., LI, M., YANG, Y., MAO, Q. & LIU, Y. H. 2014. The potential risk factors for atypical and anaplastic meningiomas: clinical series of 1,239 cases. *Int J Clin Exp Med,* 7**,** 5696-700.

LING, L., TEMPLETON, D. & KUNG, H. J. 1996. Identification of the major autophosphorylation sites of Nyk/Mer, an NCAM-related receptor tyrosine kinase. *J Biol Chem,* 271**,** 18355-62.

LINGER, R. M., COHEN, R. A., CUMMINGS, C. T., SATHER, S., MIGDALL-WILSON, J., MIDDLETON, D. H., LU, X., BARON, A. E., FRANKLIN, W. A., MERRICK, D. T., JEDLICKA, P., DERYCKERE, D., HEASLEY, L. E. & GRAHAM, D. K. 2013. Mer or Axl receptor tyrosine kinase inhibition promotes apoptosis, blocks growth

and enhances chemosensitivity of human non-small cell lung cancer. *Oncogene,* 32**,** 3420-31.

LINGER, R. M., KEATING, A. K., EARP, H. S. & GRAHAM, D. K. 2008. TAM receptor tyrosine kinases: biologic functions, signaling, and potential therapeutic targeting in human cancer. *Adv Cancer Res,* 100**,** 35-83.

LIU, J., ZHANG, W., STASHKO, M. A., DERYCKERE, D., CUMMINGS, C. T., HUNTER, D., YANG, C., JAYAKODY, C. N., CHENG, N., SIMPSON, C., NORRIS-DROUIN, J., SATHER, S., KIREEV, D., JANZEN, W. P., EARP, H. S., GRAHAM, D. K., FRYE, S. V. & WANG, X. 2013. UNC1062, a new and potent Mer inhibitor. *Eur J Med Chem,* 65**,** 83-93.

LIU, L., GREGER, J., SHI, H., LIU, Y., GRESHOCK, J., ANNAN, R., HALSEY, W., SATHE, G. M., MARTIN, A. M. & GILMER, T. M. 2009. Novel mechanism of lapatinib resistance in HER2-positive breast tumor cells: activation of AXL. *Cancer Res,* 69**,** 6871-8.

LIU, R., GONG, M., LI, X., ZHOU, Y., GAO, W., TULPULE, A., CHAUDHARY, P. M., JUNG, J. & GILL, P. S. 2010. Induction, regulation, and biologic function of Axl receptor tyrosine kinase in Kaposi sarcoma. *Blood,* 116**,** 297-305.

LOCK, R., INGRAHAM, R., MAERTENS, O., MILLER, A. L., WELEDJI, N., LEGIUS, E., KONICEK, B. M., YAN, S. C., GRAFF, J. R. & CICHOWSKI, K. 2016. Cotargeting MNK and MEK kinases induces the regression of NF1-mutant cancers. *J Clin Invest,* 126**,** 2181-90.

LOGES, S., SCHMIDT, T., TJWA, M., VAN GEYTE, K., LIEVENS, D., LUTGENS, E., VANHOUTTE, D., BORGEL, D., PLAISANCE, S., HOYLAERTS, M., LUTTUN, A., DEWERCHIN, M., JONCKX, B. & CARMELIET, P. 2010. Malignant cells fuel tumor growth by educating infiltrating leukocytes to produce the mitogen Gas6. *Blood,* 115**,** 2264-73.

LOMAS, J., BELLO, M. J., ARJONA, D., ALONSO, M. E., MARTINEZ-GLEZ, V., LOPEZ-MARIN, I., AMINOSO, C., DE CAMPOS, J. M., ISLA, A., VAQUERO, J. & REY, J. A. 2005. Genetic and epigenetic alteration of the NF2 gene in sporadic meningiomas. *Genes Chromosomes Cancer,* 42**,** 314-9.

LOPEZ-LAGO, M. A., OKADA, T., MURILLO, M. M., SOCCI, N. & GIANCOTTI, F. G. 2009. Loss of the tumor suppressor gene NF2, encoding merlin, constitutively activates integrin-dependent mTORC1 signaling. *Mol Cell Biol,* 29**,** 4235-49.

LOUIS, D. N., OHGAKI, H., WIESTLER, O. D., CAVENEE, W. K., BURGER, P. C., JOUVET, A., SCHEITHAUER, B. W. & KLEIHUES, P. 2007. The 2007 WHO classification of tumours of the central nervous system. *Acta Neuropathol,* 114**,** 97-109.

LOUIS, D. N., PERRY, A., REIFENBERGER, G., VON DEIMLING, A., FIGARELLA-BRANGER, D., CAVENEE, W. K., OHGAKI, H., WIESTLER, O. D., KLEIHUES, P. & ELLISON, D. W. 2016. The 2016 World Health Organization Classification of Tumors of the Central Nervous System: a summary. *Acta Neuropathol,* 131**,** 803-20.

LU, Q., GORE, M., ZHANG, Q., CAMENISCH, T., BOAST, S., CASAGRANDA, F., LAI, C., SKINNER, M. K., KLEIN, R., MATSUSHIMA, G. K., EARP, H. S., GOFF, S. P. & LEMKE, G. 1999. Tyro-3 family receptors are essential regulators of mammalian spermatogenesis. *Nature,* 398**,** 723-8.

LU, Q. & LEMKE, G. 2001. Homeostatic regulation of the immune system by receptor tyrosine kinases of the Tyro 3 family. *Science,* 293**,** 306-11.

LUDWIG, K. F., DU, W., SORRELLE, N. B., WNUK-LIPINSKA, K., TOPALOVSKI, M., TOOMBS, J. E., CRUZ, V. H., YABUUCHI, S., RAJESHKUMAR, N. V., MAITRA, A., LORENS, J. B. & BREKKEN, R. A. 2018. Small-Molecule Inhibition of Axl Targets Tumor Immune Suppression and Enhances Chemotherapy in Pancreatic Cancer. *Cancer Res,* 78**,** 246-255.

MACCOLLIN, M., WOODFIN, W., KRONN, D. & SHORT, M. P. 1996. Schwannomatosis: a clinical and pathologic study. *Neurology,* 46**,** 1072-9.

MADIGAN, P. & SHAW, R. V. 1988. Neurofibromatosis in 13th century Austria? *Neurofibromatosis,* 1**,** 339-41.

MAHADEVAN, D., COOKE, L., RILEY, C., SWART, R., SIMONS, B., DELLA CROCE, K., WISNER, L., IORIO, M., SHAKALYA, K., GAREWAL, H., NAGLE, R. & BEARSS, D. 2007. A novel tyrosine kinase switch is a mechanism of imatinib resistance in gastrointestinal stromal tumors. *Oncogene,* 26**,** 3909-19.

MAHBOUBI, H., MADUCDOC, M. M., YAU, A. Y., ZIAI, K., GHAVAMI, Y., BADRAN, K. W., AL-THOBAITI, M., BRANDON, B. & DJALILIAN, H. R. 2015. Vestibular Schwannoma Excision in Sporadic versus Neurofibromatosis Type 2 Populations. *Otolaryngol Head Neck Surg,* 153**,** 822-31.

MAIER, H., OFNER, D., HITTMAIR, A., KITZ, K. & BUDKA, H. 1992. Classic, atypical, and anaplastic meningioma: three histopathological subtypes of clinical relevance. *J Neurosurg,* 77**,** 616-23.

MALAWISTA, A., WANG, X., TRENTALANGE, M., ALLORE, H. G. & MONTGOMERY, R. R. 2016. Coordinated expression of tyro3, axl, and mer receptors in macrophage ontogeny. *Macrophage (Houst),* 3.

MARGARETO, J., LEIS, O., LARRARTE, E., POMPOSO, I. C., GARIBI, J. M. & LAFUENTE, J. V. 2009. DNA copy number variation and gene expression analyses reveal the implication of specific oncogenes and genes in GBM. *Cancer Invest,* 27**,** 541-8.

MARTINELLI, E., MARTINI, G., CARDONE, C., TROIANI, T., LIGUORI, G., VITAGLIANO, D., NAPOLITANO, S., MORGILLO, F., RINALDI, B., MELILLO, R. M., LIOTTI, F., NAPPI, A., BIANCO, R., BERRINO, L., CIUFFREDA, L. P., CIARDIELLO, D., IAFFAIOLI, V., BOTTI, G., FERRAIOLO, F. & CIARDIELLO, F. 2015. AXL is an oncotarget in human colorectal cancer. *Oncotarget,* 6**,** 23281-96.

MAY, C. D., GARNETT, J., MA, X., LANDERS, S. M., INGRAM, D. R., DEMICCO, E. G., AL SANNAA, G. A., VU, T., HAN, L., ZHANG, Y., KIVLIN, C. M., BOLSHAKOV, S., KALAM, A. A., LIU, J., ZHOU, F., BROCCOLI, D., WANG, W. L., LAZAR, A. J., POLLOCK, R. E., LEV, D. & TORRES, K. E. 2015. AXL is a potential therapeutic target in dedifferentiated and pleomorphic liposarcomas. *BMC Cancer,* 15**,** 901.

MCCLATCHEY, A. I., SAOTOME, I., RAMESH, V., GUSELLA, J. F. & JACKS, T. 1997. The Nf2 tumor suppressor gene product is essential for extraembryonic development immediately prior to gastrulation. *Genes Dev,* 11**,** 1253-65.

MCCUBREY, J. A., ABRAMS, S. L., FITZGERALD, T. L., COCCO, L., MARTELLI, A. M., MONTALTO, G., CERVELLO, M., SCALISI, A., CANDIDO, S., LIBRA, M. & STEELMAN, L. S. 2015. Roles of signaling pathways in drug resistance, cancer initiating cells and cancer progression and metastasis. *Adv Biol Regul,* 57**,** 75-101.

MCDANIEL, N. K., CUMMINGS, C. T., IIDA, M., HULSE, J., PEARSON, H. E., VASILEIADI, E., PARKER, R. E., ORBUCH, R. A., ONDRACEK, O. J., WELKE, N. B., KANG, G. H., DAVIES, K. D., WANG, X., FRYE, S. V., EARP, H. S., HARARI, P. M., KIMPLE, R. J., DERYCKERE, D., GRAHAM, D. K. & WHEELER, D. L. 2018. MERTK Mediates Intrinsic and Adaptive Resistance to AXL-targeting Agents. *Mol Cancer Ther,* 17**,** 2297-2308.

MENON, A. G., RUTTER, J. L., VON SATTEL, J. P., SYNDER, H., MURDOCH, C., BLUMENFELD, A., MARTUZA, R. L., VON DEIMLING, A., GUSELLA, J. F. & HOUSEAL, T. W. 1997. Frequent loss of chromosome 14 in atypical and malignant meningioma: identification of a putative 'tumor progression' locus. *Oncogene,* 14**,** 611-6.

MERKER, V. L., ESPARZA, S., SMITH, M. J., STEMMER-RACHAMIMOV, A. & PLOTKIN, S. R. 2012. Clinical features of schwannomatosis: a retrospective analysis of 87 patients. *Oncologist,* 17**,** 1317-22.

MEYER, A. S., MILLER, M. A., GERTLER, F. B. & LAUFFENBURGER, D. A. 2013. The receptor AXL diversifies EGFR signaling and limits the response to EGFR-targeted inhibitors in triple-negative breast cancer cells. *Sci Signal,* 6**,** ra66.

MIGDALL-WILSON, J., BATES, C., SCHLEGEL, J., BRANDAO, L., LINGER, R. M., DERYCKERE, D. & GRAHAM, D. K. 2012. Prolonged exposure to a Mer ligand in leukemia: Gas6 favors expression of a partial Mer glycoform and reveals a novel role for Mer in the nucleus. *PLoS One,* 7**,** e31635.

MINSON, K. A., SMITH, C. C., DERYCKERE, D., LIBBRECHT, C., LEE-SHERICK, A. B., HUEY, M. G., LASATER, E. A., KIRKPATRICK, G. D., STASHKO, M. A., ZHANG, W., JORDAN, C. T., KIREEV, D., WANG, X., FRYE, S. V., EARP, H. S., SHAH, N. P. & GRAHAM, D. K. 2016. The MERTK/FLT3 inhibitor MRX-2843 overcomes resistance-conferring FLT3 mutations in acute myeloid leukemia. *JCI Insight,* 1**,** e85630.

MIYAMOTO, Y., TORII, T., TAKADA, S., OHNO, N., SAITOH, Y., NAKAMURA, K., ITO, A., OGATA, T., TERADA, N., TANOUE, A. & YAMAUCHI, J. 2015. Involvement of the Tyro3 receptor and its intracellular partner Fyn signaling in Schwann cell myelination. *Mol Biol Cell,* 26**,** 3489-503.

MOHAMMED, H. & CARROLL, J. S. 2013. Approaches for assessing and discovering protein interactions in cancer. *Mol Cancer Res,* 11**,** 1295-302.

MOODY, G., BELMONTES, B., MASTERMAN, S., WANG, W., KING, C., MURAWSKY, C., TSURUDA, T., LIU, S., RADINSKY, R. & BELTRAN, P. J. 2016. Antibody-mediated neutralization of autocrine Gas6 inhibits the growth of pancreatic ductal adenocarcinoma tumors in vivo. *Int J Cancer,* 139**,** 1340-9.

MORRISON, H., SHERMAN, L. S., LEGG, J., BANINE, F., ISACKE, C., HAIPEK, C. A., GUTMANN, D. H., PONTA, H. & HERRLICH, P. 2001. The NF2 tumor suppressor gene product, merlin, mediates contact inhibition of growth through interactions with CD44. *Genes Dev,* 15**,** 968-80.

MOSIENIAK, G. & SIKORA, E. 2010. Polyploidy: the link between senescence and cancer. *Curr Pharm Des,* 16**,** 734-40.

MUDDULURU, G. & ALLGAYER, H. 2008. The human receptor tyrosine kinase Axl gene--promoter characterization and regulation of constitutive expression by Sp1, Sp3 and CpG methylation. *Biosci Rep,* 28**,** 161-76.

MUDDULURU, G., CEPPI, P., KUMARSWAMY, R., SCAGLIOTTI, G. V., PAPOTTI, M. & ALLGAYER, H. 2011. Regulation of Axl receptor tyrosine kinase expression by miR-34a and miR-199a/b in solid cancer. *Oncogene,* 30**,** 2888-99.

MUDDULURU, G., LEUPOLD, J. H., STROEBEL, P. & ALLGAYER, H. 2010a. PMA up-regulates the transcription of Axl by AP-1 transcription factor binding to TRE sequences via the MAPK cascade in leukaemia cells. *Biol Cell,* 103**,** 21-33.

MUDDULURU, G., VAJKOCZY, P. & ALLGAYER, H. 2010b. Myeloid zinc finger 1 induces migration, invasion, and in vivo metastasis through Axl gene expression in solid cancer. *Mol Cancer Res,* 8**,** 159-69.

MYERS, S. H., BRUNTON, V. G. & UNCITI-BROCETA, A. 2016. AXL Inhibitors in Cancer: A Medicinal Chemistry Perspective. *J Med Chem,* 59**,** 3593-608.

MYERS, S. H., TEMPS, C., HOUSTON, D. R., BRUNTON, V. G. & UNCITI-BROCETA, A. 2018. Development of Potent Inhibitors of Receptor Tyrosine Kinases by Ligand-Based Drug Design and Target-Biased Phenotypic Screening. *J Med Chem,* 61**,** 2104-2110.

N, A. G., BENSINGER, S. J., HONG, C., BECEIRO, S., BRADLEY, M. N., ZELCER, N., DENIZ, J., RAMIREZ, C., DIAZ, M., GALLARDO, G., DE GALARRETA, C. R., SALAZAR, J., LOPEZ, F., EDWARDS, P., PARKS, J., ANDUJAR, M., TONTONOZ, P. & CASTRILLO, A. 2009. Apoptotic cells promote their own clearance and immune tolerance through activation of the nuclear receptor LXR. *Immunity,* 31**,** 245-58.

NANDA, A., BIR, S. C., MAITI, T. K., KONAR, S. K., MISSIOS, S. & GUTHIKONDA, B. 2017. Relevance of Simpson grading system and recurrence-free survival after

surgery for World Health Organization Grade I meningioma. *J Neurosurg,* 126**,** 201-211.

NGUYEN, K. Q., TSOU, W. I., CALARESE, D. A., KIMANI, S. G., SINGH, S., HSIEH, S., LIU, Y., LU, B., WU, Y., GARFORTH, S. J., ALMO, S. C., KOTENKO, S. V. & BIRGE, R. B. 2014. Overexpression of MERTK receptor tyrosine kinase in epithelial cancer cells drives efferocytosis in a gain-of-function capacity. *J Biol Chem,* 289, 25737-49.

NILES, A. L., MORAVEC, R. A. & RISS, T. L. 2009. In vitro viability and cytotoxicity testing and same-well multi-parametric combinations for high throughput screening. *Curr Chem Genomics,* 3**,** 33-41.

NIU, Z. S., NIU, X. J. & WANG, W. H. 2019. Role of the receptor tyrosine kinase Axl in hepatocellular carcinoma and its clinical relevance. *Future Oncol,* 15**,** 653-662.

O'BRYAN, J. P., FRIDELL, Y. W., KOSKI, R., VARNUM, B. & LIU, E. T. 1995. The transforming receptor tyrosine kinase, Axl, is post-translationally regulated by proteolytic cleavage. *J Biol Chem,* 270**,** 551-7.

O'BRYAN, J. P., FRYE, R. A., COGSWELL, P. C., NEUBAUER, A., KITCH, B., PROKOP, C., ESPINOSA, R., 3RD, LE BEAU, M. M., EARP, H. S. & LIU, E. T. 1991. axl, a transforming gene isolated from primary human myeloid leukemia cells, encodes a novel receptor tyrosine kinase. *Mol Cell Biol,* 11**,** 5016-31.

O'SHAUGHNESSY, J. & BUSSIERES, A. 2006. Subtle clinical signs of a spinal cord ependymoma at the cervicothoracic level in an adult: a case report. *J Can Chiropr Assoc,* 50**,** 244-8.

OIEN, D. B., GARAY, T., ECKSTEIN, S. & CHIEN, J. 2017. Cisplatin and Pemetrexed Activate AXL and AXL Inhibitor BGB324 Enhances Mesothelioma Cell Death from Chemotherapy. *Front Pharmacol,* 8**,** 970.

OKA, Y., NAKAJIMA, K., NAGAO, K., MIURA, K., ISHII, N. & KOBAYASHI, H. 2010. 293FT cells transduced with four transcription factors (OCT4, SOX2, NANOG, and LIN28) generate aberrant ES-like cells. *J Stem Cells Regen Med,* 6**,** 149-56.

OKADA, T., LOPEZ-LAGO, M. & GIANCOTTI, F. G. 2005. Merlin/NF-2 mediates contact inhibition of growth by suppressing recruitment of Rac to the plasma membrane. *J Cell Biol,* 171**,** 361-71.

OKIMOTO, R. A. & BIVONA, T. G. 2015. AXL receptor tyrosine kinase as a therapeutic target in NSCLC. *Lung Cancer (Auckl),* 6**,** 27-34.

ORSO, F., JAGER, R., CALOGERO, R. A., SCHORLE, H., SISMONDI, P., DE BORTOLI, M. & TAVERNA, D. 2009. AP-2alpha regulates migration of GN-11 neurons via a specific genetic programme involving the Axl receptor tyrosine kinase. *BMC Biol,* 7**,** 25.

OSORIO, D. S., HU, J., MITCHELL, C., ALLEN, J. C., STANEK, J., HAGIWARA, M. & KARAJANNIS, M. A. 2018. Effect of lapatinib on meningioma growth in adults with neurofibromatosis type 2. *J Neurooncol,* 139**,** 749-755.

OU, W. B., CORSON, J. M., FLYNN, D. L., LU, W. P., WISE, S. C., BUENO, R., SUGARBAKER, D. J. & FLETCHER, J. A. 2011. AXL regulates mesothelioma proliferation and invasiveness. *Oncogene,* 30**,** 1643-52.

PACHOW, D., ANDRAE, N., KLIESE, N., ANGENSTEIN, F., STORK, O., WILISCH-NEUMANN, A., KIRCHES, E. & MAWRIN, C. 2013. mTORC1 inhibitors suppress meningioma growth in mouse models. *Clin Cancer Res,* 19**,** 1180-9.

PAO-CHUN, L., CHAN, P. M., CHAN, W. & MANSER, E. 2009. Cytoplasmic ACK1 interaction with multiple receptor tyrosine kinases is mediated by Grb2: an analysis of ACK1 effects on Axl signaling. *J Biol Chem,* 284**,** 34954-63.

PAOLINO, M., CHOIDAS, A., WALLNER, S., PRANJIC, B., URIBESALGO, I., LOESER, S., JAMIESON, A. M., LANGDON, W. Y., IKEDA, F., FEDEDA, J. P., CRONIN, S. J., NITSCH, R., SCHULTZ-FADEMRECHT, C., EICKHOFF, J., MENNINGER, S., UNGER, A., TORKA, R., GRUBER, T., HINTERLEITNER, R., BAIER, G., WOLF, D., ULLRICH, A., KLEBL, B. M. & PENNINGER, J. M. 2014. The E3

ligase Cbl-b and TAM receptors regulate cancer metastasis via natural killer cells. *Nature,* 507**,** 508-12.

PAOLINO, M. & PENNINGER, J. M. 2016. The Role of TAM Family Receptors in Immune Cell Function: Implications for Cancer Therapy. *Cancers (Basel),* 8.

PARK, I. K., MISHRA, A., CHANDLER, J., WHITMAN, S. P., MARCUCCI, G. & CALIGIURI, M. A. 2013. Inhibition of the receptor tyrosine kinase Axl impedes activation of the FLT3 internal tandem duplication in human acute myeloid leukemia: implications for Axl as a potential therapeutic target. *Blood,* 121**,** 2064-73.

PARKINSON, D. B., BHASKARAN, A., DROGGITI, A., DICKINSON, S., D'ANTONIO, M., MIRSKY, R. & JESSEN, K. R. 2004. Krox-20 inhibits Jun-NH2-terminal kinase/c-Jun to control Schwann cell proliferation and death. *J Cell Biol,* 164**,** 385-94.

PASQUIER, B., GASNIER, F., PASQUIER, D., KEDDARI, E., MORENS, A. & COUDERC, P. 1986. Papillary meningioma. Clinicopathologic study of seven cases and review of the literature. *Cancer,* 58**,** 299-305.

PAUL, M. K. & MUKHOPADHYAY, A. K. 2004. Tyrosine kinase - Role and significance in Cancer. *Int J Med Sci,* 1**,** 101-115.

PEREZ-MAGAN, E., CAMPOS-MARTIN, Y., MUR, P., FIANO, C., RIBALTA, T., GARCIA, J. F., REY, J. A., RODRIGUEZ DE LOPE, A., MOLLEJO, M. & MELENDEZ, B. 2012. Genetic alterations associated with progression and recurrence in meningiomas. *J Neuropathol Exp Neurol,* 71**,** 882-93.

PERRY, A., CAI, D. X., SCHEITHAUER, B. W., SWANSON, P. E., LOHSE, C. M., NEWSHAM, I. F., WEAVER, A. & GUTMANN, D. H. 2000. Merlin, DAL-1, and progesterone receptor expression in clinicopathologic subsets of meningioma: a correlative immunohistochemical study of 175 cases. *J Neuropathol Exp Neurol,* 59**,** 872-9.

PERRY, A., SCHEITHAUER, B. W., STAFFORD, S. L., LOHSE, C. M. & WOLLAN, P. C. 1999. "Malignancy" in meningiomas: a clinicopathologic study of 116 patients, with grading implications. *Cancer,* 85**,** 2046-2056.

PETRILLI, A. M. & FERNANDEZ-VALLE, C. 2016. Role of Merlin/NF2 inactivation in tumor biology. *Oncogene,* 35**,** 537-48.

PEYRE, M., STEMMER-RACHAMIMOV, A., CLERMONT-TARANCHON, E., QUENTIN, S., EL-TARAYA, N., WALCZAK, C., VOLK, A., NIWA-KAWAKITA, M., KARBOUL, N., GIOVANNINI, M. & KALAMARIDES, M. 2013. Meningioma progression in mice triggered by Nf2 and Cdkn2ab inactivation. *Oncogene,* 32**,** 4264-72.

PHILLIPS, L. E., LONGSTRETH, W. T., JR., KOEPSELL, T., CUSTER, B. S., KUKULL, W. A. & VAN BELLE, G. 2005. Active and passive cigarette smoking and risk of intracranial meningioma. *Neuroepidemiology,* 24**,** 117-22.

PIERCE, A., BLIESNER, B., XU, M., NIELSEN-PREISS, S., LEMKE, G., TOBET, S. & WIERMAN, M. E. 2008. Axl and Tyro3 modulate female reproduction by influencing gonadotropin-releasing hormone neuron survival and migration. *Mol Endocrinol,* 22**,** 2481-95.

PIERCE, A., XU, M., BLIESNER, B., LIU, Z., RICHARDS, J., TOBET, S. & WIERMAN, M. E. 2011. Hypothalamic but not pituitary or ovarian defects underlie the reproductive abnormalities in Axl/Tyro3 null mice. *Mol Cell Endocrinol,* 339**,** 151-8.

PIERCE, A. M. & KEATING, A. K. 2014. TAM receptor tyrosine kinases: expression, disease and oncogenesis in the central nervous system. *Brain Res,* 1542**,** 206-20.

PINATO, D. J., MAURI, F. A., LLOYD, T., VAIRA, V., CASADIO, C., BOLDORINI, R. L. & SHARMA, R. 2013. The expression of Axl receptor tyrosine kinase influences the tumour phenotype and clinical outcome of patients with malignant pleural mesothelioma. *Br J Cancer,* 108**,** 621-8.

PIOTROWSKI, A., XIE, J., LIU, Y. F., POPLAWSKI, A. B., GOMES, A. R., MADANECKI, P., FU, C., CROWLEY, M. R., CROSSMAN, D. K., ARMSTRONG, L., BABOVIC-VUKSANOVIC, D., BERGNER, A., BLAKELEY, J. O., BLUMENTHAL, A. L., DANIELS, M. S., FEIT, H., GARDNER, K., HURST, S., KOBELKA, C., LEE, C., NAGY, R., RAUEN, K. A., SLOPIS, J. M., SUWANNARAT, P., WESTMAN, J. A., ZANKO, A., KORF, B. R. & MESSIAEN, L. M. 2014. Germline loss-of-function mutations in LZTR1 predispose to an inherited disorder of multiple schwannomas. *Nat Genet,* 46**,** 182-7.

PLOTKIN, S. R., BLAKELEY, J. O., EVANS, D. G., HANEMANN, C. O., HULSEBOS, T. J., HUNTER-SCHAEDLE, K., KALPANA, G. V., KORF, B., MESSIAEN, L., PAPI, L., RATNER, N., SHERMAN, L. S., SMITH, M. J., STEMMER-RACHAMIMOV, A. O., VITTE, J. & GIOVANNINI, M. 2013. Update from the 2011 International Schwannomatosis Workshop: From genetics to diagnostic criteria. *Am J Med Genet A,* 161A**,** 405-16.

PLOTKIN, S. R., HALPIN, C., MCKENNA, M. J., LOEFFLER, J. S., BATCHELOR, T. T. & BARKER, F. G., 2ND 2010. Erlotinib for progressive vestibular schwannoma in neurofibromatosis 2 patients. *Otol Neurotol,* 31**,** 1135-43.

PLOTKIN, S. R., MERKER, V. L., HALPIN, C., JENNINGS, D., MCKENNA, M. J., HARRIS, G. J. & BARKER, F. G., 2ND 2012. Bevacizumab for progressive vestibular schwannoma in neurofibromatosis type 2: a retrospective review of 31 patients. *Otol Neurotol,* 33**,** 1046-52.

POLVI, A., ARMSTRONG, E., LAI, C., LEMKE, G., HUEBNER, K., SPRITZ, R. A., GUIDA, L. C., NICHOLLS, R. D. & ALITALO, K. 1993. The human TYRO3 gene and pseudogene are located in chromosome 15q14-q25. *Gene,* 134**,** 289-93.

PRASAD, D., ROTHLIN, C. V., BURROLA, P., BURSTYN-COHEN, T., LU, Q., GARCIA DE FRUTOS, P. & LEMKE, G. 2006. TAM receptor function in the retinal pigment epithelium. *Mol Cell Neurosci,* 33**,** 96-108.

PRIETO, A. L., O'DELL, S., VARNUM, B. & LAI, C. 2007. Localization and signaling of the receptor protein tyrosine kinase Tyro3 in cortical and hippocampal neurons. *Neuroscience,* 150**,** 319-34.

PROVENZANO. 2018. *The role of cellular prion protein in the development of schwannomas and other merlin-deficient tumours.* Doctorate, University of Plymouth.

PUTTMANN, S., SENNER, V., BRAUNE, S., HILLMANN, B., EXELER, R., RICKERT, C. H. & PAULUS, W. 2005. Establishment of a benign meningioma cell line by hTERT-mediated immortalization. *Lab Invest,* 85**,** 1163-71.

QIN, A. & QIAN, W. 2018. MicroRNA-7 inhibits colorectal cancer cell proliferation, migration and invasion via TYRO3 and phosphoinositide 3-kinase/protein B kinase/mammalian target of rapamycin pathway suppression. *Int J Mol Med,* 42**,** 2503-2514.

RANKIN, E. B., FUH, K. C., CASTELLINI, L., VISWANATHAN, K., FINGER, E. C., DIEP, A. N., LAGORY, E. L., KARIOLIS, M. S., CHAN, A., LINDGREN, D., AXELSON, H., MIAO, Y. R., KRIEG, A. J. & GIACCIA, A. J. 2014. Direct regulation of GAS6/AXL signaling by HIF promotes renal metastasis through SRC and MET. *Proc Natl Acad Sci U S A,* 111**,** 13373-8.

RAO, V. S., SRINIVAS, K., SUJINI, G. N. & KUMAR, G. N. 2014. Protein-protein interaction detection: methods and analysis. *Int J Proteomics,* 2014**,** 147648.

RESCIGNO, J., MANSUKHANI, A. & BASILICO, C. 1991. A putative receptor tyrosine kinase with unique structural topology. *Oncogene,* 6**,** 1909-13.

RESEARCH, C. I. 2016 January. *BGB324, a selective small molecule inhibitor of the receptor tyrosine kinase AXL, enhances immune checkpoint inhibitor efficacy* [Online]. Available: http://cancerimmunolres.aacrjournals.org/content/4/1_Supplement/B014 [Accessed].

RHO, J. K., CHOI, Y. J., KIM, S. Y., KIM, T. W., CHOI, E. K., YOON, S. J., PARK, B. M., PARK, E., BAE, J. H., CHOI, C. M. & LEE, J. C. 2014. MET and AXL inhibitor NPS-1034 exerts efficacy against lung cancer cells resistant to EGFR kinase inhibitors because of MET or AXL activation. *Cancer Res,* 74**,** 253-62.

RICCARDI, V. M. 1982. Neurofibromatosis: clinical heterogeneity. *Curr Probl Cancer.*

RIEMENSCHNEIDER, M. J., PERRY, A. & REIFENBERGER, G. 2006. Histological classification and molecular genetics of meningiomas. *Lancet Neurol,* 5**,** 1045-54.

ROGERS, C. L., PERRY, A., PUGH, S., VOGELBAUM, M. A., BRACHMAN, D., MCMILLAN, W., JENRETTE, J., BARANI, I., SHRIEVE, D., SLOAN, A., BOVI, J., KWOK, Y., BURRI, S. H., CHAO, S. T., SPALDING, A. C., ANSCHER, M. S., BLOOM, B. & MEHTA, M. 2016. Pathology concordance levels for meningioma classification and grading in NRG Oncology RTOG Trial 0539. *Neuro Oncol,* 18**,** 565-74.

ROOHULLAH, A., COOPER, A., LOMAX, A. J., AUNG, J., BARGE, A., CHOW, L., MCHALE, M., DESAI, J., WHITTLE, J. R., TRAN, B., DE SOUZA, P. & HORVATH, L. G. 2018. A phase I trial to determine safety and pharmacokinetics of ASLAN002, an oral MET superfamily kinase inhibitor, in patients with advanced or metastatic solid cancers. *Invest New Drugs.*

ROSKOSKI, R., JR. 2012. ERK1/2 MAP kinases: structure, function, and regulation. *Pharmacol Res,* 66**,** 105-43.

ROULEAU, G. A., MEREL, P., LUTCHMAN, M., SANSON, M., ZUCMAN, J., MARINEAU, C., HOANG-XUAN, K., DEMCZUK, S., DESMAZE, C., PLOUGASTEL, B. & ET AL. 1993. Alteration in a new gene encoding a putative membrane-organizing protein causes neuro-fibromatosis type 2. *Nature,* 363**,** 515-21.

RUGO, H. S., CHIEN, A. J., FRANCO, S. X., STOPECK, A. T., GLENCER, A., LAHIRI, S., ARBUSHITES, M. C., SCOTT, J., PARK, J. W., HUDIS, C., NULSEN, B. & DICKLER, M. N. 2012. A phase II study of lapatinib and bevacizumab as treatment for HER2-overexpressing metastatic breast cancer. *Breast Cancer Res Treat,* 134**,** 13-20.

RUSTAGI, T., BADVE, S. & PAREKH, A. N. 2012. Sciatica from a foraminal lumbar root schwannoma: case report and review of literature. *Case Rep Orthop,* 2012**,** 142143.

SADETZKI, S., CHETRIT, A., TURNER, M. C., VAN TONGEREN, M., BENKE, G., FIGUEROLA, J., FLEMING, S., HOURS, M., KINCL, L., KREWSKI, D., MCLEAN, D., PARENT, M. E., RICHARDSON, L., SCHLEHOFER, B., SCHLAEFER, K., BLETTNER, M., SCHUZ, J., SIEMIATYCKI, J. & CARDIS, E. 2016. Occupational exposure to metals and risk of meningioma: a multinational case-control study. *J Neurooncol,* 130**,** 505-515.

SAHM, F., BISSEL, J., KOELSCHE, C., SCHWEIZER, L., CAPPER, D., REUSS, D., BOHMER, K., LASS, U., GOCK, T., KALIS, K., MEYER, J., HABEL, A., BREHMER, S., MITTELBRONN, M., JONES, D. T., SCHITTENHELM, J., URBSCHAT, S., KETTER, R., HEIM, S., MAWRIN, C., HAINFELLNER, J. A., BERGHOFF, A. S., PREUSSER, M., BECKER, A., HEROLD-MENDE, C., UNTERBERG, A., HARTMANN, C., KICKINGEREDER, P., COLLINS, V. P., PFISTER, S. M. & VON DEIMLING, A. 2013. AKT1E17K mutations cluster with meningothelial and transitional meningiomas and can be detected by SFRP1 immunohistochemistry. *Acta Neuropathol,* 126**,** 757-62.

SAHM, F., SCHRIMPF, D., STICHEL, D., JONES, D. T. W., HIELSCHER, T., SCHEFZYK, S., OKONECHNIKOV, K., KOELSCHE, C., REUSS, D. E., CAPPER, D., STURM, D., WIRSCHING, H. G., BERGHOFF, A. S., BAUMGARTEN, P., KRATZ, A., HUANG, K., WEFERS, A. K., HOVESTADT, V., SILL, M., ELLIS, H. P., KURIAN, K. M., OKUDUCU, A. F., JUNGK, C., DRUESCHLER, K., SCHICK, M., BEWERUNGE-HUDLER, M., MAWRIN, C.,

SEIZ-ROSENHAGEN, M., KETTER, R., SIMON, M., WESTPHAL, M., LAMSZUS, K., BECKER, A., KOCH, A., SCHITTENHELM, J., RUSHING, E. J., COLLINS, V. P., BREHMER, S., CHAVEZ, L., PLATTEN, M., HANGGI, D., UNTERBERG, A., PAULUS, W., WICK, W., PFISTER, S. M., MITTELBRONN, M., PREUSSER, M., HEROLD-MENDE, C., WELLER, M. & VON DEIMLING, A. 2017. DNA methylation-based classification and grading system for meningioma: a multicentre, retrospective analysis. *Lancet Oncol,* 18**,** 682-694.

SATHER, S., KENYON, K. D., LEFKOWITZ, J. B., LIANG, X., VARNUM, B. C., HENSON, P. M. & GRAHAM, D. K. 2007. A soluble form of the Mer receptor tyrosine kinase inhibits macrophage clearance of apoptotic cells and platelet aggregation. *Blood,* 109**,** 1026-33.

SAWABU, T., SENO, H., KAWASHIMA, T., FUKUDA, A., UENOYAMA, Y., KAWADA, M., KANDA, N., SEKIKAWA, A., FUKUI, H., YANAGITA, M., YOSHIBAYASHI, H., SATOH, S., SAKAI, Y., NAKANO, T. & CHIBA, T. 2007. Growth arrest-specific gene 6 and Axl signaling enhances gastric cancer cell survival via Akt pathway. *Mol Carcinog,* 46**,** 155-64.

SCALTRITI, M., ELKABETS, M. & BASELGA, J. 2016. Molecular Pathways: AXL, a Membrane Receptor Mediator of Resistance to Therapy. *Clin Cancer Res,* 22**,** 1313-7.

SCHLEGEL, J., SAMBADE, M. J., SATHER, S., MOSCHOS, S. J., TAN, A. C., WINGES, A., DERYCKERE, D., CARSON, C. C., TREMBATH, D. G., TENTLER, J. J., ECKHARDT, S. G., KUAN, P. F., HAMILTON, R. L., DUNCAN, L. M., MILLER, C. R., NIKOLAISHVILI-FEINBERG, N., MIDKIFF, B. R., LIU, J., ZHANG, W., YANG, C., WANG, X., FRYE, S. V., EARP, H. S., SHIELDS, J. M. & GRAHAM, D. K. 2013. MERTK receptor tyrosine kinase is a therapeutic target in melanoma. *J Clin Invest,* 123**,** 2257-67.

SCHLESSINGER, J. 2000. Cell signaling by receptor tyrosine kinases. *Cell,* 103**,** 211-25.

SCHMITZ, R., VALLS, A. F., YERBES, R., VON RICHTER, S., KAHLERT, C., LOGES, S., WEITZ, J., SCHNEIDER, M., RUIZ DE ALMODOVAR, C., ULRICH, A. & SCHMIDT, T. 2016. TAM receptors Tyro3 and Mer as novel targets in colorectal cancer. *Oncotarget,* 7**,** 56355-56370.

SCHNEIDER, B., PULHORN, H., ROHRIG, B. & RAINOV, N. G. 2005. Predisposing conditions and risk factors for development of symptomatic meningioma in adults. *Cancer Detect Prev,* 29**,** 440-7.

SCHNEIDER, C. A., RASBAND, W. S. & ELICEIRI, K. W. 2012. NIH Image to ImageJ: 25 years of image analysis. *Nat Methods,* 9**,** 671-5.

SCHOUMACHER, M. & BURBRIDGE, M. 2017. Key Roles of AXL and MER Receptor Tyrosine Kinases in Resistance to Multiple Anticancer Therapies. *Curr Oncol Rep,* 19**,** 19.

SCHROEDER, G. M., AN, Y., CAI, Z. W., CHEN, X. T., CLARK, C., CORNELIUS, L. A., DAI, J., GULLO-BROWN, J., GUPTA, A., HENLEY, B., HUNT, J. T., JEYASEELAN, R., KAMATH, A., KIM, K., LIPPY, J., LOMBARDO, L. J., MANNE, V., OPPENHEIMER, S., SACK, J. S., SCHMIDT, R. J., SHEN, G., STEFANSKI, K., TOKARSKI, J. S., TRAINOR, G. L., WAUTLET, B. S., WEI, D., WILLIAMS, D. K., ZHANG, Y., ZHANG, Y., FARGNOLI, J. & BORZILLERI, R. M. 2009. Discovery of N-(4-(2-amino-3-chloropyridin-4-yloxy)-3-fluorophenyl)-4-ethoxy-1-(4-fluorophenyl)-2-oxo-1,2-dihydropyridine-3-carboxamide (BMS-777607), a selective and orally efficacious inhibitor of the Met kinase superfamily. *J Med Chem,* 52**,** 1251-4.

SCHULZ, A., ZOCH, A. & MORRISON, H. 2014. A neuronal function of the tumor suppressor protein merlin. *Acta Neuropathol Commun,* 2**,** 82.

SCHULZ, A. S., SCHLEITHOFF, L., FAUST, M., BARTRAM, C. R. & JANSSEN, J. W. 1993. The genomic structure of the human UFO receptor. *Oncogene,* 8**,** 509-13.

SCHWARTZ, M. A. & ASSOIAN, R. K. 2001. Integrins and cell proliferation: regulation of cyclin-dependent kinases via cytoplasmic signaling pathways. *J Cell Sci,* 114**,** 2553-60.

SCHWARTZBAUM, J., JONSSON, F., AHLBOM, A., PRESTON-MARTIN, S., MALMER, B., LONN, S., SODERBERG, K. & FEYCHTING, M. 2005. Prior hospitalization for epilepsy, diabetes, and stroke and subsequent glioma and meningioma risk. *Cancer Epidemiol Biomarkers Prev,* 14**,** 643-50.

SEITZ, H. M., CAMENISCH, T. D., LEMKE, G., EARP, H. S. & MATSUSHIMA, G. K. 2007. Macrophages and dendritic cells use different Axl/Mertk/Tyro3 receptors in clearance of apoptotic cells. *J Immunol,* 178**,** 5635-42.

SEN, P., WALLET, M. A., YI, Z., HUANG, Y., HENDERSON, M., MATHEWS, C. E., EARP, H. S., MATSUSHIMA, G., BALDWIN, A. S., JR. & TISCH, R. M. 2007. Apoptotic cells induce Mer tyrosine kinase-dependent blockade of NF-kappaB activation in dendritic cells. *Blood,* 109**,** 653-60.

SESTINI, R., BACCI, C., PROVENZANO, A., GENUARDI, M. & PAPI, L. 2008. Evidence of a four-hit mechanism involving SMARCB1 and NF2 in schwannomatosis-associated schwannomas. *Hum Mutat,* 29**,** 227-31.

SHARMA, S., ZENG, J. Y., ZHUANG, C. M., ZHOU, Y. Q., YAO, H. P., HU, X., ZHANG, R. & WANG, M. H. 2013. Small-molecule inhibitor BMS-777607 induces breast cancer cell polyploidy with increased resistance to cytotoxic chemotherapy agents. *Mol Cancer Ther,* 12**,** 725-36.

SINGH, H., BRAVE, M., BEAVER, J. A., CHENG, J., TANG, S., ZAHALKA, E., PALMBY, T. R., VENUGOPAL, R., SONG, P., LIU, Q., LIU, C., YU, J., CHEN, X. H., WANG, X., WANG, Y., KLUETZ, P. G., DANIELS, S. R., PAPADOPOULOS, E. J., SRIDHARA, R., MCKEE, A. E., IBRAHIM, A., KIM, G. & PAZDUR, R. 2017. U.S. Food and Drug Administration Approval: Cabozantinib for the Treatment of Advanced Renal Cell Carcinoma. *Clin Cancer Res,* 23**,** 330-335.

SLUSARZ, K. M., MERKER, V. L., MUZIKANSKY, A., FRANCIS, S. A. & PLOTKIN, S. R. 2014. Long-term toxicity of bevacizumab therapy in neurofibromatosis 2 patients. *Cancer Chemother Pharmacol,* 73**,** 1197-204.

SMART, S. K., VASILEIADI, E., WANG, X., DERYCKERE, D. & GRAHAM, D. K. 2018. The Emerging Role of TYRO3 as a Therapeutic Target in Cancer. *Cancers (Basel),* 10.

SMITH, M. J., HIGGS, J. E., BOWERS, N. L., HALLIDAY, D., PATERSON, J., GILLESPIE, J., HUSON, S. M., FREEMAN, S. R., LLOYD, S., RUTHERFORD, S. A., KING, A. T., WALLACE, A. J., RAMSDEN, R. T. & EVANS, D. G. 2011. Cranial meningiomas in 411 neurofibromatosis type 2 (NF2) patients with proven gene mutations: clear positional effect of mutations, but absence of female severity effect on age at onset. *J Med Genet,* 48**,** 261-5.

SMITH, M. J., ISIDOR, B., BEETZ, C., WILLIAMS, S. G., BHASKAR, S. S., RICHER, W., O'SULLIVAN, J., ANDERSON, B., DALY, S. B., URQUHART, J. E., FRYER, A., RUSTAD, C. F., MILLS, S. J., SAMII, A., DU PLESSIS, D., HALLIDAY, D., BARBAROT, S., BOURDEAUT, F., NEWMAN, W. G. & EVANS, D. G. 2015. Mutations in LZTR1 add to the complex heterogeneity of schwannomatosis. *Neurology,* 84**,** 141-7.

SMITH, M. J., KULKARNI, A., RUSTAD, C., BOWERS, N. L., WALLACE, A. J., HOLDER, S. E., HEIBERG, A., RAMSDEN, R. T. & EVANS, D. G. 2012. Vestibular schwannomas occur in schwannomatosis and should not be considered an exclusion criterion for clinical diagnosis. *Am J Med Genet A,* 158A**,** 215-9.

SMITH, M. J., O'SULLIVAN, J., BHASKAR, S. S., HADFIELD, K. D., POKE, G., CAIRD, J., SHARIF, S., ECCLES, D., FITZPATRICK, D., RAWLUK, D., DU PLESSIS, D., NEWMAN, W. G. & EVANS, D. G. 2013. Loss-of-function mutations in SMARCE1 cause an inherited disorder of multiple spinal meningiomas. *Nat Genet,* 45**,** 295-8.

SMITH, M. J., WALLACE, A. J., BENNETT, C., HASSELBLATT, M., ELERT-DOBKOWSKA, E., EVANS, L. T., HICKEY, W. F., VAN HOFF, J., BAUER, D., LEE, A., HEVNER, R. F., BEETZ, C., DU PLESSIS, D., KILDAY, J. P., NEWMAN, W. G. & EVANS, D. G. 2014. Germline SMARCE1 mutations predispose to both spinal and cranial clear cell meningiomas. *J Pathol,* 234**,** 436-40.

SONJA, G., HEUSER, CHROMIK, BATALLA, AKYÜZ, MICKLEM, BROWN, LORENS, KEBENKO, JANNING, BINDER, FIEDLER AND CORTES. 2016. *BGB324, an Orally Available Selective Axl Inhibitor Exerts Anti-Leukemic Activity in the First-in-Patient Trial BGBC003 and Induces Unique Changes in Biomarker Profiles* [Online]. Available: http://www.bloodjournal.org/content/128/22/592?sso-checked=true [Accessed].

STEILEN-GIMBEL, H., NIEDERMAYER, I., FEIDEN, W., FREILER, A., STEUDEL, W. I., ZANG, K. D. & HENN, W. 1999. Unbalanced translocation t(1;3)(p12-13;q11) in meningiomas as the unique feature of chordoid differentiation. *Genes Chromosomes Cancer,* 26**,** 270-2.

STENMAN, G., KINDBLOM, L. G., JOHANSSON, M. & ANGERVALL, L. 1991. Clonal chromosome abnormalities and in vitro growth characteristics of classical and cellular schwannomas. *Cancer Genet Cytogenet,* 57**,** 121-31.

STOGBAUER, L., STUMMER, W., SENNER, V. & BROKINKEL, B. 2019. Telomerase activity, TERT expression, hTERT promoter alterations, and alternative lengthening of the telomeres (ALT) in meningiomas - a systematic review. *Neurosurg Rev*.

SUFIT, A., LEE-SHERICK, A. B., DERYCKERE, D., RUPJI, M., DWIVEDI, B., VARELLA-GARCIA, M., PIERCE, A. M., KOWALSKI, J., WANG, X., FRYE, S. V., EARP, H. S., KEATING, A. K. & GRAHAM, D. K. 2016. MERTK Inhibition Induces Polyploidy and Promotes Cell Death and Cellular Senescence in Glioblastoma Multiforme. *PLoS One,* 11**,** e0165107.

SUN, C. X., ROBB, V. A. & GUTMANN, D. H. 2002. Protein 4.1 tumor suppressors: getting a FERM grip on growth regulation. *J Cell Sci,* 115**,** 3991-4000.

SUN, W., FUJIMOTO, J. & TAMAYA, T. 2004. Coexpression of Gas6/Axl in human ovarian cancers. *Oncology,* 66**,** 450-7.

TAKAHASHI, S. 2011. Downstream molecular pathways of FLT3 in the pathogenesis of acute myeloid leukemia: biology and therapeutic implications. *J Hematol Oncol,* 4**,** 13.

TAN, A. C., VYSE, S. & HUANG, P. H. 2017. Exploiting receptor tyrosine kinase co-activation for cancer therapy. *Drug Discov Today,* 22**,** 72-84.

TAN, L., ZHANG, Z., GAO, D., CHAN, S., LUO, J., TU, Z. C., ZHANG, Z. M., DING, K., REN, X. & LU, X. 2019. Quinolone antibiotic derivatives as new selective Axl kinase inhibitors. *Eur J Med Chem,* 166**,** 318-327.

TAVAZOIE, S. F., ALARCON, C., OSKARSSON, T., PADUA, D., WANG, Q., BOS, P. D., GERALD, W. L. & MASSAGUE, J. 2008. Endogenous human microRNAs that suppress breast cancer metastasis. *Nature,* 451**,** 147-52.

TAYLOR, I. C., ROY, S. & VARMUS, H. E. 1995. Overexpression of the Sky receptor tyrosine kinase at the cell surface or in the cytoplasm results in ligand-independent activation. *Oncogene,* 11**,** 2619-26.

TIAN, Y., ZHANG, Z., MIAO, L., YANG, Z., YANG, J., WANG, Y., QIAN, D., CAI, H. & WANG, Y. 2016. Anexelekto (AXL) Increases Resistance to EGFR-TKI and Activation of AKT and ERK1/2 in Non-Small Cell Lung Cancer Cells. *Oncol Res,* 24**,** 295-303.

TORRES, K. E., ZHU, Q. S., BILL, K., LOPEZ, G., GHADIMI, M. P., XIE, X., YOUNG, E. D., LIU, J., NGUYEN, T., BOLSHAKOV, S., BELOUSOV, R., WANG, S., LAHAT, G., LIU, J., HERNANDEZ, B., LAZAR, A. J. & LEV, D. 2011. Activated MET is a molecular prognosticator and potential therapeutic target for malignant peripheral nerve sheath tumors. *Clin Cancer Res,* 17**,** 3943-55.

TROFATTER, J. A., MACCOLLIN, M. M., RUTTER, J. L., MURRELL, J. R., DUYAO, M. P., PARRY, D. M., ELDRIDGE, R., KLEY, N., MENON, A. G., PULASKI, K. & ET AL. 1993. A novel moesin-, ezrin-, radixin-like gene is a candidate for the neurofibromatosis 2 tumor suppressor. *Cell,* 75**,** 826.

TWORKOSKI, K. A., PLATT, J. T., BACCHIOCCHI, A., BOSENBERG, M., BOGGON, T. J. & STERN, D. F. 2013. MERTK controls melanoma cell migration and survival and differentially regulates cell behavior relative to AXL. *Pigment Cell Melanoma Res,* 26**,** 527-41.

VALVERDE, P. 2005. Effects of Gas6 and hydrogen peroxide in Axl ubiquitination and downregulation. *Biochem Biophys Res Commun,* 333**,** 180-5.

VAN DEN MUNCKHOF, P., CHRISTIAANS, I., KENTER, S. B., BAAS, F. & HULSEBOS, T. J. 2012. Germline SMARCB1 mutation predisposes to multiple meningiomas and schwannomas with preferential location of cranial meningiomas at the falx cerebri. *Neurogenetics,* 13**,** 1-7.

VASUDEVAN, H. N., BRAUNSTEIN, S. E., PHILLIPS, J. J., PEKMEZCI, M., TOMLIN, B. A., WU, A., REIS, G. F., MAGILL, S. T., ZHANG, J., FENG, F. Y., NICHOLAIDES, T., CHANG, S. M., SNEED, P. K., MCDERMOTT, M. W., BERGER, M. S., PERRY, A. & RALEIGH, D. R. 2018. Comprehensive Molecular Profiling Identifies FOXM1 as a Key Transcription Factor for Meningioma Proliferation. *Cell Rep,* 22**,** 3672-3683.

VAUGHAN, C. A., SINGH, S., WINDLE, B., YEUDALL, W. A., FRUM, R., GROSSMAN, S. R., DEB, S. P. & DEB, S. 2012. Gain-of-Function Activity of Mutant p53 in Lung Cancer through Up-Regulation of Receptor Protein Tyrosine Kinase Axl. *Genes Cancer,* 3**,** 491-502.

VON MASSENHAUSEN, A., SANDERS, C., THEWES, B., DENG, M., QUEISSER, A., VOGEL, W., KRISTIANSEN, G., DUENSING, S., SCHROCK, A., BOOTZ, F., BROSSART, P., KIRFEL, J., HEASLEY, L., BRAGELMANN, J. & PERNER, S. 2016. MERTK as a novel therapeutic target in head and neck cancer. *Oncotarget,* 7**,** 32678-94.

VOURI, M., AN, Q., BIRT, M., PILKINGTON, G. J. & HAFIZI, S. 2015. Small molecule inhibition of Axl receptor tyrosine kinase potently suppresses multiple malignant properties of glioma cells. *Oncotarget,* 6**,** 16183-97.

VOURI, M., CROUCHER, D. R., KENNEDY, S. P., AN, Q., PILKINGTON, G. J. & HAFIZI, S. 2016. Axl-EGFR receptor tyrosine kinase hetero-interaction provides EGFR with access to pro-invasive signalling in cancer cells. *Oncogenesis,* 5**,** e266.

WANG, D. J., XIE, Q., GONG, Y., MAO, Y., WANG, Y., CHENG, H. X., ZHONG, P., CHE, X. M., JIANG, C. C., HUANG, F. P., ZHENG, K., LI, S. Q., GU, Y. X., BAO, W. M., YANG, B. J., WU, J. S., XIE, L. Q., ZHENG, M. Z., TANG, H. L., ZHU, H. D., CHEN, X. C. & ZHOU, L. F. 2013. Histopathological classification and location of consecutively operated meningiomas at a single institution in China from 2001 to 2010. *Chin Med J (Engl),* 126**,** 488-93.

WANG, X., GONG, Y., WANG, D., XIE, Q., ZHENG, M., ZHOU, Y., LI, Q., YANG, Z., TANG, H., LI, Y., HU, R., CHEN, X. & MAO, Y. 2012. Analysis of gene expression profiling in meningioma: deregulated signaling pathways associated with meningioma and EGFL6 overexpression in benign meningioma tissue and serum. *PLoS One,* 7**,** e52707.

WARREN, C., JAMES, L. A., RAMSDEN, R. T., WALLACE, A., BASER, M. E., VARLEY, J. M. & EVANS, D. G. 2003. Identification of recurrent regions of chromosome loss and gain in vestibular schwannomas using comparative genomic hybridisation. *J Med Genet,* 40**,** 802-6.

WATSON, K. L., AL SANNAA, G. A., KIVLIN, C. M., INGRAM, D. R., LANDERS, S. M., ROLAND, C. L., CORMIER, J. N., HUNT, K. K., FEIG, B. W., ASHLEIGH GUADAGNOLO, B., BISHOP, A. J., WANG, W. L., SLOPIS, J. M., MCCUTCHEON, I. E., LAZAR, A. J. & TORRES, K. E. 2017. Patterns of recurrence and survival in sporadic, neurofibromatosis Type 1-associated, and

radiation-associated malignant peripheral nerve sheath tumors. *J Neurosurg,* 126**,** 319-329.

WEITZMAN, S. P. & CABANILLAS, M. E. 2015. The treatment landscape in thyroid cancer: a focus on cabozantinib. *Cancer Manag Res,* 7**,** 265-78.

WELLENREUTHER, R., WAHA, A., VOGEL, Y., LENARTZ, D., SCHRAMM, J., WIESTLER, O. D. & VON DEIMLING, A. 1997. Quantitative analysis of neurofibromatosis type 2 gene transcripts in meningiomas supports the concept of distinct molecular variants. *Lab Invest,* 77**,** 601-6.

WESSELING, C., PUKKALA, E., NEUVONEN, K., KAUPPINEN, T., BOFFETTA, P. & PARTANEN, T. 2002. Cancer of the brain and nervous system and occupational exposures in Finnish women. *J Occup Environ Med,* 44**,** 663-8.

WILMES, L. J., PALLAVICINI, M. G., FLEMING, L. M., GIBBS, J., WANG, D., LI, K. L., PARTRIDGE, S. C., HENRY, R. G., SHALINSKY, D. R., HU-LOWE, D., PARK, J. W., MCSHANE, T. M., LU, Y., BRASCH, R. C. & HYLTON, N. M. 2007. AG-013736, a novel inhibitor of VEGF receptor tyrosine kinases, inhibits breast cancer growth and decreases vascular permeability as detected by dynamic contrast-enhanced magnetic resonance imaging. *Magn Reson Imaging,* 25**,** 319-27.

WONG, C. C. & LEE, W. M. 2002. The proximal cis-acting elements Sp1, Sp3 and E2F regulate mouse mer gene transcription in Sertoli cells. *Eur J Biochem,* 269**,** 3789-800.

WU, J., FRADY, L. N., BASH, R. E., COHEN, S. M., SCHORZMAN, A. N., SU, Y. T., IRVIN, D. M., ZAMBONI, W. C., WANG, X., FRYE, S. V., EWEND, M. G., SULMAN, E. P., GILBERT, M. R., EARP, H. S. & MILLER, C. R. 2018. MerTK as a therapeutic target in glioblastoma. *Neuro Oncol,* 20**,** 92-102.

WU, Y., SINGH, S., GEORGESCU, M. M. & BIRGE, R. B. 2005. A role for Mer tyrosine kinase in alphavbeta5 integrin-mediated phagocytosis of apoptotic cells. *J Cell Sci,* 118**,** 539-53.

WU, Y. M., ROBINSON, D. R. & KUNG, H. J. 2004. Signal pathways in up-regulation of chemokines by tyrosine kinase MER/NYK in prostate cancer cells. *Cancer Res,* 64**,** 7311-20.

XIAO, G. H., BEESER, A., CHERNOFF, J. & TESTA, J. R. 2002. p21-activated kinase links Rac/Cdc42 signaling to merlin. *J Biol Chem,* 277**,** 883-6.

XIAO, G. H., GALLAGHER, R., SHETLER, J., SKELE, K., ALTOMARE, D. A., PESTELL, R. G., JHANWAR, S. & TESTA, J. R. 2005. The NF2 tumor suppressor gene product, merlin, inhibits cell proliferation and cell cycle progression by repressing cyclin D1 expression. *Mol Cell Biol,* 25**,** 2384-94.

XU, H. M. & GUTMANN, D. H. 1998. Merlin differentially associates with the microtubule and actin cytoskeleton. *J Neurosci Res,* 51**,** 403-15.

XU, M. Z., CHAN, S. W., LIU, A. M., WONG, K. F., FAN, S. T., CHEN, J., POON, R. T., ZENDER, L., LOWE, S. W., HONG, W. & LUK, J. M. 2011. AXL receptor kinase is a mediator of YAP-dependent oncogenic functions in hepatocellular carcinoma. *Oncogene,* 30**,** 1229-40.

YAMAMOTO, R., NISHIKORI, M., KITAWAKI, T., SAKAI, T., HISHIZAWA, M., TASHIMA, M., KONDO, T., OHMORI, K., KURATA, M., HAYASHI, T. & UCHIYAMA, T. 2008. PD-1-PD-1 ligand interaction contributes to immunosuppressive microenvironment of Hodgkin lymphoma. *Blood,* 111**,** 3220-4.

YAN, D., PARKER, R. E., WANG, X., FRYE, S. V., EARP, H. S., 3RD, DERYCKERE, D. & GRAHAM, D. K. 2018. MERTK Promotes Resistance to Irreversible EGFR Tyrosine Kinase Inhibitors in Non-small Cell Lung Cancers Expressing Wild-type EGFR Family Members. *Clin Cancer Res,* 24**,** 6523-6535.

YANG, H. W., KIM, T. M., SONG, S. S., SHRINATH, N., PARK, R., KALAMARIDES, M., PARK, P. J., BLACK, P. M., CARROLL, R. S. & JOHNSON, M. D. 2012.

Alternative splicing of CHEK2 and codeletion with NF2 promote chromosomal instability in meningioma. *Neoplasia,* 14**,** 20-8.

YANG, J. J., ZHOU, C., HUANG, Y., FENG, J., LU, S., SONG, Y., HUANG, C., WU, G., ZHANG, L., CHENG, Y., HU, C., CHEN, G., ZHANG, L., LIU, X., YAN, H. H., TAN, F. L., ZHONG, W. & WU, Y. L. 2017. Icotinib versus whole-brain irradiation in patients with EGFR-mutant non-small-cell lung cancer and multiple brain metastases (BRAIN): a multicentre, phase 3, open-label, parallel, randomised controlled trial. *Lancet Respir Med,* 5**,** 707-716.

YE, X., LI, Y., STAWICKI, S., COUTO, S., EASTHAM-ANDERSON, J., KALLOP, D., WEIMER, R., WU, Y. & PEI, L. 2010. An anti-Axl monoclonal antibody attenuates xenograft tumor growth and enhances the effect of multiple anticancer therapies. *Oncogene,* 29**,** 5254-64.

YU, M., LI, W., WANG, Q., WANG, Y. & LU, F. 2018. Circadian regulator NR1D2 regulates glioblastoma cell proliferation and motility. *Oncogene,* 37**,** 4838-4853.

YUE, W. Y., CLARK, J. J., TELISAK, M. & HANSEN, M. R. 2013. Inhibition of c-Jun N-terminal kinase activity enhances vestibular schwannoma cell sensitivity to gamma irradiation. *Neurosurgery,* 73**,** 506-16.

YUZAWA, S., NISHIHARA, H., YAMAGUCHI, S., MOHRI, H., WANG, L., KIMURA, T., TSUDA, M., TANINO, M., KOBAYASHI, H., TERASAKA, S., HOUKIN, K., SATO, N. & TANAKA, S. 2016. Clinical impact of targeted amplicon sequencing for meningioma as a practical clinical-sequencing system. *Mod Pathol,* 29**,** 708-16.

ZANG, K. D. 2001. Meningioma: a cytogenetic model of a complex benign human tumor, including data on 394 karyotyped cases. *Cytogenet Cell Genet,* 93**,** 207-20.

ZHANG, P., LI, S., LV, C., SI, J., XIONG, Y., DING, L., MA, Y. & YANG, Y. 2018. BPI-9016M, a c-Met inhibitor, suppresses tumor cell growth, migration and invasion of lung adenocarcinoma via miR203-DKK1. *Theranostics,* 8**,** 5890-5902.

ZHANG, W., DERYCKERE, D., HUNTER, D., LIU, J., STASHKO, M. A., MINSON, K. A., CUMMINGS, C. T., LEE, M., GLAROS, T. G., NEWTON, D. L., SATHER, S., ZHANG, D., KIREEV, D., JANZEN, W. P., EARP, H. S., GRAHAM, D. K., FRYE, S. V. & WANG, X. 2014. UNC2025, a potent and orally bioavailable MER/FLT3 dual inhibitor. *J Med Chem,* 57**,** 7031-41.

ZHANG, Z., LEE, J. C., LIN, L., OLIVAS, V., AU, V., LAFRAMBOISE, T., ABDEL-RAHMAN, M., WANG, X., LEVINE, A. D., RHO, J. K., CHOI, Y. J., CHOI, C. M., KIM, S. W., JANG, S. J., PARK, Y. S., KIM, W. S., LEE, D. H., LEE, J. S., MILLER, V. A., ARCILA, M., LADANYI, M., MOONSAMY, P., SAWYERS, C., BOGGON, T. J., MA, P. C., COSTA, C., TARON, M., ROSELL, R., HALMOS, B. & BIVONA, T. G. 2012. Activation of the AXL kinase causes resistance to EGFR-targeted therapy in lung cancer. *Nat Genet,* 44**,** 852-60.

ZHONG, Z., WANG, Y., GUO, H., SAGARE, A., FERNANDEZ, J. A., BELL, R. D., BARRETT, T. M., GRIFFIN, J. H., FREEMAN, R. S. & ZLOKOVIC, B. V. 2010. Protein S protects neurons from excitotoxic injury by activating the TAM receptor Tyro3-phosphatidylinositol 3-kinase-Akt pathway through its sex hormone-binding globulin-like region. *J Neurosci,* 30**,** 15521-34.

ZHOU, L., ERCOLANO, E., AMMOUN, S., SCHMID, M. C., BARCZYK, M. A. & HANEMANN, C. O. 2011. Merlin-deficient human tumors show loss of contact inhibition and activation of Wnt/beta-catenin signaling linked to the PDGFR/Src and Rac/PAK pathways. *Neoplasia,* 13**,** 1101-12.

ZHOU, L. & HANEMANN, C. O. 2012. Merlin, a multi-suppressor from cell membrane to the nucleus. *FEBS Lett,* 586**,** 1403-8.

ZIZZO, G., HILLIARD, B. A., MONESTIER, M. & COHEN, P. L. 2012. Efficient clearance of early apoptotic cells by human macrophages requires M2c polarization and MerTK induction. *J Immunol,* 189**,** 3508-20.

ZORLUDEMIR, S., SCHEITHAUER, B. W., HIROSE, T., VAN HOUTEN, C., MILLER, G. & MEYER, F. B. 1995. Clear cell meningioma. A clinicopathologic study of a potentially aggressive variant of meningioma. *Am J Surg Pathol,* 19**,** 493-505.

7.0   Supplementary data

7.1   The inhibitory effect of UNC2025 and BGB324 on pFLT3 in meningioma primary cells

Incubation of meningioma primary cells with UNC2025 for 1 hr led to reduction in pFLT3 from 1.0 μM. UNC2025 was even more effective at inhibiting phosphorylation of FLT3 at 72 hrs and it nearly completely inhibited pFLT3 at 0.3 μM. A dose-dependent decrease in pFLT3 was also observed on treatment of meningioma primary cells with BGB324 for 1 hr. Although these results are preliminary and more samples needs to be tested to reach to any conclusion, the results of these experiments show that both BGB324 and UNC2025 may mediate their anti-tumorigenic effect via acting upon FLT3 in addition to AXL and MERTK respectively.
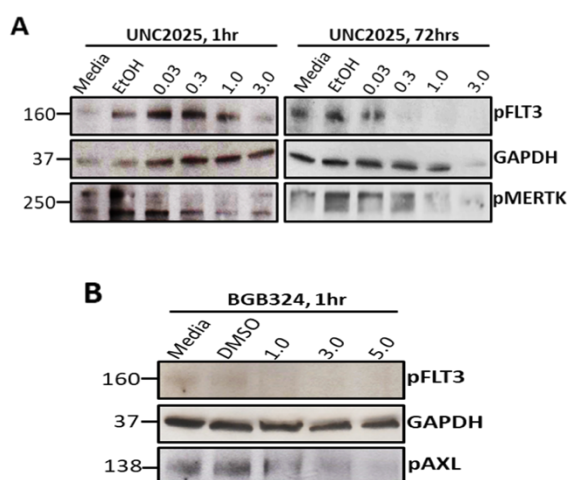

Figure S1- UNC2025 and BGB324 inhibits pFLT3 in meningioma primary cells.
A Western blot showing dose-dependent decrease in pFLT3 following treatment of meningioma primary cells with UNC2025 (1 hr and 72 hrs; n=1) **A)**; and BGB324 (1 hr; n=1) **B)**. GAPDH was used as a loading control.

7.2 The inhibitory effect of BGB324 on pAXL and pFLT3 in schwannoma cells

A strong reduction in pAXL was observed at 5 μM following incubation of schwannoma primary cells with BGB324 for 72 hrs. Interestingly, BGB324 also completely inhibited pFLT3 at 5 μM after 72 hrs. Although much more work is needed to understand the importance FLT3 in schwannoma pathogenesis, this preliminary data provides a new candidate which has not yet been investigated with respect to its role in NF2 tumorigenesis.
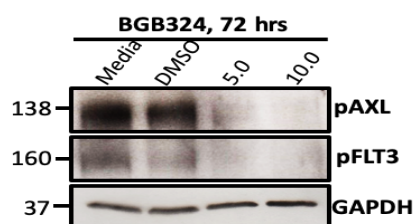

Figure S2- BGB324 inhibits pAXL and pFLT3 in schwannoma primary cells.
Decrease in pAXL and pFLT3 following treatment of schwannoma primary cells with BGB324 for 72 hrs (n=1) visualized using Western blotting. GAPDH was used as a loading control.

7.3   Macrophage infiltration in Merlin-negative human meningioma G-I tissues and the expression of AXL, TYRO3 and MERTK.

Since MERTK is highly expressed by macrophages and the TAM receptors can be activated at the cell membrane by forming a homo or hetero-dimer with the receptors of the same cells or adjacent cells, I wanted to investigate whether infiltrated macrophages influences the expression and activity of MERTK in meningiomas. To search this, firstly the levels of macrophages were investigated in each meningioma tissue sample by performing IHC or flow cytometry, followed by examination of MERTK and pMERTK levels in the same samples. In addition, the level of total AXL, TYRO3 and phospho AXL were also searched using IHC and Western blotting. IHC on meningioma tumour samples was performed in collaboration with the pathologist Dr David Hilton from the Neuropathology Department at Plymouth Hospital NHS Trust and Flow cytometry was performed by Dr Claire Adams at University of Plymouth.

IHC (Figure S3- A, B and C) and Flow cytometry (Figure S4- A and B) confirmed the infiltration of M2-polarized CD163$^+$ tumour associated macrophages in meningioma tissues and freshly isolated meningioma cells in culture, respectively.

IHC demonstrated strong cytoplasmic MERTK staining in macrophages (blue arrows) and weak variable staining in tumour cells (red arrows) (Figure-S3 D). pMERTK showed granular membrane and some cytoplasmic staining in endothelial cells (black arrows), macrophages and (blue arrows) and tumour cells (red arrows) (Figure-S3 E). AXL, pAXL and TYRO3 staining was mainly found in tumour cells (red arrows), however some staining is also observed in macrophages (blue arrows) and endothelial cells (black arrows) (Figure S3- F, G and H) confirming our group's previous data (Hilton et al., 2016). Scoring for MERTK was performed on macrophages as tumour cells displayed

only a weak, cytoplasmic staining. For pMERTK, pAXL/AXL and TYRO3 scoring was performed on tumour cells (scoring was performed by Dr David Hilton).

No significant difference in pMERTK, pAXL, and AXL or TYRO3 staining intensity was observed between tissues with low macrophage infiltration and tissues with high macrophage infiltration (Figure-S3 I). However, meningioma tissues with high macrophage infiltration showed significantly stronger MERTK staining compared to tissue with low macrophage infiltration (Figure-S3 I). Western blotting of freshly isolated meningioma primary cells (p0) from the tissues with high macrophage infiltration also demonstrated a significant increase in MERTK expression compared to samples with low macrophage infiltration (Figure-S4 C), suggesting that macrophages may contribute to the overall MERTK expression in meningioma tissues.

To verify that macrophages contribute to increased MERTK expression in meningioma tissues, freshly isolated meningioma primary cells-passage 0 (p0), were passaged to passage 1 (p1), followed by flow cytometry and detection of CD163+ macrophages. The results revealed decrease in macrophage levels from average 3.62% to average 1.20% in samples with low macrophage infiltration and from average 27.25% to average 16.84% in samples with high macrophage infiltration (Figure-S4 A and B). The same samples were then tested for MERTK expression by Western blotting, demonstrating a small but significant decrease in total MERTK levels in p1 compared to p0 cells from low macrophage infiltration tissues (Figure-S4 D). No difference in MERTK levels was observed between p0 and p1 cells from tissues with high macrophage infiltration (Figure-S4 D) as p1 still contains a proportion of macrophages (average 16.84%) expressing MERTK.
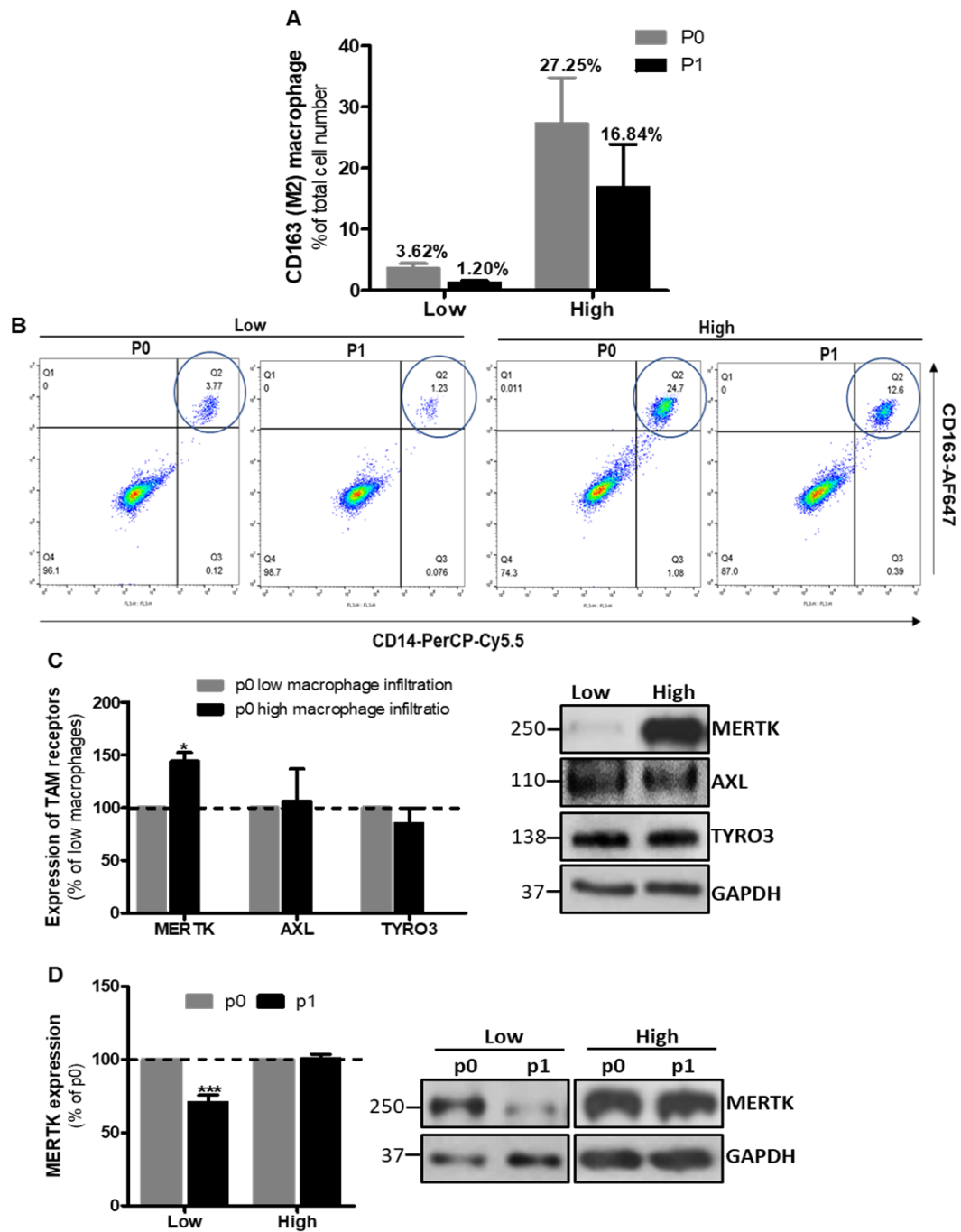
Figure S3- IHC to detect macrophage infiltration and expression of TAM receptors.
IHC demonstrate CD163 staining in tissues with low **A)** and tissue with high macrophage infiltration **B).** A scatter plot graph represents the percentage of CD163-positive cells in low (n=8) and high macrophage infiltrated meningioma tissues (n=8) **C)**. IHC shows that MERTK **D)**, pMERTK **E)**, AXL **F)**, pAXL **G)** and TYRO3 **H);** are expressed by tumour cells (red arrow), CD163+ macrophages (blue arrow) and endothelial cells (black arrow). The quantitative assessment of staining intensity for AXL, pAXL, MERTK, pMERTK and TYRO3 in tissues with low and high macrophage infiltration has demonstrated in a graph (n=8), **I)**. Scale bar 50 μM. Unpaired two-tailed student's t-test or two-way ANOVA with Bonferroni posttest was used to calculate the statistical significance; *p<0.05 and ***p<0.001. IHC staining and scoring was performed in collaboration with the pathologist Dr David Hilton from the Neuropathology Department at Plymouth Hospital NHS Trust.

Figure S4- The expression of MERTK is correlated with CD163^{+} macrophages in meningiomas.

Flow cytometery demonstrates variable level of CD163^{+} macrophage infiltration in freshly isolated- passage 0 (p0) and passaged- passage 1 (p1), meningioma primary cells in culture; (p0 and p1 for low macrophage samples (n=11) and p0 and p1 for high macrophage samples (n=6)); **A)** and **B)**. Western blot analysis shows significantly higher expression of MERTK (n=3) but not of AXL (n=3) or TYRO3 (n=3) in freshly isolated meningioma primary cell samples with high macrophage infiltration **C)**. The expression of MERTK is significantly reduced in low macrophage infiltrated samples when p0 menigioma primary cells passagd to p1 but not in samples with high macrophage infiltration (n=3) **D)**. Two-way ANOVA with Bonferroni posttest was used for statiscal significance calculation; *p<0.05 and ***p<0.001

7.4 Uncropped Western blot images of each antibodies used in this project

Figure 3.32 A

Figure 3.28 A

Figure 3.33 C (left panel)

Figure 3.5 A (left panel)

Figure S2
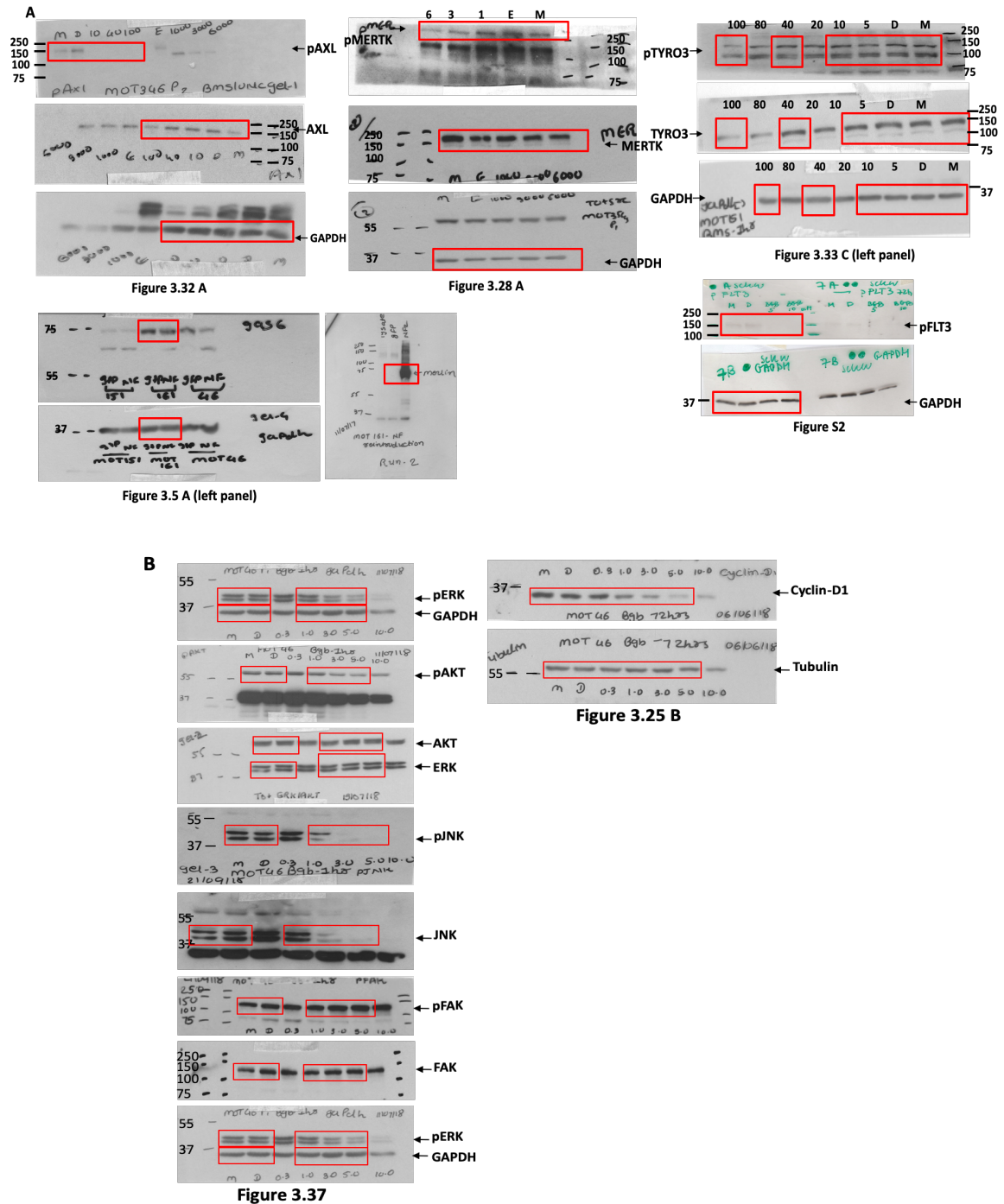
Figure 3.25 B

Figure 3.37

Figure S5- A representative uncropped Western blot images of all antibodies used in this project.

Western blot images of phosphorylated and total AXL, MERTK and TYRO3 **A)**; phosphorylated and total ERK, AKT, JNK, FAK, Src and Cyclin-D1 **B)**. The bands that used for densitometry measurements have been marked in red box.

7.5 The summary of characteristics, Merlin/NF2 status and the experiments each clinical sample used for.

The characteristics of all tumour samples (schwannomas and meningiomas) and in which particular experiments they used for, are detailed in table S1. All tumours were confirmed as Merlin-deficient using Western blot, performed by myself or one of my colleagues. The *NF2* status for some of the samples were investigated by sequencing *NF2* gene with next-generation sequencing (NGS) and multiple ligation-dependent probe amplification (MLPA) techniques at the Manchester Centre for Genomic Medicine, Mangen (Manchester Department of Clinical Genetics) depending on the project requirement and is summarized in table-S2. Table-S1 and table-S2 has been attached seperately as Excel spreadsheet.